Optimization of a supercritical assisted process for the production of liposomes for industrial applications

Paolo Trucillo

UNIVERSITY OF SALERNO

DEPARTMENT OF INDUSTRIAL ENGINEERING

Ph.D. Course in Industrial Engineering
Curriculum in Chemical Engineering - XXXI Cycle

Optimization of a supercritical assisted process for the production of liposomes for industrial applications

Supervisor
Prof. Ernesto Reverchon

PhD student
Paolo Trucillo

Scientific Referees
Ing. Roberta Campardelli
Prof. Elisabeth Badens
Prof. José Coelho

PhD Course Coordinator
Prof. Ernesto Reverchon

Acknowledgements

First of all, I would like to thank my family, my girlfriend Silvia and my friends for the daily support in overcoming all the difficulties that occurred during my path.

I would also like to thank professor Ernesto Reverchon for my cultural growth in this 3 years of research. It has been an exciting and challenging working experience as well as a continuous academic and personal exchange of ideas corroborated and continuously corrected by his vast experience.

I am also grateful to the following people I have met over the years: Roberta Campardelli for having accompanied me along this path for almost 7 years. It was 2011 when I first met her; she was the co-supervisor of my Bachelor's degree project. Then, she entrusted me with developing of a lab-scale plant for my Master's degree. Finally, I started the PhD course, having her as a member of the scientific committee, sharing academic research, joys, frustrations and then a truly fulfilling experience. Now I can run on my own thanks to her daily help and patience.

The professors Elisabeth Badens and José Coelho for being part of the Scientific Committee of this PhD project and their kindness and expertise.

Professor Patrizia Perego for giving me the possibility to work in her group for anti-microbial studies using liposomes produced at the University of Salerno.

My PhD colleagues and other brilliant researchers with whom I shared this path: Daniele Sofia, Pierfrancesco "Piffa" Ferrari, Bahar Aliakbarian, Sara Liparoti, Daniele Carullo, Marco Lupo, Veronica De Simone, Alessia Di Capua, Ida Palazzo, Paola Franco, Giovanni Cascone, Antonio Tabernero.

The Bachelor's and Master's degree students who worked on the production of liposomes using SuperLip process: Marina Iorio, Daniela Apicella, Annabella Bruno, Luca Vitale, Alessandra Saturnino, Paola Russo, Gianroberto La Corte, Ermelinda Sorrentino, Antonella Coccaro, Igino Landi and Giuseppa Del Forno.

The Day One S.r.l. staff and, in particular, Paolo De Stefanis and Valeria Guglielmotti. I had the great pleasure to meet them in the middle of my PhD activities. They helped me to increase the commercial potential of the process that we have developed at the Industrial Engineering Department of the University of Salerno.

Dr. Roberto Santoliquido from Alfatest S.r.l. (Italy) for his kind help with the NTA Nanosight measurements.

Dr. Rossella Crescitelli and especially Prof. Jan Lotval for the kind and spontaneous help in performing the Transmission Electron Microscope Analysis of liposome suspensions.

Dr. Mariarosa Scognamiglio for the kind help with the Gas Chromatographic measurements to quantify the cholesterol encapsulation efficiency in the double lipidic layer of liposomes.

Professor Iolanda De Marco for the daily advice as well as for letting me study jet atomization using her apparatus.

Dr. Sacha Anthony Berardo from the Linguistic Center of the University of Salerno, for his kind help in revising this Ph.D. manuscript.

All the other members of the supercritical assisted group: Stefano Piotto, Simona Concilio, Francesco Marra, Renata Adami, Stefano Cardea, Lucia Baldino, Giovanna Della Porta and Rosita Tulipano.

Finally, all the former colleagues that worked in our group and have now moved on: Vincenzo Cricchio, Emilia Oleandro, Mara Pascale, Valentina Prosapio, Emanuele Trucillo and Emanuela Cosenza.

List of contributions

International papers

1) R. Campardelli, P. Trucillo, E. Reverchon: "A Supercritical Fluid-Based Process for the Production of Fluorescein-Loaded Liposomes", **2016**, Industrial & Engineering Chemistry Research, Vol 55, Issue 18, pp. 5359-5365.

2) P. Trucillo, R. Campardelli, E. Reverchon, "Supercritical assisted liposomes formation: optimization of the lipidic layer for an efficient hydrophilic drug loading", **2017**, Journal of CO_2 utilization, Vol.18, p.181-188.

3) P. Trucillo, R. Campardelli, E. Reverchon, "Operative parameters optimization production of liposomes for the encapsulation of hydrophilic compounds using a new supercritical process", **2017**, Chemical Engineering Transactions, Vol. 57, pp. 799-804.

4) P. Trucillo, R. Campardelli, E. Reverchon, "Encapsulation of Hydrophilic and Lipophilic Compounds in Nanosomes Produced with a Supercritical Based Process", **2018**, Advances in bionanomaterial (book chapter), p. 23-35.

5) P. Trucillo, R. Campardelli, E. Reverchon, "Production of liposomes loaded with antioxidants using a supercritical CO_2 assisted process", **2018**, Powder Technology, Vol. 323, pp. 155-162.

6) P. Trucillo, R. Campardelli, B. Aliakbarian, P. Perego, E. Reverchon, "Supercritical assisted process for the encapsulation of olive pomace extract into liposomes", **2018**, The Journal of Supercritical Fluids, Vol. 135, pp. 152-159.

7) R. Campardelli, P. Trucillo, E. Reverchon, "Supercritical assisted process for the efficient production of liposomes containing antibiotics for ocular delivery", **2018**, Journal of CO_2 utilization, Vol.25, pp. 235-241.

8) P. Trucillo, R. Campardelli, "Production of Solid Lipid Nanoparticles with a Supercritical Fluid Assisted Process", **2019**, The Journal of Supercritical Fluids, Vol. 143, pp. 16-23.

9) P. Trucillo, R. Campardelli, M. Scognamiglio, E. Reverchon, "Control of Liposomes Diameter at Micrometric and Nanometric Level Using a Supercritical Assisted Technique", **2019**, **submitted** to Journal of CO_2 utilization.

10) P. Trucillo, R. Campardelli, E. Reverchon, "A Versatile Supercritical Assisted Process For One-Step Production of Liposomes", **2019**, The Journal of Supercritical Fluids, Vol. 146, pp. 136.143.

11) D. Apicella, M. Arruebo, R. Campardelli, M. Encabo Berzosa, P. Trucillo, E. Reverchon, V. Sebastian, J. Santamaria, "Efficent continuous production of near-infrared-sensitive liposomes for light-triggered delivery of polyinosinic-polycytidylic acid", **2019**, **submitted** to International Journal of Pharmaceutics.

12) P. Trucillo, R. Campardelli, E. Reverchon, "Antioxidant Loaded Emulsions Entrapped in Liposomes Produced with a Supercritical Assisted Technique", **2019**, **completed**.

13) R. Campardelli, P. Trucillo, M. Iorio, E. Reverchon, "Leather dyeing using a novel liposomal method assisted by a dense gas technology", **2019**, **completed**.

14) P. Trucillo, R. Campardelli, E. Reverchon, I. De Marco, "Break-up atomization study of a water jet in supercritical carbon dioxide", **2019**, **in progress**.

15) P. Trucillo, P. Ferrari, R. Campardelli, P. Perego, E. Reverchon, "Supercritical assisted method for the production of amoxicillin loaded liposomes for anti-microbial activity", **2019**, **in progress**.

National papers

1) P. Trucillo: "Produzione di liposomi con I fluidi supercritici", Jul/Aug **2016**, ICP – Rivista dell'Industria Chimica, Nr. 7-8, pp. 90-93.

2) P. Trucillo, "I nuovi orizzonti 2020 dell'Ingegneria Chimica", Oct **2016**, ICP – Rivista dell'Industria Chimica, pp. 92-94.

3) P. Trucillo, "I nanosomi, farmacie portatili", Feb **2017**, Sapere, Nr. 1, p.46.

4) P. Trucillo, "Fluidi supercritici: un convegno a Lisbona", Jun **2017**, ICP – Rivista dell'Industria Chimica, Nr. 6, pp. 90-93.

5) P. Trucillo – "Scuola di Dottorato GRICU 2017: un momento di confronto per i dottorandi", Nov **2017**, ICP – Rivista dell'Industria Chimica, Nr. 11, pp. 90-93.

6) P. Trucillo – Nanosomi: un nuovo traguardo, Nov/Dec **2017**, La Chimica e L'Industria, Nr. 6, pp. 29-33.

7) P. Trucillo – Liposomi: una tecnologia innovativa, Jan **2018**, Costo Zero, pp. 52-53.

8) P. Trucillo – Nanoliposomi: una vetrina a PharmExpo, Jan **2018**, Nr. 1, p. 78.

9) P. Trucillo – Ingegneria Chimica: l'eccellenza si incontra a Pisa, Jul/Aug **2018**, Nr. 7/8, p. 2-4.

10) P. Trucillo - DICCA: interdisciplinarietà e innovazione, Oct **2018**, Nr. 10, p. 76-79.

Conference papers

1) 8-11 May 2016: “15th European Meeting on Supercritical Fluids (EMSF 2016)”, Essen, Germany. Presentation of the poster "Liposome production using a new supercritical fluid based process: optimization of the composition of the lipidic bilayer for efficient theophylline encapsulation" (P. Trucillo, R. Campardelli, E. Reverchon).

2) 12-16 September 2016: “Convegno Nazionale GRICU 2016 – Gli orizzonti 2020 dell’Ingegneria Chimica” in Anacapri (NA, Italy). Oral presentation “Fluorescein loaded liposomes production using a new supercritical process” (P.Trucillo, R.Campardelli, E.Reverchon) and poster presentation “Production of liposomes loaded with theophylline, study and optimization of the double lipidic layer” (P. Trucillo, R. Campardelli, E. Reverchon).

3) 4-7 October 2016: “BIONAM 2016”, organized by the Pharmacy Department of the University of Salerno. Presentation of the poster “Encapsulation of hydrophilic and lipophilic compounds in nanosomes produced with a supercritical based process” (P. Trucillo, R. Campardelli, E. Reverchon).

4) 25-28 April 2017: “16th European Meeting on Supercritical Fluids (EMSF 2017)”, Lisbon, Portugal. Presentation of the poster " SuperLip Process For The Production Of Liposomes Loaded With Antioxidant Compounds" (P. Trucillo, R. Campardelli, E. Reverchon) and participation to the 1st Business Plan Competition with the project “LipoRep (Liposome Repair)” (P. Trucillo, R. Campardelli, S. Iuorio, E. Reverchon).

5) 28-31 May 2017: “13th International Conference on Chemical and Process Engineering (Icheap13)”, Milan, Italy. Oral presentation “Operative Parameters Optimization: Production of Liposomes for the Encapsulation of Hydrophilic Compounds Using a New Supercritical Process” (P. Trucillo, R. Campardelli, E. Reverchon).

6) 24-29 September 2017: GRICU 2017, Palermo, Italy. Poster presentation “Supercritical Fluids for the Production of Nutrasomes” (P. Trucillo, R. Campardelli, E. Reverchon).

7) 22-25 April 2018: “12th International Symposium on Supercritical Fluids” (ISSF 2018), held in Antibes-Juan-les-Pins, Nice, France. Presentation of the poster “Antioxidant Loaded Nanoemulsions Entrapped in Liposomes Produced with a Supercritical Assisted Technique ” (P. Trucillo, R. Campardelli, E. Reverchon), the poster “Gas to Liquid Ratio Optimization for the Reduction of Ethanol Residue for the Production of Liposomes with a Supercritical Assisted Technique” (P. Trucillo, R. Campardelli, M. Scognamiglio, E. Reverchon) and oral presentation “A Versatile Supercritical Assisted Process for the Production of Nanosomes: Development, Production and Commercialization ” (P. Trucillo, R. Campardelli, E. Reverchon).

8) 16-19 May 2018: GRICU 2018, Pisa, Italy. Poster presentation “SuperLip: Process and Product Optimization for Industrial Purposes” (P. Trucillo, R. Campardelli, E. Reverchon).

9) 20-22 June 2018: BE-Mat 2018, Business Event on Materials, Raw Materials & Circular Economy, Anacapri, Italy. Oral presentation “Nanolip” (P. Trucillo).

Summary

I. Liposomes: a full description of the state of art……1
I.1 Introduction and definition of liposomes……..…2
I.2 From history to modern times……..……..3
I.3 Classification of liposomes…….……..5
I.4 Characterization of liposomes…….……..6
I.5 Drug delivery with natural release mechanism…….....9
I.6 Artificial drug release techniques……10
I.7 Methods of production …….……..12
I.8 Comparison among liposome methods of production……19

II. Objective of this work……21

III. Plant design, materials and methods……25
III.1 Apparatus……..26
III.2 Materials……...31
III.3 Methods……31

IV. Prel. studies for the optimization of operating parameters…….37
IV.1 Effect of Pressure on empty liposomes…….....38
IV.2 A case study: the encapsulation of fluorescein……38
IV.3 Drug concentration effect…….49
IV.4 Gas to Liquid Ratio of the expanded Liquid……52

V. Liposomes double layer optimization……...……63
V.1 Cholesterol loaded liposomes……64
V.2 Production of PC/PE liposomes……68

VI. Encapsulation of antioxidant compounds……..…..…75
VI.1 Eugenol and α-lipoic acid encapsulation in liposomes……77
VI.2 Oil in Water emulsions entrapped into liposomes…….…..88

VII. Encapsulation of dietary supplements…….…..…103

VIII. Encapsulation of antibiotics……113
VIII.1 Antibiotics for ocular delivery……114
VIII.2 Encapsulation of antibodies……122
VIII.3 Anti-bacterial studies……123

IX. Encapsulation of dyes for leather treatment……131
IX.1 Process parameters optimization……134
IX.2 EDX and Colorimetric analysis……142

X. SuperLip economic and financial analysis……149
X.1 Economic analysis……151
X.2 Financial analysis……153

XI. Final discussion and conclusions……163
XI.1 Discussion……166
XI.2 Future perspectives……168

Bibliography……169

Abbreviation List……193

Index of Figures

Figure I.1 *Papers on liposomes published per country (a) and liposomes documents trend over the last decades (b). Data obtained via www.scopus.com*

Figure II.1 *A scheme of SuperLip mechanisms involved in the formation process of liposomes*

Figure II.2. *Mechanisms hypothesized for the SuperLip process*

Figure III.1 *SuperLip process layout scheme*

Figure III.2 *Homogenizer element*

Figure III.3 *High pressure vessel*

Figure III.4 *Injector for water atomization from macroscopic (a) and microscopic (b) observations*

Figure III.5 *Accumulation element*

Figure III.6 *Separator*

Figure III.7 *SuperLip apparatus*

Figure IV.1 *High pressure vapor-liquid equilibria for the system CO_2-ethanol-water at 40 °C in the pressure range 100-200 bar, adapted from (Durling et al., 2007b). Operating point of the experiments is reported (●) as a red dot.*

Figure IV.2 FE-SEM image of liposomes loaded with fluorescein at 1% theoretical loading.

Figure IV.3 *Comparison of PSDs of liposomes produced using different injector diameters, PC concentration 5 mg/mL.*

Figure IV.4 *Stability study of fluorescein loaded liposomes*

Figure IV.5 *Example of frame from NTA analysis of liposome suspensions produced at a PC concentration of 5 mg/mL and 1% fluorescein theoretical loading.*

Figure IV.6 *Comparison of PSD distribution data obtained with DLS as diameter vs intensity (a) and NTA as diameter vs concentration (b). SuperLip liposomes produced at 80 µm, PC concentration 5 mg/mL.*

Figure IV.7 *Drug release comparison: free fluorescein, 5 mg/mL PC, 7.5 mg/mL PC, 10 mg/mL PC*

Figure IV.8 *TEM image of multi-layered liposomes*

Figure IV.9 *FTIR on native BSA compared with SuperLip processed BSA*

Figure IV.10 *Particle Size Distributions (PSDs) of micrometric and nanometric empty liposomes obtained changing the Gas to Liquid Ratio of the fluid phase (GLR-EL).*

Figure IV.11 *Scanning Electron Microscope image of liposomes produced at a GLR-EL = 6.00*

Figure IV.12 *Gibbs Diagram for the CO2–EtOH–H2O system at 313K and 100 bar., adapted from (Durling, 2007).*

Figure IV.13 *Gibbs Diagram for the CO2–EtOH–H2O system at 313K and 100 bar., adapted from (Durling, 2007), with mixing paths.*

Figure IV.14 *Comparison of the Particle Size Distribution of liposome suspensions produced at GLR-EL 6.0 before and after evaporation step.*

Figure IV.15. *Particle Size Distributions of farnesol (a) and vancomycin (b) loaded liposomes produced at a GLR-EL 6.0.*

Figure IV.16 *Scanning Electron Microscope of vancomycin (a) and farnesol (b) loaded liposomes produced with GLR 6.00*

Figure V.1 *Operating points (in red) in the experiments performed at different water flow rates, reported in the carbon dioxide-*

water-ethanol ternary diagram at 40°C and 100 bar, adapted from (Durling et al., 2007a).

Figure V.2 *1% w/w theophylline loaded liposomes produced with different cholesterol percentages in the double lipidic layer (0, 1 and 2.5% w/w with respect to the PC mass concentration).*

Figure V.3 *PSD of theophylline loaded liposomes produced with increasing percentages phosphatidylethanolamine (PE) encapsulated in the double lipid layer*

Figure V.4 *Transmission Electron Microscope images of liposome vesicles.*

Figure V.5 *Stability of encapsulation of theophylline loaded liposomes (1% cholesterol, water flow rate 0.7 mL/min) observed over a 40 days period.*

Figure V.6 *Comparison of drug release kinetics of theophylline liposomes loaded with 0, 1, 2.5% cholesterol (Chol) content in the lipid double layer, produced with 0.7 mL/min water flow rate.*

Figure V.7 *Drug release kinetics comparison between un-processed theophylline, 2.5% cholesterol (Chol) loaded liposomes and 2.5% phosphatidylethanolamine (PE) loaded liposomes, produced at a water flow rate of 0.7 mL/min.*

Figure VI.1 *PSD of liposomes core loaded with 10, 20 and 30 % eugenol, produced at the temperature of 35 °C*

Figure VI.2 *PSD of liposomes core loaded with 10, 20 and 30 % eugenol, produced at the temperature of 40 °C*

Figure VI.3 *PSD of liposomes lipidic layer loaded with 10, 20 and 30 % eugenol, produced at the temperature of 40 °C*

Figure VI.4 *Cumulative curves of liposomes loaded with 10, 20 and 30 % w/w ALA, produced at the temperature of 40 °C*

Figure VI.5 *SEM images of the samples (a) eugenol loaded in the inner core at 35 °C and (b) eugenol loaded in the double lipidic layer at 40 °C.*

Figure VI.6 *SEM images of the experiments (a) ALA1, loaded with 10 % w/w (b) ALA2, 20 % w/w (c) ALA3, 30 % w/w lipoic acid at the temperature of 40 °C*

Figure VI.7 *Drug release tests on liposomes with inner core (a) and lipidic layer (b) loaded with 10 % w/w eugenol/lipids. 30°C red curve and 60 °C black curve*

Figure VI.8 *Farnesol (a), Limonene (b) and Linalool (c) loaded liposomes at different theoretical loadings (10 %, 20 % and 30 % w/w on lipid mass base)*

Figure IV.9 *Optical image of limonene loaded emulsions*

Figure IV.10 *Particle Size Distributions of empty oil in water emulsion (a) and empty emulsion loaded liposomes produced with SuperLip (b)*

Figure VI.11 *Limonene (a) and Linalool (b) loaded emulsions entrapped in the inner core of liposomes*

Figure VI.12 *FE-SEM images of double lipidic layer loaded liposomes containing (a) farnesol and (b) limonene, and inner core loaded liposomes containing limonene (c).*

Figure VII.1 *Frequency distribution curves of olive pomace loaded liposomes at 130 bar and using 60 µm injection diameter*

Figure VII.2 *FE-SEM image of liposomes loaded with 5 % mg total polyphenols from olive pomace per mg of phosphatidylcholine (TP/PC), produced at 130 bar using a 60 µm injector.*

Figure VII.3 *liposomes loaded with 5 % mg total polyphenols from olive pomace per mg of phosphatidylcholine (TP/PC)*

Figure VII.4 *Frequency distributions curves of olive pomace loaded liposomes at 170 bar and 80 µm injection diameter*

Figure VII.5 *FE-SEM image of liposomes loaded with 5 % mg total polyphenols from olive pomace per mg of phosphatidylcholine (TP/PC)*

Figure VII.6 *TP/PC % effect on encapsulation efficiency reported as a function of the pressure*

Figure VIII.1 *Cumulative distributions curves for 1 % w/w ofloxacin loaded liposomes, produced at different PC/H_2O ratios*

Figure VIII.2 *Encapsulation Efficiencies comparison at different ofloxacin theoretical loadings and different PC/H_2O ratios*

Figure VIII.3 *TEM image of ofloxacin loaded liposomes*

Figure VIII.4 *Drug release comparison between 1 % w/w ofloxacin (blue) and 1 % w/w ampicillin (red) loaded liposomes*

Figure VIII.5 *E.Coli growth kinetics in test P01bis, P05bis, P06bis, P13bis – Lipid only - (0, 25, 50, 100 ppm liposome concentration)*

Figure VIII.6 *E.Coli growth kinetics in test P02bis, P07bis, P08bis, P09bis – Lipid + cholesterol - (0, 25, 50, 100 ppm liposome concentration)*

Figure VIII.7 *E.Coli growth kinetics in lipid loaded liposomes with 0, 5, 10, 20 Amoxicillin loading and 25, 50, 100 ppm liposomes concentration*

Figure VIII.8 *Drug release tests of 1 %, 5 %, 10 % and 20 % w/w amoxicillin loaded liposomes on lipid mass basis*

Figure VIII.9 *E.Coli growth kinetics in liposomes loaded with* Albumin fluorescein isothiocyanate and amoxicillin (different liposomes concentrations)

Figure IX.1 *Particle Size Distributions of liposomes produced at a dye/lipid ratio of 5 %, 10 % and 15 % w/w*

Figure IX.2 *Particle Size Distributions of liposomes produced at a lipid concentrations of 1, 5, 7 and 10 mg/mL*

Figure IX.3 *Particle Size Distributions of liposomes produced at water flow rates of 2, 5, 10 and 20 mL/min*

Figure IX.4 *Particle Size Distributions of liposomes produced at Gas to Liquid Ratio of the Expanded Liquid at 10, 6, 4, 2.4, 1.2 (a) and at 1, 0.8, 0.7, 0.4, 0.34 (b)*

Figure IX.5 *FE-SEM characterization of aniline loaded liposomes produced with GLR-EL 0.7 (a) and GLR 2.4 (b)*

Figure IX.6 *Morphological analysis of (a) upper and (b) lower leather surface from microscopic and macroscopic (c) observations*

Figure IX.7 *Carbon and Oxygen EDX images of leather treated with native aniline (a, c) and with liposomes (b, d)*

Figure IX.8 *Red intensity of leather upper surfaces with conventional and supercritical dyeing process*

Figure IX.9 *Variation of red intensity due to thermal exposure using conventional and supercritical methods*

Figure X.1 *Comparison between Drug Delivery Systems and liposomes revenues worldwide*

Figure X.2 *Yearly market repartition of Drug Delivery Systems*

Figure X.3 *Revenues calculated for SuperLip commercialization (2018-2022).*

Figure X.4 *Net Profit diagram for SuperLip commercialization (2018-2022).*

Figure X.5 *Cash Flow Statement for SuperLip commercialization (2018-2022).*

Figure XI.1 *Working map of produced liposomes Vs encapsulation efficiency*

Index of Tables

Table I.1 *Summary of liposomes production methods compared with SuperLip technology*

Table III.1 *SuperLip main plant units*

Table III.2 *List of the entrapped compounds whose encapsulation efficiency was detected using a Uv-Vis spectrophotometer*

Table IV.1. *Mean diameter (MD) and encapsulation efficiency (EE%) of liposomes loaded with 1% of fluorescein, using injectors with different diameters and different PC concentrations. Data are not reported for the experiments that were not possible to perform.*

Table IV.2. *SuperLip size distribution data and encapsulation efficiency of liposomes loaded with 1% to 9% w/w by weight of fluorescein*

Table IV.3 *MD, PDI and EE of liposomes loaded with 1% w/w of fluorescein at 10 mL/min water flow rate*

Table IV.4 *MD, PDI and EE of liposomes loaded with 10, 20 and 30 % w/w bovine serum albumin*

Table IV.5 *Mean Diameter (MD), Standard Deviation (SD), of empty liposomes (GLR-EL in the range 0.32 to 6.00)*

Table IV.6. *Comparison between Solvent Residue (SR) measured in empty liposomes suspension after evaporation, at different values of GLR-EL.*

Table IV.7. *Mean Diameter (MD) plus Standard Deviations (SD), Encapsulation Efficiency (EE) and Solvent Residue (SR) of farnesol and vancomycin loaded liposomes at GLR-EL 6.00*

Table V.1 *Particles size distribution data for 1% theophylline loaded liposomes with 0%, 1% and 2.5% cholesterol content in the lipid layer, produced at three different water flow rates 10, 2.14 mL/min and 0.7 mL/min respectively.*

Table V.2 *Particles size distribution data of theophylline loaded liposomes with 0%, 1%, 2.5% of phosphatidylethanolammine (PE) content in the lipid layer, produced with the water flow rate of 0.7 mL/min.*

Table VI.1 *Diameter, Polydispersion Index (PDI), EE and antioxidant power of Eugenol loaded liposomes*

Table VI.2 *Mean diameters, Polydispersion index (PDI), EE and antioxidant power of ALA loaded liposomes*

Table VI.3. *Mean diameter, polydispersion index, zeta potential and encapsulation efficiency of liposomes loaded with farnesol, limonene and linalool in the double lipidic layer*

Table VI.4 *Mean diameters, polydispersion indexes and zeta potential of droplets obtained by Oil in Water emulsions loaded with limonene and linalool.*

Table VI.5 *Mean diameter, polydispersion index, zeta potential and encapsulation efficiency of liposomes loaded with limonene and linalool in the inner core*

Table VI.6 *Antioxidant activity test performed on the chosen antioxidants in different compartments of the produced liposomes*

Table VII.1 *Mean diameter (MD), standard deviation (SD) and polydispersion index (PDI) of liposomes produced using SuperLip and thin layer hydration methods, used for comparison purposes, loaded with 5 %, 10 %, 15 % 20 % mg olive pomace total polyphenols per mg of phosphatidylcholine (TP/PC).*

Table VIII.1 *Mean diameter (MD), standard deviation (SD) and encapsulation efficiency (EE) of liposomes loaded with 1, 3 and 6 % w/w ofloxacin (OF), a different PC/H_2O ratios and water flow rates*

Table VIII.2 *Liposomes produced with different Antibody/lipid ratios at different water flow rates.*

Table VIII.3 *Liposomes produced with different* Albumin fluorescein isothiocyanate mass *(FBSA) and different amoxicillin mass fixing FBSA masses*

Table IX.1 *Mean Diameter, Polydispersion Index and Encapsulation Efficiencies of liposomes loaded Dye to Lipid ratios from 5 to 15 % w/w*

Table IX.2 *Mean Diameter, Polydispersion Index and Encapsulation Efficiencies of liposomes produced with increasing lipid concentrations between 1 and 10 mg/mL ethanol solutions*

Table IX.3 *Mean Diameter, Polydispersion Index and Encapsulation Efficiencies of liposomes produced working with a decreasing water flow rate from 20 to 2 mL/min*

Table IX.4 *Mean Diameter, Polydispersion Index and Encapsulation Efficiencies of liposomes produced at different GLR-EL (from 0.34 to 10)*

Table IX.5 *Energy Dispersive X-ray spectroscopy analysis of Carbon and Oxygen contained in Leather, native dye, leather + dye and leather + dye loaded liposomes*

Table IX.6 C*olorimetric analysis on leather dyed at different contact times using conventional and supercritical techniques*

Table IX.7 *Red dye intensity of leather untreated and treated with water at 100 °C and oven at 120 °C*

Table X.1 *Pain and Gain of SuperLip Vs other methods*

Table X.2 *S.W.O.T. analysis of the SuperLip process*

Table X.3 *CAPEX cost for SuperLip apparatus*

Table X.4 *Marketing cost*

Table X.5 *Sub-contractors costs*

Table X.6 *Operating and production costs*

Table X.7 *Personnel costs*

Table X.8 *Profit & loss Statement*

Table X.9 *Cash Flow Statement*

Table X.10 *Balance Sheet*

Table X.11 *Financial indexes calculation*

Table XI.1 *List of compounds entrapped into liposomes by SuperLip, specifying the compartment of encapsulation, Mean Diameter (MD), Standard Deviation (SD) and average Encapsulation Efficiencies (EE)*

Table XI.2 *Summary of PAINS and GAINS of other liposomes production methods Vs SuperLip*

Abstract

Liposomes are spherical vesicles made of a double lipidic layer that surrounds an inner aqueous core. Several methods for the preparation of liposomes have been developed over the last decades. However, these methods present several drawbacks, such as low reproducibility, batch operations, low encapsulation efficiency of hydrophilic compounds, control difficulties in liposome size distribution and high solvent residue, thus hindering the significant industrial potential of these drug delivery systems.

Supercritical fluid (SCF) technologies have been proposed to overcome several limitations of conventional processes for the production of micronized particles carriers, coprecipitates and nanocomposite polymeric structures. Recently, some techniques based on the use of supercritical carbon dioxide have also been proposed for liposome production. However, these methods still have some limitations related to the control of liposome dimension and size distribution, while also presenting very low encapsulation efficiency of hydrophilic drug. The main limitation of the processes, both conventional and supercritical, derives from the hydration step of the lipid layer. During this step, only a part of the water used for hydration is entrapped in liposomes, resulting in a low overall encapsulation efficiency.

Therefore, the **objective of this PhD thesis** is to develop a novel technology assisted by supercritical carbon dioxide for the production of liposomes of controlled dimensions. The proposed technique is called Supercritical assisted Liposome formation (SuperLip). In this process, first water droplets are produced; then, they are rapidly covered by phospholipids.

In the **first year** of this PhD project, the effect of several process parameters were studied such as water flow rate, injector diameter, pressure and Gas to Liquid Ratio of the Expanded Liquid (GLR-EL); i.e., the mass ratio of carbon dioxide and ethanol flow rates. In addition, the composition of liposomes was modified by changing the phospholipid concentration and adding other lipids in the double lipidic layer such as cholesterol. It was then possible to produce vesicles with a good control of particle size distribution (PSD) as well as obtain a high encapsulation efficiency (EE) of the hydrophilic and lipophilic (up to 99%) compounds. The decrease of the water flow rate resulted in the increase of drug encapsulation efficiency; moreover, the use of an injector nozzle with a larger diameter resulted in the production of both larger water droplets and liposomes. The concentration of lipids did not affect the mean size of the liposomes or encapsulation efficiency, but it resulted in a delayed drug release due to the formation of several lamellae around the water droplets. Cholesterol was also recognized

as being responsible for a more compact double lipidic backbone. From previous studies, the increase of pressure resulted in the formation of smaller water droplets and liposomes. Vesicle production mechanisms involved in the SuperLip technique were studied to verify the hypothesis proposed for this process.

During the **second year**, several liposome-based product formulations were developed, according to the operating parameters already optimized during the first year of study. Antibiotics for ocular delivery, proteins and markers for molecule labeling were entrapped in liposomes for pharmaceutical purposes. Cosmetic applications were also explored, encapsulating antioxidant compounds of a hydrophilic and amphiphilic nature. Amphoteric compounds were entrapped either in the inner core or lipidic layer of liposomes to study the differences in the antioxidant inhibition power, depending on the vesicles compartment of encapsulation. Dietary supplements were also entrapped for food applications, in order to valorize the by-products that are generally discarded by the agro-alimentary field. A novel textile application was also proposed for the deposition of a dye on leather samples.

In the **third year** of this PhD project, *in vitro* studies were also performed with antibiotic loaded liposomes with *E.Coli*. An economic analysis on the proposed SuperLip technique was performed. SuperLip has a Technology Readiness Level (TRL) of 6/7, since it has been designed in a continuous lab-scale configuration, with it being possible to scale it up to industrial level. The SuperLip method can produce about 5 liters of liquid liposomes suspensions per day. The idea at the basis of the process has been already validated by product development and samples characterization, as reported in our published works. The potential of SuperLip has always been recognized by external customers, interested in the production of liposomes on demand. A business plan for the commercialization of SuperLip products was attempted to verify whether the production of liposomes using this technique could be profitable in the commercial application. A B2B model was proposed and an estimation of CAPEX and OPEX performed to produce a 5-year (2018-2022) prospective for commercialization.

Chapter I
Liposomes: a full description of the state of art

Chapter I

I.1. Introduction and definition of liposomes

Drug delivery consists of the administration of a compound to achieve a benefic and therapeutic effect in living bodies (Tiwari et al., 2012). For the treatment of human illnesses, several drug delivery systems have been developed, such as polymeric and lipidic particles, hydrogel particles, emulsions, membranes and microspheres and other molecular complexes (McClements, 2015). Nevertheless, the development of new drug formulations has recently been considered not sufficient to guarantee scientific progress in the drug therapy field. For this reason, the introduction of novel drug carriers was considered a promising strategy to enhance drug bioavailability and effectiveness of drug administration (Lesoin et al., 2011b). Among the drug delivery systems, the attention of academics and industries is focused on liposomes production and development for their high potential benefits to human body.

Liposomes are spherical vesicles characterized by an inner aqueous core surrounded by one or more lamellae of phospholipids. Each lamellae is made up of a double layer of phospholipids; the latter are amphiphilic compounds formed by a hydrophilic polar head and two hydrophilic tails. The head is mainly phosphoric acid; whereas, the chains are made of two fatty acids with approximately 10-20 carbon atoms and from 0 to 5 double bonds for each chain. For this reason, when phospholipids are added to an aqueous environment, they self assemble into spherical objects including a part of water volume. In detail, lipids form lamellar sheets that suddenly start to fold like a balloon from the corners; the polar heads face outwards to the aqueous region; whereas, the fatty acids face each other and finally form spherical vesicles. This is due to lipids natural tendency to reduce their total free energy of dispersion in an aqueous environment (Yoshimoto et al., 2013).

Liposomes are used as drug carriers because they can include water in which a hydrophilic compound has previously been dissolved. Moreover, lipophilic drugs can also be entrapped within the limited space between the two lipidic layers (Torchilin, 2005). Liposomes can entrap a wide variety of active principles, such as antibiotics, proteins, peptides, dyes, nucleic acids, antioxidants or enzymes. They are recognized as being biocompatible with the human body since they are generally delivered to living cells that essentially have the same structure: a double layer of phospholipids. Laterally thinking, liposomes are very good artificial imitations of nature; whereas, exosomes are vesicles of natural origin that are released directly by the cells for their communication (Valadi et al., 2007). Liposomes are biodegradable and characterized by low toxicity (Lian and Ho, 2001); they are non-immunogenic for systemic and non systemic administrations. Lipidic vesicles can entrap unstable compounds and shield their functional properties.

Delivery systems that use drug carriers made of phospholipids can have many applications in different industrial fields such as the cosmetics (Lohani et al., 2014), food and farming industries as well as pharmaceutics. They also have many advantages over conventional dosage formulations because they can protect the entrapped active principles after drug administration. Moreover, liposomes act as drug reservoirs and a local depot for sustained, targeted or delayed release (Pham et al., 2012). They can be applied for antimicrobial, antifungal and antiviral therapy, anti-tumor administration (Lasic, 1998, Malam et al., 2009), gene delivery (Sarisozen et al., 2015), immunology. In addition, liposomes can be programmed as targets for macrophages for blood cleaning (Jone, 2013): drugs are released when liposomes are digested by macrophages. Moreover, they are used to protect antioxidants in dermatological applications and anti-aging therapy; they are involved in food applications as additives of flavors or as dietary supplements (Keller, 2001) and food bioactive ingredients (Akhavan et al., 2018). The latter could also be oral iron supplements used to increase hemoglobin level by liposome encapsulation and delivery (Tarantino et al., 2015). Liposomes are involved in enzyme immobilization, bioreactor technology (Akbarzadeh et al., 2013) and the deposition of dyes in textile applications (Barani and Montazer, 2008a). Finally, a curious and highly interesting application is the production of Lipid Oxygen containing Microparticles (LOMs). In the case of prolonged oxygen deprivation, serious damage can be caused to the heart or brain. In this case, oxygen is fed to patients through oral injection via a mouth tube. A more difficult situation is created when access to the lungs is impeded or delayed. For this reason, oxygen loaded liposomes can be mixed with venous blood and delivery oxygen to O2-deprived hemoglobin; following initial animal trials, it was demonstrated that their health is prolonged and side effects of asphyxia delayed or avoided (Kheir et al., 2012).

I.2. From history to modern times

Liposomes were first discovered by Dr. Alec D. Bangham (1921-2010), a British hematologist of the Babraham Institute of Cambridge (United Kingdom) around 1965. While he was working on blood coagulation mechanisms applied to biological membranes, he understood that dried lipids are able to rearrange spontaneously if put in contact with a sufficient amount of water. This is considered as one of the best examples of science discoveries by serendipity. He also demonstrated that the spontaneous rearrangement of lipids is guided by unfavorable interactions between lipids and water, that generated repulsion effects (Campardelli et al., 2015). This fact contributes to placing amphiphilic molecules in the space describing a spherical shape and minimizing molecular interactions and the free Gibbs

energy of the system made of hydrophobic chains and external aqueous medium. For this reason, Bangham defined liposomes as perfect thermodynamic models (Bangham, 2005).

In the first years of his research, Bangham called these vesicles swollen phospholipids (Bangham et al., 1965), because they seemed to fold around a volume of water. Sometimes he referred to vesicles less seriously calling them banghasomes.

When convinced by the scientific editor Gerald Weissmann to find a more suitable name for them, the term liposomes was chosen, with it being made up of the two Greek words lipos (meaning fat) and soma (meaning body). Bangham also observed these vesicles using an optical microscope and verified that effectively they were characterized by two compartments: internally made of water and externally by at least one double layer of phospholipids. Bangham furthered his studies over the following decades, producing many interesting works (Bangham, 1992, Bangham, 1993) that led to numerous fields of research all over the world, with a successive high industrial potential. He was defined as "the odd pattern of a well-drawn drop of blood" (Deamer, 2010) thanks to his versatility and open-mindedness, along with the interdisciplinary of his studies.

Liposomes were seriously considered as possible precursors of living cells during the prebiological age on the Earth. According to this approach, life originated from inanimate matter via a spontaneous increase of molecular complexity and specificity. The spontaneity of liposomes self-arrangement was compatible with the theory of spontaneous evolution processes, starting from simple and small molecules to complex systems, following a bottom-up approach (Luisi et al., 1998).

Nowadays, among a great variety of drug carrier systems, the field of liposomes is one of the most growing scientific topics worldwide (see **Figure I.1**).

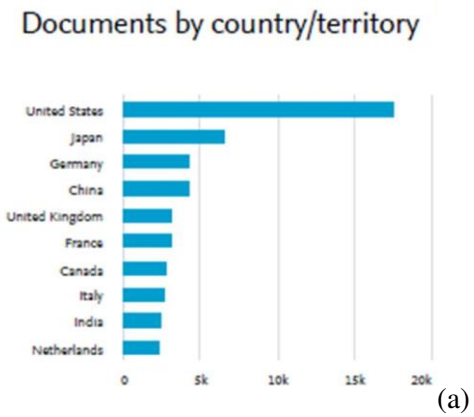

(a)

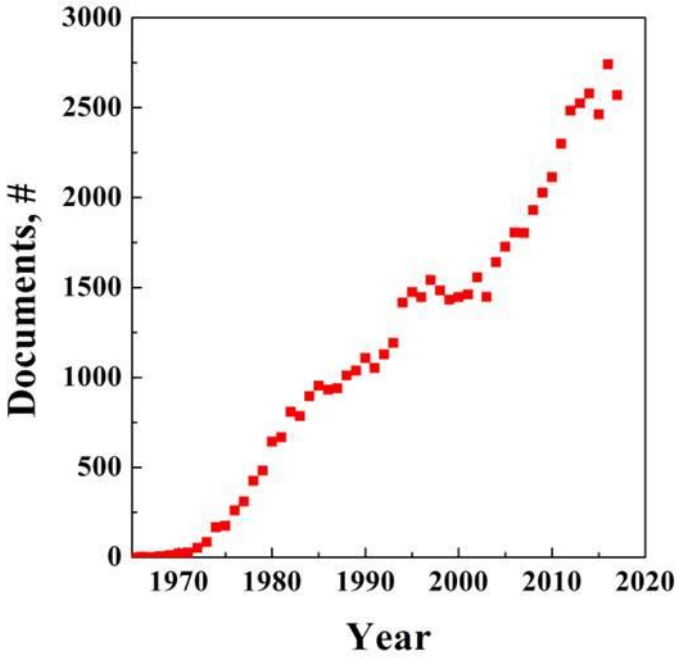

(b)

Figure I.1 *Papers on liposomes published per country (a) and liposomes documents trend over last decades (b). Data obtained by www.scopus.com*

During the last decades, about 2000 papers regarding liposomes and their applications were published each year. The first country focusing on this kind of research is the United States, followed by Japan, Germany, China and United Kingdom. Italy is placed 8th worldwide. The information was obtained from www.scopus.com.

I.3. Classification of liposomes

Liposomes are promising systems for drug delivery, but their morphology and properties can be of fundamental importance, depending on the kind of application. Lipidic vesicles can be classified according to **size** and **lamellarity**. Size means the mean diameter of the liposomes, controlled by different operating conditions and processes; whereas, the lamellarity indicates the number of double layers of phospholipids that surround the inner aqueous core containing the hydrophilic drug.
Regarding their size, liposomes can be classified as follows:

- Single Unilamellar Vesicles (SUV), characterized by only one double layer of phospholipids, with a mean diameter in a range between 20 nm and 200 nm. These are the most powerful vesicles since they can be employed in every kind of human tissue; most of them have nanometrical interstices in which nanosomes can accumulate and be taken up by the cellular barrier.
- Medium Unilamellar vesicles (MUV), with a mean diameter between 200 and 500 nm.
- Large Unilamellar Vesicles (LUV), single lamellae, with mean dimensions of about 0.5-10 µm.
- Giant Unilamellar Vesicles (GUV), a single lamellae and a mean size between 100 and 200 µm, that have been used to study the mechanical properties of lipid bilayers or as cell models for other studies (Akashi et al., 1996).

According to lamellarity, they can be divided into:

- OLV (Oligo Lamellar Vesicles), with less than 5 lipidic layers.
- MLV (Multi Lamellar Vesicles), that have a number of double lipidic layers included between 5 and 20, as if a sort of onion structure. In some cases, the number of lamellae can be greater.
- MVV (Multi Vesicular Vesicles). They are a particular category, since they are made of several lipidic layers externally, but in the inner aqueous core they are made up of other disjointed vesicles. These vesicles are multi-vesicular for this reason, because they seem to be liposomes in other liposomes. More precisely, this kind of vesicle might be called Multilamellar and Multivesicular Vesicles (MLMV). This class can be particularly interesting for the entrapment of different kinds of compound in disjointed inner vesicles, being transported by the same macro liposome (Shaheen et al., 2006).

I.4. Characterization of liposomes

Liposomes need to be characterized before massive production and subsequent administration (Laouini et al.). For this reason, many quality controls must be performed after production (Anwekar et al., 2011). The manipulation of liposomes according to their applications has brought to the production of several characterization protocols. As a consequence, many

techniques over the years have evolved to better measure the characteristics of vesicles (Perkins et al., 1993).
Liposomes suspensions can be translucent or milky, depending on the size of vesicles and concentration of lipids and drug entrapped or not. For this reason, the first important analysis to perform is the visual appearance, to define the **turbidity** of the sample.

The second step consists of measuring the mean size and standard deviation of the liposomes produced. Thus, it is possible to obtain the particle size distribution of the sample so as to have an idea of the order of magnitude of the vesicles. Vesicle size is a crucial parameter to determine the circulation half-life of the liposomes. This characterization is performed with dynamic light scattering. Liposome size also determines the extravasation, meaning the leakage of fluids from blood streams. Tumor capillaries are more permeable than others; for this reason, fluids along with small sized liposomes (at nanometric level) can pass through the gaps and increase drug accumulation directly in the tumor tissue (Sharma et al., 2018). Moreover, liposomes considered for inhalation administration need a strict control of the mean dimension, since it influences the in vivo fate of liposomes together with the encapsulated drug. Moreover, small sized liposomes resulted in an increased blood circulation ability (Woodle and Lasic, 1992). Another method to obtain the mean diameter and particle size distribution of liposomes is Nanoparticle Tracking Analysis (NTA); this technique exploits the properties of light scattering as well as the Brownian motion of colloidal particles in a background medium. Every moving element is detected with a laser and appear as a white spot followed in all its motion. In this way, a concentration of liposomes can be obtained with a good approximation.

The determination of lamellarity means to count the number of double lipidic layers of the vesicles observed. This analysis contributes to classifying liposomes as single lamellar, oligolamellar or multilamellar as well as determine their potential application and efficacy for drug delivery and administration. This operation is performed using transmission electron microscopy for the nanometric dimensions and optical microscopy for the micrometric dimensions. The thickness of each phospholipid double layer is approximately 5 nm (Wen-ChyanTsai and S.H.Rizvi, 2016).

Surface charge is generally used to predict the colloidal stability of liposomes suspended in the aqueous external medium. This measurement cannot be measured directly; for this reason, it is performed with dynamic light scattering (Gibis et al., 2014) to define the surface charge of the liposomes and their possible molecular interactions with other molecules or tissues. It is also called ζ potential, and is calculated using the equation eq. (1):

$$U_e = \frac{2\,\varepsilon\,\zeta\,f}{3\,\eta} \qquad (1)$$

where U_e is the electrons mobility, ε is the dielectric constant in the sample medium, η is the viscosity of the medium and f the function of Henry. Net charges of particle surface affect the distribution of ions within the external double lipidic layer of liposome, that determines the affinity with the drug that needs to be entrapped (Disalvo and Bouchet, 2014). According to surface charge, liposomes are classified as cationic (Barenholz et al., 2011), anionic or neutral (Patil and Jadhav, 2014). Surface charge is an important value to produce the formulation of drugs and assure their efficacy in a human medium. The choice of the bilayer components not only determines the rigidity or fluidity of the drug within the membrane, but also the average surface charge of the liposomes (Sahoo and Labhasetwar, 2003).

Morphology and shape are detected with scanning electron microscopy, with it being able to reproduce the 3-dimensional structure of liposomes. It also gives a confirmation of liposomes size and distribution. Particularly, Transmission Electron Microscope can be used to observe liposomes section to check the circularity of the vesicles, count the number of double layers of the phospholipids and measure their thickness. This can be important in delaying a controlled drug release through many layers of lipids.

Encapsulation efficiency is the percentage of compound used in the process that is effectively entrapped in the inner volume of the liposomes. This means that its complement to 100 is characterized by not entrapped compound, that will be dispersed or dissolved in the aqueous external bulk. This drug will not take part in drug administration; for this reason, it is necessary to entrap as much drug as possible so as to reduce any loss of content. This feature is taken in particular consideration in the case of highly expensive drugs to be administrated. Encapsulation efficiency can be obtained in different manners. The most direct one consists of centrifuging the liposomes suspension and separate supernatant from the vesicles. Then the vesicles are dissolved in an organic solvent to disrupt the lipidic layers (Lopes et al., 2004). The absorbance of the amount of drug diffused in the solvent is measured with an UV-Vis spectrophotometer and the encapsulation efficiency is calculated by eq. (2):

$$EE\ [\%] = \frac{Drug\ Entrapped\ Concentration}{Total\ Drug\ Concentration} * 100 \qquad (2)$$

Another possibility is to indirectly measure the absorbance of the not entrapped compound present in the supernatant, calculated as the complement to 100 % of the percentage of the drug detected in the supernatant (Nii and Ishii, 2005b, Zhao et al., 2015), following eq. (3):

$$EE = \frac{Total\ Drug\ Conc. - Drug\ Conc.in\ the\ Supernatant}{Total\ Drug\ Conc.} \qquad (3)$$

in which the supernatant is the aqueous external bulk in which liposomes are suspended. Working with both methods is always a good way to check the real EE obtained. Encapsulation efficiency or lipid content can also be measured with High Performance Liquid Chromatography (HPLC) (Onyeji et al., 1994), Gas Chromatography, special kits for specific molecules such as insulin (Park et al., 2011) or lactoferrin (Liu, 2013) or enzyme immunoassay (Ramaldes et al., 1996). High entrapment efficiencies are achievable depending not only on the solubility of the drug in the chosen compartment of encapsulation (water for inner core or ethanol/chloroform for lipidic layer), but also on the molecular interaction between the lipids and the drug.

The stability of liposomes is measured through a mean size analysis, scanning electron microscope analysis and encapsulation efficiency tests during fixed intervals of time. Storage temperature mostly affect the stability of lipidic vesicles: particles stored at room temperature (20-25 °C) lose efficacy; whereas, particles stored at -20 °C resulted in an increase of the mean diameter and polydispersity index. Refrigerator temperature (2-4 °C) seemed to be the best condition to maintain the liposomes properties unaltered for months (Ball et al., 2017).

I.5. Drug delivery with natural release mechanism

Liposomes release mechanisms can be natural or artificial. The natural mechanism is strictly linked to the similarity between the vesicle membrane and the cell membrane. Liposomes are attracted to the cell membrane and become part of the cellular barrier. For this reason, the drug can be injected directly inside the cytoplasm of the cell. In this way, liposomes can preserve the drug until they reach the target tissue or cell. These liposomes are the simplest and are recognized to be 1st generation vesicles.

Drug delivery of the liposome can be mainly performed through oral administration, transdermal delivery and systemic delivery. The oral delivery system is highly unstable since the vesicles are subjected to the hostile physiological conditions of the GastroIntestinal tract (GI) of the human body (Li et al., 2011b, Rogers and Anderson, 1998), resulting in low drug bioavailability and short half-life, that leads to the necessity of multiple dose administration per day (Franze et al., 2018). Transdermal delivery is one of the most effective methods for drug delivery using liposomes, that can be applied to most part of hydrophilic and lipophilic compounds. According to this method, the drug can move into the body through diffusion across the layers of the skin (skin penetration) (Doppalapudi et al., 2017).

Intramuscular and sub-cutaneous drug administration (systemic) represent a direct method for liposomal drug delivery that creates a local depot for the absorption process. In this case, only smaller liposomes show a fast diffusion into the lymphatic capillaries; whereas, larger liposomes

remain confined in the site of the injection (Oussoren et al., 1997). Moreover, the lymphatic system is highly exploited by tumor cells and pathogens for the creation of secondary tumors (Poste and Fidler, 1980); for this reason, the sub-cutaneous injection of liposomes containing anti-tumoral drugs could be the best drug delivery system to fight against these illnesses (Oussoren and Storm, 2001).

I.6. Artificial drug release techniques

Clinical diagnostics is characterized by an enormous range of drug molecules, whose list is added to every year. For this reason, one of the most important aims of pharmaceutical industries is to increase the therapeutic index of drugs as much as possible, minimizing the side effects and reducing drug exposure to normal tissues. The main problem of native drug molecules is related to the incapability to deliver therapeutic drug concentrations to target tissues, avoiding any toxic effects. This is particularly true for chemotherapy, that involves tissue treatment with very potent drugs. Normally, only 1% of the intravenously administered drug effectively reaches tumor tissue; the rest is dispersed throughout the whole body, damaging its safety. For this reason, sterically stabilized vesicles and targeted surfaces are the key to avoiding toxic effects during therapies. A new generation of liposomes was founded.

Drug delivery systems such as liposomes are widely used due to their ability to incorporate several compounds of a different nature. To treat a wide variety of illnesses related to cells, intelligent liposomes have been developed that can float in blood streams for a longer time (Voinea and Simionescu, 2002). For this reason, artificial release mechanisms have been created and realized. They are generally induced by external stimuli; for example, a sudden increase of temperature (Temperature Sensitive Liposomes). Some kind of lipids are sensible to temperature variation and can be activated even with a slight increase (0.1 °C). Working with temperature sensitive liposomes, the lipidic membrane can open and release the entrapped drug. In this way, it is possible to activate and stop the release according to patient necessities. Another external stimulus is the pH variation, since the formation of necrotic tissues due to the presence of cancer leads to a different pH value of the cellular environment (Bertrand et al., 2010). In fact, pH-sensitive liposomes can accumulate in the site of action for two different reasons: first, viruses develop strategies to take advantage of the acidification of the tissues to infect cells; second, it was found that such tumors or inflamed areas exhibit an acidic environment when compared to normal tissues (Tila et al., 2015). In detail, if the liposomes are programmed to recognize this variation of pH, they will also easily find a target tumoral tissue without causing dangerous toxic side effects to healthy tissues. Another artificial release is induced by ultrasound

stimulus. This can induce the opening of the lipidic barrier with subsequent drug release. Finally, it is possible to deliver a liposome in which a pharmaceutical compound and Hollow Gold Nanoshells (HGN) or Nanoparticles have been previously entrapped. Gold nanoshells are reactive to near-infrared radiation (Wu et al., 2008). When the targeted cell is reached, an infrared laser goes in resonance with the gold and the double layer opens and works as a trigger for the release of the drug. When the irradiation is stopped, the structure closes and the drug is no longer released. This kind of drug release is called pulsed and should be programmed carefully. Drug concentration must be included in the therapeutic window, above the lower limit (efficacy) and under the upper limit (toxicity). Also ultrasound stimuli or electroporation applying a directly a constant magnetic field (Casciola et al., 2014) that disturbs the integrity of the double lipidic layer and induce lamellae rupture and the consequent drug loss. These systems were considered to be part of the second generation of liposomes.

The third generation of liposomes was obtained with the fabrication of surface modified and engineered lipidic vesicles. Liposomes external surfaces can be decorated with labels such as peptides (Ravikumar et al., 2012), opsonines, antibodies (Papadia et al., 2014) or polymer fragments (Karanth and Murthy, 2007) so as to obtain specific delivery or a long delayed drug release to target tissues. Opsonins are ligands to activate endocytosis in other cell types; whereas, antibodies are used as “homing” devices capable of transforming into a binding element for analytical applications. However, the large number of active groups that can be linked onto liposomes surface are able to favor their binding to their complementary cell receptor; this is known as multivalent effect (Paleos et al., 2016).

One of the most important liposomes drawbacks is the fast elimination from blood, since they are captured by the reticulo-endothelial system, first of them, the liver. For this reason, vesicles were furthermore improved to overcome this problem. Immunoliposomes are vesicles with a modified surface programmed to be digested by macrophages. This plays a fundamental role in keeping human tissues clean. Since artificial liposomes are recognized to be external elements, macrophages tend to eat them. For this reason, liposomes were used as Trojan horses to be digested by macrophages (Jain et al., 2013). During the digestion, the vesicles are dissolved and the drug is transferred to target tissues through the macrophages. For this reason, the immune response of the human body is exploited. Long circulating immunoliposomes are able to recognize and blind target cells with great specificity, especially for anti-cancer therapy (Benech et al., 2002).

Long-Circulating liposomes can be prepared by coating their surface with PolyEthylene Glycol (PEG). This modification can be obtained by absorbing the polymer physically on the surface of liposomes or by chemical reaction

between lipids and polymer fragments. The presence of PEG filaments can improve drug distribution in target tissues. PEG also avoids vesicles attraction (Van Der Waals forces) and aggregation phenomena, thus improving their stability (Immordino et al., 2006). Another important characteristic of the PEG link to liposomes is their improved half-life, resulting in longer circulating times in humans. Long circulating vesicles can detect occult inflammations, demonstrating a high potential for all the alternative drug delivery systems (Crommelin et al., 1999).

I.7. Methods of production

There was a global welcome of liposomes as drug carriers for medical and nutraceutical applications, but they joined the market with many difficulties, linked to the low encapsulation efficiencies of compounds, low reproducibility and high cost of production and scale up. These were the main problems of the conventional methods developed from 1965 up to 2000. Especially for pharmaceutical and clinical uses, an appropriate formulation of liposomes should follow very strict production criteria depending on the size, zeta potential, morphology and stability. For example, it was discovered that liposomes smaller than 70 nm are taken up by liver parenchymal cells, whereas vesicles larger than 300 nm tend to accumulate in the spleen (Liu et al., 1992). Micrometric liposomes have a very limited bioavailability because they are larger than the cells where they should be taken up.

Over the last two decades, supercritical assisted methods of production were proposed to overcome the problems found in the conventional methods, such as the entrapment efficiency, reproducibility, reduction of the solvent residue and mean dimensions of the vesicles. Nonetheless, the control of particle size distribution particularly at nanometric level was still a challenge.

Conventional and supercritical assisted methods are described in detail in the following paragraphs, including their advantage and disadvantages.

I.7.1 Conventional methods

Liposomes can be prepared from several kinds of phospholipids, using them singularly or with lipidic mixtures, with the eventual addition of cholesterol. In particular, phosphatidylcholines are the most often used because they are amphiphilic molecules characterized by two carbon chains linked by a glycerol bridge and a hydrophilic polar head. They can be derived both by natural and synthetic sources. Phosphatidylethanolamine has a different tendency to form hexagonal micelles, whereas phosphatidylserines may be responsible for packing irregularities and instability (Suetsugu et al., 2014a). The mixing of phospholipids can be

responsible for the permeability of the lipidic double layer, as well as their lipid chain melting temperature. This means that an increased temperature may induce drug delivery after lipidic membrane melting (Ulrich, 2002). The addition of cholesterol is recognized to be responsible for lipid permeability reduction (Cathcart et al., 2015, Collins and Phillips, 1982).

Conventional techniques for liposomes production generally consist of 4 main steps: drying of lipids from organic solvents, dispersion of the lipids in an aqueous medium, purification of obtained liposomes and eventual post-processing steps such as probe or bath sonication or extrusion (Mozafari, 2005a).

I.7.1.1 Thin Film Hydration

Also known as the Bangham method, Thin Layer Hydration (TLH) is considered the earliest liposomes preparation method; it is also particularly simple because it can be performed at room temperature and at atmospheric pressure. According to the Thin Layer Hydration method, lipids are first dissolved into a chloroform solution; the hydrophilic drug is dissolved into an aqueous bulk. The organic solvent is evaporated at 30 °C for 30 minutes, under vacuum and a thin lipid layer is formed on the walls of the glass flask. The lipidic layer is then hydrated using the aqueous solution under gentle agitation (250 rpm). After 1 hour of agitation, liposomes are formed and analyzed. The removal of the organic solvent may have a different duration, depending on the kind of solvent employed. This method produces liposomes of 10-100 μm, not easily absorbable by human cells; for this reason, this method is generally coupled with sonication to obtain smaller mean dimensions. The encapsulation efficiencies are as low as 20-30 % and the shape of the liposomes produced is not in all cases spherical; an ellipsoidal shape and sphericity can be calculated observing vesicles populations obtained with conventional methods (Imura et al., 2003b). Despite all these limitations, this method is still one of the most widely used (Lesoin et al., 2011a).

I.7.1.2 Ethanol Injection method

The ethanol (or ether) injection method involves the dissolution of the lipid into an organic phase, followed by the drop wise injection of the lipid solution into an aqueous media (Santo et al., 2015). A fine needle is used to inject the lipidic solution into the water bulk containing a hydrophilic drug. This method is very simple because it works in the absence of pressure, but high solvent residue is present in the final suspension, and the removal of ethanol is difficult since it forms an azeotropic mixture in direct contact with water (Meure et al., 2008). Moreover, the evaporation step risks damaging the vesicle structure and alter their dimensions. For this reason, the

population of the liposomes produced is generally heterogeneous and its particle size distribution is difficult to control. Encapsulation efficiencies are lower than 20 % for hydrophilic compounds and around 60 % for lipophilic molecules (Jaafar-Maalej et al., 2010).

I.7.1.3 Emulsion method

There are several versions of the emulsion method. One of these, implies that phospholipids are dissolved into an organic solvent and mixed with a solution to form a water in oil emulsion. The mixture is then added to another water solution to form a double emulsion w/o/w (Nii and Ishii, 2005b). The organic solvent is then evaporated, generating liposomal aqueous suspension. This method does not work continuously, and the production volumes are limited (10, 20 and 150 mL for water, oil and water solutions respectively). Micrometric and multivesicular liposomes are obtained this way. Large amounts of organic solvent need to be eliminated.

I.7.1.4 Reverse phase Evaporation Vesicles (REV)

This technique is based on the formation of water droplets surrounded by lipids and dispersed in an organic solvent to form a Water in Oil (W/O) emulsion. Since phospholipids behave as surfactants, they rearrange at the interface between oil and water, creating inverted micelles. Then, the solvent is eliminated slowly and the micelles are converted into a gel form. The gel state collapses and the excess of phospholipids in the environment creates a second layer of lipids around the first inverted one. The formation of a complete bilayer around the residual micelles results in the formation of liposomes. Among the disadvantages of this technique, there is the long-lasting contact between the drug and organic solvent, that can lead to drug denaturation in case of fragile compounds such as proteins and peptides. An encapsulation efficiency variable from 30 to 65% is obtained from this technique (Szoka and Papahadjopoulos, 1978).

I.7.1.5 Freeze drying

This method consists of the homogeneous formation of a dispersion of lipids in water soluble carrier materials. The first step is the dissolution of the lipids in tert-butyl alcohol and water-sucrose to form an isotropic monophase solution and then the freeze dying of the solution. Freeze drying is characterized by two main steps; first, the sample is freezed at -40 °C for a time of 8 hour, followed by a second longer time of drying at room temperature. Upon adding water, the lyophilized system spontaneously form lipidic spherical vesicles (Li and Deng, 2004). The presence of sucrose can prevent the formation of aggregated minidomains during the drying steps.

The mean dimensions of the liposomes are between 100 and 300 nm. Encapsulation efficiency is between 40 and 60 %, but the storage stability is no more than 60 days (Yang et al., 2013).

I.7.1.6 Microfluidic channel method

This method consists of the development of a rigid silicon support in which microfluidic channels of 100 µm in depth have been previously designed and printed (Jahn et al., 2007), with a tendency to fuse and aggregate, and low stability. The cost of the production of the micro-circuit is higher than other conventional methods. A lipidic solution is injected into the central feeding channel, whereas aqueous solutions are fed from side channels, that intersect the central channel at the center of the support. In the outer channels, liposomes are created. Monodisperse suspensions of liposomes are obtained optimizing water to the lipid ratio. Nanometric liposomes are obtained, and a decrease of liposome diameter is obtained by increasing the flow rate feeding ratio. This method risks containing high levels of solvent residue in the final liposomes suspensions. This method has also been used to entrap bacteriophage agents into liposomes (Leung et al., 2018), with encapsulation efficiencies up to 50%.

I.7.1.7 Heating method

The heating method (Mozafari et al., 2002) is very simple regarding the production of liposomes. It does not involve the use of organic solvents. Phospholipids are added to an aqueous solution together with 3% v/v glycerol and the temperature of the batch is increased up to 120 °C. Glycerol is water soluble and is an isotonic agent able to increase the stability of lipid vesicles, preventing any coagulation and agglomeration phenomena. Lipids are not subject to high temperature degradation with this technique. Moreover, the sterilization step is not needed. The liposomes produced have nanometric dimensions, a long-term stability (12 – 14 months) but quite low encapsulation efficiencies (12 – 54 %) (Colas et al., 2007).

I.7.1.8 Hollow fiber membrane contactor

Membrane contactors have already been applied to the preparation of emulsions, precipitates, polymeric and lipid particles. For the preparation of liposomes, the principle of the membrane contactor is used with a hollow fiber module (Laouini et al., 2011). An aqueous medium in which a drug has been dissolved is pumped in a hollow fiber module. The organic phase containing lipids is set in a pressurized vessel (1.8 – 5 bar) with nitrogen. Bubbling in the vessel, nitrogen transports the lipidic solution to the hollow fiber; lipids permeate through a membrane directly into the aqueous phase

and liposomes are spontaneously obtained. The process works at room temperature in batch mode and the feeding tanks need to be refilled at the end of the experiments. Moreover, at the end of the production, the hollow fiber module needs to be regenerated and washed with a water/ethanol solution.

I.7.2 Supercritical assisted methods

After the diffusion of the concept of green chemistry in the early 1990s, the interest in supercritical fluids grew exponentially (Zhong and Dai, 2011). With the development of high technology disciplines and biotechnology, academics transferred their newest knowledge to industrial enterprises for the development of novel methods of production on large scale. These methods have been proposed taking the advantage of an enhanced mass transfer coefficient of supercritical fluids. This was obtained working at high pressures, involving an increasing level of risks and cost, especially in the aim of scaling up from laboratory to industrial level.

I.7.2.1 Depressurization of an Expanded solution into an aqueous medium (DESAM)

According to this method, (Meure et al., 2009) lipids are dissolved in ethanol. Then, working at a pressure of 35-55 bar, the solution is expanded into carbon dioxide and injected into a water bath in a vessel and left bubbling for at least 1 hour. Working during this time at the temperature of about 75 °C, part of the ethanol is evaporated. A hydrophilic compound can be previously dissolved in water and receives the expanded liquid containing the lipids. Lipids transported by bubbles and water containing drug are in contact and produce liposomes. The ethanol content is reduced to 2.2 % v/v, that is still too high to guarantee safety and biocompatibility of the drug carrier. The nanometric dimensions of the liposomes are obtained with a good stability over a period of 8 months. The main problem of this method is related to the low encapsulation efficiency of hydrophilic drugs, that is about 30 %. This means that most of the drug dissolved in the water solution remains in the external bulk, resulting in huge wastes of drug and high production costs.

I.7.2.2 Supercritical fluid method

This system is characterized by two parts: the high-pressure part is used to dissolve lipids and cholesterol in supercritical carbon dioxide at the pressure of 250 bar; whereas, in the low-pressure part, the homogeneous supercritical solution is expanded with the addition of 7 % v/v ethanol at the temperature of 60 °C. The expanded liquid is then mixed with (Frederiksen

et al., 1997) a water phase to obtain liposomes encapsulating a water soluble compound. Only 3 % of the vesicles are subjected to degradation and the mean diameter is about 200 nm, whereas the particle size distribution is generally bimodal. The encapsulation efficiency of the hydrophilic compounds is particularly low (15 %). The total amount of ethanol content is 15 times lower than the ethanol injection method.

I.7.2.3 Supercritical Anti-Solvent method

The organic solvent containing phospholipids is spayed continuously in the supercritical CO_2, that act as an anti-solvent. The dissolution of supercritical carbon dioxide in the liquid phase and the subsequent evaporation of the organic solve leads to the precipitation of the lipidic particles. A washing step with pure carbon dioxide is performed to remove any excess organic solvent. Finally, these particles are hydrated in an aqueous buffer to obtain liposomes (Lesoin et al., 2011c). SAS is a green process that is able to produce nanometric or micrometric liposomes, depending on the kind of application needed. The encapsulation efficiency is similar to the thin layer hydration method, but the sphericity of the lipidic particles is highly improved. The particles size distribution is more controlled and repeatable; the liposomes are also more stable.

I.7.2.4 Rapid Expansion of a Supercritical Solution (RESS)

According to this method, lipids are dissolved in supercritical carbon dioxide; generally, 5-10 % v/v ethanol is added to favor the dissolution phenomena. The solution is then released through a small orifice and mixed with an aqueous solution containing the drug. A rapid depressurization follows; the pressure drop results in the desolvation of the lipids forming layers around the droplets (Imura et al., 2003a). However, this method has some problems such as the difficult separation between the lipid particles and co-solvent during depressurization. Even if the mean diameters of the liposomes are included between 130 and 190 nm and the particle size distributions are monodispersed, the encapsulation efficiencies are still a challenge.

I.7.2.5 SuperCritical fluid Reverse Phase Evaporation (SCRPE)

This technique is similar to the conventional Reverse phase Evaporation Vesicles; the techniques differs in the use of supercritical carbon dioxide in substitution of the organic solvent (Otake et al., 2001). Lipids are put in contact with SC-CO_2 in a view cell in batch mode, reaching the temperature of 60 °C and the pressure in a range of 12-30 bar. After reaching the equilibrium of the system, an aqueous solution including glucose is slowly

inserted into the vessel with a precision pump and large unilamellar lipidic vesicles are obtained. Working under these conditions, the liposomes produced have a mean diameter between 200 and 1200 nm; whereas, decreasing the lipid concentration, the mean diameter decreases to 100-250 nm. The average encapsulation efficiency is 10 %. A lower depressurization rate could be used to obtain higher encapsulation efficiencies but also higher mean dimensions (Otake et al., 2006).

I.7.2.6 Particles from gas saturated solution (PGSS)

This method consists of dissolving a bioactive compound in an organic solvent; then, supercritical carbon dioxide is introduced into the solution. After saturation is reached, this solution is sprayed through a nozzle into a high-pressure vessel. Liposomes are formed and a rapid depressurization of carbon dioxide eliminates the solvent, leaving supercritical conditions (M. J. Cocero et al., 2009, de Paz et al., 2012). The saturation temperature is 100-130 °C at the pressure of 80-100 bar; the liposomes produced have a mean diameter of 1-5 µm and the encapsulation efficiency is about 60 %.

I.8 Comparison among liposome methods of production

A comparison of the operating conditions, the number of steps of production, average mean diameters produced, average encapsulation efficiency, stability of the vesicles over fixed times of observation and solvent residue have been summarized. The characteristics of conventional and dense gas techniques have been summarized in **Table I.1**.

Table I.1 *Summary of liposomes production methods compared with SuperLip technology*

Method	Operating conditions	steps	Average Mean diameter	Encapsulation efficiency	Stability	Solver Residue
Bangham	20-25 °C, 1 bar	2	10-100 µm	10-20 %	low	high
Ethanol injection	40-60 °C, 1 bar	One-shot	100-300 nm	16 %	---	40000 ppm
Emulsion method	20-25 °C, 1 bar	2	variable	50 %	---	high
Hollow fiber membrane contactor	1.8-5 bar, 20-25 °C	2	110-230 nm	93 %	2-3 months	---
Reverse Phase Evaporation	20-25 °C, 1 bar	2	variable	30 - 65 %	---	high
Heating method	20.25 °C, 120 °C	One-shot	200-300 nm	12-54 %	12-14 months	none
Freeze drying method	-40 to 25°C, 1 bar	3 steps	100-300 nm	44-62 %	2 months	---
Microfluidic channel	25 °C, 1 bar	One-shot	100-200 nm	50 %	---	high
Supercritical Reverse Phase evaporation	60 °C, 12-30 bar	One-shot	100-1200 nm	10 %	---	---
RESS	31 °C, 74 bar	2	130-190 nm	low	---	low
DESAM	25-55 bar, 75 °C	2	200 nm	29 %	8 months	2.2 % v/v
Sup.Flu method	250 bar, 60 °C	One-shot	200 nm	15 %	---	1/15 of ethanol injection
SAS method	90-130 bar, 35 °C	2 steps	0.1-100 µm	20 %	---	low
PGSS	100-130 °C, 80-100 bar	2	1-5 µm	60 %	---	low

Chapter II
Objectives of this work

Considering the papers reported in current literature, it appears that additional work is required to improve the technologies based on supercritical fluids and, generally speaking, to produce liposomes. These kinds of processes still have limitations related to the control of liposomes dimension and size distribution, especially at nanometric scale, batch or semi-continuous layout and also show very low encapsulation efficiencies. For these reasons, the **MAJOR SCOPE** of this PhD thesis is to develop and optimize a new continuous supercritical CO_2 based process, so as to produce liposomes to be used mainly in pharmaceutical and biomedical field. In order to overcome the major drawbacks of the other preparation methods, it is necessary to change the order of the process steps involved in liposomes production. Differently from the previously proposed processes, the idea at the basis of this new process is to first produce water-based droplets and, then, form liposomes around them. To obtain this result, it was decided to atomize water directly in a near supercritical solution in which phospholipids are dissolved.

The key process of SuperLip (Supercritical assisted Liposome formation) consists of the creation of water droplet containing the drug, followed by a fast surrounding of a double layer of phospholipids. The main steps of the SuperLip process are presented in **Figure II.1**.

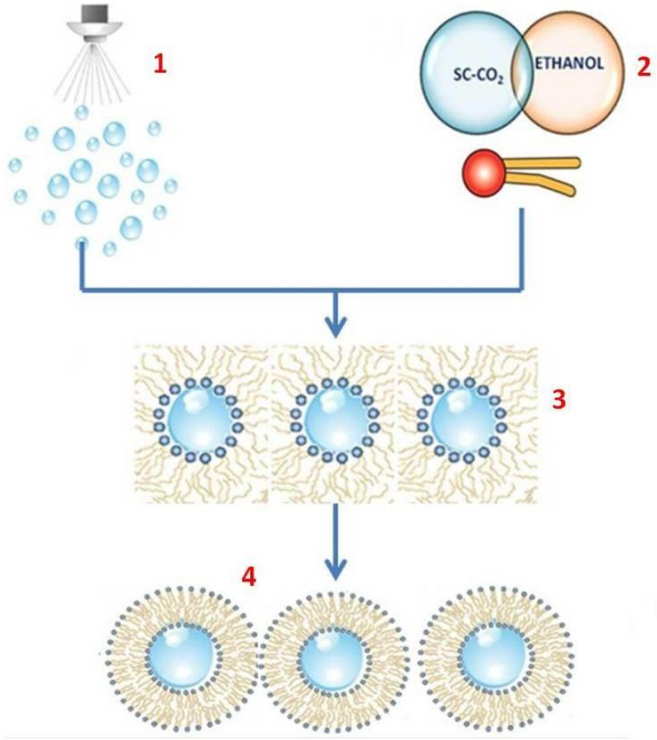

Figure II.1 *A scheme of SuperLip mechanisms involved in the formation of liposomes*

As described in the figure, water droplets are atomized in a high pressure formation vessel (1); whereas, an expanded liquid of ethanol and carbon dioxide transports phospholipids to the formation vessel (2). Subsequently, a first layer of lipids surrounds the water droplets, creating inverted micelles (3); then, a second layer of lipids is created around the micelles (4). A diagram of the proposed phenomena is reported in **Figure II.2**.

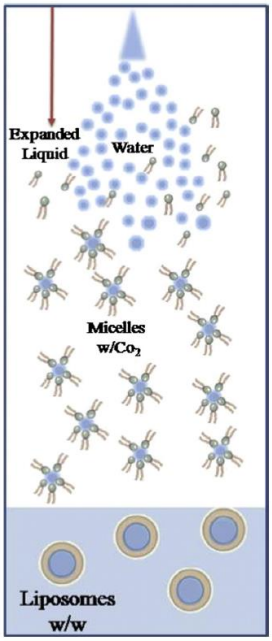

Figure II.2. *Mechanisms hypothesized for the SuperLip process*

Some preliminary tests were successfully performed, confirming the high potential of this technique at a micrometric dimension (Santo et al., 2014). Feasibility tests revealed that the spontaneous organization of liposomes in the high-pressure vessel is fast enough to allow for the formation of micrometric/sub-micrometric liposomes. The first experimental evidence obtained also seems to indicate that the mechanism of liposomes formation is related to favourable interactions between the expanded liquid phospholipid mixture and the water droplets: water-based droplets are rapidly surrounded by a layer of the lipids dissolved in the expanded liquid and a water in CO_2 emulsion is formed. The obtained liposomes maintain a diameter similar to the original droplets produced during the atomization step. High water soluble drug entrapments are confirmed by the measured encapsulation efficiencies, around 80%.

Therefore, the **aim of this thesis** is to orientate this proof of concept towards a process applicable on large scale. Intense research is required to reach this ambitious goal.

The effect of several process parameters will be studied such as water flow rate, injector diameter, pressure and the Gas to Liquid Ratio of the Expanded Liquid (GLR-EL), i.e. the mass ratio of the carbon dioxide and ethanol flow rate. The composition of liposomes will be varied, changing the phospholipid concentration and adding other lipids in the double lipidic layer such as cholesterol.

Several liposome-based product formulations will be developed, according to the operating parameters previously optimized. Antibiotics for ocular delivery, proteins and markers for molecule labeling will be entrapped into liposomes for pharmaceutical purposes. Then, cosmetic applications will be explored, encapsulating antioxidant compounds of a hydrophilic and amphiphilic nature. Amphoteric compounds will be entrapped either in the inner core, or in the lipidic layer of liposomes so as to study the differences in the antioxidant inhibition power, depending on the vesicles compartment of encapsulation. Dietary supplements will be also entrapped for food applications, in order to valorize the by-products that generally are discarded from the agro-alimentary field. A novel textile application will be also proposed for the deposition of dye on leather fragments. *In vitro* studies will be also performed with antibiotic loaded liposomes against *E.Coli*.

An economic and financial analysis on the SuperLip technique will be performed. SuperLip has a Technology Readiness Level (TRL) of 6/7, since it has been designed in a continuous lab-scale configuration and it is possible to scale it up to industrial level. The SuperLip method can produce about 5 liters of liquid liposomes suspensions per day, working at lab-scale. The idea at the basis of the process has already been validated by product development and samples characterization, as reported in our published works. The potential applications of SuperLip has always been recognized by external customers, interested in the production of liposomes on demand. A business plan for the commercialization of SuperLip products will be attempted to verify whether the production of liposomes with this technique could be profitable in the markets. A B2B model and an estimation of CAPEX and OPEX will be performed to produce a 5-years (2018-2022) prospective for commercialization.

Chapter III
Plant, materials and methods

***Note**: in this chapter a full description of the process layout has been provided, as well as the methods and the materials involved in the SuperLip process. However, the experimental protocol is confidential and protected by industrial secrets.*

Chapter III

III.1 Apparatus

Liposomes were prepared using the SuperLip technology. The apparatus consists of three different feeding lines for the delivery of CO_2, water and ethanol-phospholipids solution respectively.

CO_2 is taken from a reservoir (1) and delivered to the homogenizer using a membrane pump (Lewa Eco model LDC-M-2, Germany). The ethanolic solution and the water phase are pumped using two different precision pumps (Gilson model 305, France).

The ethanol solution and CO_2 are continuously fed to the stainless steel homogenizer (Swagelok, 150 cm3, Pmax 5000 psig, USA) forming an expanded liquid. The mixing of the two components occurs at a fixed Gas to Liquid Ratio of the Expanded Liquid (GLR-EL).

The homogenizer (2) is heated using band heaters (Watlow Thinband, 240 V, 140 W, Italy) and contains stainless steel packings (Sigma Aldrich, ProPak, 1889 m^{-1} specific surface, 0.94 void degree, Italy). The packing elements allow for an intimate mixing among the ethanol solution and CO_2, producing the expanded liquid, that is, then, delivered to the precipitation vessel. In the same vessel, water (or a water solution in the case of loaded liposomes) is atomized through a nozzle with a 80 μm internal diameter. The atomization and the delivery of the expanded liquid is co-currently performed.

The precipitation vessel (3) is a high-pressure stainless steel cylinder, with an internal volume of 1600 cm^3. It is thermally heated using heating bands (Watlow, Thinband 240 V, 800 W, Italy).

At the exit of the precipitation vessel, a smaller stainless steel cylinder (4) (Compliant Sample Cylinder, ¼ in, FNPT, internal volume 150 cm^3, 5000 psig, 344 bar) is used to allow for the accumulation and homogenization of the suspension produced during the experiment. The suspension is collected at fixed time intervals using an on-off valve.

A separator (5) is located downstream the precipitation vessel and is used to recover CO_2 and ethanol after depressurization. The separator is a stainless steel vessel with a 330 cm^3 internal volume, in which the pressure is regulated using a backpressure valve (model 26-1723-44, Tescom, Italy). A micrometric valve is also located on the CO_2 vent line for a fine regulation of the pressure in the precipitation vessel. A rotameter and a dry test meter are used to measure the CO_2 flow rate.

A first scheme of the SuperLip apparatus is shown in **Figure III.1**.

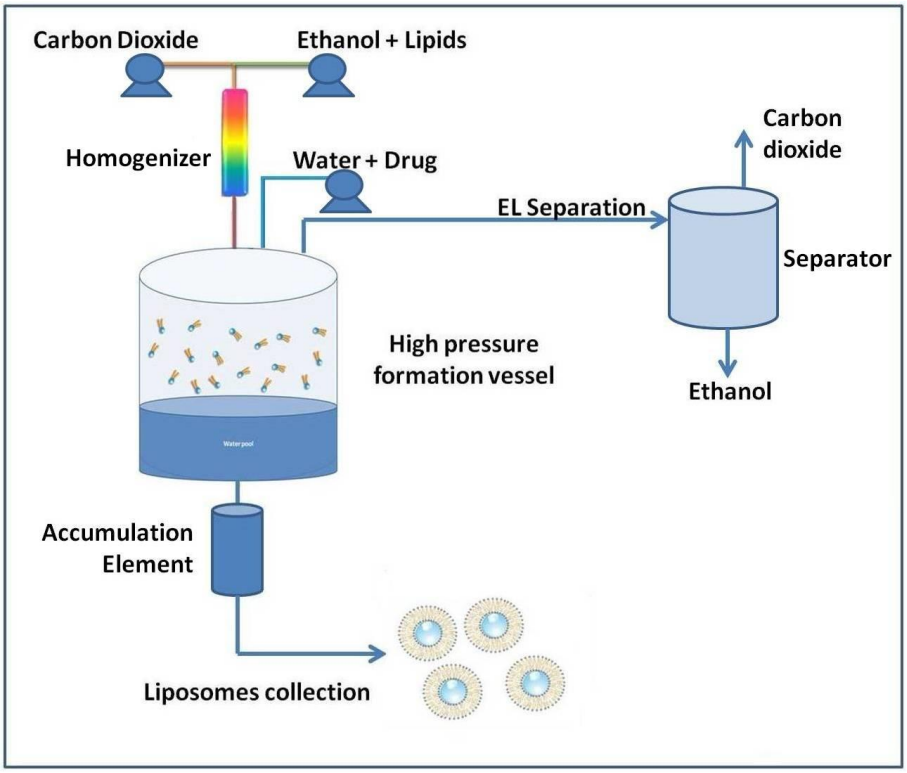

Figure III.1 *SuperLip process layout scheme*

In summary, the SuperLip apparatus consists of four main steps:

Homogenizer (**Figure III.2**): in this part of the plant the formation of the expanded liquid, characterized by the system ethanol–CO_2–phospholipids, takes place. Then, the expanded liquid is fed to the precipitation vessel.

Figure III.2. *Homogenizer element*

High pressure formation vessel (**Figure III.3**): in this part of the apparatus the droplets come into contact with the expanded liquid formed in the homogenizer.

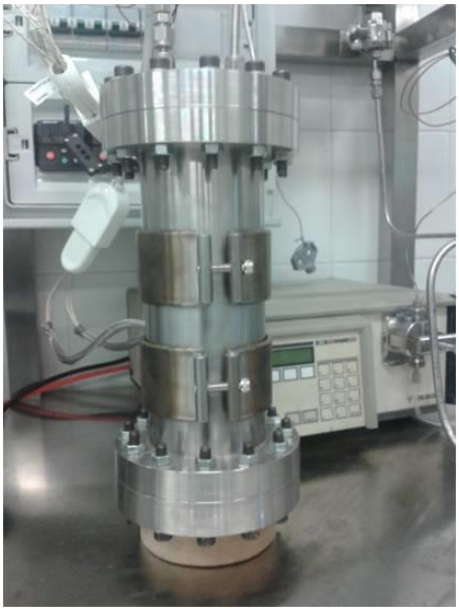

Figure III.3. *High pressure formation vessel*

Atomization: a nozzle (**Figure III.4**) located at the top of the precipitation vessel allows for the formation of water droplets.

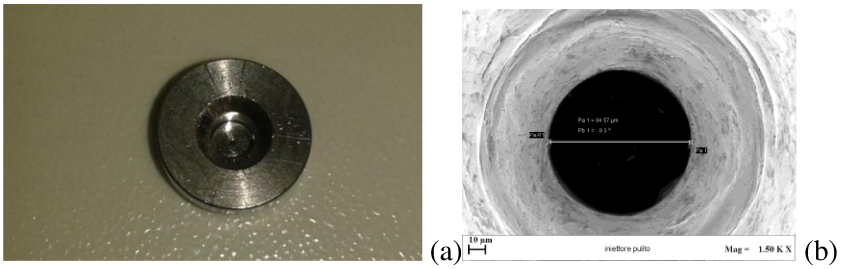

(a) (b)

Figure III.4. *Injector for water atomization from macroscopic (a) and microscopic (b) observation*

Suspension recovery: the produced suspension is withdrawn at fixed time intervals from an accumulation element (**Figure III.5**).

Figure III.5. *Accumulation element*

Separator (**Figure III.6**): the solvent, used for the expanded liquid formation, is recovered after depressurization.

Figure III.6. *Separator*

Finally, a photograph of the SuperLip apparatus is presented in **Figure III.7**.

Figure III.7. *SuperLip apparatus*

In **Table III.1** the construction properties of the SuperLip elements are summarized.

Table III.1 *SuperLip main plant units*

Unit	Internal Diameter [cm]	Height [cm]	Internal volume [cm^3]
Homogenizer	4.5	17.5	150
Formation vessel	9	25	1600
Separator	6.5	10	330
Accumulation	4.5	17.5	150

III.2. Materials

L-α-Phosphatidylcholine (PC) from egg yolk (99 % pure) was purchased from Sigma-Aldrich, Milan, Italy. The hydrophilic, amphoteric and lipophilic compounds presented in this work were all bought from Sigma Aldrich, Milan, Italy. The lipids were stocked in absence of light at the temperature of -20 °C before the experiments.

Phospholipids were dissolved in ethanol bought from Sigma-Aldrich, Milan, Italy (> 99.8% pure). Carbon dioxide was provided by Morlando Group, Naples, Italy (> 99.4% pure, at gas-liquid equilibrium). Distilled water was self-produced through a lab-scale distillator.

For the antioxidant activity, Folin & Ciocalteu's phenol was purchased from Sigma Aldrich (Milan, Italy).

Regarding olive pomace extract, anti-bodies and E.Coli, they were given by the Department of Civil, Chemical and Environmental (DICCA) Engineering of the University of Genoa, Italy.

Antibodies Mouse IgG Isotype Control (Catalog Number 02-6502) were used for liposomes entrapment in the inner core. The antibody was provided in liquid PBS form at the concentration of 2.5 mL/min in a purified form.

All the materials and reagents were used as received.

III.3. Methods

The **morphology** of the produced liposomes was studied using a Field Emission-Scanning Electron Microscope (FESEM mod. LEO 1525; Carl Zeiss SMT AG, Oberkochen, Germany). The samples were prepared spreading a drop of liposome suspension over an adhesive carbon tab placed on an aluminum stub. The drop was left to dry at air over-night. The sample was, then, covered with gold, using a sputter coater (thickness 250 Å, model B7341; Agar Scientific, Stansted, UK).

A **dynamic laser scattering** (DLS) instrument (mod. Zetasizer Nano S, Worcestershire, UK) was used to measure the particle size distribution (PSD), mean diameter (MD), standard deviation (SD), and zeta potential of the liposomes. The suspension was analyzed as produced, without any dilution step or addition of stabilizing agents. Three measurements of the same sample were performed for all the produced suspensions.

Nanoparticle tracking analysis (NTA) was also used to provide complementary information about the liposome size distribution. In particular, this technique, thanks to the possibility of the on-line monitoring of liposomes in suspension, provides information about liposome concentration in the sample. A laser beam is used to irradiate the sample. The particles in suspension scatter the light and can be visualized via a long working distance microscope onto which a video camera is mounted. The camera captures a video file of the particles moving under Brownian motion. In this way, the Nanoparticle Tracking Analysis (NTA) software tracks many particles individually, providing an evaluation of the concentration of the sample.

The NTA measurements were performed using a NanoSight LM20 (NanoSight, Amesbury, UK), equipped with a sample vessel and a 640-nm laser. The samples were injected into the vessel using sterile syringes (BD Discardit II, New Jersey, USA) until the liquid reached the tip of the nozzle. All the measurements were performed at room temperature. The data were analyzed using NTA 2.0 Build 127 software. The samples were measured for 40 s with manual shutter and gain adjustments. Three measurements of the same sample were performed for all the produced suspensions.

To determine **encapsulation efficiency**, the procedure of evaluation of the drug leakage was adopted, as reported in current literature (Nii and Ishii, 2005a). The liposome suspension was centrifuged at 6500 rpm for 45 minutes at 4 °C. Then, the concentration of the drug in the water supernatant was analyzed using UV-Vis spectroscopy, at the wave length of 515 nm. The encapsulation efficiency (EE) was calculated as the complement to 100% of the percentage of drug present in the supernatant. Each encapsulation efficiency test was repeated in triplicates, and the results are the mean over 3 different measurements.

Several hydrophilic, amphoteric and lipophilic compounds were entrapped into liposomes and their encapsulation efficiencies were obtained with UV-Vis spectrophotometer. In **Table III.2** a list of this compounds with their absorbance peak is reported.

Table III.2 *List of the entrapped compounds whose encapsulation efficiency was detected using Uv-Vis spectrophotometer*

Compound	Peak of UV-Vis absorbance [nm]
Fluorescein	515
Red Aniline	500
Bovine Serum Albumin	280
Albumin fluorescein isothiocyanate	280; 515
Ofloxacin	290
Theophylline	275
Ampicillin	225
Amoxicillin	280
Vancomycin	230
Eugenol	280
Linalool	220
α-lipoic acid	325
Limonene	270
Farnesol	260

The **antioxidant activity** of extracts entrapped into liposomes was measured in terms of hydrogen-donating or radical-scavenging ability by means of the radical 2,2-diphenyl-1-picrylhydrazyl (DPPH•). In detail, 0.0197 g of DPPH were dissolved in 500 mL of ethanol to obtain a 10-4 M DPPH in ethanol solution. 0.01 g of the antioxidant compound was dissolved in 1000 mL pure water to obtain a 100 ppm concentration. From this solution, 4 diluted solutions were obtained (50, 20, 10 and 5 ppm). 1 mL of each diluted sample was mixed with 3 mL of DPPH in ethanol solution.

The mixed solutions were stored in glass vials for 30 minutes and incubated in the dark. Then, a micro-volume UV-Vis spectrophotometer as described above was used to measure the absorbance of the solutions at the wavelength of 517 nm (Brandwilliams et al., 1995). The absorbance at 517 nm of DPPH in ethanol was also measured. A reference sample was prepared with 1 mL of pure water mixed with 3 mL of pure ethanol. Liposomes suspensions were ultra-centrifuged at 13000 rpm for 50 min at -4 °C and the pellet was separated from the supernatant. The pellet was then dissolved in ethanol and the DPPH method was applied. The DPPH inhibition percentage was calculated according to eq. (4):

$$Inhibition\ [\%] = 100 * \left(1 - \frac{A_a}{A_b}\right) \quad (4)$$

where A_a is the absorbance at 517 nm of the sample treated with DPPH in ethanol solution, and Ab is the control absorbance at 517 nm of DPPH in ethanol. The inhibition percentage obtained in this way was compared to the one of pure unprocessed samples percentage, to calculate the decrease of the DPPH inhibition capacity between the unprocessed and processed samples.

Transmission electron microscopy, TEM, (JEOL 1400, 100 kV accelerating voltage) was used with negative staining to investigate the morphology and size of the liposomes produced. For the preparation of the samples, a droplet of liposome suspension was placed on a copper grid and allowed to sit for 60 s. The droplet was then dried with filter paper. A droplet of staining agent was subsequently placed on top of the grid and left reacting for 30 s, the excess was then removed with filter paper.

Theophylline **drug release test** at 37 °C were studied using a UV-Vis spectrophotometer. The drug profiles were determined in 80 mL of distilled water continuously stirred at 100 rpm. For each study, 5 mL of theophylline loaded liposome suspension were charged in a dialysis sack (MWCO 3500 Da, Sigma Aldrich, Milan, Italy). Every 30 minutes, the absorbance of theophylline in the aqueous external bulk was measured, drug release tests were performed in triplicates and the curves proposed in the results are the mean profile obtained.

The amount of Chol entrapped in the lipidic double layer was measured with **Gas Chromatography** (GC) assay (GC-FID, mod. 6890 Agilent Series, Agilent Technologies Inc), according to the method reported in current literature (Lozada-Castro and Santos-Delgado, 2016). For the preparation of the samples, a defined volume of liposome suspension was centrifuged for 50 min at -4 °C, then the pellet was re-suspended in 3 mL of hexane and gently agitated for 30 min. Finally, 2 µL of this solution were used for GC analysis.

Leather fragments were characterized by **Energy-Dispersive X-ray spectroscopy** (EDX) microanalysis. An elemental analysis and element mapping were performed using the FE-SEM equipped with an Energy Dispersive X-ray spectroscopy (EDX-INCA Energy 350, Oxford Instruments, Witney, United Kingdom).

Color measurements were carried out on a leather fragment surface using a colorimeter CIE-Lab (Chroma Meter II Reflectance CR-300,

Minolta, Japan), equipped with a CIE standard D65 illuminant. Color redness a* values were recorded and compared in the Results section.

Solvent residue was measured using a head space sampler (mod. 50 Scan; Hewlett & Packard, Palo Alto, California) coupled with a Gas Chromatograph interfaced with a Flame Ionization Detector (GC-FID; mod. 6890 Agilent Series; Agilent Technologies Inc., Wilmington, Delaware). Ethanol was separated using a fused-silica capillary column of 50 m in length, with a 0.25 mm internal diameter and 0.40 µm film thickness (mod. DB-WAX; Agilent, United States). The GC oven temperature was set at 40 °C and maintained constant for 8 min. The injector was maintained at 180 °C (split mode, ratio 1:1) and helium was used as the carrier gas at a flow rate of 1 mL/min. The head space conditions were: equilibration time of 60 min at the temperature of 100 °C, pressurization time of 2 min and loop fill time of 1 min. The analyses were performed on each sample in triplicates.

Water in Oil (W/O) **emulsions** preparation procedure: emulsions were prepared following this standard procedure: the water phase was obtained dissolving 0.18 g of surfactant Tween 80 in 90 mL distilled water and the solution was stirred with a magnetic stirrer at 250 rpm for 30 min at room temperature. The oil phase was prepared dissolving 5 %, 10 % and 15 % w/w of the chosen antioxidants (on lipid mass base) in 10 g isopropyl myristate and the solution was agitated under the same conditions. Then, the Oil phase was gently added to the Water phase and agitated using an emulsifier (mod. L4RT, Silverstone, USA), working at 7000 rpm for 6 min. The obtained emulsion was finally fed to the SuperLip apparatus and atomized directly in the formation vessel.

Fourier transform infrared (FT-IR) spectra were obtained via M2000 FTIR (MIDAC Co, Costa Mesa, CA), at a resolution of 0.5 cm−1. The scan wave number range was 4000–400 cm−1, and 16 scan signals were averaged to reduce the noise. The solution spectra were collected using a 5.4 m path length liquid cell with CaF2 windows.

To evaluate the **growth of *Escherichia coli***, bacteria were inoculated in liquid medium in the presence of different concentrations of nanoliposomes. To allow for the growth of this microorganism Luria-Bertani medium (10 g/L of triptone, 10 g/L of sodium chloride, and 5 g/L of yeast extract) was used (Sezonov et al., 2007). Before using the medium, it was sterilized by autoclaving at 121°C for 20 minutes. In order to have a sterile suspension of the liposomes, they were filtered by 0.22 µm filters. *E.Coli* was grown at 37 ± 1°C (incubator VWR, Radnor, PA, USA). To obtain the growing curves, the optical density (O.D.) of the samples, after opportune dilution, was read at 600 nm (spectrophotometer Genova, Jenway, Staffordshire, UK). The

control samples were represented by microorganisms grown in the presence of empty liposomes. The O.D. of the samples were registered after 1, 2, 4, 5, 18, 26 e 48 after the inoculum.

Chapter IV

Preliminary studies for the optimization of operating parameters

Chapter IV

IV.1 Effect of Pressure on empty liposomes

In this first set of experiments, empty liposomes were produced in order to study the effect of pressure variation on liposome mean size. The temperature in the vessel and mixer was set at 40 °C, with the vessel and mixer pressure being set at 100, 150 or 175 bar. The nozzle used for atomization had an 80 µm internal diameter and the water flow rate was set at 10 mL/min. The Gas to Liquid Ratio (GLR w/w) in the mixer was fixed at 2.42 using a carbon dioxide flow rate of 6.5 g/min and an ethanol flow rate of 3.5 mL/min. The PC concentration in the ethanol solution was fixed at 5 mg/mL.

The liposomes mean diameter varied between 289 ± 50 nm to 184 ± 20 nm when the pressure was increased from 100 and 175 bar. Increasing the pressure, a smaller mean size and standard deviation were obtained. The effect of pressure on liposome mean size can be explained considering that, increasing the pressure, an increase of CO_2 density and, consequently, of expanded liquid mixture density is obtained, that favors the atomization of the water injected into the high pressure vessel (Platzer and Maurer, 1989).

Another explanation is that at higher pressure a higher amount of water is dissolved in the formation vessel in which the mixture CO2/Ethanol is injected. Therefore, at higher pressure, the droplets loose a higher amount of water to their environment, which also causes the formation of smaller droplets.

The generation of smaller water droplets could lead to the formation of liposomes with a smaller diameter.

IV.2 A case study: the encapsulation of fluorescein

Fluorescent dyes are widely used as encapsulated agents in liposome-based biosensors for signal amplification, to realize biosensors with increased sensitivity and lower detection limits (Chu and Wen, 2013). In particular, fluorescein is a synthetic dye commonly used as a liposome biosensor based on fluorescence signals (Ligler et al., 1987, Katoh et al., 1993, Zhou and Li, 2015, Chu and Wen, 2013). Various attempts to encapsulate fluorescein into liposomes can be found in current literature for different applications. It has been encapsulated into liposomes as a model drug (Espirito Santo et al., 2015b) and as a marker to study liposomes permeation through skin (Coderch et al., 1996, Coderch et al., 2000) or to detect liposomes in ocular blood flow after administration (Niesman et al., 1992). However, an efficient production of liposomes encapsulating fluorescein is still challenging. The results reported in current literature show fluorescein encapsulation efficiencies lower than 50% (van Elk et al., Mahrhauser et al., 2015, Peer and Margalit, 2004, Hwang et al., 1999).

The optimization of the SuperLip operating parameters has to be performed with the objective of encapsulating fluorescein into liposomes trying to increase its encapsulation efficiency, while controlling liposome

dimensions in the sub-micrometric range. The SuperLip process parameters, such as the diameter of the injector used for water atomization, phospholipids concentration and fluorescein concentration in the water solution, have been studied to obtain liposomes of controlled size and distribution with high fluorescein encapsulation efficiency. The stability during the time of liposomes loaded with fluorescein was also investigated.

IV.2.1 Effect of injector diameter

The experiments discussed in this part of the thesis were performed at 100 bar and 40 °C. The CO_2 flow rate was set at 6.5 g/min and ethanol solution flow rate was set at 3.5 mL/min, to obtain a Gas to Liquid Ratio (GLR) in the homogenizer of 2.4 (on mass basis). The water solution flow rate was set at 10 mL/min. Selecting these operating conditions and assuming that the presence of PC does not modify the high pressure water-ethanol-CO_2 ternary equilibrium, the operating point of the experiments in the ternary diagram of **Figure IV.1** (Durling et al., 2007b) is located inside the miscibility gap. In the two-phase region, the 3 components (ethanol, carbon dioxide and water) are not completely miscible with each other. Depending on the position of the operating point, mass transfer of water into the ethanol/CO_2-rich phase and mass transfer of ethanol and CO_2 into the water-rich phase can modify the composition of the system.

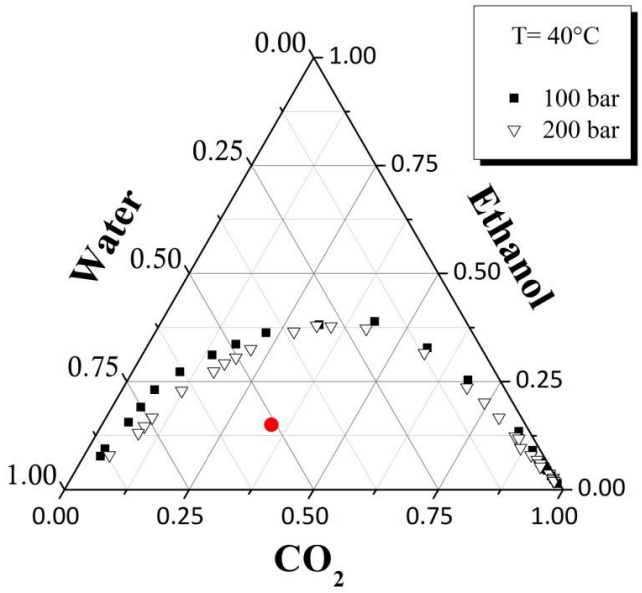

Figure IV.1. *High pressure vapor-liquid equilibria for the system CO_2-ethanol-water at 40 °C in the pressure range 100-200 bar, adapted from (Durling et al., 2007b). Operating point of the experiments is reported (●) as a red dot.*

In a first experiment, liposomes encapsulating fluorescein at a loading of 1% (weight of fluorescein/PC, % w/w) were produced. Phospholipids were dissolved in 100 mL of ethanol at a concentration of 5 mg/mL. Fluorescein was dissolved in 300 mL of water at a concentration of 0.017 mg/mL, to obtain a 1% by weight theoretical loading. An injector with the diameter of 80 µm was used for the atomization of the water solution in the formation vessel. The experiment was successful and liposomes with a nanometric diameter and a sharp PSD were produced. The DLS measured mean diameter (MD) of the fluorescein loaded liposomes was about 289±50 nm. This data are summarized in **Table IV.1**.

Table IV.1. *Mean diameter (MD) and encapsulation efficiency (EE%) of liposomes loaded with 1% of fluorescein, using injectors with different diameters and different PC concentrations. Data are not reported for the experiments that were not possible to perform.*

Injector Diameter [µm]	**Data**	**Lipid concentration [mg/mL]**				
		5		**7.5**	**10** **12**	**15**
80	MD ± SD (nm)	289± 50	283±58	305± 91	298 ± 89	---
	PDI	0.17	0.20	0.30	0.30	---
	EE%	90	92	90	81	---
60	MD ± SD (nm)	260± 48	262± 50	267± 53	268± 69	---
	PDI	0.18	0.19	0.20	0.26	---
	EE%	61	58	60	56	---
40	MD ± SD (nm)	249± 46	---	---	---	---
	PDI	0.18				
	EE%	58	---	---	---	---

A FE-SEM image of the produced liposomes is shown in **Figure IV.2**; they are characterized by an irregular spherical shape, with a rough surface. Furthermore, it is possible to see that their mean diameter seems smaller than the one measured by DLS (around 200 nm, see reference bar in SEM image). This result can be attributed to the shrinkage of the vesicles during the preparation of the sample for electronic microscopy.

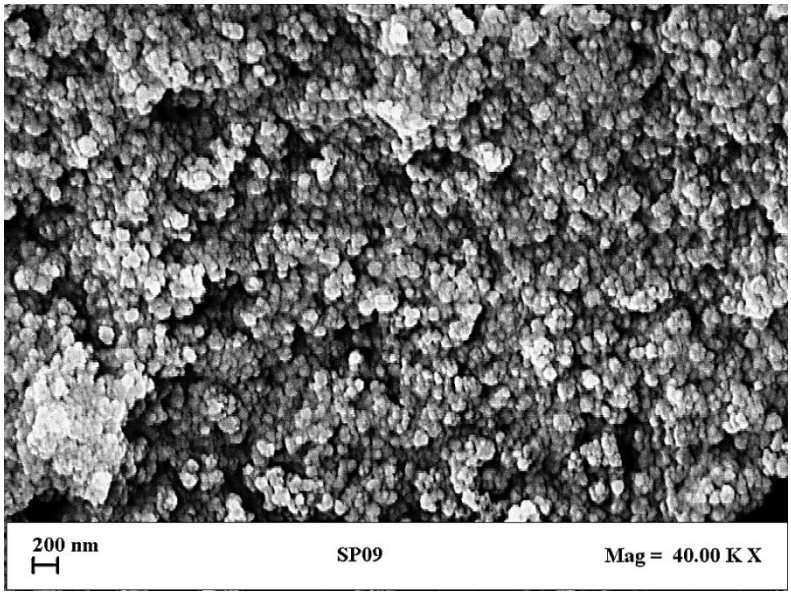

Figure IV.2. FE-SEM image of liposomes loaded with fluorescein at 1% theoretical loading.

Fluorescein was entrapped successfully in these liposomes, with high encapsulation efficiency (90%), as reported in **Table IV.1**. This result confirms that the water solution sprayed in the formation vessel was efficiently covered by phospholipids, leading to the formation of fluorescein loaded liposomes. This result is significantly better when compared to those obtained for fluorescein encapsulation, reported in current literature (Frederiksen et al., 1997, Hwang et al., 1999), confirming the high potential of this process in the encapsulation of hydrophilic compounds.

Considering the success of the first encapsulation test, a systematic study was performed to understand how the SuperLip operating parameters affect the drug entrapment in the liposomes. Experiments with larger PC concentrations were performed and the results are summarized in **Table IV.1**. PC concentration was increased from 5 to 15 mg/mL; the other operating conditions were left unchanged (pressure 100 bar, temperature 40 °C, GLR = 2.4). A stable liposome suspension was produced at all the values of PC concentration, except for the test performed at 15 mg/mL. In this case, the experiment was unsuccessful due to the blockage of the injector. The explanation of this result is that this PC concentration caused the deposition of part of phospholipids on the tip of the injector in the formation vessel, thus hindering the atomization of water. From the data reported in **Table IV.1** for the other experiments, it is possible to observe that the increase of the PC concentration in the ethanol solution did not produce a significant effect on the mean diameter of the liposomes. Increasing the PC

concentration from 5 mg/mL to 12 mg/mL, the liposome mean diameter, measured by DLS, slightly increased from 289±50 nm to 298±89 nm respectively; an enlargement of PSD can be noted (see standard deviations).

Considering the encapsulation efficiency, fluorescein was entrapped for values larger than 80% (measured using a UV-Vis spectrophotometer). This efficiency remained practically constant when the concentration of PC was increased from 5 to 10 mg/mL (see **Table IV.1**). The overall results suggest that a sufficient amount of lipid for droplets coverage is present in the formation vessel at 5 mg/mL and, therefore, a further increase to 7.5 and 10 mg/mL did not produce an improvement of EE. The reduction of EE to 81% is observed at 12 mg/mL, a condition very near to the operability threshold of 15 mg/mL (injector blockage). Near this condition, the partial blockage of the injector may cause phenomena of instability of the jet.

Experiments using injectors of 60 and 40 µm were then performed. For each injector, the same set of experiments with different PC concentrations, from 5 to 15 mg/mL, was performed. The other operating parameters were kept constant (pressure 100 bar, temperature 40 °C, GLR = 2.4). These results are summarized in **Table IV.1**. For the case of 60 µm injector, at the PC concentration of 15 mg/mL the experiment was not successful and the explanation is the same as in the previous case. Considering PC concentrations lower than 15 mg/mL, successful production of liposome suspensions was obtained. The data reported in **Table IV.1** show that using the 60 µm injector, liposomes with a smaller mean diameter, around 260 nm, were obtained, according to DLS measurements. In this case, the increase of PC concentration had an effect on the enlargement of the PSD curve, whereas the MD of the suspension was not significantly affected.

A smaller injector diameter (40 µm) was used to confirm the trend observed until now. Only one experiment was possible using this injector (see **Table IV.1**); for values of PC concentration larger than 5 mg/mL the injector blockage systematically took place. Using this injector, at 5 mg/mL, liposomes with a mean diameter of 249±46 nm, measured by DLS were produced (**Table IV.1**).

It is possible to compare the results obtained at the same PC concentration (5 mg/mL) using different injector diameters, as reported in **Figure IV.3**. In this figure, it is possible to see a progressive reduction of the liposome mean diameter when smaller injectors are used. In summary, the three injectors (80, 60 and 40 µm) produced liposomes with different mean diameters of about 300 nm, 260 and 240 nm, respectively. Furthermore, the smaller is the injector, the narrower the PSDs are.

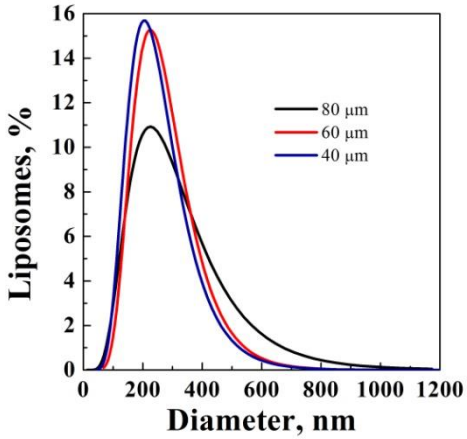

Figure IV.3. *Comparison of PSDs of liposomes produced using different injector diameters, PC concentration 5 mg/mL.*

The results obtained until now confirm that, in this process, the diameter of liposomes does not depend on the PC concentration but is connected to the dimension of the injector used for the water solution atomization; i.e., it influences the diameter of the atomized droplets in the formation vessel. A reduction of the diameter of the injector can improve the efficiency of the water atomization, allowing for the generation of a water spray formed by smaller droplets. It has also to be considered that, generally, when the turbulence of the spray is increased, as in the case of the reduction of the injector diameter, a better control of the PSD can also be obtained.

The data reported in **Table IV.1**, show that the fluorescein encapsulation efficiency decreases when using smaller injectors. Using the 60 µm injector fluorescein was entrapped with an efficiency of about 60%. As observed in the case of the experiments performed using the 80 µm injector, at values of the PC concentrations between 5 and 10 mg/mL, the encapsulation efficiency was practically constant; a reduction of 56% was obtained for the value of PC concentration near the threshold. Using the 40 µm injector, the encapsulation efficiency was 58%. These results can be explained considering that using an injector with smaller diameter (or partially blocked injector) an increase of the velocity of the liquid jet exiting the nozzle is obtained; therefore, water droplets, falling along the formation vessel, impact on the surface of the water bulk at a higher velocity. This phenomenon may cause the disruption of the lipid layer and can produce a consequent leakage of the drug content.

A set of experiments with different fluorescein loadings was also performed; the results are reported in **Table IV.2**. The operating conditions for the encapsulation tests were selected considering the previous

experiments: PC concentration of 5 mg/mL, using the 80 µm injector. These conditions were selected because they allowed for the highest fluorescein encapsulation efficiency in the previous experiments (92%). Empty PC liposomes were also produced under the same process conditions, to verify the effect of the presence of a solute on liposome PSD.

Table IV.2. *SuperLip size distribution data and encapsulation efficiency of liposomes loaded with 1 % to 9 % w/w by weight of fluorescein*

Fluorescein theoretical loading [%]	MD ± SD [nm]	PDI	Real Loading [%]	EE [%]
0	291±62	0.21	---	---
1	289±50	0.17	0.90	90
3	277±55	0.20	2.88	96
6	269±51	0.19	5.58	93
9	268±53	0.20	7.83	87

Liposomes produced using different fluorescein theoretical loading were characterized by a mean diameter of about 280 nm, that was not evidently affected by the different amount of fluorescein dissolved in the water phase. The presence of the solute did not produce any valuable effects on liposome PSD. The possible explanation is that the presence of the solute did not alter the atomization efficiency. Fluorescein encapsulation efficiency was high in all cases. Encapsulation efficiencies between 87-96% were obtained upon increasing the theoretical fluorescein loading from 1 to 9% respectively. This result is extremely relevant since SuperLip overcomes the drawback of traditional methods used for liposomes preparation, in which, in most of the cases, the encapsulation efficiency is negatively affected by an increase of the theoretical loading (Berger et al., 2001).

IV.2.2 Characterization of liposome suspensions

Liposome suspensions produced by SuperLip, at the optimized operating conditions (pressure of 100 bar, 80 µm injector and 5 mg/mL PC concentration), were also characterized in terms of liposome stability over the time and concentration of the liposomes in the final suspension.

Liposome suspensions were stored at 4 °C and PSD measurements were performed at fixed time intervals for more than 120 days using DLS. The results obtained are shown in **Figure IV.4**. The mean diameter of the fluorescein loaded liposomes remained relatively constant for more than four months. The liposome zeta potential was always about -20 mV, indicating a good suspension stability. The general dividing line between stable and unstable suspensions is generally taken as +30 or -30mV with the particles having zeta potentials outside of these limits normally considered stable (Larsson et al., 2012). The value of the zeta potential of the liposomes

produced in this paper is near the region of stability. The concentration of fluorescein in the external medium of the suspension was measured during storage; the data collected confirmed that there were no significant fluorescein leakages from the liposomes.

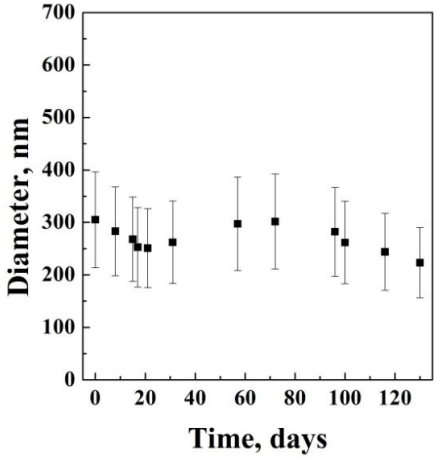

Figure IV.4 *Stability study of fluorescein loaded liposomes*

The NTA technique was used to measure the liposome concentration in the suspension and gain further indications about their diameter. The particles detected by the laser beam are counted by the NTA, obtaining the sample concentration in terms of number of particles per mL of suspension. A typical frame acquired for the sample obtained at 5 mg/mL and with fluorescein theoretical loading of 1% is proposed in **Figure IV.5**. The liposome population is represented by white points in a dark background. The quantitative data show that the suspension produced is characterized by a liposome concentration of about 280 million of vesicles per mL of suspension.

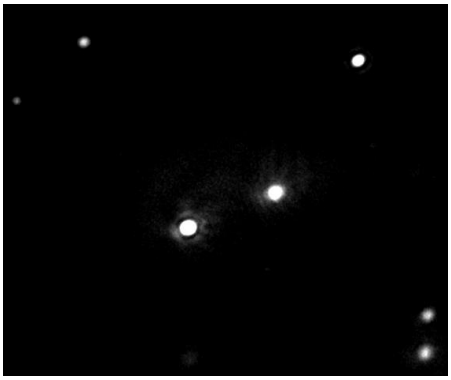

Figure IV.5 *Example of frame from NTA analysis of liposome suspensions produced at a PC concentration of 5 mg/mL and 1% fluorescein theoretical loading.*

The software can also calculate the liposome hydrodynamic diameters using the Stokes Einstein equation smoothing the results and eliminating possible aggregates. NTA measurement can be even more accurate than DLS. NTA measured PSD of a SuperLip suspension is reported in **Figure IV.4.6b**, and a comparison of distribution data of the same sample, obtained using the DLS technique, is shown in **Figure IV.6a**. The mean size obtained by NTA was about 166±60 nm. Both techniques show that the suspension is characterized by a relatively narrow distribution; nevertheless, it is possible to observe a tail of the DLS size distribution towards larger sizes, that can be mostly due to the contribution of large particles to the overall scattering (Filipe et al., 2010). The DLS technique also considers as single particles the scattering produced by aggregates; therefore, the overall mean diameter measurement could be modified by the aggregates contribution.

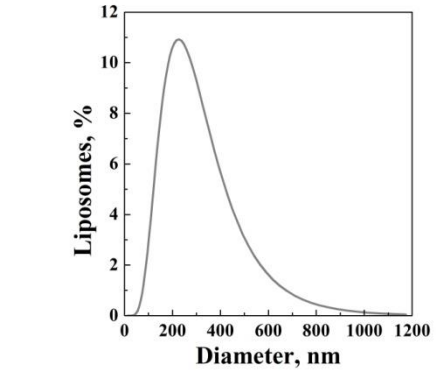

(a)

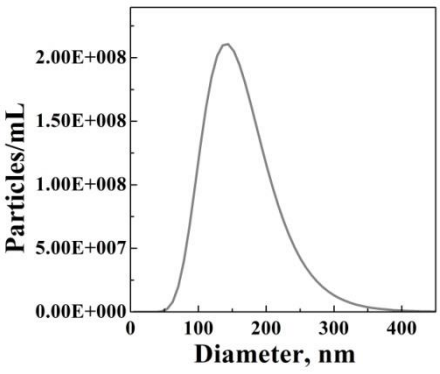

(b)

Figure IV.6 *Comparison of PSD distribution data obtained with DLS as diameter vs intensity (a) and NTA as diameter vs concentration (b). SuperLip liposomes produced at 80 µm, PC concentration 5 mg/mL.*

Thanks to the accuracy of the NTA measurement, it can be observed that the liposome size distributions of the suspensions produced by SuperLip are even narrower with respect to the data obtained using DLS, confirming the good control of PSD allowed for by this process.

The efficient production of liposomes loaded with fluorescein characterized by nanometric diameter and narrow PSD was demonstrated using the SuperLip process. The analysis of the process parameters allowed to obtain encapsulation efficiencies up to 97%. The diameter of the injector had a significant effect on the fluorescein encapsulation efficiency. The smaller the injector used is, the lower the encapsulation efficiency is. The concentration of phospholipids in the supercritical solution and the concentration of fluorescein in the aqueous phase did not produce any significant effects on the fluorescein encapsulation efficiency that remained constant and very high. The liposomes were stable during storage (4 months), retaining the drug in the inner compartment.

IV.2.3 Lipidic concentration effect

As further proof of the versatility of SuperLip, the effect of lipid concentration variation was studied: 500 mg, 750 mg and 1000 mg of PC were dissolved in 100 mL of ethanol to obtain 5, 7.5 and 10 mg/mL lipid concentration. Two sets of experiments were performed with these lipid concentrations, first setting water flow rate at 10 mL/min and then at 0.7 mL/min. 1 % w/w fluorescein was also loaded into liposomes in every experiment. The pressure was set at 100 bar. Mean diameters, PDI and Encapsulation Efficiencies are reported in **Table IV.3.**

Table IV.3 *MD, PDI and EE of liposomes loaded with 1% w/w of fluorescein*

Water Flow rate [mL/min]	**Lipid Conc. [mg/mL]**	**PC/H_2O**	**MD [nm] ± SD**	**PDI**	**EE [%]**
10	5	2	204.4 ± 38.8	0.38	87.5
mL/min	7.5	3	188.7 ± 37.7	0.40	76.5
	10	4	160.3 ± 32.1	0.40	87.9
0.7	5	25	476.5 ± 127.7	0.54	96.4
mL/min	7.5	38	448.3 ± 132.5	0.59	99.9
	10	50	912.3 ± 329.8	0.72	99.4

By increasing the PC mass used to prepare the samples, a slight decrease of the mean diameters was observed. The sample prepared with 5 mg/mL of PC had a diameter of 204.4 ± 38.8 nm while the sample with maximum lipid concentration had a mean diameter of 160.3 ± 32.1 nm. The measured EE was between 76.5 and 87.9 % without a significant trend, since it was not affected by the PC concentration.

The same set of experiments for the production of fluorescein loaded liposomes was performed with a smaller water flow rate, 0.70 mL/min. In this case, the PC/Water ratio was furthermore modified because the PC and water mass fed into the system were both changed. In **Table IV.3,** the mean diameters, PDI and EE of this set of experiments are reported.

Increasing the lipidic concentration, a progressive increase of the average liposomes dimensions was observed, from a mean diameter of 476.5 ± 127.7 nm to 912.3 ± 329.8 nm for the 10 mg/mL lipidic concentration. This effect was mainly due to the formation of more lipidic double layers around the water droplets. This phenomenon was highly evident with this kind of compound and especially for a reduced water flow rate. The reduced speed of the water droplets traduced into a larger residence time of the water droplets in the formation vessel, giving the lipids the time to produce a higher number of layers.

Moreover, the mean dimensions of the liposomes were larger than the set produced at 10 mL/min because with a lower water flow rate, the fluid velocity at the exit of water injector is reduced. This caused a minor phenomenon of jet break up and the formation of bigger droplets. The probable presence of a higher number of lipidic layers gave the possibility to entrap further quantities of fluorescein in the inner core, from 96.4 % to 99.9 %, higher than the EE of the previous fluorescein samples. Since the water speed is decreased, a major number of water droplets is covered by the phospholipids before the drug diffuses into the external bulk.

To complete the study of fluorescein encapsulation efficiency, drug release experiments were performed in vitro at 37 °C on samples loaded with 1 % w/w fluorescein and 5, 7.5 and 10 mg/mL lipid concentration (0.70 mL/min water flow rate), comparing them with free fluorescein drug release. The kinetics curves are compared in **Figure IV.7**.

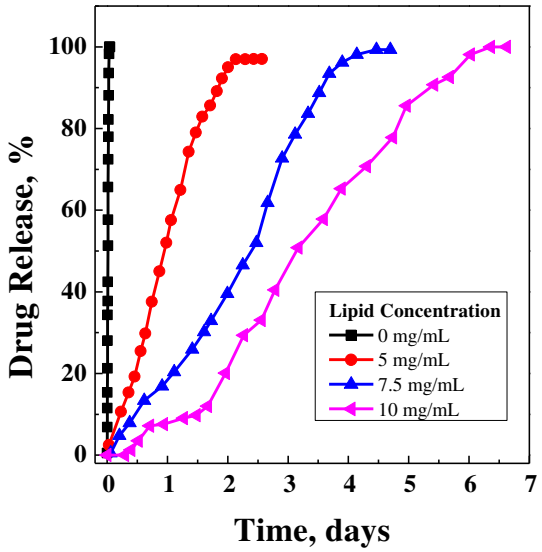

Figure IV.7 *Drug release comparison: free fluorescein, 5 mg/mL PC, 7.5 mg/mL PC, 10 mg/mL PC*

Native fluorescein was totally released after 2 hours. Liposomes prepared with 5 mg/mL lipid concentration reached the maximum values after 2 days, the sample with 7.5 mg/mL reached it after 5 days and the most loaded one released all its content after almost 7 days. What was evident is the delaying effect on drug release, due to the presence of a higher lipidic content. This result confirmed the hypothesis that a greater amount of PC caused the formation of a greater number of lipidic double layers, making the vesicles more compact and giving the fluorescein more obstacles to overcome during diffusion into the external bulk. An explanation was also found in the literature, where it is confirmed that the difference in the release rate is due overall to the number of double lipidic layers that hydrophilic drug has to cross before being released into the external medium (Bozzuto, 2015).

IV.3 Drug concentration effect

Bovine serum albumin (BSA) was encapsulated into liposomes. Ampicillin is a hydrophilic protein with a higher molecular weight compared to the previous studied compounds. BSA was chosen to demonstrate that it is possible to encapsulate also molecules bigger than ampicillin and fluorescein, using SuperLip. The water flow rate was set to 10 mL/min, pressure was set at 100 bar and the other process parameters were not

changed. A set of experiments was performed by varying the BSA theoretical loading from 10 % w/w to 30 % w/w and then to 60 % w/w in ratio with the PC mass. The PC/Water ratio did not change since the water flow rate and lipid concentration were not modified.

Table IV.4 *MD, PDI and EE of liposomes loaded with 10, 20 and 30 % w/w bovine serum albumin*

BSA Loading [w/w, %]	PC/H_2O	Mean Diameter MD [nm] ± SD	PDI	EE [%]
10		123.0 ± 12.3	0.20	62.5
30	2	144.7 ± 16.0	0.22	83.5
60		244.6 ± 36.7	0.30	93.9

Upon increasing the drug loading (**Table IV.4**), the liposome mean diameter increased. With a 10 % w/w theoretical loading, liposomes of 123.0 ± 12.3 nm were obtained. Increasing it to 30 % w/w, the vesicles mean size became 144.7 ± 16.0 nm and for a 60 % w/w theoretical loading, it became 244.6 ± 36.7 nm. The increased mean diameter was ascribed to the increased viscosity of a higher BSA concentration in the water solution. The PDI were also increased by increasing the theoretical loading, because the PSDs became polydispersed. The EE was increased from 62.5 % for 10 % w/w loaded sample to 93.9 % for 60 % w/w loaded sample, because the high viscosity of the water solution slows the drug diffusion to the external bulk.

Fluorescein and BSA encapsulation experiments were performed with SuperLip by varying some of the process parameters. Upon increasing the Ampicillin theoretical loading, nanometric and stable liposomes with high EE were produced. Increasing the lipidic concentration, the liposomes mean diameters were not modified by higher water flow rates, while they significantly increased at lower water flow rates. The higher lipidic concentration caused the formation of a major number of lipidic layers that showed a delaying effect on fluorescein drug release. EE were still high, up to 99.9 %. These good results were also confirmed for the BSA loaded liposomes, that become smaller by increasing the drug theoretical loading.

A TEM image on this sample is reported in **Figure IV.8**, followed by an IR characterization of the BSA native compared with SuperLip processed BSA (**Figure IV.9**).

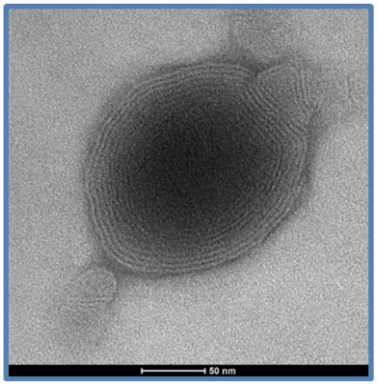

Figure IV.8 *TEM image of multi-layered liposomes*

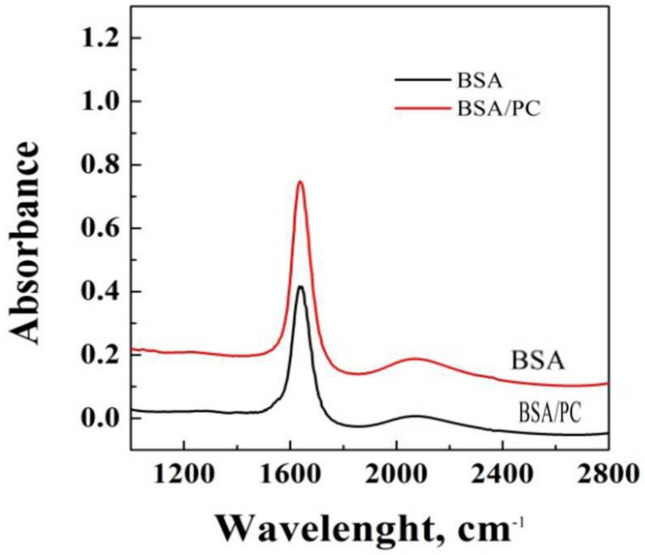

Figure IV.9 *FTIR on native BSA compared with SuperLip processed BSA*

A Fourier-transform infrared spectroscopy (FTIR) analysis of the BSA loaded liposomes, compared to native BSA solution spectrum shows that SuperLip did not damage the protein structure, preserving its functionality. From the deconvolution of FTIR spectrum, it was observed that the content in the native BSA is 66% and remained practically unchanged (at 64%) in the processed BSA.

IV.4 Gas to Liquid Ratio of the expanded Liquid

Despite the SuperLip process having demonstrated to be able to produce micrometric and nanometric stable liposomes, the control of their mean dimensions, especially at nanometric level, required further studies. For this reason, the main aim of this work was to explore the effect of Gas to Liquid Ratio of the Expanded Liquid (GLR-EL) on the diameter of produced liposomes at micrometric and nanometric level. The entrapment of vancomycin (Lankalapalli et al., 2015, Uhl et al., 2017) and farnesol (Bandara et al., 2016) was attempted to verify the results also on loaded liposomes.

IV.4.1 Production of empty liposomes at different GLR-EL

A relevant parameter still unexplored is the composition of the Expanded Liquid (EL), i.e. the Gas to Liquid Ratio of the fluid phase (GLR-EL). It is defined as the ratio between the carbon dioxide and ethanol flow rate, and its effect on liposomes diameter has been studied.

In previous papers, GLR-EL was set at 2.4 (Campardelli et al., 2016a, Santo et al., 2014) to study the effect of other process parameters such as pressure, water flow rate, nozzle diameter, lipid concentration and double layer composition (Campardelli et al., 2018, Trucillo et al., 2018a, Trucillo et al., 2018b, Trucillo et al., 2018c, Trucillo et al., 2017, Campardelli et al., 2016c).

Empty liposomes were produced modifying the ethanol flow rate from 1.46 mL/min to 7.71 mL/min; whereas, CO_2 flow rate was regulated with a micrometric valve, varying it from 2.47 g/min to 11.28 g/min. As a consequence, the Gas to Liquid Ratio of the Expanded Liquid (GLR-EL) varied from 0.32 to 6.00 on the mass basis (as reported in **Table IV.5**). The water flow rate was set at 10 mL/min. The pressure in the formation vessel was set at 100 bar and temperature at 40 °C.

Table IV.5 *Mean Diameter (MD), Standard Deviation (SD), of empty liposomes (GLR-EL in the range 0.32 to 6.00)*

GLR-EL	Ethanol flow rate [mL/min]	Carbon dioxide flow rate [g/min]	MD ± SD [nm]
0.32	**7.71**	**2.47**	1729 ± 733
0.44	**7.71**	**3.39**	1324 ± 537
1.33	**6.94**	**9.23**	963 ± 230
1.50	**6.94**	**10.40**	940 ± 263
1.83	**6.17**	**11.28**	878 ± 170
2.20	**4.62**	**10.17**	139 ± 49
3.85	**2.70**	**10.39**	155 ± 71
4.86	**2.16**	**10.49**	145 ± 65
6.00	**1.46**	**8.79**	150 ± 72

The experiments performed with a GLR-EL between 0.32 and 1.83 resulted in the formation of liposomes of micrometric dimensions (see **Table IV.5**); the particle size distributions of these samples are reported in **Figure IV.10**.

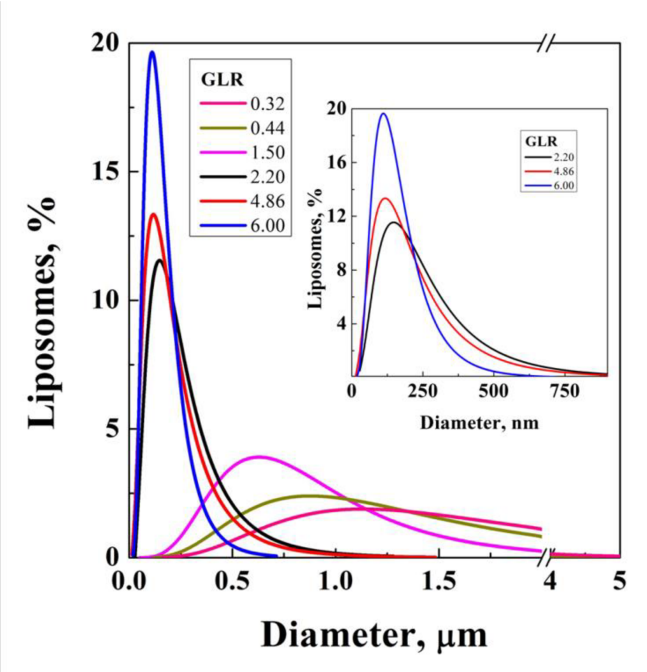

Figure IV.10. *Particle Size Distributions (PSDs) of micrometric and nanometric empty liposomes obtained changing the Gas to Liquid Ratio of the fluid phase (GLR-EL).*

In particular, the mean diameters of micrometric samples are included between a minimum of 878 ± 170 nm and a maximum of 1729 ± 733 nm.

Figure IV.10 shows the decreasing trend of the mean diameters, as well as the size distributions that become narrower upon increasing GLR-EL from 0.32 to 1.50. Data in **Table IV.5** and **Figure IV.10**, also show that, for GLRs-EL values included between 2.20 and 6.00 on the mass basis, the mean size of the liposomes is in the nanometric range, between a minimum of 139 ± 49 nm and a maximum of 155 ± 71 nm. The Particle Size Distributions of the nanometric samples are also added to **Figure IV.10** for GLRs-EL larger than 2.20. For these cases, an increase of GLR-EL Gas results in the production of liposomes with narrower particle size distributions. PSDs in **Figure IV.10** have been reported together to allow for the observation of results at micro and nano level, that cover more than one order of magnitude. In particular, looking at the results summarized in **Table IV.5**, the overall comment is: changing the GLR from 0.32 to 6.00, a progressive reduction of the liposomes mean diameter was observed, from micrometric liposomes to nanometric level.

A FE-SEM image of nano-liposomes obtained working at GLR-EL 6.00 is shown in **Figure IV.11.**

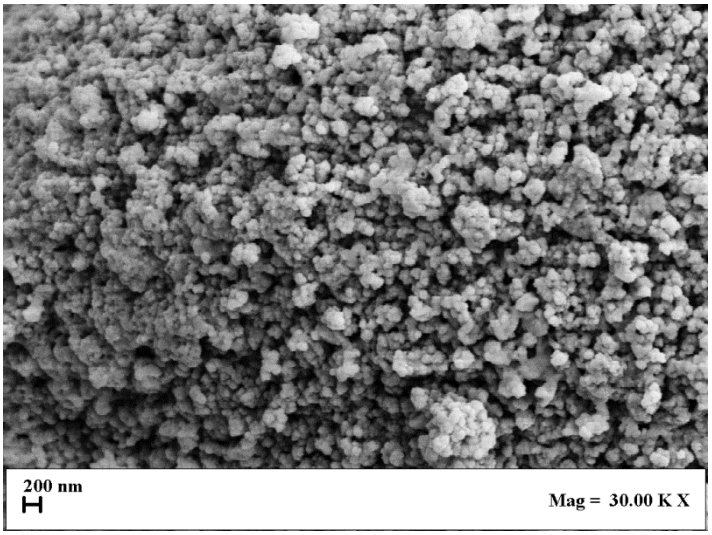

Figure IV.11. *Scanning Electron Microscope image of liposomes produced at a GLR-EL = 6.00*

In summary, these experiments demonstrated that it is possible to tune the mean dimensions of the liposomes changing the GLR-EL using SuperLip. Working with a GLR-EL lower than 1.83 on the mass basis, sub-micrometric and micrometric vesicles have been produced. Working at GLRs-EL larger than 1.83, nanometric mean dimensions smaller than about 150 nm have been obtained.

It is necessary to recall the theory studied by Brunner on the surface tension between two coexisting phases (Brunner, 2013). In the particular case of this work, it should be considered the surface tension between the water-rich phase and the other phase that is rich in ethanol and CO_2. Carbon dioxide and water are slightly miscible, but ethanol is miscible with CO_2 (at 100 bar and 40°C) and with water. Thus, the ethanol can be considered as a mediator between CO_2 and water, being directly responsible of reducing the surface tension. Indeed, for small Gas to Liquid Ratios, the surface tension is smaller than for large Gas to Liquid Ratios.

A Gibbs diagram of the ternary system water-carbon dioxide-ethanol was provided in **Figure IV.12**.

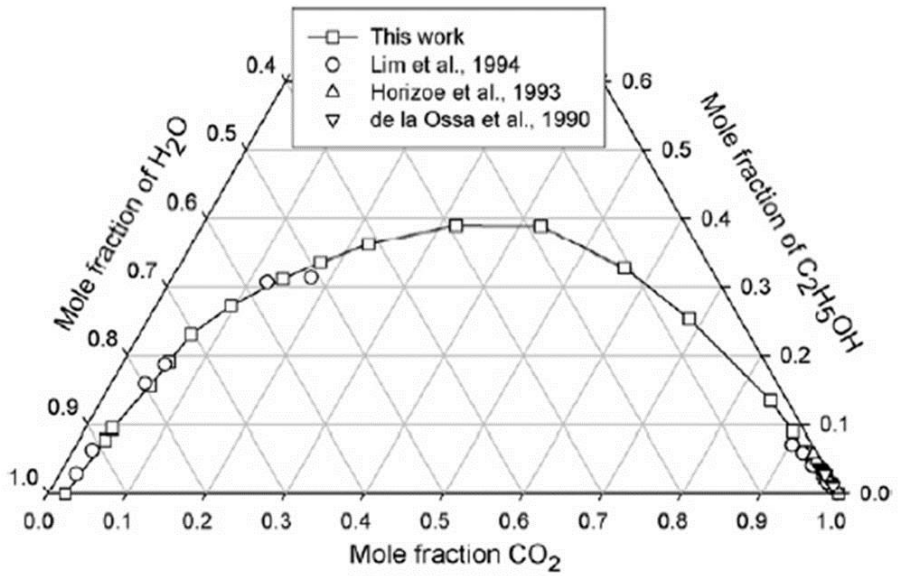

Figure IV.12. *Gibbs Diagram for the CO_2–EtOH–H_2O system at 313K and 100 bar., adapted from (Durling, 2007).*

The **Solvent Residue** (SR) present in the liposomes after SuperLip production was also studied for all the experiments. The samples recovered after SuperLip were subjected to evaporation under vacuum. This operation was performed at 40 °C and 150 rpm for 20 minutes; these mild conditions were chosen to preserve the integrity of the liposomes vesicles. The results are reported in **Table IV.6**. However, it is necessary to consider the Gibbs diagram adapted from (Druling, 2007), containing the mixing paths for the different compositions water-ethanol-carbon dioxide (**Figure IV.13**).

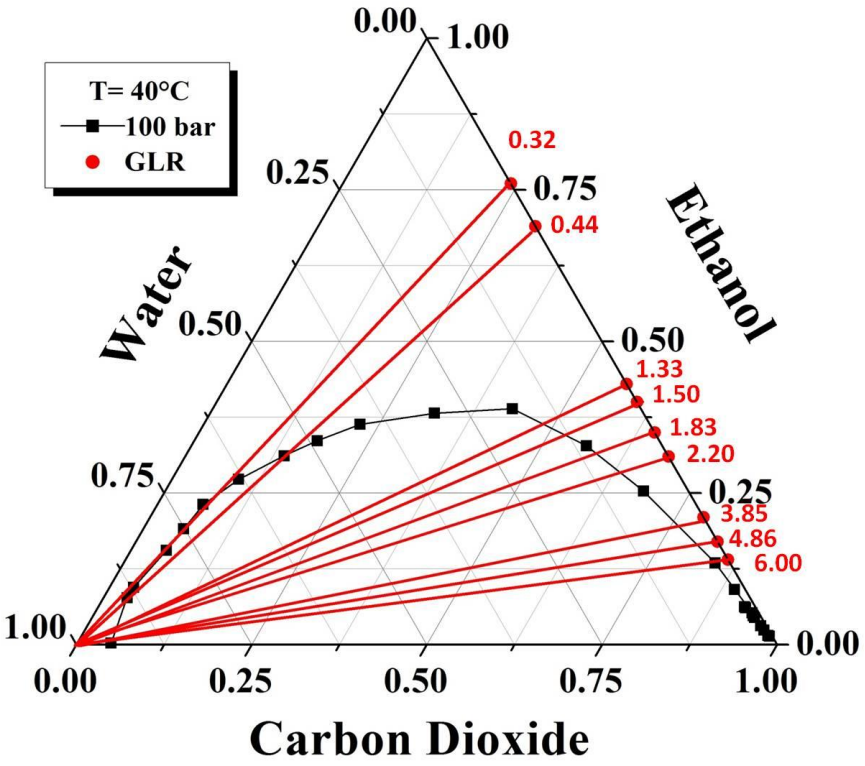

Figure IV.13. *Gibbs Diagram for the CO_2–EtOH–H_2O system at 313K and 100 bar., adapted from (Durling, 2007), with mixing paths.*

The system obtained in the high pressure vessel of SuperLip is characterized by a mixture of ethanol, carbon dioxide and water, hypothesized at their equilibrium. Then, looking at the equilibrium diagram, the composition of the binary mixture ethanol-carbon dioxide is modified by the GLR-EL. The mixing paths (drawn in red), that link the ethanol molar fraction in the binary mixture with water, describe different intersections with the miscibility gap, changing the composition of the expanded liquid (ethanol + carbon dioxide), and consequently of the water phase at the bottom of the formation vessel. As described by mixing paths, the segment that links the binary mixture with the binodal curve indicates the maximum amount of ethanol that can enrich the water bulk, set at the bottom of the formation vessel of SuperLip. Moreover, increasing GLR-EL, the paths demonstrate that the system will be characterized by a smaller amount of ethanol residue.

Table IV.6. *Comparison between Solvent Residue (SR) measured in empty liposomes suspension after evaporation, at different values of GLR-EL.*

GLR-EL	SR after evaporation, [ppm]
0.32	4 567
0.44	4 102
1.33	3 214
1.50	3 023
1.83	2 832
2.20	2 641
3.85	2 450
4.86	2 259
6.00	1 890

Solvent in the liposomes suspensions after the SuperLip process was above the limit of Drug & Food Administration guidelines for this class of solvent (< 5000 ppm). For this reason, an evaporation step was required. Looking at the results reported in **Table IV.6**, it is possible to see that after 20 min of mild evaporation, final solvent residues were always less than the fixed admissible limit for this solvent. It is interesting to note that different GLR-EL values determine different final contents of ethanol; i.e., decreasing the amount of ethanol in the EL mixture (increase of GLR-EL), the final amount of ethanol in liposome suspensions was lower. Solvent Residues ranged between a maximum of 4 567 ppm for a GLR-EL of 0.32 to a minimum of 1890 ppm for a GLR-EL of 6.00. To verify if liposomes subjected to evaporation were damaged by the post-processing step, samples were characterized using Dynamic Light Scattering to study their Particle Size Distributions and stability before and after the evaporation step. A comparison between the particle size distributions of the vesicles produced at a GLR-EL of 6.0 is proposed in **Figure IV.14**.

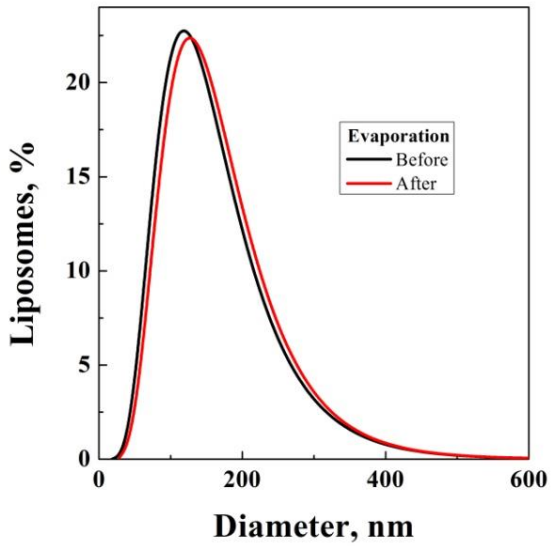

Figure IV.14 *Comparison of the Particle Size Distribution of liposome suspensions produced at GLR-EL 6.0 before and after evaporation step.*

It shows that the two distributions substantially overlap and this result means that post-processing by evaporation has a negligible effect on the liposomes diameter.

IV.4.2 Production of loaded liposomes

A hydrophilic antibiotic such as vancomycin was entrapped in the inner core of liposomes with theoretical loadings from 5 % to 15 % on the lipid mass base. The same theoretical loadings were repeated for the entrapment of the lipophilic antioxidant farnesol in the lipidic double layer. Pressure and temperature were set at 100 bar and 40 °C. The aim of this part of the work is twofold: first, to verify if it is possible to load these compounds in liposomes produced by SuperLip and, second, to verify that diameter control at nano level is still possible, when producing loaded liposomes. GLR-EL was fixed to 6.00 as optimized with the previous set of experiments.

In **Table IV.7**, the Mean Diameters (MD), Encapsulation Efficiencies (EE) and Solvent Residue (SR) are reported; whereas, the particle size distributions are compared in **Figure IV.15**.

Table IV.7. *Mean Diameter (MD) plus Standard Deviations (SD), Encapsulation Efficiency (EE) and Solvent Residue (SR) of farnesol and vancomycin loaded liposomes at GLR-EL 6.00*

Compound	Theor. Loading [%]	Mean Diameter MD± SD [nm]	Encapsulation Efficiency [%]	Solvent Residue [ppm]
Farnesol (lipophilic)	5	133 ± 76	22.9 ± 1.4	1900
	10	150 ± 80	65.2 ± 2.3	1868
	15	159 ± 95	74.0 ± 1.1	1680
Vancomycin (hydrophilic)	5	250 ± 93	76.7 ± 1.9	134
	10	201 ± 58	61.3 ± 1.0	23
	15	180 ± 48	60.0 ± 0.8	10

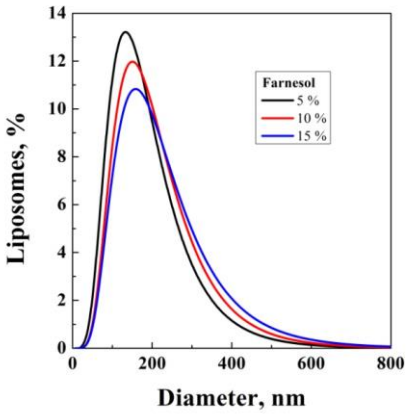

(a)

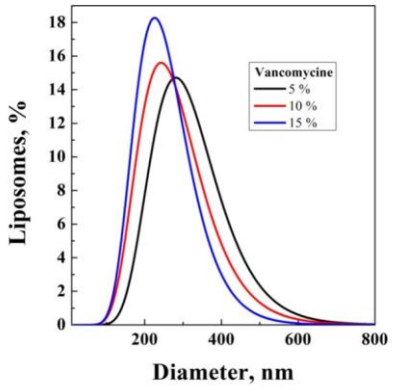

(b)

Figure IV.15. *Particle Size Distributions of farnesol (a) and vancomycin (b) loaded liposomes produced at a GLR-EL 6.0.*

It is possible to observe that the farnesol loaded liposomes had a mean diameter between a minimum of 133 ± 76 nm for the lowest drug theoretical loading (5 % w/w) and a maximum of 159 ± 95 nm for the highest (5 % w/w). The liposome mean dimensions showed a decreasing trend by increasing the drug cargo (see **Figure IV.15a**).

In the same way, the vancomycin loaded liposomes showed a mean size from 180 ± 48 nm to a maximum of 250 ± 93 nm, as shown in **Figure IV.15b**. These results demonstrated that the particle size distribution of the loaded liposomes remained at nanometric level.

The encapsulation efficiency was up to 74.0 ± 1.1 % for the farnesol loaded liposomes and up to 76.7 ± 1.9 % for the vancomycin loaded liposomes. The encapsulation efficiency of the hydrophilic compound was almost constant upon increasing the drug theoretical loading; whereas, it showed an increasing trend for the lipophilic loaded liposomes. This last result was already obtained for other lipophilic compounds entrapped in the double lipidic layer of vesicles and explained in our previous work (Trucillo et al., 2018c).

After evaporation under vacuum, the Solvent Residue (SR) of the vancomycin loaded liposomes was 134 ppm for 5 % vancomycin loading, 23 ppm for 10 % and 10 ppm for 15 % loaded vesicles. Comparing these results with empty liposomes, the ethanol residue was much lower. A possible explanation of these results can be provided considering the different solubility of the drugs in ethanol. Vancomycin is slightly soluble in ethanol; for this reason, this antibiotic dissolved in water droplets probably repels ethanol during the liposome formation. This results in the smaller SR of the vancomycin loaded liposomes. Farnesol has good affinity with ethanol and does not modify the interaction between water droplets and the Expanded Liquid during the formation of liposomes in the high pressure vessel. Due to its lipophilic nature, Farnesol was dissolved into ethanol together with lipids and participated in the formation of the vesicles lamellae as well as Phosphatidylcholine (PC), resulting in SRs similar of those obtained for empty liposomes. A confirmation of this explanation is given by the results of the SRs obtained for the sample with the increased vancomycin loadings. In the case of farnesol, SR was almost constant when the drug loading was increased. Upon increasing the drug theoretical loading on lipid mass base, the solvent residue showed a decreasing trend. In particular, for 5 % vancomycin loaded liposomes, the measured residue was 134 ppm; it was 23 ppm for 10 % loaded vesicles and 10 ppm for 15 % loaded carriers. Examples of Field Emission-Scanning Electron Microscope (FE-SEM) images of vancomycin and farnesol loaded liposomes are reported in **Figure IV.16**.

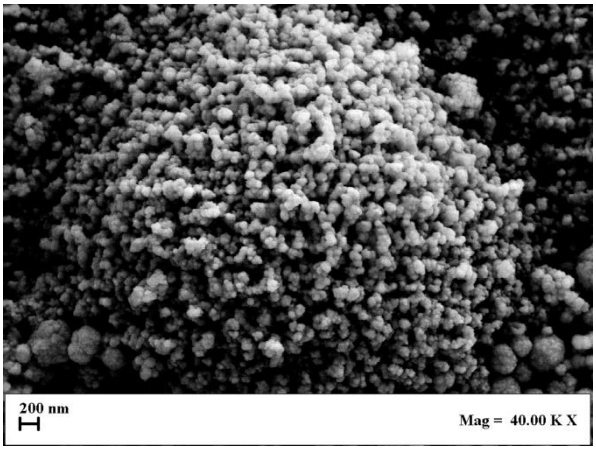

(a)

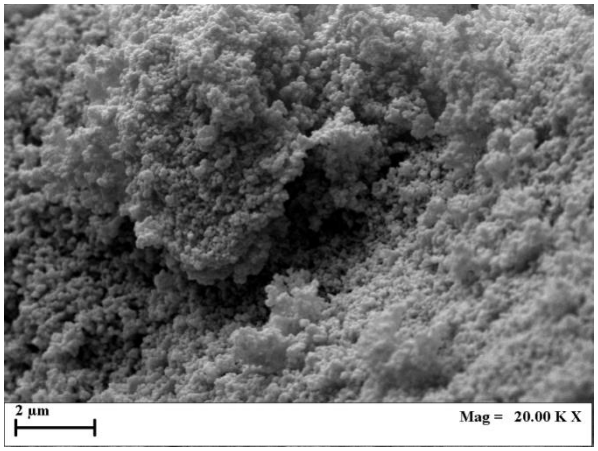

(b)

Figure IV.16 *Scanning Electron Microscope of vancomycin (a) and farnesol (b) loaded liposomes produced with GLR 6.00*

This figure shows that the nanometric mean dimensions were confirmed; the shape of the vesicles is spherical. In the case of farnesol loaded vesicles (**Figure IV.16b**), larger aggregation phenomena can be observed. This fact is probably due to the presence of farnesol in the lipidic barrier. Farnesol is liquid at room temperature and for this reason its presence in the liposome membrane can produce a stickier sample.

Control of the liposomes diameter is one of the key questions in their production, especially at nanometric level. This study revealed that in the case of SuperLip, the key parameter that mainly controls liposome diameter is GLR-EL. This result is somewhat surprising but a possible explanation, based on its influence on the properties of the receiving EL during atomization and their influence on the forming droplets, has been proposed. Another relevant result of this study is the reduction of solvent residue changing GLR-EL and based on the ethanol percentage in the EL.

The encapsulation study with vancomycin and farnesol confirmed that GLR-EL can give a good control of the liposome size and solvent residue, both for lipophilic and hydrophilic compounds entrapment.

Chapter V

Liposomes double layer optimization

Chapter V

V.1 Cholesterol loaded liposomes

The characteristics of liposomes are strictly related to the chemical properties of the phospholipids used during the preparation. The kind of lipids selected for the liposome formation may modify the total surface charge of liposomes, the permeability, the encapsulation efficiency and the drug release (Nagahiro et al., 2000, Filion and Phillips, 1997, Gregoriadis, 2016). The membrane solidity is often linked to the shape of the phospholipids, particularly to the corner amplitude described by their two tails (Nogueira et al., 2015). Phosphatidylcholine (PC) is the most commonly used phospholipid in liposomes membrane (Li et al., 2015). Cholesterol (Chol) is recognized as being compatible with the formation of vesicles. It is reported that it is able to prevent the formation of aggregates and has stabilizing effects. However, a high percentage of cholesterol in liposome formulation can cause liposome destabilization and the presence of Chol crystals in the aqueous bulk. The amount necessary to achieve stable carriers has yet to be clarified (Eloy et al., 2014). Phosphatidylethanolamine (PE) is another kind of phospholipid used in many cases for liposomes double layer formulations (Hwang et al., 2007). In this case, the main difference with the PC tridimensional structure is the presence of a larger angle between the two lipid chains. The PE general shape is truncated conical, while PC has a cylindrical shape (Suetsugu et al., 2014b). Despite these interesting properties, a systematic study on the effect of PE or Chol incorporation in liposome membranes on the vesicles mean diameter, drug encapsulation efficiency, drug release has not been performed yet. For example, some liposome formulations have been developed adding synthetic lipids to PE vesicles, obtaining nanoparticles but with low encapsulation efficiencies of the active principles (Blume and Cevc, 1990). The effect of cholesterol incorporation was studied together with PEGylation or chitosan coating; but, focusing especially on the permeability effect on the membrane (Wang et al., 2010).

The SuperLip process has been proposed to explore the possibility to produce liposomes with a high encapsulation efficiency of the hydrophilic compounds and using different lipid mixtures in the bilayer membrane, to understand the effects of lipid composition on drug encapsulation efficiency and drug release kinetics.

In particular, the possibility of production of PC based liposomes with Chol and PE in the lipid bilayer (with different w/w percentages) using the SuperLip process is studied, using theophylline as a model hydrophilic drug. The effect of the water solution flow rate, the presence of Chol and PE is considered on the Particle Size Distribution (PSD), encapsulation efficiency (EE), vesicles stability and drug release kinetics. Liposome stability as well as Chol and PE entrapment efficiency into liposomes bilayer was also investigated.

A first set of experiments was performed at different water solution flow rates to verify the possibility of the encapsulation of theophylline in PC/Chol based liposomes.

The experiments were performed at a pressure of 100 bar and a temperature of 40 °C. The flow rate of the ethanol solution was set to 3.5 mL/min and carbon dioxide flow rate was calculated to obtain a gas to liquid ratio by mass weight (GLR) of about 2.4. The water flow rate was initially set at 10 mL/min. The corresponding composition of the system during the experiments can be represented on the ternary vapor liquid equilibrium diagram of **Figure V.1** (Durling et al., 2007a) water-CO_2-ethanol (neglecting the presence of the solutes). In order to obtain liposomes, the operating point should be located inside the miscibility gap, where the immiscibility between the water droplets and the expanded liquid can be obtained. Outside the miscibility gap, water can be extracted by the expanded liquid solution ethanol-CO_2.

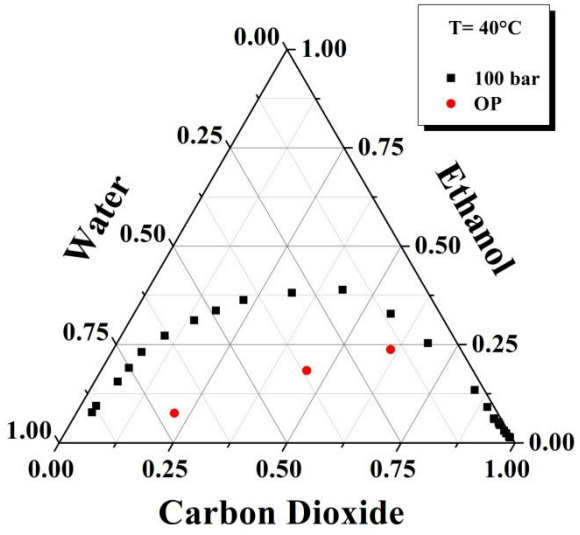

Figure V.1. *Operating points (in red) in the experiments performed at different water flow rates, reported in the carbon dioxide-water-ethanol ternary diagram at 40°C and 100 bar, adapted from (Durling et al., 2007a).*

PC and Chol were dissolved in the ethanol solution (100 mL total volume) to obtain a total lipid concentration in the ethanol solution of 5 mg/mL. Cholesterol was loaded at 1% and 2.5% by weight, with respect to the PC amount. PC only based liposomes were also produced for comparison purposes. The theophylline theoretical loading was fixed at 1% w/w with respect to the lipid content. The results are summarized in **Table V.1**.

Table V.1 *Particles size distribution data for 1% theophylline loaded liposomes with 0%, 1% and 2.5% cholesterol content in the lipid layer, produced at three different water flow rates 10, 2.14 mL/min and 0.7 mL/min respectively.*

Chol. Theor. Loading [%]	1% [w/w] theophylline theoretical loading				
	WFR [mL/min]	MD± SD [nm]	PDI	Drug EE [%]	Chol EE [%]
0	10.0	192.2 ± 32	0.171	2.0	---
1	10.0	240.5 ± 40	0.170	7.3	25.9
2.5	10.0	218.7 ± 55	0.252	5.5	23.7
0	2.14	165.9 ± 60	0.362	59.5	---
1	2.14	180.1 ± 70	0.390	59.9	75.8
2.5	2.14	189.8 ± 81	0.426	58.8	76.2
0	0.70	140.5 ± 54	0.470	96.3	---
1	0.70	136.2 ± 86	0.636	98.0	80.5
2.5	0.70	170.5 ± 59	0.693	97.7	81.7

As shown in **Table V.1**, the addition of Chol in the membrane forming liposomes does not significantly affect liposome formation; the suspensions were successfully produced at all the value of Chol concentrations. The size distribution of the liposomes produced at different Chol percentages are reported in **Figure V.2**. Comparing the PSD of the PC based liposomes and PC/Chol liposomes, reported in **Figure V.2**, it is possible to observe that the presence of Chol in the lipid membrane composition did not produce any significant effects on the vesicles mean diameters and PSDs. In particular, the liposome mean diameter values were in the range between 192.2 ± 32 nm and 240.5 ± 40 nm. Nanometric liposomes were produced for all the cholesterol concentrations with PDI < 0.2. The experiment with 2.5% of Chol in the lipid layer presented the highest PDI, of about 0.252, with a longer tail. A higher amount of Chol in the lipid bilayer probably causes an enlargement of the liposome particle size distribution due to the higher steric volume of Chol crystals in the lipid membrane.

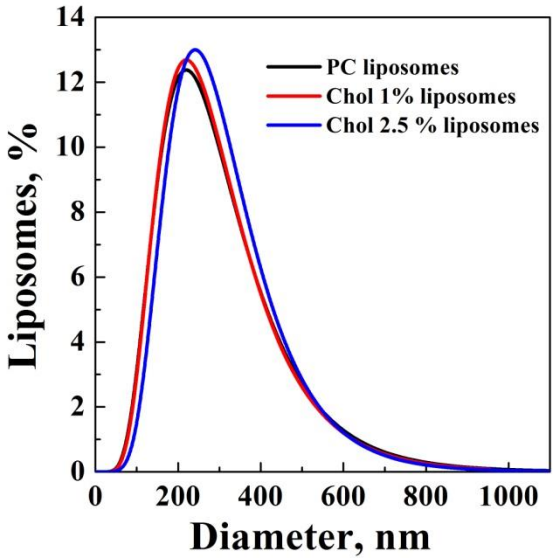

Figure V.2 *1% w/w theophylline loaded liposomes produced with different cholesterol percentages in the double lipidic layer (0, 1 and 2.5% w/w with respect to the PC mass concentration).*

The theophylline encapsulation efficiency seemed to be not affected by the Chol percentage in the lipid composition. In addition, the effective Chol loading inside the lipid membrane, measured using GC analysis, was low with an overall entrapment efficiency of Chol in the bilayer of about 25%. The increase of the Chol theoretical loading in the initial solution did not largely modify the Chol entrapment efficiency. Therefore, some experiments where performed at different water solution flow rates, according to the hypothesis that low encapsulation efficiencies were probably caused by the high velocity of the droplets atomized at the exit of the nozzle as well as by the disruption of the droplets when they impacted on the water pool located at the bottom of the formation vessel. If these events are considered, the loss of theophylline content from the water internal core of the liposomes, along with a disaggregation of the lipid bilayer could be explained.

In order to improve the theophylline encapsulation efficiency and to verify the hypothesis of the negative effect of high water flow rate on liposome efficient production, the water flow rate was reduced. The same set of experiments with different Chol loadings from 0 to 2.5% was repeated at the lower water flow rates of 2.14 and 0.7 mL/min. The theophylline theoretical loading with respect to the lipid content was maintained at 1% w/w. The results are shown in **Table V.1**. An improvement of both the Chol entrapment in the lipid layer and the theophylline encapsulation efficiency in the inner water core was successfully obtained operating with a water flow

rate of 2.14 mL/min. Chol was entrapped in the liposome membrane with a trapping efficiency of about 76.2% and theophylline encapsulation efficiency was improved up to 59.9%. At a reduced water flow rate, the phenomenon of disruption of the water droplets during the impact with the receiving water bath, at the bottom of the formation vessel, is probably reduced. This allows to obtain a higher theophylline encapsulation efficiency as well as avoid the loss of part of the lipid content from the liposome membrane. Reducing the water flow rate to 2.14 mL/min, the mean diameter of the liposome suspensions was also slightly reduced. In particular, the liposome mean diameter values were in the range between 165.9 ± 60 nm and 189.8 ± 81 nm. However, an increase of PSD amplitude was observed, PDI in the range between 0.362 and 0.426 were obtained. The reduction of the water flow rate produced a spray of water droplets characterized by a larger size distribution. Comparing the data of the PC based liposomes and the PC/Chol liposomes, it can be observed that also in this case the presence of Chol in the lipid bilayer composition did not produce any significant effects on the vesicle mean diameters, but, as also observed in the set of experiments at 10 mL/min of the water flow rate, the wider PSD was obtained at 2.5% of the Chol loading in the lipid layer. This test presented the highest PDI of the experiments at 2.14 mL/min, of about 0.426, with a longer tail of the PSD, due to a higher steric volume of Chol crystals in the liposome lipid membrane. The theophylline and Chol entrapment efficiency was not affected by the amount of Chol in the lipid composition of the liposome membrane.

A further successful increase of the Chol and theophylline entrapment efficiency was observed operating with a water flow rate of 0.7 mL/min. The theophylline encapsulation efficiency was significantly improved up to 98% and the Chol entrapment efficiency was improved up to 81.7%. 0.7 mL/min seems to be the best flow rate for an efficient PC/Chol theophylline loaded liposomes production. Liposomes suspensions were successfully produced obtaining a further reduction of the liposome mean diameters with values in the range from 136.2 ± 86 nm and 170.5 ± 79 nm. The reduction of the water flow rate produced an enlargement of the PSDs again, with PDI over 0.6, confirming the previously observed results.

These results seem to confirm that the reduction of the water flow rate from 10 to 0.7 mL/min, allows to reduce the droplets disruption at the impact on the final water bath avoiding a loss of the encapsulated drugs.

V.2 Production of PC/PE liposomes

Another set of experiments was performed using Phosphatidylethanolammine (PE) rather than Cholesterol in the lipid solution. Chol is a one-tail surfactant; whereas, PE is a two-tail surfactant. PC is classified as a cylindrical shaped phospholipid, PE is truncated conical

shaped [50]. The experiments were performed to verify if the shape of phospholipids may play a significant role in the mean dimensions of the produced vesicles. Furthermore, the composition of the lipid bilayer can affect both drug encapsulation efficiency and release kinetics. For this reason, experiments with PC and 0, 1, 2.5% (w/w) of PE content were performed at the operating conditions previously optimized for PC/Chol theophylline loaded liposomes: 100 bar, 40 °C and 0.7 mL/min water flow rate. The results are summarized in **Table V.2** and PSDs are compared in **Figure V.3**.

Table V.2 *Particles size distribution data of theophylline loaded liposomes with 0%, 1%, 2.5% of phosphatidylethanolammine (PE) content in the lipid layer, produced with the water flow rate of 0.7 mL/min.*

PE. Theor. Loading [%]	MD± SD [nm]	PDI	Drug EE [%]	PE EE [%]
0	192.2 ± 32	0.171	2.0	---
1	240.5 ± 40	0.170	7.3	25.9
2.5	218.7 ± 55	0.252	5.5	23.7

The data reported in **Figure V.3** and **Table V.2** show that the mean diameter of the liposomes is not significantly affected also by the presence of PE in the double layer. A slight decrease of the liposome mean diameter is observed increasing the PE percentage. Due to the particular shape of PE tails, a lipidic membrane with a denser packing was probably formed, resulting in lower vesicle mean dimensions. In this case, it was not possible to evaluate the PE entrapment efficiency in the lipidic double layer because PC and PE were detected in a single GC peak and it was not possible to separate the contribution of the two compounds. Regarding theophylline, the encapsulation efficiency up to 95.1 % was obtained using the optimized operating parameters.

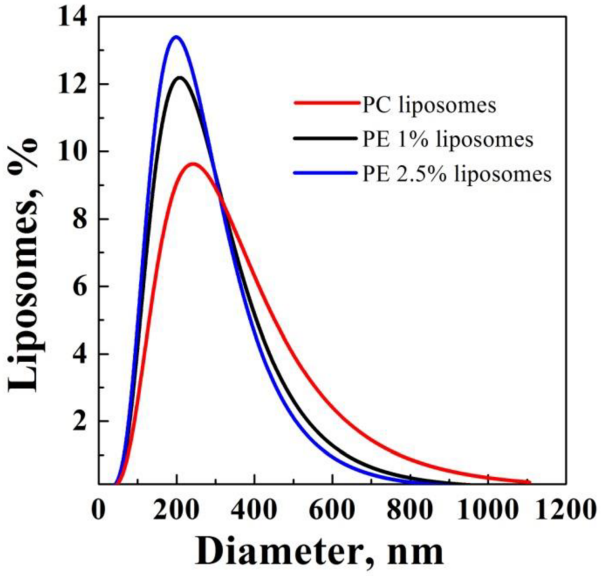

Figure V.3 *PSD of theophylline loaded liposomes produced with increasing percentages phosphatidylethanolamine (PE) encapsulated in the double lipid layer*

Transmission Electron Microscope images of the liposomes with 1% (w/w) Chol content in the lipidic layer have been produced and reported as examples in **Figure V.4**.

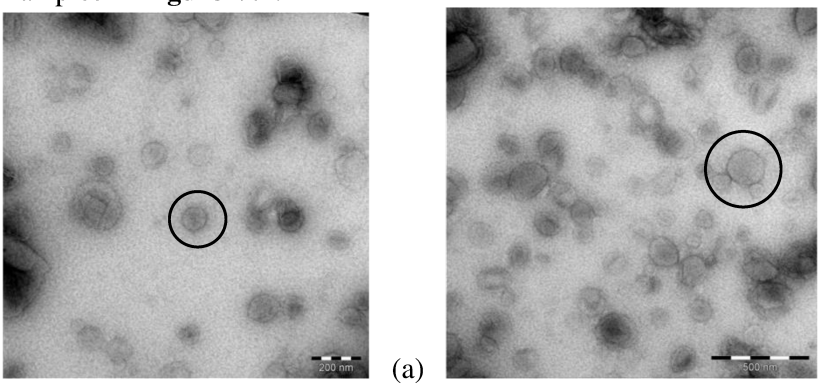

Figure V.4 *Transmission Electron Microscope images of liposome vesicles.*

These images report qualitative information about the morphology of the vesicles produced. In particular, it is possible to verify the spherical shape of the vesicles. The sample also shows a relatively wide population of liposomes. It is also possible to observe the presence of the double layer of the liposomes, whose thickness is about 30-40 nm. The concentration of the

vesicles in the aqueous bulk, obtained by Nanoparticle Tracking Analysis (NTA), was about 28.8*106 liposomes/mL.

The stability of the vesicles is the capability to retain the drug in the inner core. It was measured through the encapsulation efficiency of the liposomes sample stored at 4°C for over 40 days and controlled every 7 days. The results are reported in **Figure V.5** for the sample containing 0.5% of Chol in the lipid membrane and 1% of theophylline in the inner core, produced at 0.7 mL/min of water flow rate.

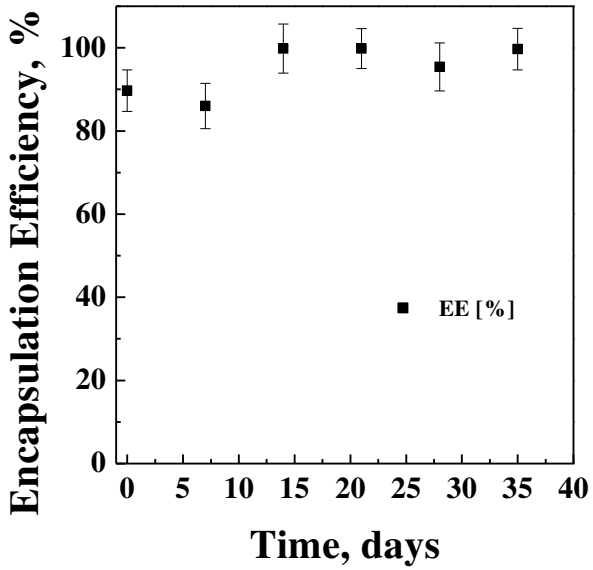

Figure V.5 *Stability of encapsulation of theophylline loaded liposomes (1% cholesterol, water flow rate 0.7 mL/min) observed over a 40 days period.*

As shown in **Table V.5**, the encapsulation efficiency remains stable over 5 weeks, without significative drug leakages. The same behavior was observed for the sample loaded using PE and for PC based liposomes. In conclusion, the presence of different lipids in the liposome membrane did not alter the vesicles stability.

In order to understand the effect of the lipid composition in the liposomes membrane on the drug release kinetics, samples produced at 0.7 mL/min water flow rate, theophylline loaded at 1% and with 0, 1 and 2.5% w/w of Chol were used to perform drug release tests at 37 °C (**Figure V.6**).

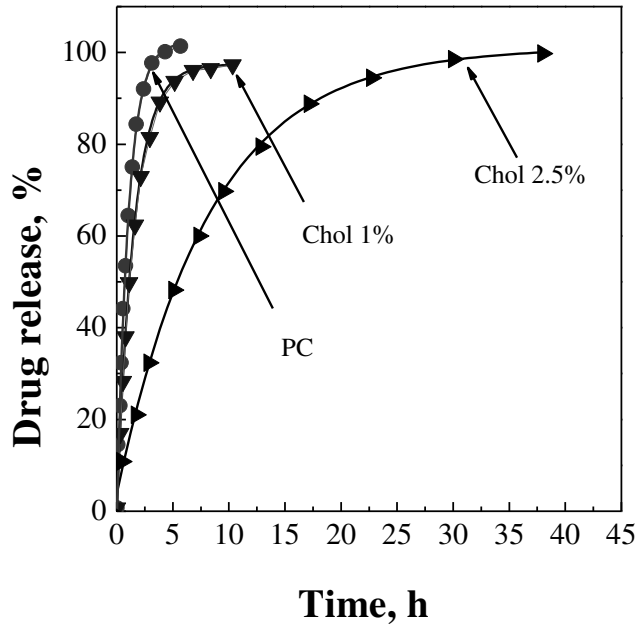

Figure V.6 *Comparison of drug release kinetics of theophylline liposomes loaded with 0, 1, 2.5% cholesterol (Chol) content in the lipid double layer, produced with 0.7 mL/min water flow rate.*

From **Figure V.6**, the liposomes with 0% cholesterol (PC based liposomes) released their total content of theophylline in about 5 hours. The 1% Chol loaded liposomes completed the release of the drug in about 9 hours; whereas, 2.5% cholesterol loaded vesicles released the total drug content after 40 h (about 2 days).

These results show that the presence of small quantities of Chol largely modify the drug release kinetics. This experimental evidence is explainable considering that Chol is reported to modify the microviscosity of the lipid membrane, affecting its fluidity; but, also to improve the integrity and the stability of the vesicles' membrane (Sankaram and Thompson, 1990). Furthermore, cholesterol is capable of increasing the hydrophobicity of the membrane (Subczynski et al., 1994), inducing a longer time retention of the hydrophobic molecules, like theophylline, encapsulated in the inner core.

For a further confirmation of the previous results, the same tests were performed for the sample produced at 2.14 mL/min of water flow rate and at different Chol percentages. These experiments confirmed the trend observed; i.e., increasing the Chol amount loaded in the lipid bilayer, slower drug release kinetics were obtained. In order to understand the effect of PE on

theophylline drug release kinetic, a release test was performed for liposomes loaded with 2.5% of PE. The results are shown in **Figure V.7**, where also the release kinetics obtained for the sample at 2.5% of Chol and for un-processed theophylline are reported for comparison purposes.

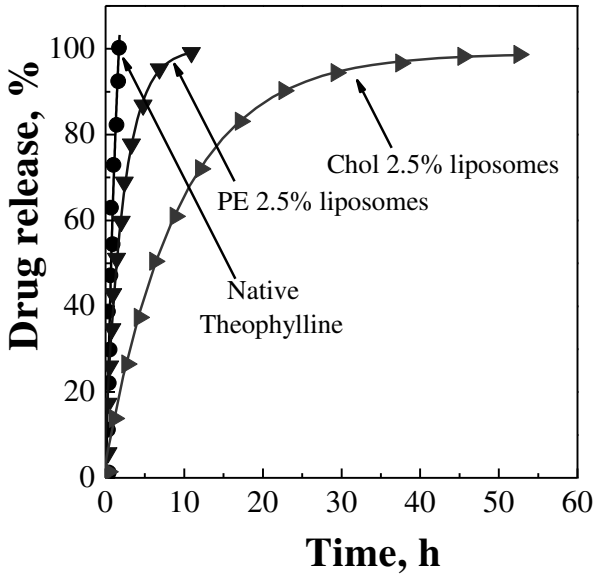

Figure V.7 *Drug release kinetics comparison between un-processed theophylline, 2.5% cholesterol (Chol) loaded liposomes and 2.5% phosphatidylethanolamine (PE) loaded liposomes, produced at water flow rate of 0.7 mL/min.*

The presence of PE again slows down the release kinetics of theophylline, the PC/PE liposomes released the total drug content after about 10 h; whereas, un-processed theophylline is rapidly dissolved in less than 1.5 hours. Comparing this result with the PC/Chol drug release kinetic, it is possible to observe that the strongest effect on the drug release kinetic decrease was obtained when 2.5% of Chol was loaded into the lipid bilayer. This result can be explained considering that, probably, the addition of Chol contributes to increasing the integrity and stability of the lipid membrane more than PE.

The composition of the lipid layer did not significantly affect the liposome size distribution, vesicles stability over time and drug encapsulation efficiency, but demonstrated, even at low concentrations, considerable effects on the drug release kinetics. The modifications of the fluidity and the permeability of the lipid bilayer with the addition of different

lipids into liposome membrane are relevant to prolong drug release rate from these liposomes.

Chapter VI

Encapsulation of antioxidants

The controlled delivery of antioxidants (Turek and Stintzing, 2013) is of interest for therapeutic (Stone and Smith, 2004) and cosmetic (Jiang et al., 2011) applications. For example, eugenol (EUG, 4-allyl-2-methoxyphenol) has a remarkable antioxidant activity, thanks to its antibacterial and antifungal properties (Guan et al., 2016). It is generally used as a food flavoring agent, as an additive to fragrances and in active packaging applications (Baskaran et al., 2010, Devi et al., 2010, Zhang et al., 2000). In addition, α-lipoic acid (ALA) (Packer et al., 1995) possesses an antioxidant activity and is often used in human diets due to its functional properties (Abdel-Zaher et al., 2008). Moreover, it can be used as a therapeutic agent to prevent some pathologies, like diabetes (Zhang et al., 2016, Alvarez-Rivera et al., 2016). However, antioxidants are generally unstable and sensitive to oxygen, light and heat (Garg and Singh, 2011, Choi et al., 2009, Mourtzinos et al., 2008). Microorganisms can also use these compounds as substrates (Tadasas, 1983). For these reasons, it is preferable to protect and deliver them using a carrier.

It has been recognized that nanoencapsulation offers various benefits such as enhanced stability, protection against oxidation, retention of volatile compounds, reduced toxic effects and enhanced bioavailability (Neethirajan and Jayas, 2011, Nedovic et al., 2011).

EUG loaded liposomes were produced using thin film hydration and reversed-phase evaporation methods (Sebaaly et al., 2016b, Sebaaly et al., 2016a, Espirito Santo et al., 2015a). However, these techniques suffer from many drawbacks because they require complex post-treatment steps. The produced liposomes are not homogeneous and Particle Size Distribution (PSD) is difficult to replicate. Encapsulation Efficiencies (EE) are generally lower than 30 % of the theoretical loading for hydrophilic compounds. For example, some authors attempted to protect EUG using encapsulation in nanoparticles, nanocapsules, microcapsules and liposomes (Woranuch and Yoksan, 2013). Nanoparticles with antioxidant EE of about 20% were produced under optimized operating conditions. Some authors tried to entrap ALA in microspheres, using chitosan as the polymeric matrix (Weerakody et al., 2008), obtaining micrometric ALA-loaded particles with 55 % encapsulation efficiency; however, a reduction of the antioxidant activity of lipoic acid of 25% after encapsulation in the chitosan matrix was observed.

SuperLip has been tested for the entrapment of lipophilic compounds that in principle can only be included in the lipid bilayer. This operation can destabilize the vesicles integrity. Therefore, the production of submicro liposomes containing EUG and ALA considered as model lipophilic antioxidant compounds was attempted to avoid drug degradation caused by light and heat as well as improve drug vehiculation and its bioavailability.

VI.1 Eugenol and α-lipoic acid encapsulation in liposomes

It is possible, in principle, to encapsulate EUG either in the lipophilic core or in the lipidic layer, since this compound is soluble both in ethanol and water. The first experiments were performed to try to encapsulate EUG in the classical way, using the hydrophilic core, adopting theoretical loadings of 10, 20 and 30 % w/w with respect to phosphatidylcholine (PC).

The process temperature was set at 35 °C in the first set of experiments; then, it was set to 40 °C.

The **possibility of changing the temperature in the SuperLip** system was limited by the lower limit of 31.1 °C (critical temperature for carbon dioxide) and 45 °C, when not modified lipids are subjected to degradation.

Pressure was fixed at 100 bar and water flow rate to 10 mL/min. The first The mean diameters, polydispersion indexes (PDI), encapsulation efficiencies (EE) and antioxidant power of the EUG-loaded liposomes are summarized in **Table VI.1**.

Table VI.1 *Diameter, Polydispersion Index (PDI), EE and antioxidant power of Eugenol loaded liposomes*

Test	Theoretical Loading [%, p/p]	Mean Diameter [nm ± SD]	PDI	EE [%]	Inhibition reduction [%]
35 °C	10	224 ± 81	0.36	84.3	8.2
inner	20	151 ± 69	0.46	86.2	6.4
core	30	139 ± 69	0.50	84.1	7.5
40 °C	10	260 ± 91	0.35	80.4	10.0
inner	20	196 ± 76	0.39	92.5	9.6
core	30	188 ± 113	0.60	94.2	10.7
40 °C	10	255 ± 122	0.48	83.9	10.6
lipid	20	234 ± 101	0.43	86.3	22.2
layer	30	230 ± 96	0.42	84.9	41.9

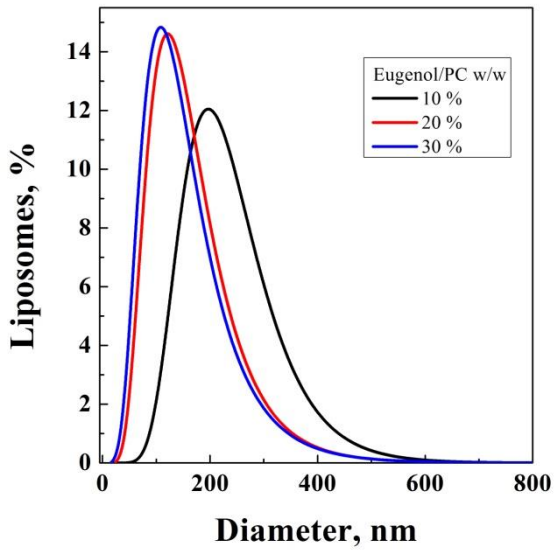

Figure VI.1 *PSD of liposomes core loaded with 10, 20 and 30 % eugenol, produced at the temperature of 35 °C*

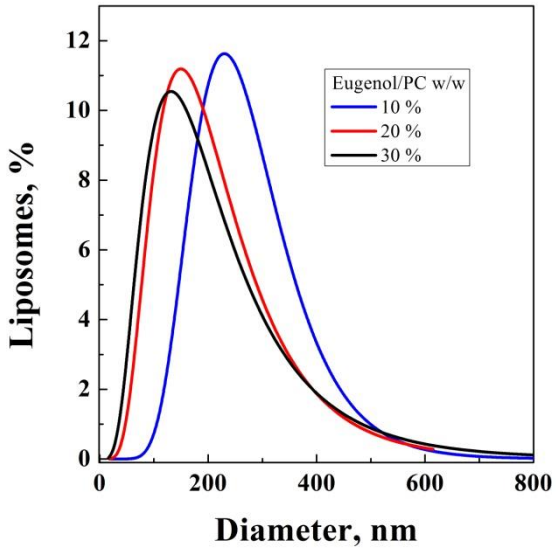

Figure VI.2 *PSD of liposomes core loaded with 10, 20 and 30 % eugenol, produced at the temperature of 40 °C*

In detail, operating at 35 °C the liposomes mean diameter decreased from 224 ± 81 nm to 139 ± 69 nm by increasing the EUG theoretical loading from 10 to 30 % w/w; PDI also increased from 0.36 to 0.50. These results are well represented by the particle size distributions reported in **Figure VI.1**. The entrapment of the hydrophilic drug seemed not to be affected by the concentration of drug. EE was nearly constant, ranging from a minimum of 84.1 % to a maximum of 86.2 %. Antioxidant activity of the encapsulated EUG was measured using the DPPH assay, as described in the Methods section; processed EUG showed an almost constant inhibition capacity, with a slight decrease of the inhibition compared to the native compound. The inhibition reduction ranged between 6.4 and 8.2 %, meaning that the molecules entrapped in the liposomes have approximatively the same antioxidant power of the unprocessed compound. These results confirmed that the mild operating conditions adopted in SuperLip allow to encapsulate EUG with high EE, preserving its antioxidant power.

The second set of experiments was performed to explore the effect of the temperature on liposome formation. In these experiments, the process temperature was set to 40 °C, maintaining constant all the other operating parameters (see **Table VI.1).**

The data reported in **TableVI.1** and the particle size distributions of **Figure VI.2**, show that the EUG containing liposomes were still of nanometric dimensions; the vesicles' mean diameter was included between 260 ± 91 nm and 188 ± 113 nm, with a PDI from 0.35 to 0.60. In this case, the mean diameters decreased when the EUG theoretical loading was increased. Furthermore, PSDs maintained the same trend observed in the experiments performed at 35 °C. Regarding EUG EE, the samples processed at 40 °C showed larger encapsulation efficiencies. For this set of experiments, EE increased up to 94.2 %; i.e., with an increase of about 10 % with respect to EE obtained at 35 °C. The antioxidant power of the processed eugenol was still not largely reduced with respect to the unprocessed compound, with an inhibition reduction between 9.6 and 10.7 %. According to the results obtained, 40 °C can be considered a better condition to obtain a good control of PSD and high EE and antioxidant power preservation. Therefore, this parameter was fixed at 40 °C in all the following experiments.

The successive set of experiments was performed to study the possibility to incorporate EUG in the lipidic double layer. Theoretical loadings of EUG with respect to lipid content in ethanol solution were fixed again at 10, 20 and 30 % w/w in PC for comparison purposes; but, in this case, EUG was dissolved in the ethanolic solution instead of the water solution. The working temperature was set to 40 °C, as well as the pressure at 100 bar and the water flow rate at 10 mL/min.

Looking at results shown in **Table VI.1** and **Figure VI.3**, it is possible to see that liposomes of nanometric dimensions were produced and their mean

diameters ranged between 255 ± 122 nm and 230 ± 96 nm; in this case, only a slight decrease of the mean diameter, increased EUG theoretical loading, was observed. Comparing these results with the liposomes obtained when EUG was loaded in the inner core at the same temperature, in this case, the mean diameters are larger. Regarding the EE of the samples loaded with 10, 20 and 30 % w/w theoretical loading, EUG was entrapped successfully also in the lipidic double layer, with EE up to 86.3 %. This result means that PC, dissolved in the expanded liquid, succeeds in holding the compound during the process of liposome formation. However, looking at **Table VI.1**, it is possible to note that EUG entrapped in the lipidic membrane was more significantly damaged. The reduction of the antioxidant power is more relevant, if compared to liposomes with eugenol encapsulated in the inner core and, also, an increase of the inhibition reduction can be noted at larger EUG theoretical loadings. This degradation phenomenon could be due to the fact that EUG dissolved in ethanol is subjected to harder process conditions, compared to EUG dissolved in the inner liposome core.

The possibility to encapsulate lipophilic compounds in a liposome double lipidic layer was also tested for ALA. Since ALA is not soluble in water but highly soluble in organic solvents, the encapsulation tests were performed only in the lipidic layer of liposomes, using the same parameters found for EUG-loaded liposomes: the temperature was set to 40°C, the water flow rate to 10 mL/min and the pressure to 100 bar (**Table V.2**). To compare them to the eugenol-loaded liposomes, the concentration of ALA was 10, 20 and 30 % w/w in PC, as well. The particle size distributions are compared in **Figure VI.4**.

Table VI.2 *Mean diameters, Polydispersion index (PDI), EE and antioxidant power of ALA loaded liposomes*

Test	Theoretical Loading [%, p/p]	Diameter [nm ± SD]	PDI	EE [%]	Inhibition reduction [%]
40 °C	10	244 ± 86	0.35	**55.7**	13.3
lipid	20	187 ± 75	0.40	**68.1**	22.6
layer	30	109 ± 49	0.45	**63.1**	62.8

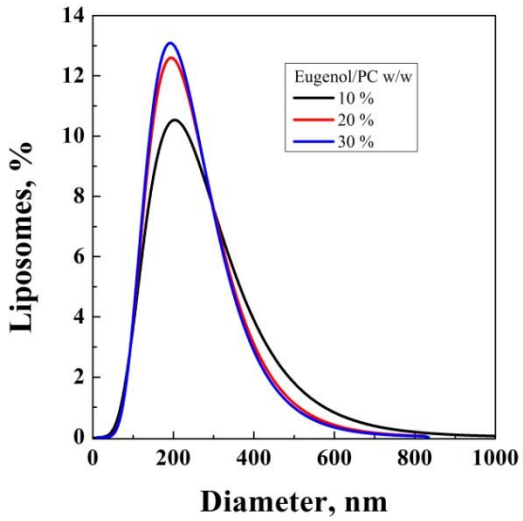

Figure VI.3 *PSD of liposomes lipidic layer loaded with 10, 20 and 30 % eugenol, produced at the temperature of 40 °C*

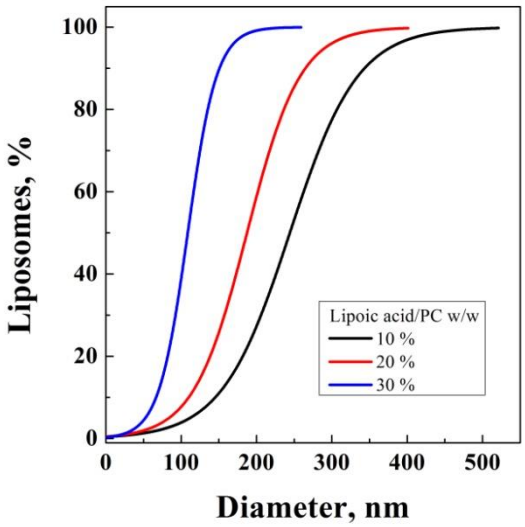

Figure VI.4 *Cumulative curves of liposomes loaded with 10, 20 and 30 % w/w ALA, produced at the temperature of 40 °C*

The liposomes mean diameters decreased from 244 ± 86 nm to 109 ± 49 nm, increasing the theoretical loading of the lipophilic drug. **Figure VI.4** shows the PSDs of the experiments performed using different percentages of ALA in the lipidic solution: it is possible to observe that increasing the ALA content in the lipidic double layer, a reduction of the vesicles mean diameters was obtained. Moreover, also the PDI of the ALA-loaded samples decreased, increasing the ALA theoretical loading. The same trend was observed for the EUG double layer encapsulation experiments, but the average mean diameters were higher in the case of the ALA loaded vesicles. This decreasing trend is a general behavior of additives introduced into liposome double layers, as reported in literature for other lipidic compounds such as cholesterol (Bae et al., 2016).

EEs measured for this set of experiments ranged between 55.7 % and 68.1 %, that are lower if compared to EEs obtained for EUG double layer encapsulation tests. The inclusion of ALA in the phospholipids double layer structure is probably more difficult than EUG due to the higher molecular weight and steric volume of ALA. Regarding the antioxidant power of processed ALA, the results related to the inhibition of the processed compound compared to the inhibition of the native compound, presented in **Table VI.2**, show that the reduction of the inhibition property is higher at increased ALA theoretical loadings. Inhibition reduction is 13.3, 22.6 and 62.8 % for 10, 20 and 30 % w/w in PC loaded liposomes, respectively. The last result indicates that 30 % w/w loading in PC is particularly unfavorable.

EUG and ALA entrapped in the lipidic layer showed similar trends: a higher inhibition reduction is detected by increasing the drug theoretical loading, for both compounds. As a general comment, higher inhibition reductions are observed in the case of antioxidants encapsulation in the lipid compartment of liposome vesicles. Probably, when the molecule is confined in the water inner core, it is better protected from external degradation agents.

EUG loaded liposomes were observed by Scanning Electron Microscopy (SEM). In **Figure VI.5a,** liposomes loaded with EUG in the inner water core are reported, whereas, in **Figure VI.5b** liposomes loaded with EUG in the lipidic layer are shown.

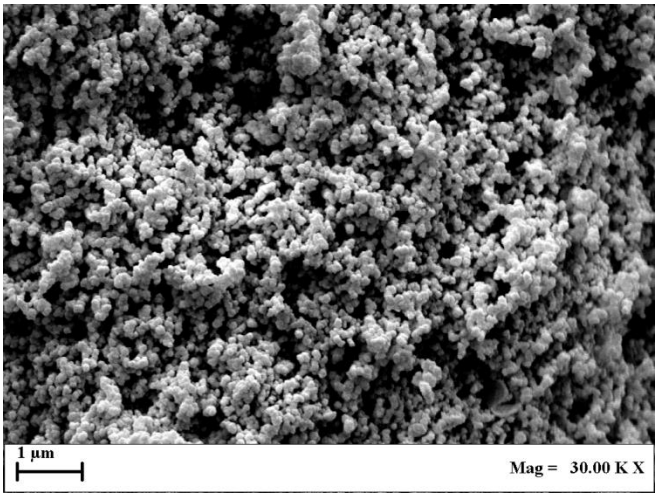

(a)

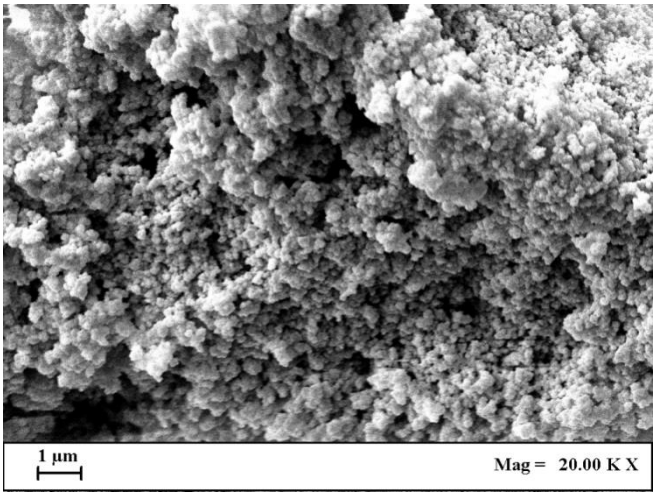

(b)

Figure VI.5 *SEM images of the samples (a) eugenol loaded in the inner core at 35 °C and (b) eugenol loaded in the double lipidic layer at 40 °C.*

The liposomes in **Figure VI.5** present a spherical shape and a smooth surface. The size analysis performed on SEM images confirm the liposome mean diameters between 100 and 200 nm when EUG is loaded in the inner core, whereas mean diameters of about 250 nm are observed in the case of lipophilic loaded liposomes.

ALA-loaded samples are also observed by SEM for the three different loadings, as shown in **Figure VI.6**.

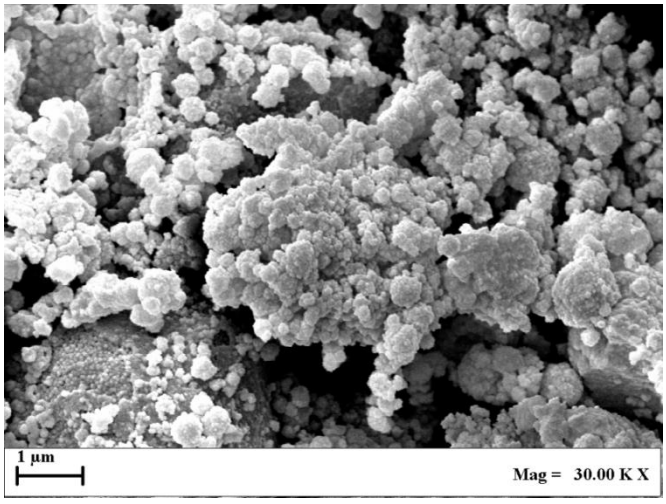

(a)

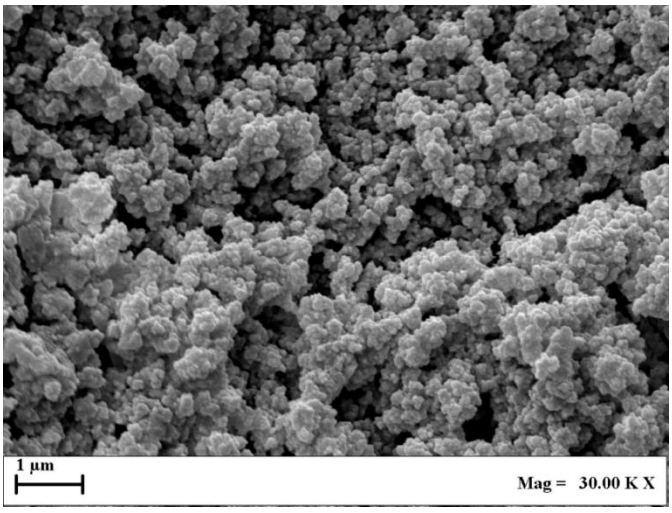

(b)

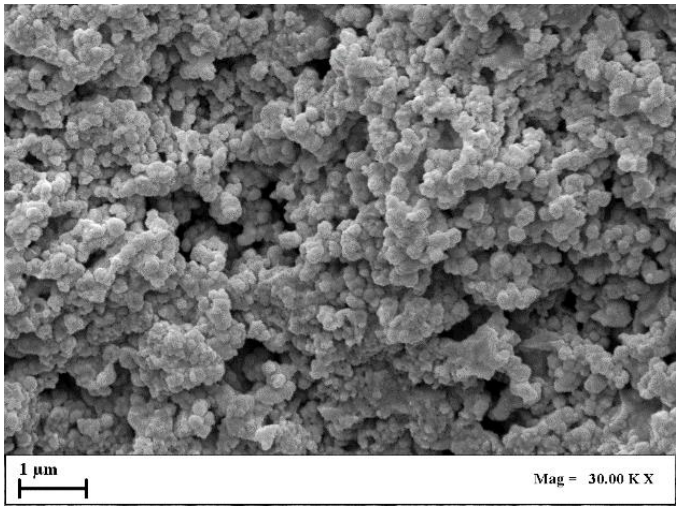

(c)

Figure VI.6 *SEM images of the experiments (a) ALA1, loaded with 10 % w/w (b) ALA2, 20 % w/w (c) ALA3, 30 % w/w lipoic acid at the temperature of 40 °C*

The inclusion of ALA in the lipid double layer does not modify the shape and morphology of the produced liposomes. However, the vesicles appear aggregated probably due to sample dehydration and metallization procedure for microscopy observation.

To further characterize the obtained liposomes, drug release tests were performed on liposomes loaded with 10 % w/w EUG in the inner core and in the lipidic layer. Drug release tests were performed at 30°C and 60 °C, to study the different release behavior of the antioxidant loaded in the water or in the lipidic compartment (see **Figure VI.7**).

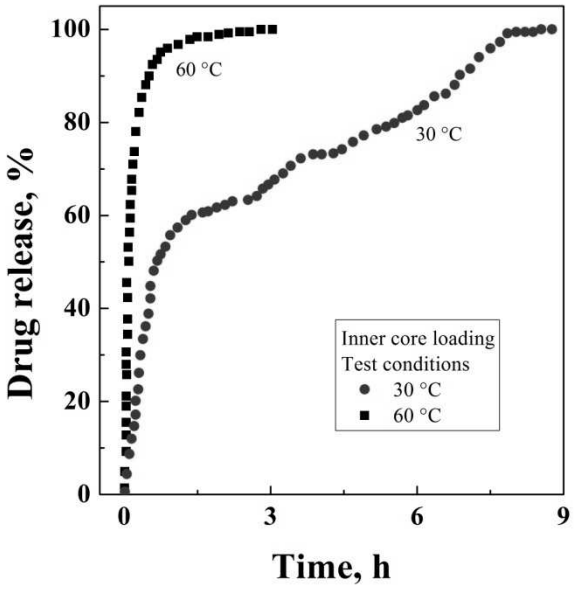

(a)

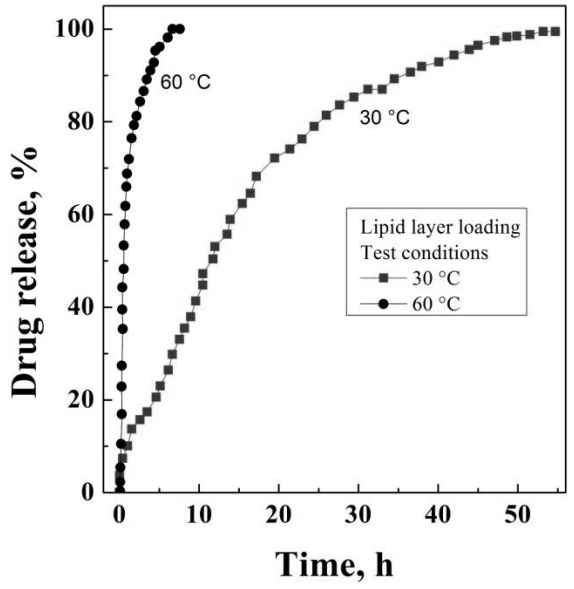

(b)

Figure VI.7 *Drug release tests on liposomes with inner core (a) and lipidic layer (b) loaded with 10 % w/w eugenol/lipids*

Considering the release of EUG from the inner water core of the liposomes, reported in **Figure VI.7a**, drug release performed at 30 °C (red line) reached the plateau after about 8 h. When the temperature was increased to 60 °C (black line), 100 % drug release was obtained after about 3 h. Furthermore, in the test performed at 60 °C, about 80 % of the release is obtained in the first minutes in about 0.15 h. These results indicate that these liposomes are temperature sensitive. Increasing the temperature an increased mobility of the lipidic membrane is probably obtained causing a faster drug release from the inner water core to the external release medium. When EUG is entrapped in the external liposome lipidic layer, slower EUG release rates are observed both at 30°C and 60 °C, as it is possible to note from **Figure VI.7b**. In particular, it is possible to see that the release curves follow the same trend observed for the inner core loaded liposomes (**Figure VI.7a**): an increase of the drug release rate is observed at higher temperatures, but the release times of the drug entrapped in the lipidic layer are higher than the ones shown in **Figure VI.7a**. When EUG is loaded in the lipidic layer, drug release performed at 30 °C is completed after about 55 h, while the drug release test performed at 60 °C is completed after about 10 h. This general behavior is probably due to the fact that EUG molecule is confined to the lipidic compartment of the double phospholipid membrane and, in this way, is less available for dissolution in the external water release medium with respect to EUG dissolved in the inner water core.

It has been verified whether SuperLip can produce liposomes loaded with antioxidant lipophilic compounds included in the phospholipid double layer structure and a comparison with inner core encapsulation performed, obtaining indications about the encapsulation efficiency and reduction of the antioxidant activity. Considering the SuperLip liposome formation mechanism, it could be hypothesized that the lipidic drug spontaneously distributes in the lipidic compartment of the vesicles during liposome formation thanks to the chemical affinity with lipids and water repulsion. The inclusion of the drug in the lipid membrane is more successful for the antioxidant with the lower molecular weight, EUG, that was entrapped with an overall efficiency of 86.3 %, ALA was entrapped with a maximum EE of 68.1 %. It is confirmed that encapsulation in the aqueous phase is the most successful route to obtaining high drug entrapment efficiencies. Furthermore, it was also possible to better preserve the antioxidant power of the entrapped molecules. Longer release times were obtained for the encapsulated compounds in the lipidic layer. This result could be considered an advantage of this location of the active compounds.

VI.2 Oil in Water emulsions entrapped into liposomes

Lipophilic antioxidants (farnesol, limonene, linalool) were entrapped in liposomes double lipidic compartment, using SuperLip. A novel idea of entrapping lipophilic molecules has also been proposed: first they were dissolved in an oil phase of an Oil in Water emulsion (O/W); then, the emulsion is entrapped in the inner core of the liposomes. Vesicles loaded with antioxidants in the lipidic layer showed a mean size from 116 ± 32 nm to 230 ± 103 nm, with EE up to 74 % for farnesol, 87 % for limonene and 54 % for linalool; whereas, O/W entrapment in the inner core resulted in higher mean dimensions (from 397 ± 103 nm to 605 ± 175 nm), and EE up to 99 %. The reduction of inhibition power was up to 22.47 % for lipidic layer entrapment; whereas, it was down to 1.93 % for O/W entrapment.

For this reason, 3 lipophilic antioxidant model molecules such as limonene, linalool and farnesol were chosen to be entrapped in the lipidic layer of liposomes, with the SuperLip process. Since only hydrophilic compounds can be entrapped in the inner core of vesicles, lipophilic antioxidants will be dissolved in the oil phase of an Oil in Water emulsion to entrap the antioxidants in the inner aqueous core. A novel approach for the encapsulation of lipidic compounds will be presented, with the aim of preserving the antioxidant properties. The inhibition power reduction of lipophilic antioxidants loaded in the double lipidic layer of liposomes will be compared with the encapsulation in the inner core. Moreover, the simultaneous entrapment of antioxidants in liposomes will be studied to verify the effects of molecules interactions on encapsulation efficiencies and antioxidant activity.

Despite their efficiency, antioxidants are generally characterized by high volatility and low bioavailability and can suffer from degradation caused by contact with oxygen, light and heat. This was thought as a way to overcome those problems, entrapping antioxidants into liposomal drug carriers.

VI.2.1 Antioxidants lipidic layer entrapment

To preserve antioxidant properties, liposomes were employed to entrap farnesol, linalool and limonene in their lipidic layer, i.e. in the external lipophilic compartment of the vesicles. The chosen antioxidants are lipophilic and not available for the entrapment in the aqueous core.

The experiments were divided into two groups: lipidic compartment and emulsion core entrapment. For this reason, the SuperLip process was used, setting the pressure at 100 bar, lipidic mass at 500 mg and ethanol flow rate at 3.5 mL/min, Gas to Liquid Ratio of the Expanded Liquid at 2.4 and water flow rate at 10 mL/min.

The first set of experiments was characterized by liposomes loaded with a farnesol theoretical loading of 10 %, 20 % and 30 % w/w on a lipid mass

base. The same concentration trends were also repeated for linalool and limonene loaded liposomes, using the same process parameters. Then, the simultaneous entrapment of linalool + limonene and limonene + farnesol was finally attempted.

The mean diameters, polydispersion indexes, zeta potentials and encapsulation efficiencies are reported in **Table VI.3**. The particles size distributions of the 3 sets of experiments are compared in **Figure VI.8**.

Table VI.3. *Mean diameter, polydispersion index, zeta potential and encapsulation efficiency of liposomes loaded with farnesol, limonene and linalool in the double lipidic layer*

Compound	Theoretical loading [%, w/w]	Mean Diameter [nm ± SD]	PDI	Zpot [mV]	EE [%]
Farnesol	10	146 ± 44	0.30	-13.6	22
	20	132 ± 45	0.34	-12.3	65
	30	126 ± 35	0.27	-10.2	74
Limonene	10	121 ± 42	0.35	-13.2	67
	20	116 ± 32	0.28	-10.9	87
	30	159 ± 44	0.28	-9.4	87
Linalool	10	197 ± 122	0.62	- 16.4	5
	20	213 ± 128	0.60	- 10.2	36
	30	230 ± 103	0.45	-4.9	54
Lin + Far	30 ; 30	81 ± 23	0.28	-11.4	Lin 61 Far 70
Lim + Lin	30 ; 30	121 ± 44	0.36	-8.83	Lim 90 Lin 61

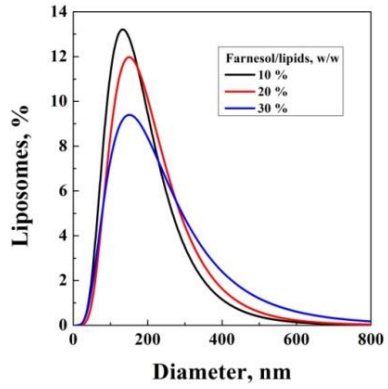

(a)

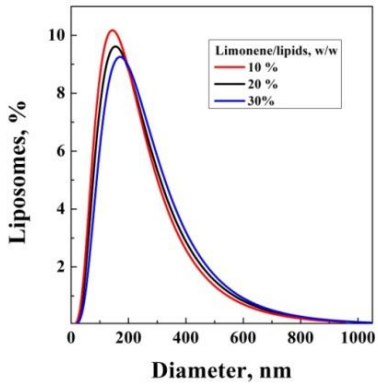

(b)

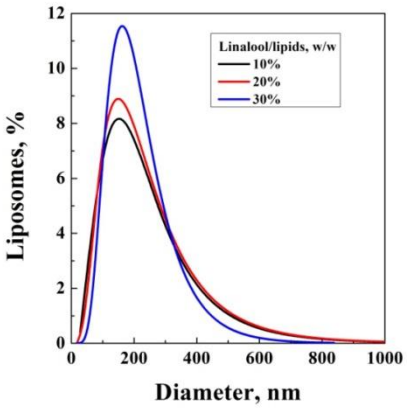

(c)

Figure VI.8 *Farnesol (a), Limonene (b) and Linalool (c) loaded liposomes at different theoretical loadings (10 %, 20 % and 30 % w/w on lipid mass base)*

The mean diameter of farnesol loaded liposomes decreased by increasing the farnesol theoretical loading, with values included between 146 ± 44 nm for 10 % loaded liposomes and 126 ± 35 nm for 30 % theoretical loading. The trend is confirmed by **Figure VI.8a**. However, the mean dimensions do not change significantly by increasing the farnesol loading, as well as the sample polydispersion indexes: a minimum value of 0.27 was obtained for 30 % loaded liposomes; whereas, a maximum of 0.34 was registered for 20 % farnesol/lipid ratio. The surface charge of the vesicles was characterized by a decreasing trend from -13.6 mV to -10.2 mV, describing a general stability of the lipidic vesicles. The encapsulation efficiency was 22 % for the experiment performed at the lowest farnesol concentration; whereas, it was 65 % for 20 % w/w theoretical loading and 74 % for 30 % w/w farnesol cargo on the lipid mass base.

The second set of experiments was performed at the same operating conditions of the first set, using the same theoretical loading of limonene on the lipidic mass ratio. The particle size distributions are compared in **Figure VI.8b**. The liposomes average dimensions are included between a minimum of 116 ± 42 nm and 159 ± 32 nm, describing a slight increase by increasing the antioxidant theoretical loading to 30 % w/w. PDIs decreased from a maximum of 0.35 to 0.28. In this case, the zeta potential showed a decreasing trend from -13.2 mV to -9.4 mV. The encapsulation efficiency was characterized by the same increasing trend obtained for the previous set, from 67 % (10 % w/w) to 87 % (30 % w/w).

The third set was finally realized entrapping linalool inside liposomes produced with SuperLip (**Figure VI.8c)**. In this case, a more significant increasing trend in the liposomes mean diameters was obtained, with a minimum of 197 ± 122 nm to a maximum of 230 ± 103 nm. The particles size distributions of **Figure VI.8c** are polydispersed, confirming the decreasing trend of the PDI from 0.62 of the less concentrated sample to 0.45 produced at higher linalool concentrations. The decreasing trend is also confirmed for the zeta potential, whose values varies from -16.4 mV to -4.9 mV, indicating a higher stability of the sample at a lower concentration (10 % w/w on lipid mass base). The encapsulation efficiencies again showed an increasing trend by increasing the linalool theoretical loading, but the values were significantly lower than the farnesol and limonene entrapped vesicles (from 5 % to 54 %). This is probably linked to the molecular interactions of the linalool loaded samples, that maybe were affected by the Wan Der Walls forces between the lipids and not entrapped antioxidant molecules.

Since the experiments performed on the single compound entrapment were successful using the SuperLip process, the simultaneous encapsulation of antioxidants was attempted to verify the feasibility of an antioxidant mixture entrapment in liposomes. Farnesol and linalool were first entrapped into liposomes with a theoretical loading of 30 % w/w (farnesol to lipid ratio) and 30 % w/w (linalool to lipid ratio) on the mass base. The mean

diameter of the liposomes produced were 81 ± 23 nm and the PDI was equal to 0.28. Zeta potential was -11.4 mV; whereas, the encapsulation efficiency was 61 % for the linalool entrapment efficiency and 70 % for the farnesol entrapment efficiency. The two values of the encapsulation efficiencies were detected separately since the detection peak of the two compounds are sufficiently different. In the case of simultaneous encapsulation, the linalool entrapment efficiency was higher than the single entrapment, varying from 54 % to 61 %. A more evident increase was obtained for the farnesol entrapment loading from 4 % to 70 % switching from a single to simultaneous encapsulation.

A second mixture of the antioxidants of limonene and linalool were entrapped in the double lipidic layer of liposomes, maintaining the operating and composition parameters of the previous experiment constant. In the second attempt of simultaneous entrapment, the sample obtained was less dispersed, showing a mean diameter of 121 ± 44 nm, a PDI reduced to 0.36 with respect to the linalool loaded liposomes and a zeta potential of -8.88 mV. In this case, the simultaneous entrapment resulted in an increased EE of the two compounds, that were 90 % for limonene and 61 % for linalool, whereas they were 87 % and 54 % respectively.

VI.2.2 Emulsions inner core entrapment

The second part of this study consisted of the optimization of the SuperLip process to increase antioxidant encapsulation efficiencies. Instead of modifying the operating parameters such as pressure, gas to liquid ratio or water flow rate, the entrapment of antioxidant compounds was attempted in the aqueous compartment of liposomes. Nevertheless, the lipophilic nature of the antioxidants such as limonene and linalool did not allow to perform this step in the aqueous core. For this reason, the antioxidants were first emulsified in Oil in Water emulsions and then the emulsions were processed with SuperLip and entrapped in the inner core of the liposomes.

Limonene and linalool were first emulsified in oil in water emulsions and then the emulsions were processed with SuperLip and entrapped in the inner core of liposomes. Farnesol was not tested for emulsion encapsulation, because its solubility into isopropyl myristate was negligible and also not indicated in literature.

Limonene and linalool oil in water emulsions were produced and the amount of antioxidant dissolved in the oil phase of the emulsion was the same loaded in the double lipid compartment in the previous set of experiment. In this way 10 %, 20 % and 30 % w/w theoretical loading of antioxidant were tested. The results are reported in **Table IV.4**.

Table VI.4 *Mean diameters, polydispersion indexes and zeta potential of droplets obtained by Oil in Water emulsions loaded with limonene and linalool.*

Compound	Theoretical loading [%, w/w]	Mean Diameter [µm ± SD]	PDI	Zpot [mV]
Limonene	10 %	4.1 ± 2.3	0.56	-17.0
	20 %	3.9 ± 1.3	0.33	-15.1
	30 %	3.7 ± 0.8	0.21	-16.5
Linalool	10 %	3.5 ± 1.6	0.46	-14.7
	20 %	3.4 ± 1.3	0.38	-10.1
	30 %	2.5 ± 0.8	0.33	-9.0

From **Table VI.4**, it is possible to observe a decreasing trend of the droplets mean diameter, from 4.1 ± 2.3 µm for 10 % w/w loaded sample to 3.7 ± 0.8 µm for the 20 % w/w loaded droplets. The same decreasing trend was obtained for the PDI of the droplets size distributions from 0.56 to 0.21 by increasing the limonene theoretical loading, related to a less dispersed sample (**Figure VI.8a**). The zeta potential was again decreased from -17 mV to -16.5 mV, but not significantly. Since the encapsulation efficiency was measured from the supernatant of the liposomes centrifuged suspensions, it was not measured only for emulsions, but directly from the final liposomes in which the emulsions were then entrapped.

The second set of emulsions was obtained entrapping limonene in the oil phase. In this case, the droplets mean dimensions showed a decreasing trend increasing antioxidant theoretical loading, included from a maximum of 3.5 ± 1.6 µm for 10 % w/w to 2.5 ± 0.8 µm for 30 % w/w loaded emulsions; the same decreasing trend was obtained for PDI from 0.46 to 0.33, resulting in a narrower particle size distribution by increasing DLR (**Figure VI.8b**). Sample zeta potentials showed a decreasing trend from -14.7 mV to -9 mV. These two results confirmed the trend reported for the limonene loaded emulsions.

Optical microscope was employed to observe oil in water emulsions before their entrapment into liposomes; an example of limonene loaded emulsion is reported in **Figure IV.9**.

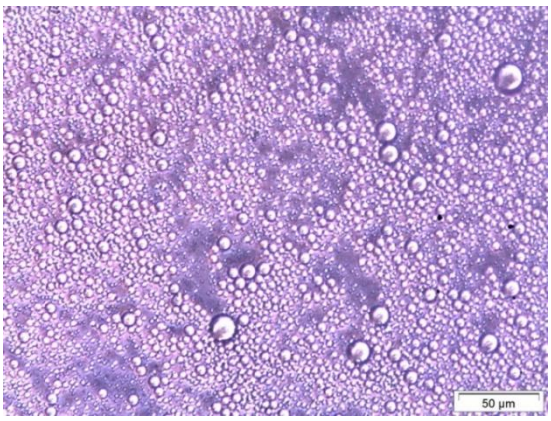

Figure IV.9 *Optical image of limonene loaded emulsions*

It is possible to observe that droplets have micrometric mean dimensions, with an almost good control of particle size distribution. The emulsion is also successfully formed and stable in the aqueous bulk.

The produced emulsions were processed with SuperLip process, maintaining the process conditions: pressure set at 100 bar, temperature at 40 °C, Gas to Liquid Ratio of the Expanded Liquid at 2.4, water flow rate at 10 mL/min and ethanol flow rate at 3.5 mL/min.

To study the effect of liposomes in SuperLip process and its rearrangement in the formation vessel, an empty oil in water emulsion was prepared and then processed in SuperLip to create liposomes loaded with empty emulsions.

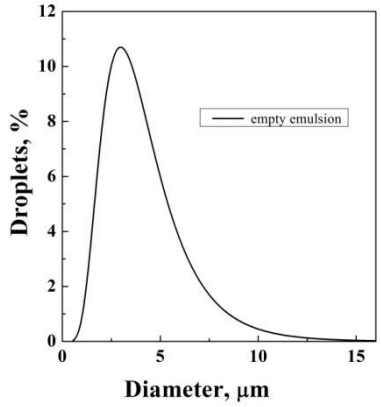

(a)

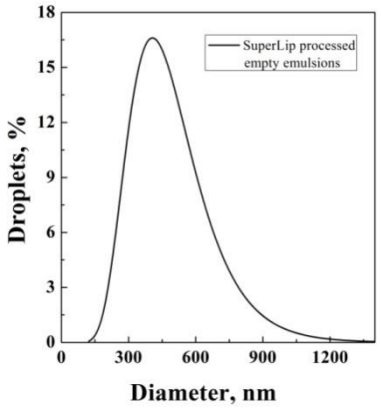

(b)

Figure IV.10. *Particle Size Distributions of empty oil in water emulsion (a) and empty emulsion loaded liposomes produced with SuperLip (b)*

From **Figure IV.10** it was possible to affirm that the re-assemblement of emulsions in SuperLip process was confirmed, obtaining droplets at sub-micrometric and nanometric level, with a narrower particle size distribution. The hypothesized phenomenon was not affected by the antioxidant entrapped in the emulsions, but by fluid dynamics. In details, the mechanisms involved in particle re-arrangement could be affected by several parameters, such as the Gas to Liquid Ratio of the liquid phase in the receiving medium (Ochowiak, 2012), turbulent shear forces and viscosity of the medium (Perrier-Cornet et al., 2005). In particular, increasing the viscosity of the system, a mitosis-like jet disruption occurs (Floury et al., 2000). Moreover, high pressure jet technique is already commonly used to obtain emulsion droplets at nanometric level; the higher is the energy density (Karbstein, 1995) of the atomization due to nozzle micrometric diameters and high pressure, the smaller the droplets (Marie et al., 2002). A

corroborative explanation of this theory is linked to the use of a surfactant in the prepared emulsions, stabilizing emulsions droplets during jet break up, avoiding their coalescence (Dickinson and Whyman, 1996).

The produced emulsions were fed as aqueous solutions to the SuperLip process, maintaining the ratio between the mass of the antioxidant entrapped in the liposomes and lipids employed in the process. The SuperLip process conditions were repeated as in the first set: the pressure set at 100 bar, the temperature at 40 °C, the Gas to Liquid Ratio of the Expanded Liquid at 2.4, the water flow rate at 10 mL/min and the ethanol flow rate at 3.5 mL/min.

Table VI.5 *Mean diameter, polydispersion index, zeta potential and encapsulation efficiency of liposomes loaded with limonene and linalool in the inner core*

Compound	Theoretical loading [%, w/w]	Mean Diameter [nm ± SD]	PDI	Zpot [mV]	EE [%]
Limonene	10 %	655 ± 218	0.33	-9.8	93
	20 %	492 ± 148	0.30	-5.1	91
	30 %	397 ± 103	0.26	-4.5	92
Linalool	10 %	424 ± 165	0.39	-5.1	96
	20 %	521 ± 167	0.32	-4.3	97
	30 %	605 ± 175	0.29	-2.2	99
Lim + Lin	30 % + 30 %	489 ± 117	0.24	-0.4	99 Lim 99 Lin

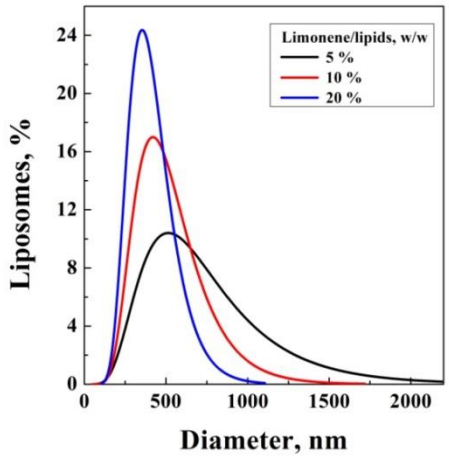

(a)

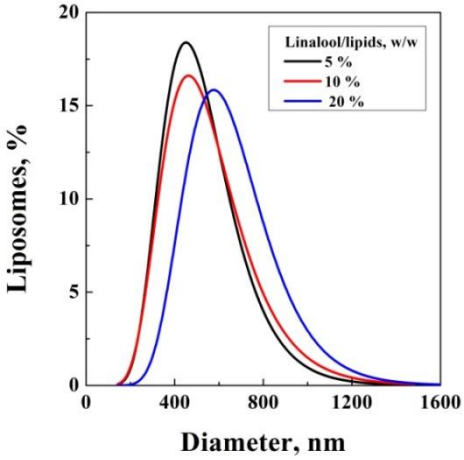

(b)

Figure VI.11. *Limonene (a) and Linalool (b) loaded emulsions entrapped in the inner core of liposomes*

Analyzing the data of **Table VI.5** in detail, a first major observation is that the liposomes mean diameters were significantly smaller than the droplets average mean size. The mean size of the emulsion droplets were reduced during the atomization of the aqueous feeding inside the SuperLip formation vessel, due to the high pressure of the process involved in the jet break-up phenomena. Once atomized in the vessel, the emulsion was subjected to a rearrangement with the formation of oil droplets of sub-micrometric dimensions in a water bulk. Since in the formation vessel phospholipids are also present, sub-micrometric liposomes were obtained containing the atomized emulsion inside the aqueous core of the vesicles.

The limonene loaded vesicles had a decreasing mean diameter from 655 ± 218 nm to 397 ± 103 nm, with a decreasing trend of PDI from 0.33 to 0.26. The linalool loaded samples show an increasing trend from 424 ± 165 nm to 605 ± 175 nm; whereas, a decreasing trend was obtained for PDI from 0.39 to 0.29. The different trend of the two samples is probably dependent on the molecular interactions with the lipids; the particle size distributions of the two sets of experiments are compared in **Figure VI.11**. The simultaneous encapsulation of both emulsions into liposomes resulted in the production of a population of 489 ± 117 nm with a PDI of 0.24.

Another interesting datum that needs to be commented is the variation of the zeta potential values from the emulsions to liposomes. The surface zeta potential of the limonene emulsions was between a minimum of -17 mV and -15.1 mV; whereas, they were between -9.8 mV and -4.5 mV for liposomes. The same data were obtained for linalool: the zeta potential of the droplets was between -14.7 mV and -9 mV; whereas, it was between -5.1 mV and -2.2 mV for liposomes. This is due to the fact that the droplets were entrapped inside the liposomes double lipidic layer, confirming the variation of the surface charge of the particles. The structure of the sample was modified by SuperLip processing, and the significant variation for the production of lipidic vesicles. The variation of the zeta potential could be an important indication of the effective entrapment of antioxidants inside the liposomes.

Regarding the encapsulation efficiencies, the limonene emulsified loaded liposomes retained 93 %, 91 % and 92 % respectively for 10 %, 20 % and 30 % w/w antioxidant theoretical loading on the mass base; whereas, EE was 67 %, 87 % and 87 % for the lipidic layer entrapment. Analogously, the linalool loaded vesicles showed an encapsulation efficiency of 96 %, 97 % and 99 % for 10 %, 20 % and 30 % antioxidant theoretical loading on the lipid mass base; whereas, it was 5 %, 36 % and 54 % for the double lipidic entrapment. Finally, the simultaneous entrapment of limonene and linalool resulted in an EE of 99 % for both compounds; whereas, it was 90 % (limonene) and 61 % (linalool) in the case of the lipidic compartment encapsulation. Even if the EEs were higher than conventional methods when entrapped in the lipidic layer, they were much higher when encapsulated in the inner core using the novel method of emulsion entrapment.

The effect of the SuperLip process on the morphology of lipidic samples was verified using Field Emission Scanning Electron Microscope (FE-SEM). **Figure VI.12** reports lipidic layer and inner core loaded liposomes; whereas, **Table VI.10** regards the optical observation of emulsions (optical microscope) and its inner core encapsulation in liposomes (FE-SEM), respectively.

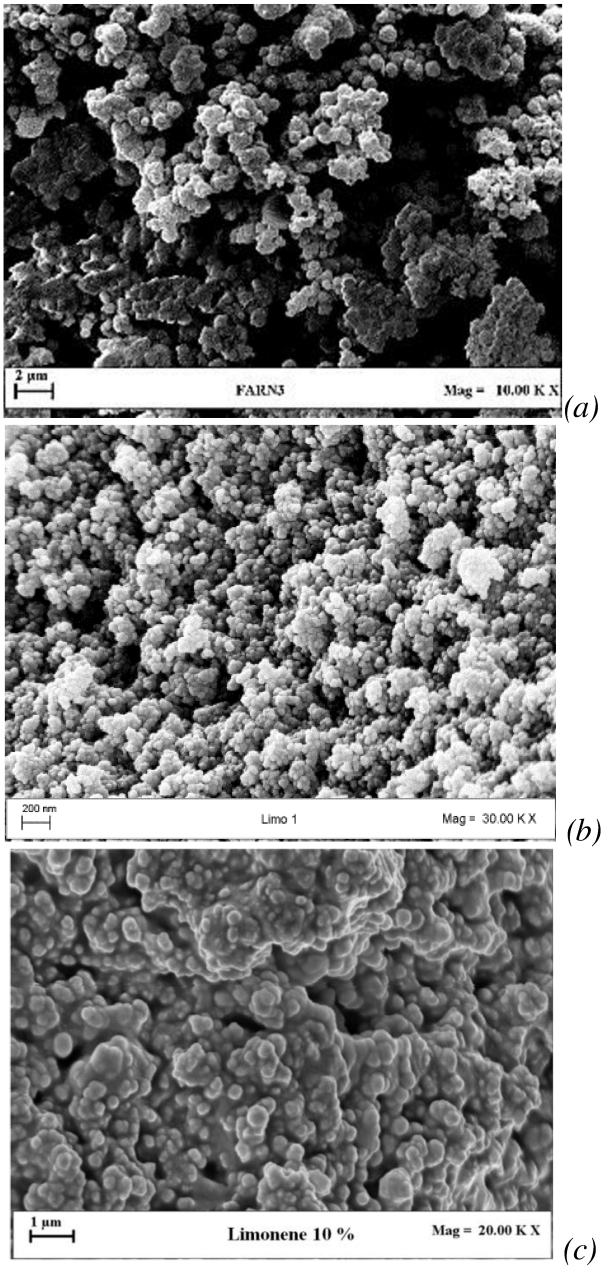

Figure VI.12 *FE-SEM images of double lipidic layer loaded liposomes containing (a) farnesol and (b) limonene, and inner core loaded liposomes containing limonene (c).*

As reported in **Figure VI.12**, liposomes are characterized by nanometric and sub-micrometric dimensions, showing a spherical and smooth surface. The distribution of the vesicles is homogenous. The proposed images of farnesol (**Figure VI.12a**) and limonene (**Figure VI.12b**) loaded samples do not show any significant differences by varying the entrapped compound.

Regarding **Figure VI.12c**, liposomes have a smooth and spherical surface and the vesicles distribution is still homogenous. The high polydispersion index observed in liposomes loaded with 10 % w/w limonene (on the mass base) is probably due to the interaction between the antioxidant molecule and lipids, that in case of low drug concentration resulted in a wider lipid aggregation phenomena. The aggregation of liposomes could also be due to the preparation of stubs followed by metallization pre-processing for microscopic observations (dried samples). The aggregation phenomena are not evident in optical images since the observation happens in a liquid bulk and the sample was opportunely diluted before observation.

It was possible to observe how the encapsulation efficiencies were higher in the case of Oil-in-Water entrapment into liposomes than in double lipidic layer encapsulation. On the other hand, the encapsulation of O/W emulsions in the inner core resulted in many advantages in the production process, such as the preservation of the integrity of the molecules, protected by layers of lipids, as already obtained in a previous study with SuperLip (Trucillo et al., 2018c). A compound entrapped in the external lipidic layer is easily exposed to degrading agents such as high pressures of the system. By entrapping molecules in the inner core, they have more chances to arrive integrally at the target delivery site. To verify this hypothesis, the reduction of the inhibition power was measured in order to establish if the antioxidant activity is better preserved after the entrapment in the inner core than the lipidic layer. The inhibition reduction of the antioxidant power was measured for each sample produced with SuperLip and loaded in the inner core or double lipidic layer. A summary of the results obtained is reported in **Table VI.6**.

Table VI.6 *Antioxidant activity test performed on the chosen antioxidants in different compartment of the produced liposomes*

Compound	Theoretical loading [%, w/w]	Compartment	Reduction of the Inhibition Power, %	
Linalool	10	Lipidic layer	4.32	
	20		10.26	
	30		14.60	
	10	Aqueous core	1.93	
	20		3.32	
	30		7.90	
Limonene	10	Lipidic layer	13.11	
	20		12.87	
	30		12.42	
	10	Aqueous core	2.63	
	20		4.01	
	30		3.85	
Limonene + Linalool	30	Lipidic layer	Limonene 8.43	Linalool 7.21
		Aqueous core	4.19	2.04
Farnesol	10	Lipidic layer	16.78	
	20		18.86	
	30		22.47	
Farnesol + Linalool	30		Farnesol 7.40	Linalool 3.02

Looking at **Table VI.6**, it is possible to observe how linalool entrapped in the double lipidic layer showed an inhibition reduction of the antioxidant power from a minimum of 4.32 % to a maximum of 14.60 % for the higher antioxidant concentrations (increasing trend). The same increasing trend was observed for linalool emulsions entrapped in the inner core, but the average inhibition power reduction was much lower than the lipidic layer, from a minimum of 1.93 % to a maximum of 7.90 % for the highest antioxidant concentration.

Similarly, limonene entrapped into the lipidic layer showed an almost stable behavior by increasing the antioxidant concentration, from 12.42 % to 13.11 %; whereas, emulsion entrapment guaranteed an inhibition reduction from 2.63 % to 4.01 %, increasing drug concentration.

Analogously, farnesol entrapped in the lipidic layer had an inhibition reduction from 16.78 % to 22.47 %, confirming the increasing trend and the higher molecule degradation in the case of double lipidic entrapment. The simultaneous entrapment of linalool and farnesol in the lipidic layer resulted

in an inhibition power reduction of 7.40 % for farnesol and 3.02 % for linalool.

Regarding the simultaneous encapsulation tests, the antioxidant power of the compounds entrapped in the lipidic layer was reduced to 8.43 % for limonene and 7.21 % for linalool, lower than single double layer entrapment. Moreover, the inhibition reduction of emulsion simultaneous entrapment was even lower: 4.19 % for limonene and 2.04 % for linalool.

A general comment on these results could be that, since the compounds entrapped in the lipidic layer are directly in contact with the expanded liquid, the effect of high pressures could cause molecule degradation phenomena due to turbulences created in the system. The entrapment in emulsions loaded in the inner core of liposomes better preserved the compounds, during production.

The SuperLip process was employed to produce liposomes of nanometric and sub-micrometric dimensions loaded with antioxidants and mixtures of them. Farnesol, linalool and limonene were chosen for their lipophilic nature; for this reason, the only possible compartment for liposome encapsulation was the lipidic layer. However, to enhance the encapsulation efficiency and better preserve the inhibition power, the antioxidants were entrapped in Oil in Water emulsions and the emulsions were loaded in the inner core of the liposomes.

Regarding single compounds, the encapsulation efficiencies were significantly increased from the lipidic entrapment to emulsion loading, up to 92 % for limonene and 99 % for linalool. The EE of limonene and linalool was increased to 99 % for both compounds in the case of simultaneous emulsion entrapment. The SuperLip process did not cause antioxidant molecules to denaturate, especially for emulsion entrapped liposomes, with an inhibition reduction of 1.93 % for linalool and 2.53 % for limonene.

More studies on the mean diameters, encapsulation efficiencies and inhibition power stability will be performed on vesicles produced with SuperLip. Comparisons will be also provided with conventional methods. Drug release tests among double lipidic layer and emulsion entrapment will be also performed.

Chapter VII

Encapsulation of dietary supplements

Chapter VII

Polyphenols are compounds largely available in nature; for example, vegetables, cereals and fruit have a high content in polyphenols (Pandey and Rizvi, 2009). These compounds are generally produced by the secondary metabolism of plants (Beckman, 2000). In general, they are found in different quantities in cellular and sub-cellular plant tissues; in particular, water soluble phenolic compounds generally occur in cell vacuoles (Wink, 1997). Phenolics can be divided into flavonoids (Terahara, 2015), phenolic acids (Vinayagam et al., 2016), stilbenes (Likhitwitayawuid, 2008) and lignans (Adlercreutz and Mazur, 1997).

The food industry uses phenolic compounds as additives to cover bitterness, to add color, flavor as well as to protect products against oxidative stress (Papuc et al., 2010, Reverchon et al., 1994). Moreover, polyphenols are frequently added to human diets (Manach et al., 2004) because they can have beneficial bioactive properties for humans (Cevallos-Casals and Cisneros-Zevallos, 2010). They are used to prevent cardiovascular and heart diseases (Scalbert and Mazur, 2002), cancer (Sancho and Mach, 2015), type 1 and type 2 diabetes (Solayman et al., 2016, Dragan et al., 2015), osteoporosis (Hagiwara et al., 2011) and neuronal illnesses (Scarmeas et al., 2006). Anti-aging (Harman, 2006, Biesalski, 2002), anti-viral (Eichhorn et al., 1985) and antimicrobial (Daglia, 2012) activities are also recognized for many polyphenols, according to their antioxidant powers (Vissers et al., 2004), that help to inhibit degenerative body processes (Mantovani et al., 2008). Olive and olive oil by-products are well-known resources of natural phenolic compounds. In particular, olive pomace has been identified as an inexpensive source of phenolic compounds (Aliakbarian et al., 2012, Aliakbarian et al., 2011, Palmieri et al., 2012).

However, polyphenols are extremely volatile, unstable, and sensitive to light (Gellerstedt, 1975, Barth et al., 1994), heat (Sauvage et al., 2010) and oxygen (Volf et al., 2014, De Leonardis et al., 2013). The antioxidant property of polyphenols (Fang and Bhandari, 2010) can be preserved, by enhancing their stability (Volf et al., 2014), bioactivity (Taamalli et al., 2012) and bioavailability (Williamson and Manach, 2005) using polymer carriers.

The technologies commonly used to perform polyphenols encapsulation are spray drying (Desai and Park, 2005, Paini et al., 2015a), coacervation (Gouin, 2004), co-crystallization (Deladino et al., 2007), yeast encapsulation (Blanquet et al., 2005), and microcapsules and membranes entrapment (Paini et al., 2015b, De Marco et al., 2017). However, these conventional processes suffer from several drawbacks related to high process temperatures, low polyphenols encapsulation efficiencies and difficult control of the particle size distribution.

The aim of this part of the work is to apply SuperLip to the encapsulation of aqueous phenolic compounds extracted from olive pomace, for nutraceutical purposes. The advantage of SuperLip in the encapsulation of

this extract is linked to the possibility to work at mild operating conditions, crucial in the preservation of these temperature sensitive compounds. Furthermore, this process allows for the continuous production of stabilized water liposome suspensions with a good control of liposome dimension, also at nanometrical level. The effects of some process parameters such as operating pressure, injector diameter, phenolic compounds loading on the encapsulation efficiency, liposomes morphology and diameters were studied. A conventional thin layer hydration method was also used to encapsulate phenolic compounds from olive pomace and the results are compared with those obtained using SuperLip.

For the first time in the SuperLip process, a natural extract is directly atomized to generate a liposome inner core. The operating pressure was set at 130 bar and temperature was fixed to 40 °C in the homogenizer and in the formation vessel. A 60 μm injector diameter was used for water atomization. The water extract of the olive pomace, obtained by the HPHT extractor, have a TP concentration of 2.6 ± 0.1 mgCAE/mL. The water flow rate was set at 5 mL/min for all the experiments.

Liposomes suspensions loaded with olive pomace extract were successfully obtained. The increase of the extract flow rate allowed to atomize the olive pomace water solution without any nozzle blockage. A minor flow rate facilitated the deposition of solids causing the fouling of the nozzle. The liposomes produced, operating in this way, were characterized by a mean diameter of 134±76 nm. Experiments at 10, 15 and 20 % of TP/PC were conducted. The experiments were performed successfully producing stable liposome suspensions. However, at the end of the experiments at higher TP/PC loadings (15 and 20%), a partial occlusion of the nozzle was observed.

In the experiments presented in **Table VII.1**, the liposomes showed mean dimensions between a minimum of 148 ± 59 nm and a maximum of 250 ± 100 nm; the mean size of the vesicles increased with the increase of the theoretical loading of olive pomace extract. PDIs ranged between a minimum of 0.37 to a maximum of 0.40, increasing the drug theoretical loading. This means that at higher bioactive compounds, the loading of liposomes larger dispersions were obtained, as also shown in **Figure VII.1**, where the PSDs of the liposomes loaded upon increasing the content of the olive pomace were compared.

Table VII.1 *Mean diameter (MD), standard deviation (SD) and polydispersion index (PDI) of liposomes produced using SuperLip and thin layer hydration method, used for comparison purpose, loaded with 5 %, 10 %, 15 % 20 % mg olive pomace total polyphenols per mg of phosphatidylcholine (TP/PC).*

Pressure [bar]	Injector diameter [µm]	TP/PC [%, w/w]	MD [nm ± SD]	PDI	EE [%]
130	60	5	134 ± 50	44.9	44.9
		10	148 ± 59	47.9	47.9
		15	210 ± 84	49.0	49.0
		20	250 ± 100	50.3	50.3
130	80	5	245 ± 76	34.2	34.2
		10	260 ± 91	45.0	45.0
		15	264 ± 98	56.7	56.7
		20	265 ± 101	58.1	58.1
170	80	5	165 ± 26	25.4	25.4
		10	171 ± 31	40.9	40.9
		15	185 ± 46	44.9	44.9
		20	199 ± 52	45.5	45.5
Thin layer hydration		15	50 ± 8	0.18	10.1

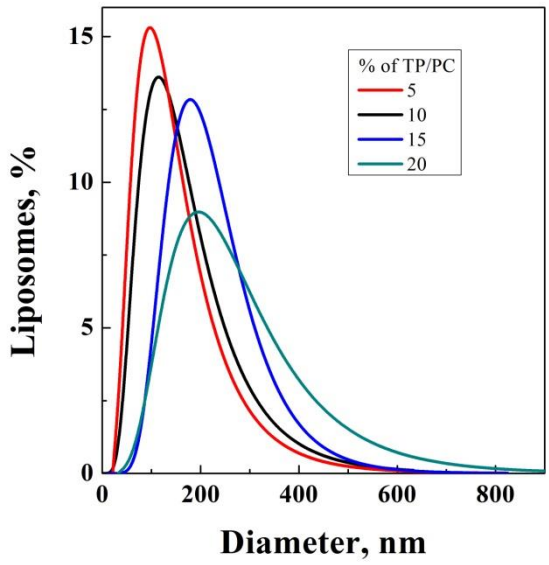

Figure VII.1 *Frequency distribution curves of olive pomace loaded liposomes at 130 bar and using 60 µm injection diameter*

The general observed effect was an increase of the liposome diameter with the increase of TP/PC loading. This effect can be explained considering that at higher concentrations of extract also correspond increased viscosity and density of the solution. These properties of the atomized fluid play an important role in the efficiency of the atomization process. Higher fluid cohesive forces generally determine larger droplets production (Manna et al., 2017).

FE-SEM was used to confirm mean size and morphology of the vesicles produced with SuperLip. As an example, a 5 % TP/PC loaded liposomes FE-SEM image is reported in **Figure VII.2**.

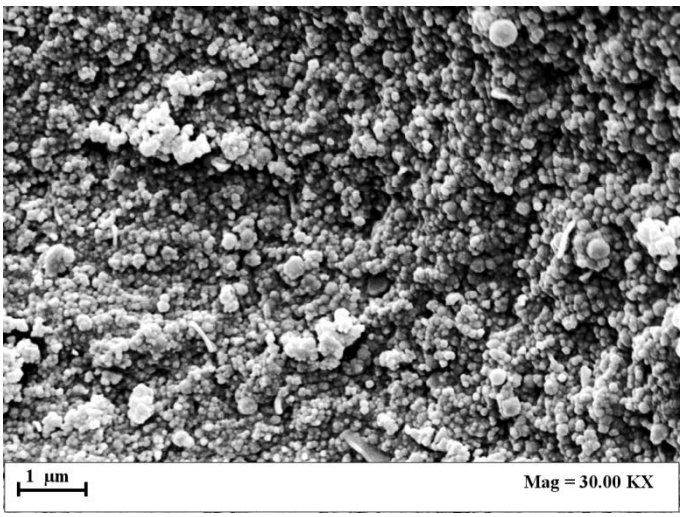

Figure VII.2 *FE-SEM image of liposomes loaded with 5 % mg total polyphenols from olive pomace per mg of phosphatidylcholine (TP/PC), produced at 130 bar using a 60 µm injector.*

As shown in **Figure VII.2**, liposomes are characterized by a spherical shape and a slightly smooth surface. The mean dimensions measured using specialized software on SEM image, confirmed the values reported in **Table VII.1**.

A second set of experiments was performed using a larger nozzle diameter of 80 µm, all the other process parameters were maintained constant. This choice was made in order to try to avoid nozzle fouling problems. At a 60 µm nozzle diameter and with the higher water flow rate of 5 ml/min, the extract was processed successfully but a partial deposition of solid residue was observed on the nozzle surface. This condition did not compromise the experiment but is still not desirable. The same set of experiments, with different TP/PC loadings, was performed. The experiments were performed successfully and no nozzle fouling was observed at the end of the experiment.

As shown in **Table VII.1,** the increase of the injector diameter produced liposomes with larger average diameters. The mean diameters ranged between a minimum of 245 ± 76 nm to a maximum of 265 ± 101 nm. As observed for the liposomes produced with the smaller nozzle, also in this case, the polydispersion index slightly increased from a minimum of 0.31 to a maximum of 0.38 when TP/PC increased from 5 to 20 %. In this case, the mean dimensions of the liposomes were practically constant; however, the distribution curves are narrower than the 60 µm produced samples. The effect of the nozzle diameter can be explained considering that larger nozzle diameters generally generate larger droplets during the atomization process.

For this reason, the produced liposomes are characterized by increased mean diameters.

Characterization of the size and morphology of the liposomes produced with SuperLip using an 80 µm injector was also performed using FE-SEM. An example of the vesicle image is reported in **Figure VII.3** for the sample produced at 130 bar using a nozzle of 80 µm for 5 % TP/PC ratio.

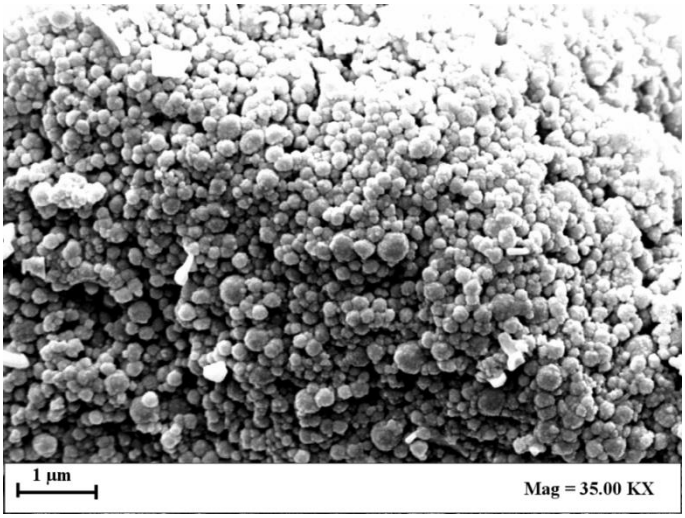

Figure VII.3 *liposomes loaded with 5 % mg total polyphenols from olive pomace per mg of phosphatidylcholine (TP/PC)*

The increase of the nozzle diameter allowed to obtain a good processability of the extract, but an increase of the liposomes mean diameters was observed. In order to try to reduce the liposome dimensions and have a better control of the particle size distributions, another set of experiments was performed increasing the formation vessel pressure to 170 bar, all the other operating parameters remained unchanged.

Liposomes with mean diameters in the range from 165 ± 26 nm and 199 ± 52 nm with PDI from 0.16 to 0.26 were obtained. In particular, looking at the results for different TP/PC % as reported in **Figure VII.4**, increasing the theoretical loading of TP, the mean diameter, increased from a minimum of 165 ± 26 nm for 5 % w/w TP/PC to a maximum of 199 ± 52 nm for 20 % w/w TP/PC. The polydispersion indexes increased from a minimum of 0.16 for the lowest TP/PC ratio to 0.26 for the highest ratio. Summarizing these results, the increase of the operating pressure produced smaller liposomes with a narrow PSD. In this case, there is a double positive effect of the pressure and water injector nozzle on vesicles formation. The increase of the pressure produces a significant effect on the decrease of the mean diameter and control of PSD. The simultaneous positive effects of the pressure increase (Espirito Santo et al., 2015b) and the use of a larger nozzle allowed

for a better control of the water droplets atomization and, as a consequence, of the PSD of liposomes loaded with olive pomace extract (Espirito Santo et al., 2014a).

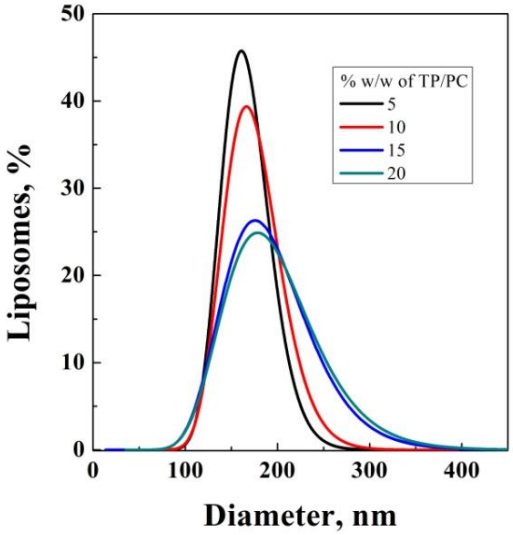

Figure VII.4 *Frequency distributions curves of olive pomace loaded liposomes at 170 bar and 80 μm injection diameter*

A FE-SEM image of the liposomes produced at 170 bar is reported in **Figure VII.5** and allows to qualitatively compare these vesicles with those produced at a lower pressure.

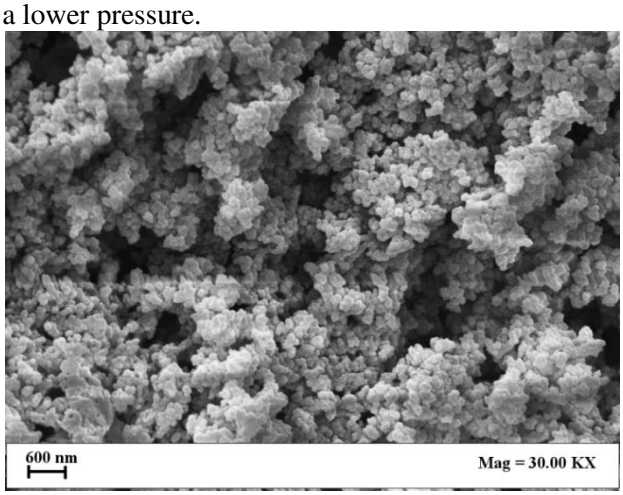

Figure VII.5 *FE-SEM image of liposomes loaded with 5 % mg total polyphenols from olive pomace per mg of phosphatidylcholine (TP/PC)*

The FE-SEM image confirms that mean diameter of the liposomes is smaller when the vesicles are produced at a lower pressure.

The samples prepared with SuperLip at the bioactive compounds loading of 15 % w/w were compared with liposomes produced using the thin layer hydration method. Olive pomace extract was diluted in water to obtain a theoretical olive pomace loading of 15% with respect to the lipid content. The results are shown in **Table VII.1**. The general problem, related to the use of a conventional method, is the production of vesicles generally larger than 10 μm if post-processing steps such as sonication or extrusion are not added. In this particular case, the experiment at 15 % TP/PC loaded liposomes resulted in the production of vesicles with a diameter of 50 ± 8 μm with a PDI of 018; i.e. more than 350 times larger than the liposomes produced using SuperLip at the same theoretical loading. These larger liposomes did not maintain their stability over time, due to vesicles aggregation; therefore, the mean diameter modified with time and drug leakage was obtained during storage (Nedovic et al., 2011).

Liposomes produced using the 60 μm nozzle working at 130 bar showed a slight increase of the EE percentage by increasing the ratio of TP/PC. TP encapsulation efficiencies ranged between 44.9 % and 50.3 % for this set of experiments. Using an 80 μm nozzle and working at the same pressure, the trend is confirmed, by increasing the bioactive compounds loading. However, in this case, the range of TP encapsulation efficiency is wider, from a minimum of 34.2 % to a maximum of 58.1 %. Looking at the set of experiments performed at 170 bar, TP content entrapped by liposomes also increased when increasing the TP/PC theoretical loading from a minimum of 25.4 % to a maximum of 45.5 %. Comparing the results obtained, the injector diameter had no significant effect on EE. The only remarkable effect on the TP encapsulation efficiency was due to the TP/PC total loading. Considering the experiments performed at the same injector diameter but at different pressures, a slight effect of pressure on EE can be observed. In particular, upon increasing the operating pressure, a slight reduction of EE can be noted. In this case, an increase of EE can be obtained by increasing the TP/PC loading. **Figure VII.6** highlights the main effect of the TP/PC loading and pressure effect on EE.

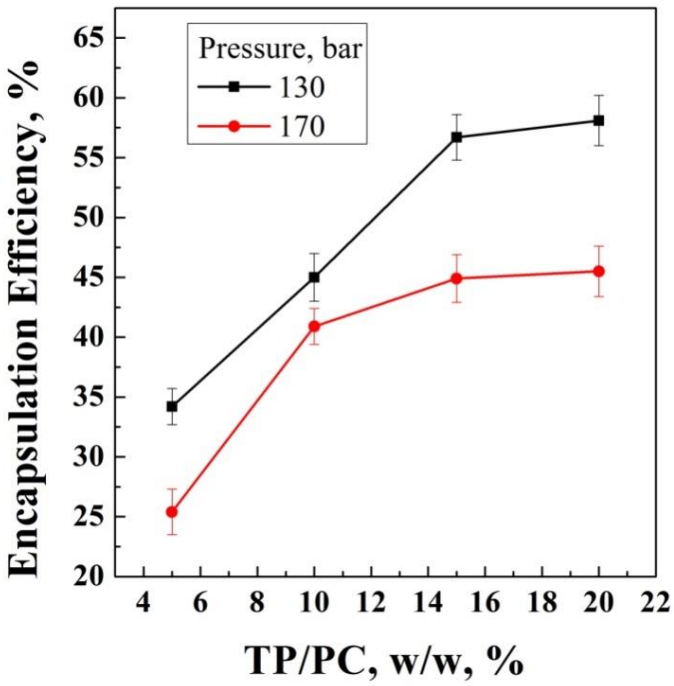

Figure VII.6 *TP/PC % effect on encapsulation efficiency reported as a function of the pressure*

As a final comparison, conventional loaded samples had an EE of 10.1 % of TP, much smaller than the vesicles produced directly using SuperLip (Campardelli et al., 2016c).

It was demonstrated that SuperLip can be successfully used for the production of liposomes entrapping polyphenolic compounds extracted from olive pomace. A good compromise between particle size and encapsulation efficiency was achieved. Liposomes of 265 ± 101 nm mean diameter entrapped up to 58.1 %. The systematic study of the SuperLip operating parameters showed the simultaneous effects of a larger nozzle diameter and higher working pressure on the control of PSDs.

It is also worth considering the encapsulation efficiency: it is not high as generally obtained using SuperLip. The encapsulation of the polyphenols contained in olive pomace remains extremely difficult because the natural extract contains a lot of different compounds. However, the encapsulation results obtained in this study are 6 times higher than those reported in current literature (Atefe et al., 2018).

Chapter VIII

Encapsulation of antibiotics

Chapter VIII

VIII.1 Antibiotics for ocular delivery

The human eye has a complex anatomy and the delivery of drugs to targeted ocular tissues is restricted by various precorneal, dynamic and static ocular barriers (Meisner, 1995). Ocular drug systemic delivery suffers from the difficulty of reaching the specific target of ocular tissue. For this reason, topical delivery is preferred and can be directly performed by patients (Gulsen and Chauhan, 2004, Le Bourlais, 1998).

Cyclodestrins have been used as ocular drug carriers for hydrophilic molecules, but drug leakage occurs. Other side effects include ocular irritation, redness and inflammation (Mannermaa et al., 2006). Emulsions for ocular delivery are preferred in water/oil formulation (Chan et al., 2007, Vandamme, 2002), because less irritation and better tolerance of the eye has been observed (Liang et al., 2008). Mucoadhesive polymers such as chitosan have been introduced to improve pre-corneal residence time (Yamaguchi et al., 2009). Other conventional drug carriers developed for topical ocular delivery are suspensions and ointments. To overcome the problems related to the direct administration of ocular drugs, nanocarriers have been proposed that can assure reduced eye tissues irritation, a better bioavailability as well as a better biocompatibility with the eye cells. The most widespread examples of nanodrug carriers (Salgado et al., 2017) for ocular delivery are nanomicelles (Vaishya et al., 2014), colloids (Popowchak et al., 1996), dendrimers (Kalomiraki et al., 2016, Spataro et al., 2010), gels (Patel et al., 2016, Mundada and Avari, 2009), microneedles (Khandan et al., 2016, Khandan et al., 2012) and liposomes (Chen et al., 2016, Dong et al., 2015, Niesman, 1992).

Liposomes are particularly indicated for topical ocular drug delivery due to their biocompatibility. They are artificial vesicles formed by an inner water core, surrounded by an external double lipidic layer. Their similarity to human membrane cells, along with the amphoteric behavior of phospholipids make it possible to encapsulate both hydrophilic and lipophilic compounds. Liposomes show good efficacy in delivering drugs to the posterior and anterior segments of the eye tissues. For this reason, they are considered the most valuable eye drug delivery systems (Zhang et al., 2009, Bochot et al., 2000, Lajunen et al., 2014, Sasaki et al., 2013).

Ampicillin and ofloxacin, antibacterial drug used to stop ocular post-surgery infections, are often delivered using liposomes. (Liu et al., 2010, Guliy et al., 2005, Kim et al., 2001, Luo et al., 2013, Navaratnam and Claridge, 2000). However, encapsulation efficiencies (EE) in liposomes produced using conventional techniques, reported in current literature, are low (Furneri et al., 2000, Pardue and White, 1997). For example, ofloxacin encapsulation efficiency in multilammellar micrometric liposomes ranging between 53 and 65% was reported by Hosnoy et al. (Hosny, 2009) using the thin layer hydration method. Similar results were reported in the case of

ampicillin encapsulation into liposomes, using the same production method, with encapsulation efficiencies in the range from 10 to 50% (Schumacher and Margalit, 1997).

Therefore, the aim of this section is to attempt the encapsulation of ofloxacin and ampicillin into liposomes using SuperLip. The process parameters, such as water flow rate and drug concentration have been studied to obtain high EE, and the correlation between these process parameters, size and drug EE of the vesicles has been proposed. Storage stability and drug release kinetics have also been performed.

The effect of the lipid to water ratio (PC/H_2O) on the mass base was studied. For these experiments, all the previously described operating parameters were already optimized. However, to obtain a different PC/H_2O ratio, different water flow rates were used. Ofloxacin theoretical loading of 1% w/w was adopted. The data are listed in **Table VIII.1**, along with the liposomes mean diameters and encapsulation efficiencies for ofloxacin loaded liposomes production.

Table VIII.1 *Mean diameter (MD), standard deviation (SD) and encapsulation efficiency (EE) of liposomes loaded with 1, 3 and 6 % w/w ofloxacin (OF), a different PC/H_2O ratios and water flow rates*

Ofloxacin theoretical loading [w/w, %]	PC/H_2O [mg/g]	Water Flow Rate [mL/min]	MD [nm] ± SD	EE [%]	Zeta potential [mV]
1	1.7	10.00	281±194	0	-15.7
	2.1	8.57	325±110	0	-12.2
	4.2	4.28	331±234	29	-14.4
	8.3	2.14	670±235	54	-21.4
	25	0.70	1760±792	86	-27.9
3	1.7	10.00	202±125	20	-14.4
	2.1	8.57	295±112	20	-15.1
	4.2	4.28	328±115	69	-14.7
	8.3	2.14	750±188	94	-25.1
	25	0.70	1150±518	95	-35.7
6	1.7	10.00	275± 125	20	-16.5
	2.1	8.57	275±103	20	-15.5
	4.2	4.28	325±223	60	-16.2
	8.3	2.14	770±188	90	-38.1
	25	0.70	1523±694	97	-39.4

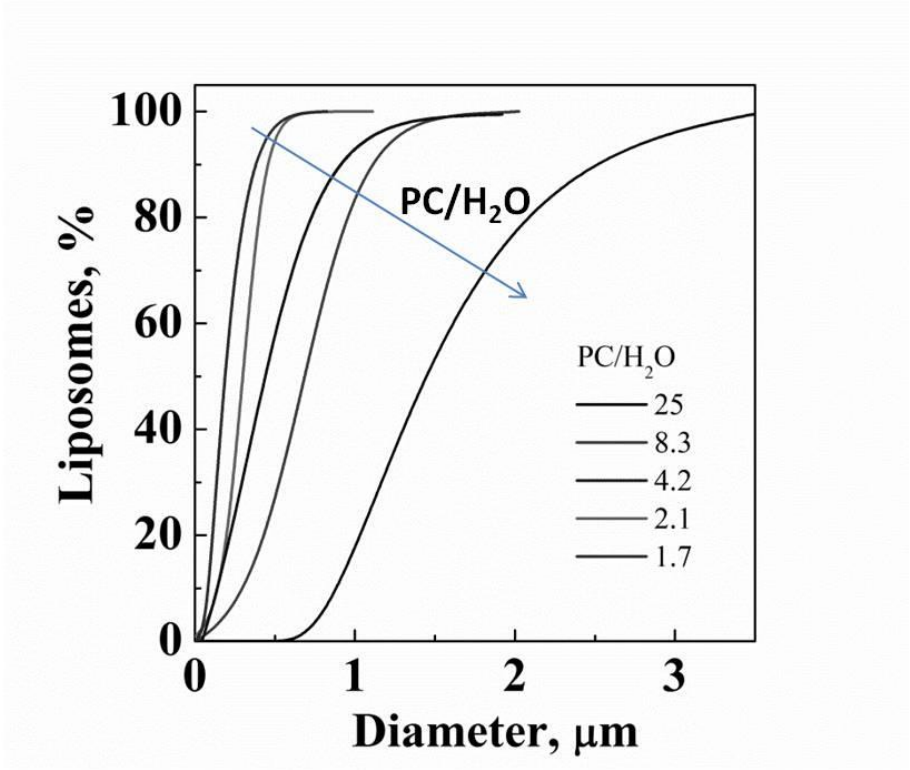

Figure VIII.1. *Cumulative distributions curves for 1 % w/w ofloxacin loaded liposomes, produced at different PC/H_2O ratios*

As reported in **Table VIII.1**, these experiments were largely successful. A first observation is possible: when higher PC/H_2O ratios were used, more concentrated liposomes samples were collected. Considering the results reported in **Table VIII.1**, there is a significant increase of the mean size of the liposomes upon increasing the PC/H_2O ratio from 1.7 to 25 mg/g. In particular, 1% w/w ofloxacin loaded liposomes showed mean diameters between 281±194 nm for 1.7 mg/g PC/H_2O ratio and 1760±792 nm for 25 mg/g PC/H2O ratio. The effect of this parameter on the PSD curves is plotted in **Figure VIII.1**.

It is possible to observe that increasing PC/H_2O, an overall enlargement of liposome size distribution was obtained. For ratios lower than 4.2 mg/g, only a slight increase of PSD was noted. The effect on MD can be due to the different water flow rate used in these experiments that can influence the atomization regime inside the formation vessel. At the highest water flow rate (10 mL/min), the Reynolds number (Re) at the exit of the injector is higher than 106, whereas for the lowest water flow rate of 0.70 mL/min Re is about 104. In the first case, the jet break up is in the full atomization regime; whereas, in the second case the jet break up regime is defined as

second wind induced (Reitz, 1978). In the full atomization region (at 10 mL/min), the drop size is largely smaller than the jet diameter. As a consequence, the mean liposomes diameter is nanometric. At the lowest water flow rate, the atomization regime is near the second wind (Faeth, 1990). In this case, the drop sizes are not significantly smaller than the jet diameter, resulting in micrometric liposomes.

However, the most relevant effects are related to the EE. The best results in terms of EE were obtained at high PC/H_2O ratios. For 1.7 and 2.1 ratios, it is near to zero; EE increased to 54 % at a ratio of 8.3 and at 86 % for 25 ratio. The general trend observed was a large increase of EE with the increment of the quantity of the phospholipids available per unit of water volume.

Considering these results, the EE tests were also repeated for other percentages of ofloxacin theoretical loadings (3 % and 6 % w/w). Experiments at 3 % and 6 % w/w, with different water to lipid ratios were performed, while leaving all the other operating parameters constant. The results are reported again in **Table VIII.1**. For 3 % loading, the mean diameter of the liposomes was included between a minimum of 202±125 nm to a maximum of 1150±518 nm. For 1 % loaded liposomes, increasing the PC/H_2O ratio, a general enlargement of the liposome mean size was observed. In addition, the encapsulation efficiency increased when increasing the PC/H_2O ratio from a minimum of 20 % at PC/H_2O of 1.7 mg/g to a maximum of 95 % at 25 mg/g of PC/H_2O ratio. The same effect was also observed for 6 % w/w ofloxacin loaded liposomes, with the mean diameters increasing from 275±125 nm to 1523±694 nm, when the PC/H_2O ratio from 1.7 to 25 mg/g was increased. In this case, the ofloxacin encapsulation efficiency also increased from a minimum of 20 % for the lowest PC/H_2O ratio to a maximum of 97 % for the highest PC/H_2O ratio.

Comparing all the results obtained, the encapsulation efficiency always enlarged by increasing the drug to lipid ratio. In particular, the PC/H_2O ratio 25 mg/g allowed to obtain almost total drug entrapment in the liposomes. The EE results of the set of experiments performed at different PC/H_2O ratios and different ofloxacin loadings are graphically reported in **Figure VIII.2**.

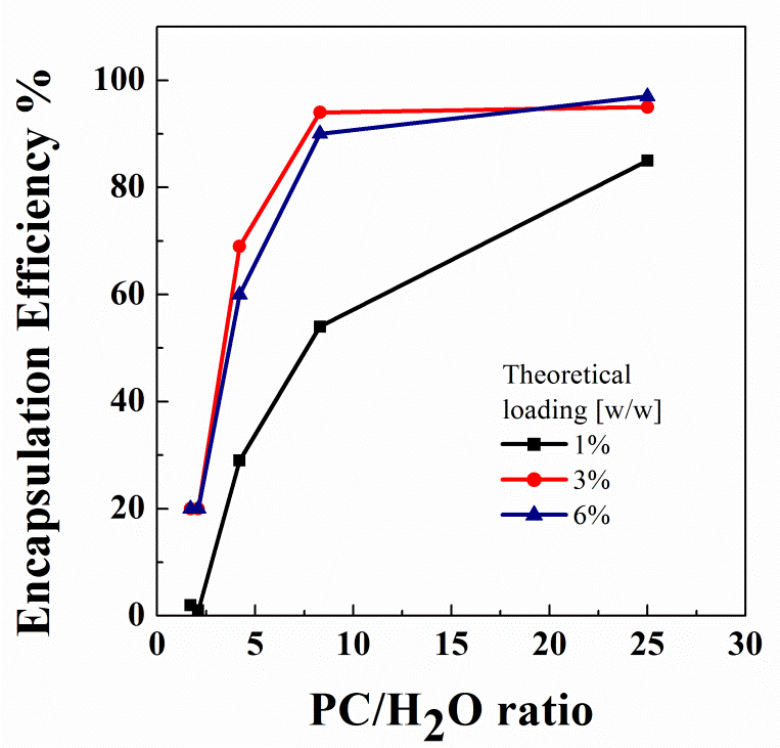

Figure VIII.2 *Encapsulation Efficiencies comparison at different ofloxacin theoretical loadings and different PC/H_2O ratios*

The general explanation of these results is that at higher PC/H_2O ratios, a larger amount of lipids per volume of water is available, and this condition enhances the coverage of the droplets, resulting in higher encapsulation efficiencies. Furthermore, looking at **Figure VIII.2**, an EE dependency on ofloxacin theoretical loading can be also observed. Using 1 to 3 % theoretical loadings, there was a significant increase of EE values; a further increment to 6 %, did not lead to any significant EE improvement.

The positive effect of the PC/H_2O ratio on the encapsulation efficiency can be also explained considering that the high PC/H_2O ratio were obtained in correspondence with the smallest water flow rate. In this case, the mean velocity of the water droplets at the exit of the nozzle was reduced and the water droplets flying time was increased. The greater contact time between the atomized water droplets and phospholipids improved the droplet lipid coverage, resulting in a higher ofloxacin EE.

At this point of the work, the positive results obtained for ofloxacin encouraged to try to improve the ampicillin encapsulation in the liposomes with 1 % w/w theoretical loading, in the hydrophilic water core of the vesicles using a PC/H_2O ratio of 25 mg/g. Ampicillin loaded liposomes were

successfully produced, with a mean diameter of 313 ± 143 nm and a large improvement of the encapsulation efficiency: ampicillin EE equal to 99%. was obtained. This test demonstrated that the operating conditions used for the ofloxacin loaded liposomes can be successfully applied for the encapsulation of ampicillin and probably of other antibiotics.

As a further confirmation of versatility of SuperLip in entrapping ocular delivery antibiotics, another experiment was performed, for the simultaneous entrapment of ampicillin and ofloxacin, with 1 % w/w theoretical loading for both drugs.

Liposomes loaded with both ampicillin and ofloxacin showed a mean diameter of 957 ± 335 nm. This value is included between the mean sizes of single drug loaded liposomes. The encapsulation efficiencies for the two compounds simultaneously entrapped in the vesicles are 86 % for ofloxacin and 99 % for ampicillin, these values reflect the EE of the vesicles loaded only with ampicillin or ofloxacin under the same conditions. This means that the simultaneous entrapment of both compounds did not modify the encapsulation efficiency of the single drug.

A TEM image of the liposome loaded with ofloxacin produced using SuperLip is shown in **Figure VIII.3**. The vesicles are unilamellar and their lipidic double layer can be observed. The liposome mean dimension is in the range of the measures obtained using the DLS technique and gives a cross confirmation of the results.

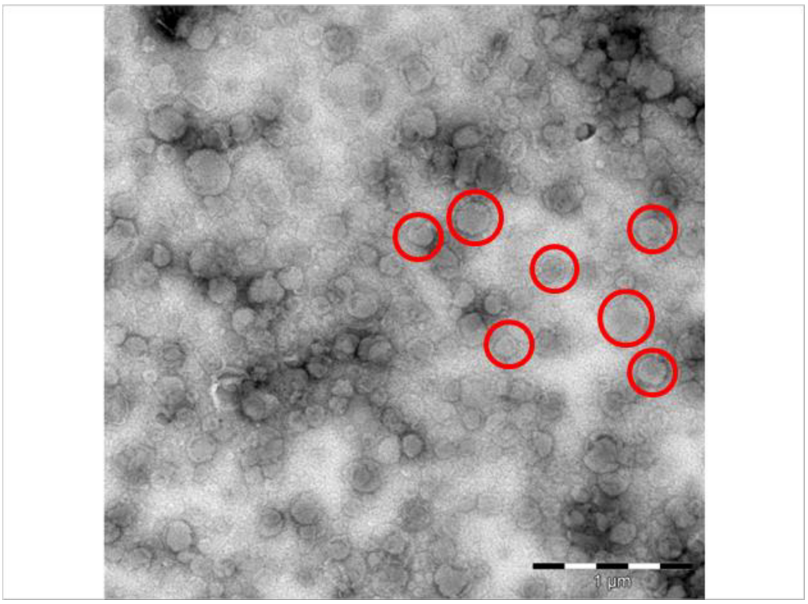

Figure VIII.3 *TEM image of ofloxacin loaded liposomes*

The zeta potential of the produced suspensions was measured for the samples loaded with ofloxacin, for all the drug concentrations previously considered. The zeta potential was in the range of stable vesicles and increased with the increase of PC/H_2O ratio. The maximum value of the zeta potential was obtained at 25 mg/g PC/H_2O ratio for each drug concentration. In particular, at 25 mg/g of PC/H_2O ratio the zeta potential value of the liposome suspension was -27.9, -35.7 and -39.4 mV for the 1%, 3% and 6% w/w ofloxacin loading respectively. This means that more stable liposomes were produced when a higher lipid to water ratio was used. Furthermore, the zeta potential mean value increased with the increase of the drug loading from 1% to 6% w/w; the same trend was also confirmed for ampicillin loaded vesicles, that showed a mean zeta potential between -16.2 mV for 1.7 PC/H_2O ratio and -54.5 mV for 25 PC/H_2O ratio. In conclusion, lipid vesicles with higher PC/H_2O ratio and higher drug loading are characterized by an increased surface charge and better suspension stability.

Drug release tests at 37 °C were performed for ampicillin and ofloxacin vesicles loaded with 1 % w/w drug and prepared with a PC/H_2O ratio of 25 mg/g. Ofloxacin was completely released in 180 min; whereas, the release of ampicillin was completed after 240 min. These results are the demonstration that antibiotics loaded liposomes are suitable for ocular delivery providing a sustained drug release and thereby enhancing drug ocular bioavailability.

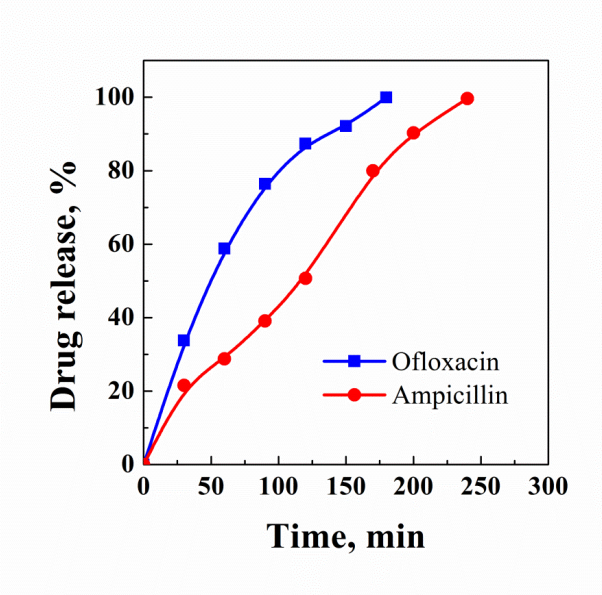

Figure VIII.4 *Drug release comparison between 1 % w/w ofloxacin (blue) and 1 % w/w ampicillin (red) loaded liposomes*

A new selection of the SuperLip process parameters was required for the successful production of liposomes encapsulating ophthalmic antibiotics. The application of the operating parameters previously used for other molecules was unsuccessful for the encapsulation of antibiotics for ocular delivery. This could probably be due to a higher steric volume of these molecules and also explains the results generally reported in current literature for the liposome encapsulation of this class of compounds. The variation of the lipid to water ratio reveled to be the key parameter to obtaining an improvement of the encapsulation efficiency. This ratio affected the mean size and encapsulation efficiency of the vesicles produced. An increase of this ratio allowed for the production of vesicles with an encapsulation efficiency up to 97 % for ofloxacin and 99 % for ampicillin. High PC/H_2O ratios produced higher EE thanks to a longer water droplets flying time in the formation vessel and better lipid coverage.

The simultaneous entrapment of compounds was also attempted for the first time using the SuperLip process. Their successful encapsulation showed that water droplets behave like discrete volumes in which the compounds remains confined without interfering with other water volumes.

VIII.2 Encapsulation of antibodies

Another pharmaceutical application was studied for the entrapment of antibodies into liposomes (see Material section). These antibiotics were suspended in an aqueous solution and entrapped in the inner core of liposomes. The antibodies were entrapped with different ratios on the lipid mass base from 0.635 % up to 2.5 % w/w working at a water flow rate of 10 mL/min; whereas, concentrations up to 12 w/w on the lipid mass base were chosen for lower water flow rates (1 mL/min). The results are reported in **Table VIII.1.**

Table VIII.1 *Liposomes produced with different Antibody/lipid ratio at different water flow rates.*

Water flow rate [mL/min]	Antibody/Lipid [%]	MD ± SD [nm]	PDI	Zpot [mV]	EE [%]
10 mL/min	0	245 ± 101	0.41	-3.55	//
	0.625	398 ± 139	0.35	-8.14	57.66
	1.25	524 ± 176	0.33	-3.84	74.67
	2.5	587 ± 201	0.34	-31.0	39.32
1 mL/min	1.25	264 ± 108	0.41	-33.5	40.20
	2.5	297 ± 121	0.41	-16.2	54.60
	4	366 ± 176	0.48	-7.49	73.66
	12	451 ± 239	0.53	-15.2	89.79

Liposomes produced in this manner showed nanometric and sub-micrometric dimensions. Working at higher water flow rates, the dimensions were in the range 245 ± 101 nm and 587 ± 201 nm, with a growing trend of the mean dimensions upon increasing the antibody to lipid ratio. The encapsulation efficiencies were lower than 57 %, with a decreasing trend. For this reason, the water flow rate was changed to 1 mL/min and higher encapsulation efficiencies were obtained, with an increasing trend from 40 % to almost 90 %, upon increasing the theoretical loading from 1.25 to 12 w/w on the lipid mass base.

Future developments will consist in the production of liposomes stealth, linking antibodies on the external surface of the phospholipids. In this way, a targeted delivery could be performed in order to reduce any toxic effects of the drugs. The antibodies on the surface could be coupled with an antibiotic or a protein entrapped in the inner core of lipidic vesicles. PEGilated liposomes could also be produced in this manner. Together with antibodies substituting them, PEG fragments could be linked to the external surface of the liposomes, as already performed for several anti-carcinogenic drugs such as Doxorubicin. Moreover, coated liposomes will be produced to enhance drug protection in long circulating drug delivery systems (PEGilated liposomes).

VIII.3 Anti-bacterial studies

The supercritical assisted method for the production of liposomes was also used for the production of antibiotic loaded vesicles to study their anti-microbial activity. In particular, amoxicillin loaded liposomes were produced changing the water flow rate as well as the drug to lipid ratio. The results are proposed in **Table VIII.2**.

Table VIII.2 *Liposomes produced with different Antibody/lipid ratio at different water flow rates.*

Test	Water flow rate [mL/min]	Drug/lipid [w/w, %]	Lipid employed		EE [%]
			PC	Chol	
P01	10	0%	100%	0%	---
P04	10	1%	100%	0%	0%
P13	10	20%	100%	0%	41%
P01bis	2	0%	100%	0%	---
P04bis	2	1%	100%	0%	2%
P05bis	2	5%	100%	0%	55%
P06bis	2	10%	100%	0%	39%
P13bis	2	20%	100%	0%	84%
P02bis	2	0%	99%	1%	---
P07bis	2	1%	99%	1%	0%
P08bis	2	5%	99%	1%	25%
P09bis	2	10%	99%	1%	61%

The first set of experiments was performed working at a water flow rate of 10 mL/min, changing the Drug to Lipid Ratio from 0 % (no drug) to 20 % w/w. However, the Encapsulation Efficiencies (EE) were not higher than 41 %. For this reason, the water flow rate was reduced to 2 mL/min, obtaining EE as high as 84 %.
To verify the effect of additives against *E.Coli*, 1 % cholesterol (Lipid to Lipid ratio on the mass base) was inserted in the liposomes double layer. The encapsulation efficiencies obtained were up to 61 %, in this case.

E.Coli growth profiles were analyzed as described in the Methods section. In particular, it was studied for:
- vesicles only prepared with phosphatidylcholine (PC), upon increasing the liposomes concentrations.
- vesicles prepared with PC and cholesterol, upon increasing the liposomes concentrations
- lipid loaded liposomes with 0, 5, 10, 20 Amoxicillin loading and 25, 50, 100 ppm liposomes concentration
- lipid+cholesterol loaded liposomes with 0, 5, 10, 20 Amoxicillin loading and 25, 50, 100 ppm liposomes concentration.
The results are reported in sets in **Figures VIII.5, VIII.6, VIII.7, VIII.8**.

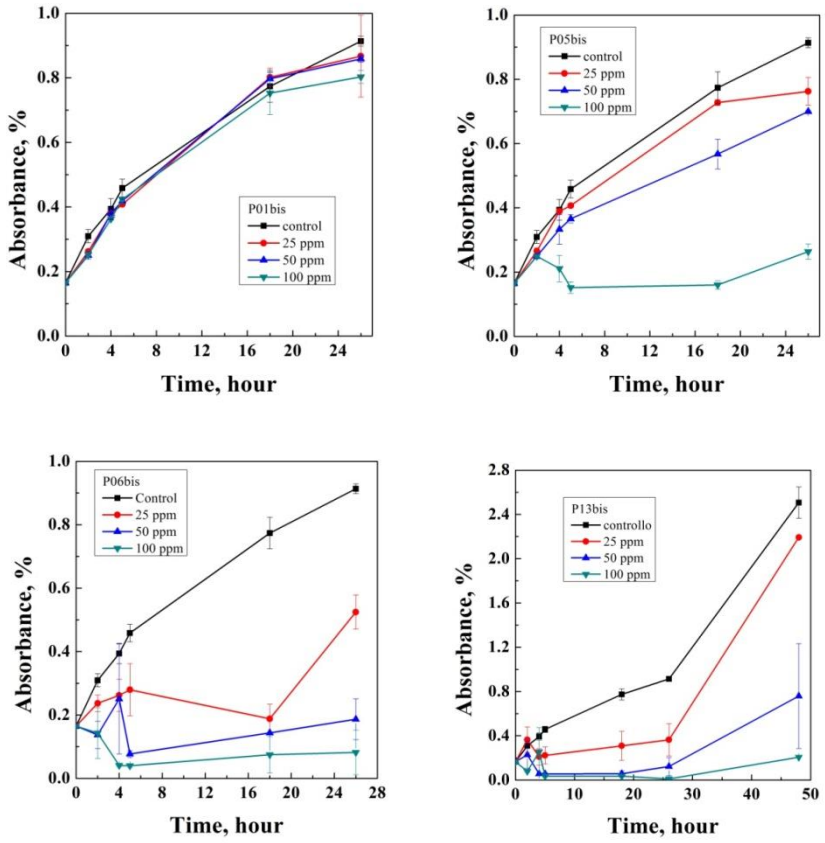

Figure VIII.5 *E.Coli growth profiles in test P01bis, P05bis, P06bis, P13bis – Lipid only - (0, 25, 50, 100 ppm liposome concentration)*

Experiment P01bis regards empty liposomes. For this reason, there is no effect of the different liposomes concentrations on *E.Coli* growth. Native phosphatidylcholine did not alter the response on the bacteria growth profiles. Increasing the amoxicillin loading, the liposomes concentration started to be more significant on *E.Coli* growth; in particular, a growth delay was detected for the 100 ppm liposome concentration. The best conditions were reached for 10 % and 20 % w/w amoxicillin loading at 50 and 100 ppm liposome concentrations.

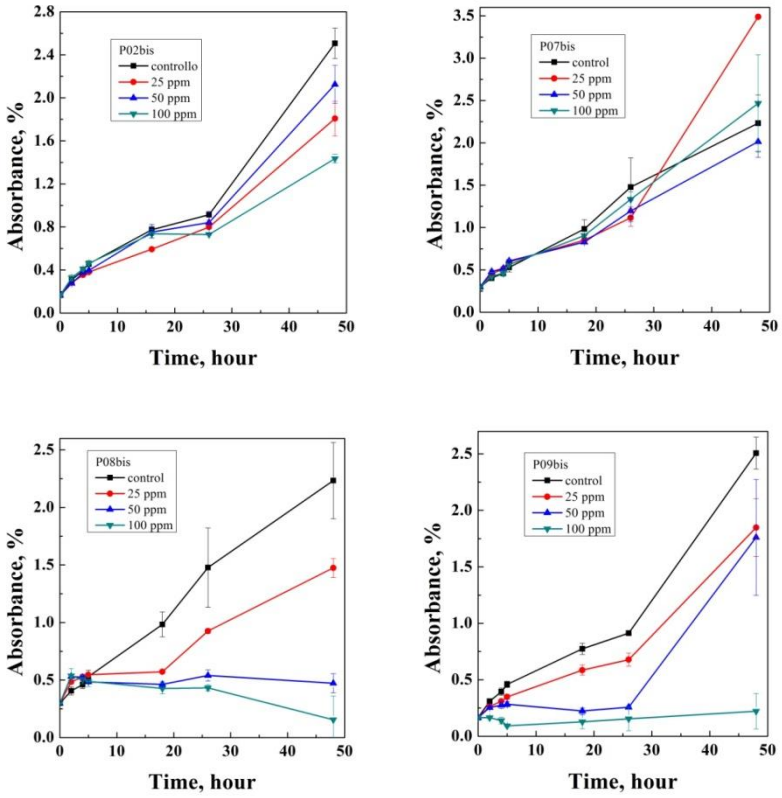

Figure VIII.6 *E.Coli growth kinetics in test P02bis, P07bis, P08bis, P09bis – Lipid + cholesterol - (0, 25, 50, 100 ppm liposome concentration)*

Similar results were obtained by repeating the previous experiments, adding 1 % w/w cholesterol on the lipid mass base during the liposomes production. *E.Coli* growth was not delayed as in the case of the phosphatidylcholine liposomes. This is due to the fact that the addition of cholesterol compacted the structure of the vesicles, delaying the drug release time. This was also confirmed in Chapter V. For this reason, the *E.Coli* growth rate was not decreased as rapidly as in liposomes with only lipids.

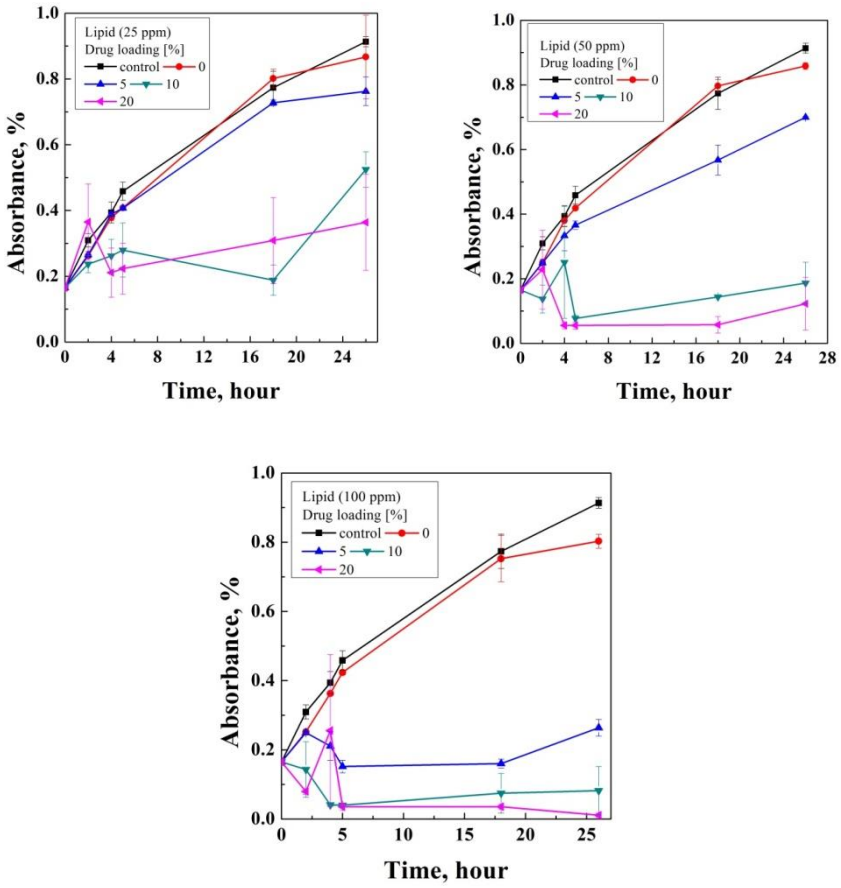

Figure VIII.7 *E.Coli growth kinetics in lipid loaded liposomes with 0, 5, 10, 20 Amoxicillin loading and 25, 50, 100 ppm liposomes concentration*

In this set of figures, the amount of the liposomes concentration was fixed; whereas, the amoxicillin loading was varied from 0 to 20 %. In this case, the best bacteria inhibition was reached for 10 and 20 % drug loading and 50 and 100 ppm of the liposomes concentrations.

Drug release tests were added to this study to compare *E.Coli* growth profiles with amoxicillin drug release from liposomes. The external medium for this tests was the same prepared for the determination of *E.Coli* growth profiles. For this study, vesicles made of only phospholipids were taken as models.

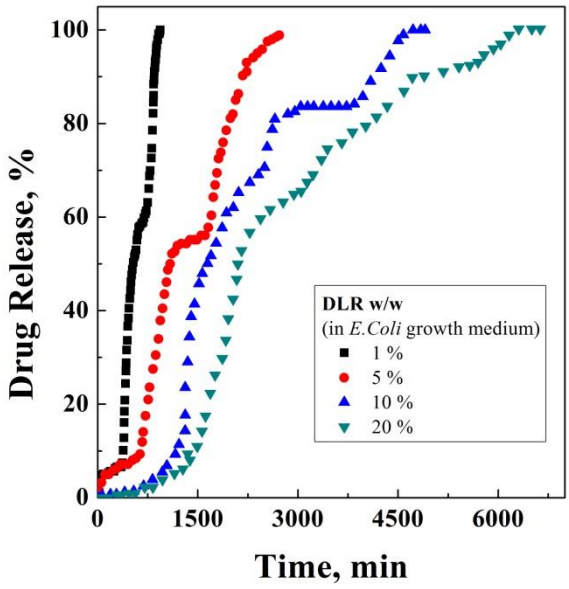

Figure VIII.8 *Drug release tests of 1 %, 5 %, 10 % and 20 % w/w amoxicillin loaded liposomes on lipid mass basis*

As is it possible to see in **Figure VIII.8**, drug release from 1 % loaded liposomes was completed after almost 1500 min; whereas, the 5 % loaded samples continued the release up to 3000 min. This means that a higher content of drug can contrast *E.Coli* growth for a longer time.
Moreover, in both profiles, a lag-phase was observed after drug initial burst. The latter is due to not entrapped drug which is suddenly released from the supernatant. Then, drug release is delayed for about 500 min, and then antibiotic diffuses in the external medium with higher velocity. This could explain why in some *E.Coli* profiles, the growth of bacteria is observed during the first five hours, before decreasing definitely.

Another pharmaceutical application that has been attempted is the encapsulation of albumin fluorescein isothiocyanate. This molecule is characterized by the classical protein Bovine Serum Albumin to which the fluorescein molecule has been previously chemically bonded. This molecule has many applications in the pharmaceutical field since it can be used for cellular uptake studies.

In this case, it was entrapped into liposomes to study the morphology of vesicles and to be co-encapsulated with an antibiotic for anti-bacterial applications. A first set of experiments was performed entrapping only Albumin fluorescein isothiocyanate (FBSA). Then, another set of

experiments was performed with the simultaneous encapsulation of FBSA and amoxicillin. The results are reported in **Table VIII.3**.

Table VIII.3 *Liposomes produced with different* Albumin fluorescein isothiocyanate mass *(FBSA) and different amoxicillin mass fixing FBSA mass*

Drug	**Drug mass [mg]**	**Diamentro medio DM [nm] ± DS**	**PDI**	**EE% media ± SD**	
Albumin fluorescein isothiocyanate (FBSA)	25	411 ± 133	0.32	84.41	
	50	426 ± 150	0.35	88.53	
	100	482 ± 310	0.64	80.61	
Amoxicillin	25	342 ± 101	0.29	95.0	74.9
	50	350 ± 122	0.35	91.8	78.7
	100	362 ± 168	0.46	98.8	76.0

Liposomes of sub-micrometrical dimensions were obtained. The first set was characterized by encapsulation efficiencies up to 88 % for FBSA. In the second set, FBSA was entrapped with an EE of 98.8 % of FBSA and 78 % for amoxicillin. Since the encapsulation of both the labeled protein and antibiotic was successfully achieved, the liposomes were put in contact with *E. Coli* to study the anti-bacterial response of this vesicles. The results are shown in **Figure VIII.9.**

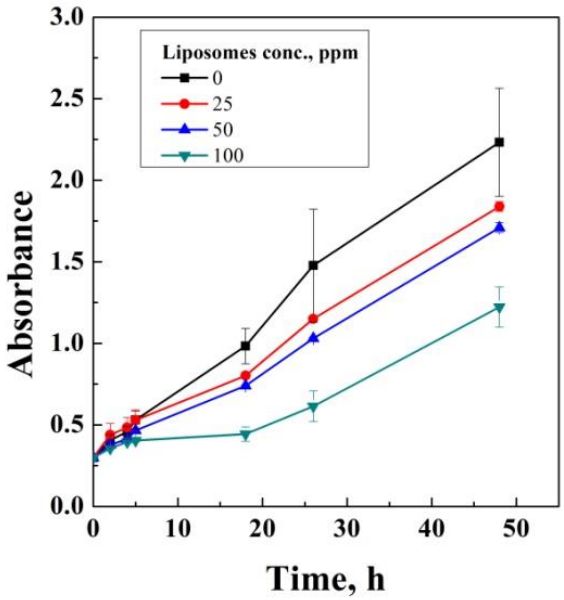

Figure VIII.9 *E.Coli growth kinetics in liposomes loaded with Albumin fluorescein isothiocyanate and amoxicillin (different liposomes concentrations)*

Even if the MIC concentration was not obtained for *E. Coli*, the increased liposomes concentrations put in contact with the bacteria resulted in a decrease in the bacterial growth rate.

Chapter IX

Encapsulation of dyes for leather treatment

Chapter IX

Leather manufacturing has ancient origins since primitive humans produced suits from the hunted animals and used vegetal tannins to process them (Falcao and Araujo, 2018). However, the leather obtained from animals had many drawbacks, such as the fast degradation caused by the decomposition of the dead skin. For this reason, the primitive humans tried to dry the leather so as to inhibit the decomposition process and soften up dried leather with fats. This method caused problems of rigidity.

The modern process of leather manufacturing (Sathish et al., 2016) is classically called tanning and its purpose is to transform the dead skin of the animal into a hygienic, transpiring and resistant suitable product. One of the last steps of the tanning process is the dyeing with the use of coloring substances. The purpose of dyeing is to improve the appearance of the leather so as to increase its commercial value. The following step is called fattening and gives to the leather softness and hydrophobicity. Usually, this operation is performed by applying natural or synthetic oils and fats.

Some artificial dyes are called anilines, that are substances responsible for the molecular interactions with the surface of the materials to be treated. Dyes are not only characterized by the spectral absorption functions of the visible light, but also by a high affinity with the material that should absorb it. Moreover, once the dyeing bath has been used, no residual dye should remain in the bath. This last property is known as the covering power. Generally, dyes have to be specific for the material that should be colored.

Several techniques have been developed for the coloring of leather (Priya et al., 2016, Chen et al., 2015, Sivakumar et al., 2009, Kyu, 2006, Rafidinarivo and Delmas, 1996); this is performed either directly in tanneries or in specific chemical factories. Dyeing is the process of applying the dye to textile substrates that frequently recur at high temperatures and pressures steps. During this process, dyes and chemical agents such as surfactants, acids alkalis, bases, electrolytes, leveling agents, chelating, emulsifying and softening agents are applied to leather to achieve a uniform dye penetration and strength properties (Kyu, 2006, Mandal et al., 2015). This process includes the diffusion of the dye in the aqueous phase followed by adsorption on the outer surface of the fibers, and finally diffusion and adsorption on the inner surface of the fibers. Depending on the final use of the fabrics, different dye strength properties may be required. For example, swimwear should not lose color in water and textiles for vehicles should not fade after prolonged exposure to sunlight. Dye can be fixed to the fiber by different mechanisms, typically working in aqueous solutions and ionic bonds. Van Der Waals interaction, hydrogen bonds and covalent bonds can be involved.

The leather dyeing process (Prakash et al., 2016, Venba et al., 2015, Lee et al., 2014, Purev et al., 2013, Page et al., 2009) can be performed continuously or in batch (Kore and Shukla, 2017, Li et al., 2011a). In general, the choice can depend on different factors, such as the type of

material and dye bath size; whereas, discontinuous processes are more automated but they are characterized by several expensive steps and also by environmental problems caused by process effluents (Rosa et al., 2017, Laurenti et al., 2017).

The major drawbacks of conventional dyeing techniques are linked to the consumption of a high energy request, especially for the optimization of the operating parameters to obtain a homogeneous dye distribution. For this reason, the idea of using liposomes has been considered in current literature for textile applications (Marsal et al., 2003, Delamaza et al., 1992, Marti et al., 2014, Montazer et al., 2009, El-Zawahry et al., 2009, Marsal et al., 2002, Marti et al., 2001) since they are eco-friendly carriers, non toxic and require lower production temperatures. Liposomes are spherical vesicles made of double layer of phospholipids and an inner core of water (Garcon et al., 1989). Liposomes production methods have also evolved over the last decades, first with the development of conventional techniques and then with dense gas assisted methods (Maherani et al., 2011, Mozafari, 2005b, Watwe and Bellare, 1995).

In the textile field, the higher interest of dyeing using liposomes is for wool treatment (Pause, 2007), in which a reduction of process temperature was also achieved (Coderch et al., 1997). However, it has been proved that liposomes have the ability to work as vehicles for several kind of synthetic compounds commonly used in dyeing processes (Sheveleva et al., 2003). Working at low temperatures gave the possibility to preserve fibers and limiting the energy cost (Lei et al., 1992). In tanning, the increasing interest in working with sustainable processes encouraged the use of natural matter such as phospholipids to reduce the environmental impact (El-Zawahry et al., 2007). Some studies present techniques for the removal of dyes using Pseudomonas (Roy et al., 2018), but almost no data are reported in the literature about the encapsulation efficiency of red aniline loaded liposomes for textile applications, probably for the limitations linked to the most common encapsulation techniques.

The main aim of this work is to achieve a significant encapsulation efficiency in stable vehicles for dye deposition on sheep leather surface. A novel supercritical assisted process will been employed for the production of liposomes called Supercritical assisted Liposome formation (SuperLip). SuperLip method has been already tested and used for the production of nanometric vesicles with high encapsulation efficiencies of hydrophilic and lipophilic compounds (Campardelli et al., 2016c, Campardelli et al., 2018, Trucillo et al., 2018a, Trucillo et al., 2017, Trucillo et al., 2018b, Trucillo et al., 2018c). Liposomes can be used for the vehiculation of dyes on leather surface, thanks to the fat nature of both lipids and leather skin (Barani and Montazer, 2008b). Therefore, the aim of this work will be achieved optimizing operating parameters of SuperLip process for the production of

liposomes loaded with red aniline, a hydrophilic dye, in the inner aqueous core.

In particular, effects on particle size distributions and encapsulation efficiencies will be studied varying dye and lipid concentration, water flow rate and the gas to liquid ratio of ethanol and carbon dioxide feeding lines. Morphological and atomic characterization will be performed on colored leather samples. Moreover, in order to give to this technique an increased commercial value, thermal exposition tests and colorimetric analysis will be performed to compare the efficiency of conventional coloration techniques with supercritical assisted liposomal method. This could reduce energy cost and production timing in tanning process, reducing also the environmental impact.

This section is divided into two main parts; the first describes the optimization of the operating parameters of the production process of liposomes; whereas, the second focuses on the dyeing of leather fragments with the liposomes produced, with a proper colorimetric analysis.

IX.1 Process parameters optimization

For the optimization of the process parameters, a first set of experiments was carried out, varying the mass ratios between the dye (synthetic red aniline) and lipids for the production of liposomes. This dye has a hydrophilic nature; for this reason, it was entrapped in the aqueous inner core of the liposomes. The ratio of dye/lipids was varied from 5 % w/w to 15 % w/w. The SuperLip experiment was performed at the pressure of 100 bar, temperature of 40 °C and a fixed Gas to Liquid Ratio of the Expanded Liquid of 2.4, with an ethanol flow rate of 3.5 mL/min. The water flow rate was fixed at 10 mL/min and the lipid concentration in ethanol was 5 mg/mL. The aim of this first set of experiments was to study the effect of the mass percentage on the particle size distribution of the obtained liposomes and encapsulation efficiencies. The mean diameters of the vesicles produced, polydispersion indexes and EE are reported in **Table IX.1** and the PSDs are compared in **Figure IX.1**.

Table IX.1 *Mean Diameter, Polydispersion Index and Encapsulation Efficiencies of liposomes loaded Dye to Lipid ratios from 5 to 15 % w/w*

Dye/PC [w/w, %]	Mean Diameters MD±DS [nm]	Encapsulation Efficiency EE [%]
5	174±70	23.7
10	185±78	23.7
15	196±94	27.3

Table IX.2 *Mean Diameter, Polydispersion Index and Encapsulation Efficiencies of liposomes produced with increasing lipid concentrations between 1 and 10 mg/mL ethanol solution*

Lipid conc. in Ethanol [mg/mL]	Mean Diameters MD±DS [nm]	Encapsulation Efficiency EE [%]
1	153±57	19.1
5	174±70	23.7
7	197±98	29.0
10	243±101	40.6

As seen in **Table IX.1**, increasing the dye mass with respect to the lipids from 5 to 15 % w/w, there is no macroscopic increase of the mean dimensions (MD) of the liposomes produced; MD are between a minimum of 174±70 nm for 5 % w/w loaded liposomes to a maximum of 196±94 nm for 15 % w/w loaded vesicles. Since there is no significant effect on liposomes production, the PSDs reported in **Figure IX.1** confirm the mean diameters trend. The encapsulation efficiencies are always less than 30 % of the theoretical dye entrapped, from a minimum of 23.7 % and a maximum of 27.3 %. No trends were detected in EEs.

For this reason, a new set of experiments was performed to study the effect of the lipid concentration in the ethanol flow rate for the preparation of liposomes. The concentrations studied were 5 mg/mL (used for the first set of experiments), 7 mg/mL, 10 mg/mL and 12 mg/mL. The mass of the dye entrapped in the liposomes was fixed to 50 mg, as well as the other process parameters used in the previously described set. The mean diameters of the vesicles produced, polydispersion indexes and EE are reported in **Table IX.2** and the PSDs are compared in **Figure IX.2**.

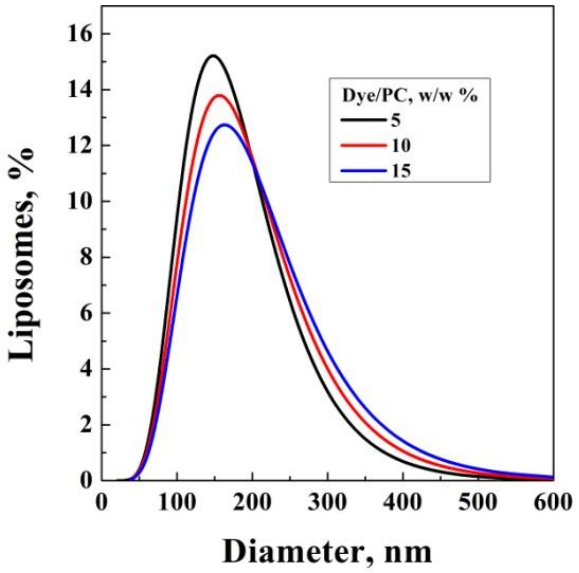

Figure IX.1 *Particle Size Distributions of liposomes produced at a dye/lipid ratio of 5 %, 10 % and 15 % w/w*

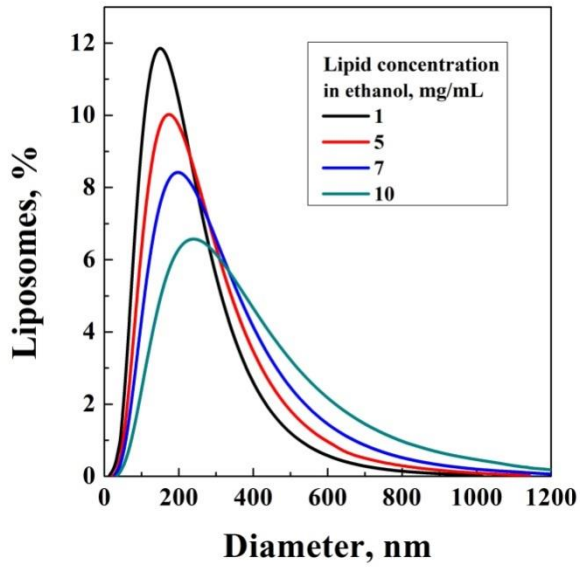

Figure IX.2 *Particle Size Distributions of liposomes produced at a lipid concentrations of 1, 5, 7 and 10 mg/mL*

As reported in **Table IX.2** and **Figure IX.2**, the mean values of the diameters have significantly increased by increasing the lipid concentration, from a minimum of 153±57 nm for 1 mg/mL ethanol concentration to a maximum of 243±101 nm with 10 mg/mL. The last concentration of 12 mg/mL was not explored due to a blockage of the injection for water atomization. The liposomes produced with an increased lipid concentration can be characterized by a higher number of double lipidic layers that surround the inner core. this could confirm the higher mean dimensions and polydispersion index than previous sets of experiments. The encapsulation efficiency increases upon increasing the lipid concentration; it is 19.1 % for 1 mg/mL lipid in ethanol concentration; whereas, it became 23.7 % for 5 mg/mL, 29.0 % for 7 mg/mL and 40.6 % for 10 mg/mL.

A new set of experiments was performed setting the concentration of lipids at 10 mg/mL. The water flow rate was varied from a minimum of 2 mL/min to a maximum of 20 mL/min.

The aim of this section is to verify if this process parameter can have an increasing effect on the encapsulation efficiencies of dyes into liposomes. The other process parameters were maintained constant.

Table IX.3 *Mean Diameter, Polydispersion Index and Encapsulation Efficiencies of liposomes (decreasing water flow rate from 20 to 2 mL/min)*

Water Flow Rate [mL/min]	Mean Diameters MD ± SD [nm]	Encapsulation Efficiency EE [%]
20	191±76	15.2
10	243±101	40.6
5	256±143	50.3
2	271±158	62.0

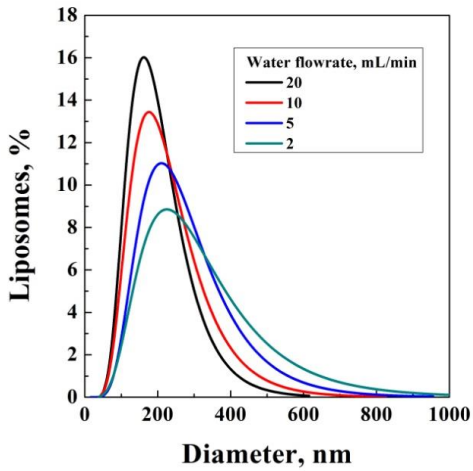

Figure IX.3 *Particle Size Distributions of liposomes produced at water flow rates of 2, 5, 10 and 20 mL/min*

The liposome mean dimension increases by decreasing the water flow rate (WFR), from a minimum of 191±76 nm for the highest water flow rate (20 mL/min) to 251±158 nm for the lowest water flow rate (2 mL/min). The decrease of the water flow rate resulted in the formation of more lipidic layers around the water droplets as described in other works and, as a consequence of this, a higher mean diameter was obtained for these vesicles. The encapsulation efficiency increased from 15.2 % for the case of 20 mL/min WFR up to 62 % for 2 mL/min WFR. This confirmed the hypothesis of the formation of more lipidic layers around the water droplets with lower WFR; with more layers, the drug content is highly protected and confined in the inner core of the liposomes.

To increase the values of the encapsulation efficiency of red aniline dye, another set of experiments was performed setting the concentration of the lipids at 10 mg/mL and the water flow rate at 2 mL/min. The other process parameters remained constant, except for the Gas to Liquid Ratio of the Expanded Liquid (GLR-EL), i.e. the mass ratio of the carbon dioxide and ethanol flow rate that are fed into SuperLip. This parameter was varied from 0.34 to 10, with the aim of studying the probable differences by changing the composition of the system. The carbon dioxide and ethanol flow rate were changed together in order to modify the GLR-EL. The mean diameters of the vesicles produced, polydispersion indexes and EE are reported in **Table IX.4** and the PSDs are compared in **Figure IX.4**. Again, aniline theoretical loading was fixed at 5 % w/w on lipid base.

Table IX.4 *Mean Diameter, Polydispersion Index and Encapsulation Efficiencies of liposomes produced at different GLR-EL (from 0.34 to 10)*

Scale	GLR-EL	Mean Diameters [μm]± DS	PDI	Encapsulation Efficiency EE [%]
NANO	10	0.17±0.08	0.48	32.2
	6	0.20±0.10	0.50	49.5
	4	0.23±0.12	0.51	57.7
	2.4	0.27±0.13	0.54	62.0
	1.2	0.28±0.16	0.57	74.7
MICRO	1	2.07±1.08	0.52	76.0
	0.8	3.32±1.56	0.47	79.6
	0.7	3.96±1.70	0.43	82.2
	0.4	4.52±1.72	0.38	76.3
	0.34	5.06±1.40	0.28	77.3

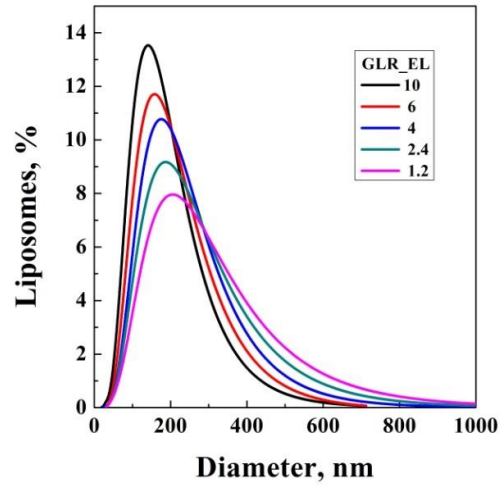

(a)

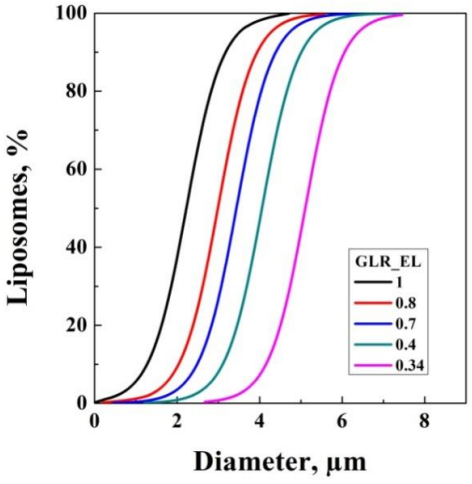

(b)

Figure IX.4 *Particle Size Distributions of liposomes produced at Gas to Liquid Ratio of the Expanded Liquid at 10, 6, 4, 2.4, 1.2 (a) and at 1, 0.8, 0.7, 0.4, 0.34 (b)*

Looking at **Table IX.4**, the liposomes produced with the Gas to Liquid Ratio of the Expanded Liquid included between 10 and 1.2 resulted in the production of liposomes with a mean diameter from 0.17±0.08 µm to 0.28±0.16 µm, showing an increasing trend, but always at a nanometric level. The particles size distribution was more dispersed when decreasing GLR-EL (**Figure IX.4a**); PDI increased from 0.48 to 0.57 when reducing the content of ethanol. The encapsulation efficiencies showed an increased

trend from 32.2 % for the higher GLR-El to 74.7 % for a GLR-EL of 1.2. The same increasing trend of the mean dimensions of indeed, vesicles was obtained working at lower values of GLR-EL, from 1.00 to 0.34. In this case, indeed, liposomes mean size increased from a minimum of 2.07±1.08 µm to a maximum of 5.06±1.40 µm, at a micrometric level. The order of magnitude was changed by decreasing the GLR-EL, but indeed, polydispersion indexes showed a decreasing trend from 0.52 to 0.28. The encapsulation efficiencies were higher than indeed, nanometric level liposomes, from a minimum of 76.0 % to a maximum of 82.2 % without showing any trend. The higher EE is probably due to the higher volume of water entrapped into the liposomes. On the other hand, decreasing the GLR-EL involves more ethanol in the system; if GLR-EL tends to zero, the SuperLip technique could be overlapped with the Ethanol Injection method (Shaker et al., 2017, Maitani, 2010), with consequent higher incompatibility with pharmaceutical applications. As already verified in previous studies with SuperLip, GLR-EL was the main process parameters which is responsible for controlling liposomes dimensions and particle size distributions, as already verified in previously cited studies.

Morphological studies were performed on liposomes produced with a GLR-EL of 0.7 and 2.4, with the aim of observing the differences between the liposomes produced at nanometric and micrometric levels. In **Figure IX.5,** the different morphologies are compared.

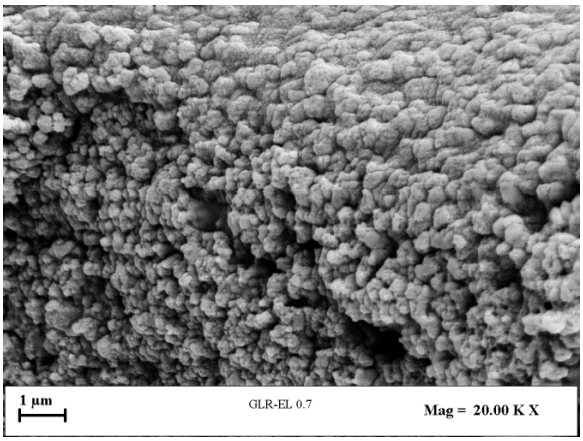

(b)

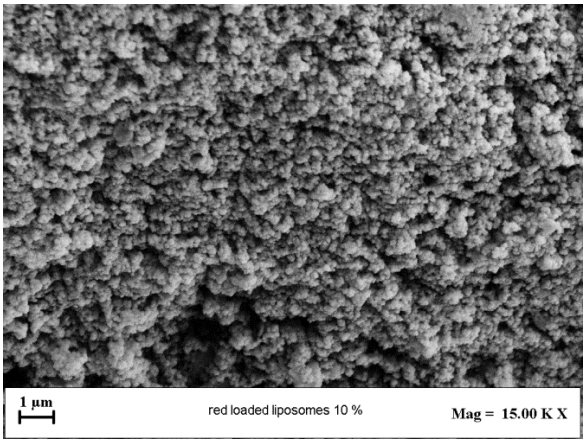

(b)

Figure IX.5 *FE-SEM characterization of aniline loaded liposomes produced with GLR-EL 0.7 (a) and GLR 2.4 (b)*

In **Figure IX.5ab,** liposomes are present. In the first one (**Figure IX.5a**) liposomes are obtained working at a GLR-EL of 0.7, showing sub-micrometric liposomes whose aggregates are of 2-3 microns in diameter (as shown in **Table IX.4**). These liposomes have a tendency to aggregate in larger vesicles, with a difficult control of the vesicles morphology; they are more dispersed as shown in **Figure IX.5a**. Whereas, in **Figure IX.5b**, liposomes of nanometric dimensions are obtained, with a more homogeneous population distribution and higher sphericity of the vesicles. The surface is smooth and regular.

Leather slices were put in contact with 20 mL of a bath containing red aniline dye in a gently stirred solution. Then, the same treatment was repeated submerging slices in a bath containing an aqueous suspension of liposomes loaded with the same amount of red aniline, taking into account the encapsulation efficiency of the vesicles. In this manner, it was possible to compare the results obtained using the traditional dyeing method and the supercritical method.

Further observations were performed on sheep leather after dyeing with liposomes with a Field Emission Scanning Electron Microscope. The upper surface can be seen in **Figure IX.6a**; whereas, the underneath surface in **Figure IX.6b**. Finally, a macroscopic image of the leather fragments is reported in **Figure IX.6c**, showing the upper and underneath surface.

Figure IX.6 *Morphological analysis of (a) upper and (b) underneath leather surfaces from microscopic and macroscopic (c) observations*

The leather upper surface is more compact since it is the surface exposed to external agents, i.e. it is more hydrophobic and its coloration is brighter (**Figure IX.6ac**). The underneath surface (**Figure IX.6bc**) is more frayed and sliced since it is linked to fibers and muscles. In general, it can absorb the dye but the final coloration is not as bright as the upper surface.

IX.2 EDX and Colorimetric analysis

Dye powder, not colored leather, leather colored with native dye and leather colored with dye loaded liposomes were analyzed with Energy Dispersive X-ray spectroscopy to obtain more quantitative and qualitative information on their chemical structure. The main results on the Carbon, Oxygen, Phosphor and Sulfur atoms are summarized in **Table IX.5**; whereas, the qualitative maps of the Carbon and Oxygen distribution are reported in **Figure IX.7**.

Table IX.5 *Energy Dispersive X-ray spectroscopy analysis of the Carbon and Oxygen contained in Leather, native dye, leather + dye and leather + dye loaded liposomes*

Element [%]	Leather	Dye	Leather+Dye	Leather+Liposomes+ Dye
O	46.08	36.51	51.77	53.92
P	0.51	-	0.50	0.98
S	1.78	8.69	2.38	2.83
C	50.49	44.81	44.80	39.42

Oxygen is one of the two main components of leather, with 46.08 %. Dye also contains it at 36.51 %; for this reason, the coupling of leather + native dye and leather + liposome deposed dyes increases its percentage (51.77 % native dye and 53.92 % dye loaded liposome).

Sulfur is contained more significantly in dye powder (8.69 %). During the dyeing process, it is deposited on the leather, increasing its sulfur content from 1.78 % to 2.38 % on conventionally colored leather and to 2.83 % on liposome colored leather. For this reason, the dye is better deposited on the leather using the method with liposomes.

Phosphorus is contained only in pure leather but not in powder dye. For this reason, the deposition on leather increases the content of phosphorous to 0.50 % using conventional coloration method; whereas, it increases up to 0.98 % using the liposomes method dye deposition.

Carbon is one of the main components of leather since it comes from an organic material. However, carbon atoms are prevalent also in phospholipids molecules since it is contained in the double tailored part of the molecule. The dye also contains it; for this reason, it is not possible to find any particular comments on its deposition since it is always present.

Energy Dispersive X-ray qualitative data are also reported in **Figure IX.7** to compare the carbon and oxygen distribution maps. The choice of showing these two elements distribution maps is linked to the fact that they are the main components of these fragments and better describe their deposition. The native aniline deposition is described in **Figure IX.7bd**; whereas, the liposomes loaded aniline is shown in **Figure IX.7ac**.

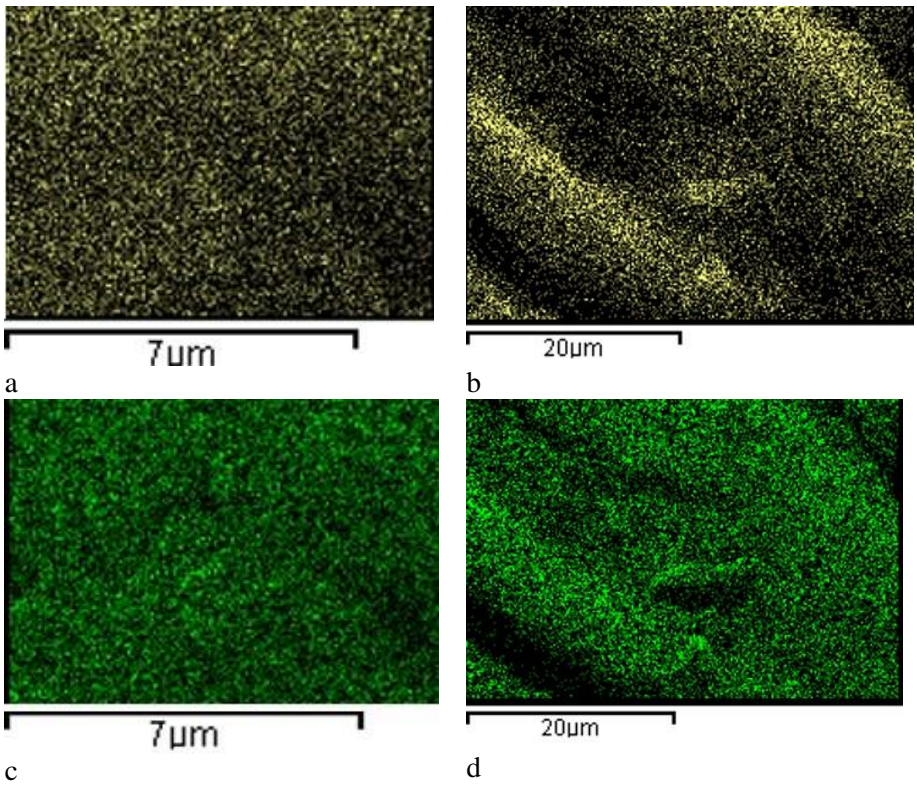

Figure IX.7 *Carbon and Oxygen EDX images of leather treated with native aniline (a, c) and with liposomes (b, d)*

Looking at **Figure IX.7ac**, a more homogeneous distribution of the Carbon and Oxygen can be observed for the liposomes treated leather fragments. The surface of the fragment treated with liposomes is smoother and more regular; whereas, in **Figure IX.7bd** a fragment treated with native red aniline appears more irregular and inhomogeneous.

As a further confirmation of the results obtained, the leather fragments were subjected to a colorimetric analysis to study any eventual variations in red dyeing on leather by changing the method from conventional to liposomal. For this reason, colorimetric coordinates were used according to the CIELAB scale, as reported in the Methods section. The conventional method was also compared with the liposomes method in terms of different time contacts (15, 30, 60 and 120 min) for the deposition of dye on leather. The time contact and redness intensity (a*) are reported in **Table IX.6** and **Figure IX.8**.

Table IX.6 C*olorimetric analysis on leather dyed at different contact times using conventional and supercritical techniques*

Dyeing method	Time contact [min]	a*±SD
Conventional	15	30.14±0.07
	30	34.61±0.09
	60	36.69±0.08
	120	36.30±0.06
Liposomes	15	27.20±0.04
	30	33.42±0.09
	60	32.51±0.12
	120	33.15±0.05

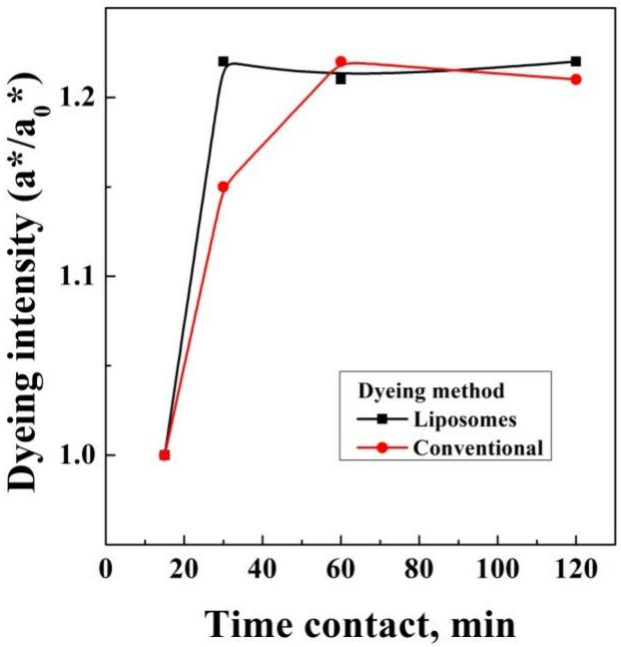

Figure IX.8 *Red intensity of leather upper surfaces with conventional and supercritical dyeing process*

From **Table IX.6**, the conventional method for the deposition of dye on leather results in a redness intensity of 30.14±0.07 % after 15 minutes of time contact; whereas, it becomes 34.61±0.09 % after 30 minutes, 36.69±0.08 % after 60 minutes and 36.30±0.06 % after 120 minutes; this means that the redness saturation limit is reached at 60 minutes using a

conventional technology. Using the liposomes deposition method, 27.20±0.04 % redness intensity is reached after 15 minutes, 33.42±0.09 % after 30 minutes, 32.51±0.12 % in 60 minutes and finally 33.15±0.05% in 120 minutes. In this case, the saturation limit was reached only after 30 minutes of time contact between the leather and red aniline. These results are confirmed in **Figure IX.8**, where each redness intensity value a* was made dimensionless with the starting value a_0^* to make the comparisons.

Colored leather fragments were subjected to thermal exposure tests. Two kind of tests were performed: colored leather was put in contact with water at the temperature of 100 °C for 24 hours and then in an oven at 120 °C for the same contact time. The redness intensity of the untreated leather was compared with the thermal exposed leather to evaluate the eventual intensity variations and dye adhesion stability after external stimuli. The results of the leather fragments colored with the conventional and liposomal methods are compared in **Table IX.7** and **Figure IX.9**.

Table IX.7 *Red dye intensity of leather untreated and treated with water at 100 °C and oven at 120 °C*

Thermal test	Dyeing method	a*±SD	Decoloration [%]
Untreated leather	Liposomes	37.50±0.05	-
	Conventional	30.05±0.11	
Water 100°C	Liposomes	33.66±0.06	10.2
	Conventional	22.50±0.04	25.1
Oven 120°C	Liposomes	36.63±0.04	2.3
	Conventional	25.76±0.07	14.3

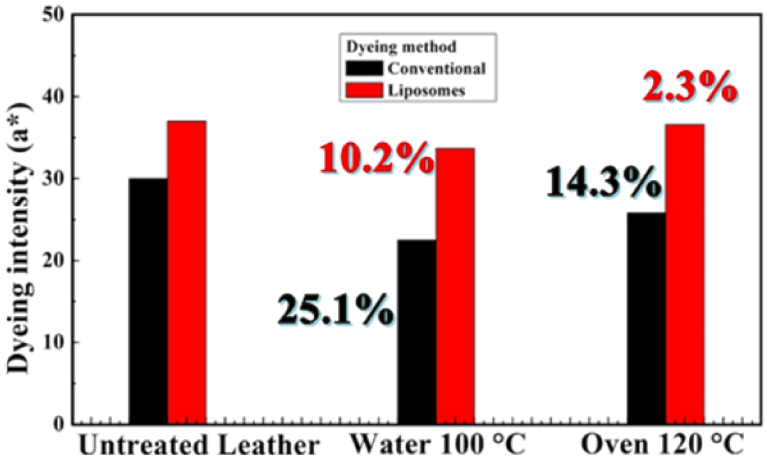

Figure IX.9 *Variation of red intensity due to thermal exposure using conventional and supercritical methods*

The redness intensity of an untreated fragment of leather was 37.50±0.05 %; it was reduced to 33.66±0.06 % with liposomal dye deposition after treatment in water at 100 °C; whereas, it was 36.63±0.04 % after the treatment in the oven at 120 °C. Decoloration was 10.2 % after hot water treatment and 2.3 % after oven treatment. The native dyeing method caused a decoloration of 25.1 % in the case of the hot water treatment and 14.3 % in the case of the oven treatment. For this reason, it is possible to affirm that in the case of liposome treatment, the dye adhesion is high performing on the leather fragments. This novel method shows an increased resistance to heat exposure, also showing a greater softening of the leather.

In this section, the SuperLip operating parameters have been optimized to obtain the best performance on the encapsulation efficiency and red aniline deposition on sheep leather fragments. The key parameters responsible for the highest encapsulation efficiencies were the water flow rate and Gas to Liquid Ratio of the Expanded Liquid. The reducing of the water flow rate

increased EE to 75 %. GLR-EL resulted mainly responsible in the control of the particle size distributions and mean diameters, that were nanometric at GLR-EL lower than 1.2 and micrometric when higher up to 10. The dyeing tests confirmed that saturation deposition is obtained in 30 minutes with the liposomal method and in 60 minutes with the conventional process. The most interesting results is linked to the use of liposomes; they guarantee the coloration and fattening of the leather, that generally are performed with two expensive steps in the tanning process. Using liposomes, the two steps are obtained simultaneously and the greater softening of leather could also speed up the classic tanning process. Finally, leather treated with dye loaded liposomes was more resistant to heat exposure, showing slightly more decoloration than conventional colored liposomes.

Chapter X
SuperLip economic and financial analysis

Supercritical assisted Liposome formation (SuperLip) is a lab scale plant for the production of lipidic drug carriers. After almost 4 years of experiments, SuperLip has been recognized to be particularly versatile in the encapsulation of molecules of different sizes, solubility and industrial fields of application.

A business plan for the commercialization of SuperLip products was attempted to verify whether the production of liposomes using this technique could be profitable. A B2B model has been proposed and an estimation of CAPEX and OPEX was performed to produce a 5-year (2018-2022) prospective for commercialization.

The analyzed market segment is 1.7 M€ large; whereas, the SuperLip apparatus could obtain a 0.1 % market share. From its discounted cash-flow, it was possible to evaluate the SuperLip market value at about €3 million.

The high versatility of the SuperLip process has already been recognized in terms of process biocompatibility and applications in several industrial fields such as nutraceutical, cosmetic, pharmaceutical and textile. The gain of this process is referred to the one-shot production of liposomes with a continuous reproducible plant layout.

This developed technology has a Technology Readiness Level (TRL) of 7, since it has been developed in a continuous lab-scale configuration and it is possible to scale it up to an industrial level. Nowadays, the SuperLip method is designed to produce about 5 liters of liquid liposomes suspensions per day. The idea at the basis of the process has already been validated by product development and samples characterization, as reported in previously published works. SuperLip potential applications have also been recognized by external customers, interested in a Business To Business (B2B) production of liposomes on demand.

The validation of the system is guaranteed by their main potential applications for skin care treatment, tissues infections, antioxidant preservation and dye deposition. A comparison of the SuperLip process with other techniques reported in current literature is summarized in **Table X.1**.

Table X.1 *Pain and Gain of SuperLip Vs other methods*

Other processes	SuperLip	Utility	Potential application
Micrometric level (0.5-50 µm)	Nanometric level (100 – 300 nm)	Drug carriers for nanometric interstices tissues	Pharmaceutical formulations for anti-carcinogenic therapies
Polydispersed samples	Monodispersed samples	Replicable granulometric control of liposomes	
Solvent Residue	Green process	Carbon dioxide is not toxic; ethanol is biocompatible. Organic solvent is removed	Food industry for the production of additives and dietary supplements
Encapsulation efficiencies low than 30 %	Encapsulation efficiencies higher than 95 %	Cost reduction	Encapsulation of markers, genes and high weight proteins
Vesicles aggregation	Vesicles distinction	Vesicles stability	Long targeted release of drugs
Sensitive to external stimuli	Drug protection from heat and oxidation	Preservation of antioxidant power	Cosmetic industries for skin penetration products
Post-production steps	1-shot	Replicability of the process and reduced cost	Production of liposome based vaccines in brief times
Discontinuous processes	Continuous processes	Scalability of the process to industrial level	Large scale production

X.1 Economic analysis

Nutraceuticals is the field of compounds content in food that can prevent the human body from developing illnesses. Even if many samples were obtained for pharmaceutical applications, the nutraceutical market segment seems to be the most interesting one for the production of liposomes, since its barriers are less severe than the pharmaceutical and cosmetic fields. Italy is ranked as the first European country for the consumption of nutraceutical products; the Italian market of dietary supplements has grown by 7.4 % between 2014 and 2016, especially for multi-vitamin additives. They are sold in pharmacies and mass markets; every Italian spends around €40 on

dietary supplements per year, followed by Austria and Belgium with €33 each. The last place in the European ranking is occupied by France, with €12 per annum. The main reason for this high market increase originates from the recommendations of doctors and specialists. 90% of Italian family doctors advise using food supplements to patients.

Not only liposomes, but also other Drug Delivery Systems (DDS), nanocrystals, polymer microspheres, gold nanoparticles, micelles, nanotubes and patches are commonly used to vehiculate nutraceutical compounds. In **Figure X.1,** a comparison between worldwide overall drug delivery systems sold and liposome sold is presented.

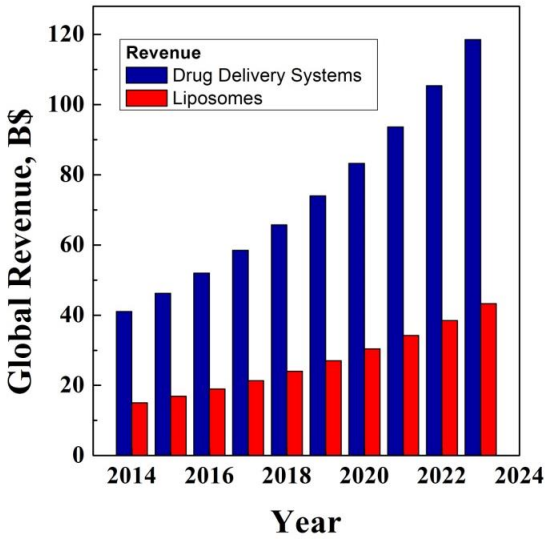

Figure X.1 *Drug Delivery Systems Vs liposomes revenues worldwide*

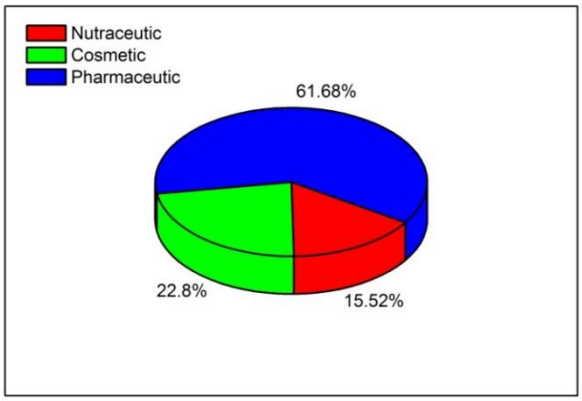

Figure X.2 *Yearly market repartition of Drug Delivery Systems*

It is possible to see in **Figure X.1**, the worldwide market is represented by all DDS sold for nutraceutical purposes, represented with blue columns. The volume of the business linked to the DDS of nutraceuticals started from €40 billion in 2014 with an estimation growth up to €100 billion in 2024. Liposomes had a market value of around €20 billion in 2014, whereas it is estimated to become around €40 billion by 2024.

The liposomes market can be furthermore divided into nutraceutical, cosmetic and pharmaceutic, as shown in the diagram of **Figure X.2**. Despite the nutraceutical field being represented by 15.52 % of the worldwide marked linked to liposomes, it is the easiest segment to join, avoiding in vitro and in vivo tests, that are generally time consuming and particularly expensive. The nutraceutical field also guarantees a shorter payback time.

In 2018, the estimation of liposomes for nutraceutical purposes will be around €1.7 million worldwide, with an estimated €3.12 billion market volume. Since the SuperLip productive capability is around 1500 liters per year (300 working days), the plant capacity will guarantee around 0.1 % of the market share.

X.2 Financial analysis

The idea is to develop a Business to Business (B2B) model. Potential customers are nutraceutical companies that would be interested in encapsulating their chosen molecule using this technology for the production of liposomes on demand. Several applications are possible, such as liposomes for iron additives to dietary supplements for sport enhanced performance. The high encapsulation efficiencies of active compounds can reduce costs and acquire more customers, especially among food industry companies linked to anti-age and antimicrobial product development as well as the prevention of cardiovascular illnesses. A scheme of the Strengths, Weaknesses, Opportunities and Threats of the SuperLip process is proposed in **Table X.2**.

Table X.2 *S.W.O.T. analysis of SuperLip process*

Strengths	Weaknesses
Liposomes produced with SuperLip have the possibility to entrap more than 95 % of the compound and tune their drug release, activated by external stimuli on demand.	The high potential of SuperLip could not be quickly understood by medical doctors and healthcare system. For this reason, an expensive advertising campaign could be necessary to be activated.
Competitive cost compared to average market price.	Several companies are still linked to conventional methods for the production of liposomes, despite their weaknesses.
Opportunities	**Threats**
Fast growth of the liposomal market	SuperLip is not a patented process, even if there are many publications discussing its several studied applications.

The idea of commercialization of SuperLip liposomes needs to be divided into OPEX (Operative Expenditures) and CAPEX (Capital Expenditures). OPEX is referred to marketing campaigns, such as participating in events and fairs. Digital advertisement is one of the main instruments to be known in a huge market environment. This area also includes utilities cost (power and water supply), chemical reagents, packaging and expedition. Human costs are also included for plant operators, technicians and maintenance. Subcontractors will require legal services, technical characterizations and business strategies, software renewal licenses and insurance costs. 10 % of the plant maintenance cost was also be considered. CAPEX is linked to the setting up of the SuperLip plant on a lab-scale configuration, but also for desks, computers, mobile phones and cars and packaging machines. 20 % automation costs have been considered for the start up of the plant. This point should cover the maintenance and safety expenditures linked to the current functioning of the plant.

CAPEX amortization was fixed as linear, with a yearly depreciation of 10 % over a period of about 10 years. Productivity was fixed at 5 Liters per day and 300 working days per year. The selling price was set at 1.8 €/mL liposome suspension. **Table X.3** contains the CAPEX cost of SuperLip; whereas, **Table X.4** represents advertising campaign costs, **Table X.5** subcontractor costs, **Table X.6** operating and production costs, **Table X.7** personnel costs.

Table X.3 *CAPEX cost for the SuperLip apparatus*

ASSET description	Cost of 1 unit	Number of units	TOTAL
Patent	10000	1	10000
pump Gilson	8000	2	16000
pump Lewa	15000	1	15000
Thermostatic bath Julabo	6000	1	6000
valves on/off	50	4	200
Micrometric valves	400	1	400
Backpressure valves	1500	1	1500
Glass burette	150	2	300
Stainless steel elements	400	2	800
Stainless steel formation vessel	1700	1	1700
Stainless steel separator	600	1	600
Thermocouples and relais	500	1	500
Electrical works	500	1	500
30 Liter compressed gas tank	4000	1	4000
Manometers	50	3	150
Electrical resistance	40	1	40
Asameter	70	1	70
Gas flow meter	30	1	30
Stainless steel plant backbone	1500	1	1500
Laboratory extractor hood	5000	1	5000
Piping	500	1	500
Maintenance elements	39970	1	39970
Packaging machinery	5000	1	5000
Desks	200	10	2000
Drawer units	50	10	500
Cupboards	66.7	10	667
Computer	800	10	8000
Company cars	14950	2	29900
Sample stock	973	1	973
Mobile phones	150	6	900
TOTALE ASSETS			152700

Table X.4 *Marketing cost*

MARKETING COSTS	PRICE	UNITS	notes	2018	2019	2020	2021	2022
# Events & Fairs				2	1	1	1	1
fee	2000	1	x event	4000	2000	2000	2000	2000
stand preparation	2500	1	x event	5000	2500	2500	2500	2500
flights, hotels, meals	1760	2	# persons for 7 days	7040	3520	3520	3520	3520
other costs	10%	1	% (staying)	704	352	352	352	352
EVENTS & FAIRS				16744	8372	8372	8372	8372
Advertising %Δ				0%	2%	4%	6%	8%
magazines	500	1	advertising/year	500	510	530	562	607
TV & Radio	2500	1	advertising/year	2500	2550	2652	2811	3036
digital advertising	500	12	monthly fee	6000	6120	6242	6367	6495
Brochure % gadgets	1500	1	x # events & fairs	3000	1500	1500	1500	2250
Professional video	2000	1	x events	4000	2.000	2000	2000	2000
Sponsorships	2000	1	at events and fairs	4000	2000	2000	2000	225
COMMUNICATION				20000	14680	14925	15241	14613
costs %Δ				0%	1%	2%	3%	4%
Social media strategy	200	12	monthly fee	2400	2424	2472	2547	2649
WEB				2400	2424	2472	2547	2649
MARKETING				39144	25476	25769	26159	25633
# Events & Fairs				2	1	1	1	1
fee	2000	1	x event	4000	2000	2000	2000	2000
stand preparation	2500	1	x event	5000	2500	2500	2500	2500
flights, hotels, meals	1760	2	# persons for 7 days	7040	3520	3520	3520	3520
other costs	10%	1	% (staying)	704	352	352	352	352
EVENTS & FAIRS				16744	8372	8372	8372	8372
Advertising %Δ				0%	2%	4%	6%	8%
magazines	500	1	advertising/year	500	510	530	562	607
TV & Radio	2500	1	advertising/year	2500	2550	2652	2811	3036
digital advertising	500	12	monthly fee	6000	6120	6242	6367	6495
Brochure and gadgets	1500	1	x # events & fairs	3000	1500	1500	1500	2250
Professional video	2000	1	x events	4000	2.000	2000	2000	2000
Sponsorships	2000	1	at events and fairs	4000	2000	2000	2000	225
COMMUNICATION				20000	14680	14925	15241	14613
costs %Δ				0%	1%	2%	3%	4%
Social media strategy	200	12	monthly fee	2400	2424	2472	2547	2649
WEB				2400	2424	2472	2547	2649
MARKETING				**39144**	**25476**	**25769**	**26159**	**25633**

Table X.5 *Sub-contractors costs*

SUBCONTRACTORS	2018	2019	2020	2021	2022
Project and management	0	0	25000	0	0
Transport of plant elements	0	0	10000	0	0
Automation cost	0	0	18952	0	0
Pharma consultancy	2500	2500	2500	2500	2500
Web content	750	750	750	750	750
Patent	10000	0	0	0	0
Legal expenses	3000	3000	3000	3000	3000
SUBCONTRACTORS	16250	6250	60202	6250	6250

Table X.6 *Operating and production costs*

OPERATING	PRICE	UNITS	notes	2018	2019	2020	2021	2022
costs %Δ				0%	2%	2%	2%	2%
Mobile phones	30	6		0	0	2247	2292	2338
Power & water supply	4560	1	yearly fee	0	0	4744	4839	4936
Internet	100	12	monthly fee	0	0	1248	1273	1299
Bank account	3	12	monthly fee	40	41	42	42	43
PEC email	30	12	monthly fee	0	0	375	382	390
insurance	3883	1	yearly fee	0	0	4040	4121	4203
Software license	100	12	monthly fee	1200	1224	1248	1273	1299
Rent	20000	1	yearly fee	20000	20400	20808	21224	21649
Reagents	23702	1	yearly	23702	24176	24660	25153	25656
Packaging	1719	1	yearly	1719	1753	1788	1824	1861
Mailing service	4000	12	monthly fee	4000	4080	4162	4245	4330
Maintenance	10%	1		6282	6408	6536	6667	6800
OPERATING				69106	70489	71898	73336	74803
costs %Δ				0%	5%	10%	15%	20%
accounting, tax e legal	10000	1	yearly fee	10000	10500	11550	13283	15939
business & strategy	3500	1	yearly fee	3500	3675	4043	4649	5579
other services	10%	1	% (other cost lines)	1350	1418	1559	1793	2152
SERVICES				14850	15593	17152	19725	23669

Table X.7 *Personnel costs*

ROLE	COST [€] [2018]	% ETF 2018	% ETF 2019	% ETF 2020-2022	2018	2019	2020	2021	2022
CEO	33600	50%	100%	100%	16800	35280	37044	38896	40841
Project manager	31200	50%	100%	100%	15600	32760	34398	36118	37924
Operator	28800	50%	75%	100%	14400	30240	31752	33340	35007
Operator	28800	0%	0%	100%	0	30240	31752	33340	35007
Technician	26400	50%	75%	100%	13200	27720	29106	30561	32089
Administrative	21600	50%	75%	100%	10800	22680	23814	25005	26255
Total cost personnel					70800	178920	187866	197259	207122

The first year of investments will be used to obtain customers contracts and start the production of the first amount of liposomes requested. By the second year, the steady state production and sale of products will be obtained. By the third year, the construction of a scaled pilot plant will be started. For this reason, in **Table X.8** a Profit & Loss Statement is proposed; whereas, in **Table X.9** a Cash Flow Statement is reported and finally in **Table X.10** a five year Balance Sheet.

Table X.8 *Profit & loss Statement*

PROFIT & LOSS	**2018**	**2019**	**2020**	**2021**	**2022**
Liposomes sold	75586	869234	1417230	1606194	1700676
TOTAL REVENUES	**75586**	**869234**	**1417230**	**1606194**	**1700676**
Liposomes not sold	56689	75586	94482	94482	94482
TOTAL COGS	56689	75586	94482	94482	94482
COST OF NOT SOLD	**5669**	**7559**	**9448**	**9448**	**9448**
GROSS MARGIN	**13227**	**786090**	**1313300**	**1502264**	**1596746**
GROSS MARGIN %	**17.50%**	**90.43%**	**92.67%**	**93.53%**	**93.89%**
PERSONNEL	70800	148680	187866	197259	207122
EVENTS & FAIRS	16744	8372	8372	8372	8372
COMMUNICATION	20000	14680	14925	15241	14613
WEB	2400	2424	2472	2547	2649
MARKETING	39144	25476	25769	26159	25633
OPERATING	56943	58082	71898	73336	74803
SERVICES	14850	15593	17152	19725	23669
SUBCONTRACTORS	16250	6250	60202	6250	6250
TOTAL COSTS	**197987**	**254081**	**362887**	**322729**	**337478**
EBITDA	**-184760**	**532009**	**950412**	**1179534**	**1259268**
DEPRECIATION	1000	1000	15270	15270	15270
EBIT	**-185760**	**531009**	**935142**	**1164264**	**1243998**
INTEREST	0	0	0	0	0
EBT	**-185760**	**531009**	**935142**	**1164264**	**1243998**
Taxes	0	196474	346003	430778	460279
NET PROFIT	**-185760**	**334536**	**589140**	**733487**	**783719**

Table X.9 *Cash Flow Statement*

CASH FLOW	2018	2019	2020	2021	2022
EBITDA	-184760	532009	950412	1179534	1259268
Δ INVENTORY	7559	79365	54800	18896	9448
Δ TAXES	0	196474	346003	430778	460279
CFO: OPERATING CASH FLOW	-192318	256171	549610	729860	789540
CFI: INVESTING CASH FLOW	10000	0	142700	0	0
PROVISION	4885	10259	12963	13611	14291
LONG TERM DEBT	0	0	0	0	0
EQUITY INJECTION	20000	0	0	0	0
CFF: FINANCING CASH FLOW	24885	10259	12963	13611	14291
CASH FLOW = CF + CFI + CFF	**-177433**	**266430**	**419873**	**743471**	**803832**

Table X.10 *Balance Sheet*

BALANCE SHEET	2018	2019	2020	2021	2022
TANGIBLE FIXED ASSETS	0	0	142700	142700	142700
DEPRECIATION FUND	0	0	14270	28540	42810
NET TANGIBLE FIXED ASSETS	0	0	128430	114160	99890
INTANGIBLE FIXED ASSETS	10000	10000	10000	10000	10000
DEPRECIATION FUND	1000	2000	3000	4000	5000
NET INTANGIBLE FIXED ASSETS	9000	8000	7000	6000	5000
LONG TERM ASSETS	9000	8000	135430	120160	104890
INVENTORY	7559	86923	141723	160619	170068
CASH	-177433	88997	508870	1252341	2056173
CURRENT ASSETS	-169875	175920	650593	1412960	2226240
ASSETS	-160875	183920	786023	1533120	2331130
EQUITY	**20000**	**20000**	**20000**	**20000**	**20000**
LEGAL RESERVE	-9288	7439	36896	73570	112756
RETAINED EARNING	-176472	141337	701020	1397832	2142365
EQUITY	-165760	168776	757916	1491402	2275121
LONG TERM DEBT	0	0	0	0	0
PROVISION (TFR)	4885	15144	28107	41718	56009
LIABILITIES	**4885**	**15144**	**28107**	**41718**	**56009**
LIABILITIES & EQUITY	**-160875**	**183920**	**786023**	**1533120**	**2331130**

From the previously proposed Tables, the Revenues, Profit and Cash Flow diagrams in **Figure X.3, Figure X.4** and **Figure X.5** were obtained.

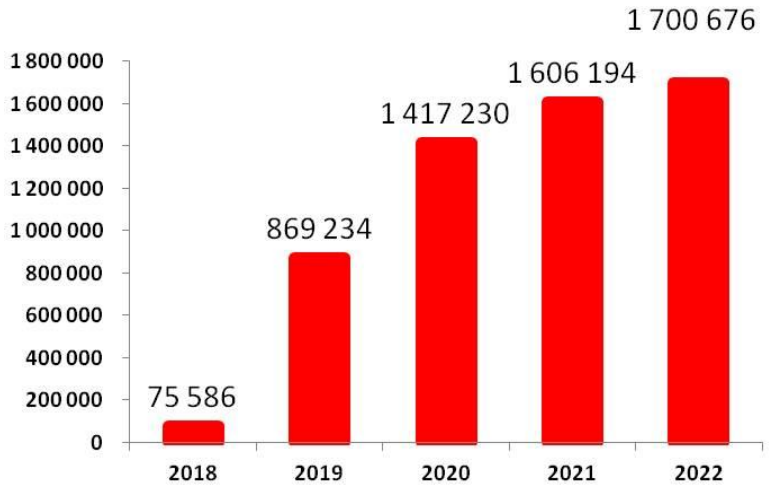

Figure X.3 *Revenues calculated for SuperLip commercialization (2018-2022).*

During the first year of production, SuperLip will obtain Revenues for as little as € 75, 000 for the reason stated above and linked to the acquisition of contracts and start up of the society. Sales will then significantly increase up to €1.7 million by 2022.

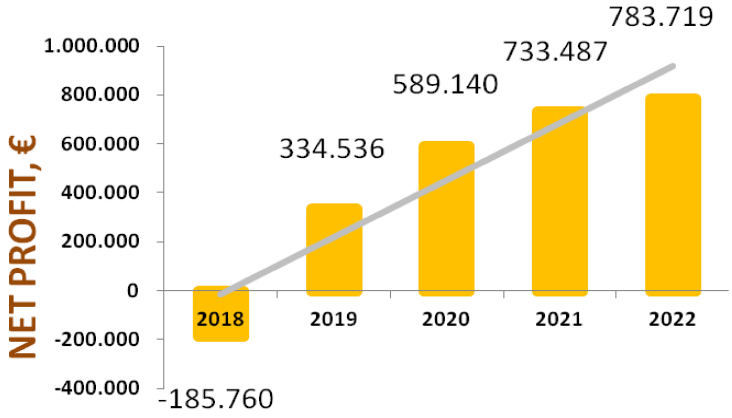

Figure X.4 *Net Profit diagram for SuperLip commercialization (2018-2022).*

Figure X.4 shows how a negative net profit is reached the first year, since the activity needs to be financed to be commercialized. Then, by the following year, the hypothesis of a higher commercialization of products has been considered, resulting in an increasing net profit up to €780,000 in 2022.

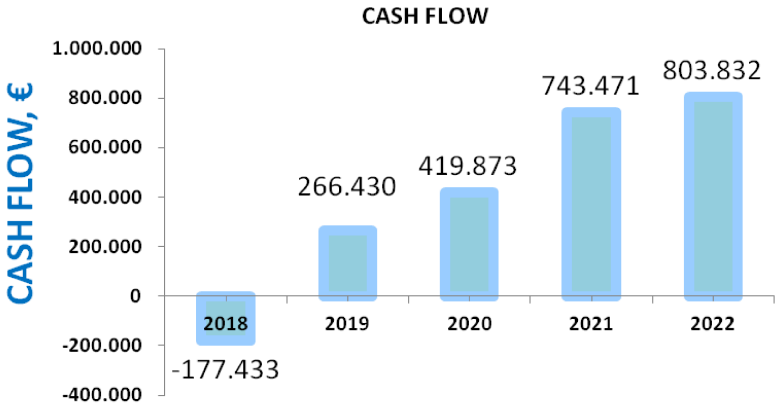

Figure X.5 *Cash Flow Statement for SuperLip commercialization (2018-2022).*

Starting from the assumptions in the previous Tables, it is possible to affirm that the payback time is reached at the second year of investment.

An index analysis was finally performed on the SuperLip proposal of commercialization. The Return On Sales (ROS) value was calculated on product selling and commercialization. Then, the Internal Rate of Return (IRR) was calculated (186 %), to indicate the interest value that indicates the interest rate, with the sum of discounted cash flows becoming zero (**Table X.11**).

Table X.11 *Financial indexes calculation*

€	2018	2019	2020	2021	2022
REVENUES	75586	869234	1417230	1606194	1700676
NET PROFIT	-185760	334536	589140	733487	783719
CASH FLOW	-177433	266430	419873	743471	803832
ROS	-245.8%	38.5%	41.6%	45.7%	46.1%
discount factor	0.83	0.69	0.58	0.48	0.40
Discounted cash flow	-124384	130930	144645	179547	515600

Using the Discount Cash Flow method (sum of the yearly discount cash flow), the hypothesized value for the SuperLip commercialization is around €3 million.

SuperLip has been demonstrated to be a relatively cheap process to develop, especially when considering the high potential applications described.

In the future, the idea of a scale up to industrial level of this chemical process plant will be considered, in order to produce a greater continuous daily production.

Chapter XI
Final discussion and conclusions

The aim of this PhD project has been to develop a new lab scale process for the production of liposomes, overcoming the limitations linked to the previously developed processes.

SuperLip process was designed and successfully tested for the encapsulation of different compounds: proteins (bovine serum albumin), dyes (fluorescein and aniline), antibodies, antibiotics (ampicillin, ofloxacin, vancomycin, theophylline, amoxicillin), essential oils (eugenol, lipoic acid, farnesol, linalool, limonene) and dietary supplements (olive pomace extract and coffee seed root extract).

In **Table XI.1**, the list of compounds for which the encapsulation has been obtained is reported. The proposed molecules have been divided into three groups: water core entrapment, lipidic layer encapsulation and encapsulation in both compartments.

The mean dimensions and average encapsulation efficiencies are reported in **Figure XI.1**. **Figure XI.1** summarizes the results obtained in this set of experiments in terms of Encapsulation Efficiency Vs Mean Diameter.

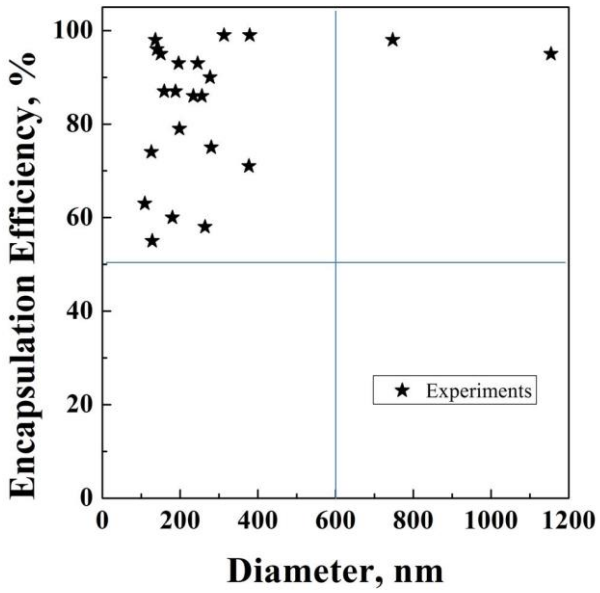

Figure XI.1 *Working map of produced liposomes Vs the encapsulation efficiency*

Table XI.1 *List of compounds entrapped into liposomes by SuperLip, specifying the compartment of encapsulation, Mean Diameter (MD), Standard Deviation (SD) and average Encapsulation Efficiencies (EE)*

Compound	Liposome Compartment	Mean diameter (MD) nm ± SD	Average Encapsulation Efficiency, %
Fluorescein	Water core	277 ± 61	90
Bovine Serum Albumin		245 ± 73	93
Albumin fluorescein isothiocyanate		379 ± 91	99
Antibody Mouse IgG Isotype Control		142 ± 33	93
Ofloxacin		256 ± 71	86
Theophylline		136 ± 86	98
Ampicillin		313 ± 69	99
Amoxicillin		198 ± 57	79
Vancomycin		180 ± 48	60
Olive pomace extract		264 ± 98	58
Caffeine from spent coffee ground		188 ± 36	87
Eugenol (inner core)	Both	196 ± 76	93
Eugenol (lipidic layer)		234 ± 101	86
Linalool	Lipidic layer	128 ± 49	55
Lipoic acid		109 ± 49	63
Limonene		159 ± 44	87
Farnesol		126 ± 35	74
Cholesterol		140 ± 27	96
Phosphatidyletanolamine		150 ± 25	95

Summarizing the content of the upper part of **Table XI.1**, it is possible to see that the liposomes of nanometric or sub-micrometric dimensions were produced in all the experiments using the SuperLip technique, with encapsulation efficiencies as high as 99 %. Most of the hydrophilic compounds were encapsulated with an EE greater than 90 %.

The amphiphilic chosen compound was eugenol, entrapped both in the lipidic layer (86 %) as well as in the inner water core (93 %). Water entrapped eugenol caused the production of liposomes with a mean diameter of 196 ± 76 nm; whereas, the lipidic layer entrapped eugenol produced more dispersed samples of liposomes, with a mean diameter of 234 ± 101 nm.

The lipophilic compounds used for the encapsulation tests were antioxidants particularly sensible to light and oxygen exposure. The obtained liposomes were substantially smaller, with mean diameters from 109 ± 49

nm (lipoic acid) to 159 ± 44 nm (limonene). The samples were less dispersed while the average encapsulation efficiencies were smaller than the hydrophilic entrapped compounds, from a minimum of 55 % (linalool) to a maximum of 87 % (limonene).

Regarding the additives of the lipidic double layer, cholesterol and phosphatidylethanolamine were also entrapped in the lipidic compartment of liposomes, and a more compact structure was obtained, with encapsulation efficiencies of 96 % (cholesterol) and 95 % (phosphatidylethanolamine).

The map of **Figure XI.1** represents how most of the experiments are collocated in the area of the graph characterized by a high entrapment efficiency and smaller diameters. These two combined parameters are significant since the liposomes of nanometric dimensions can be up taken more easily by cells and the high encapsulation efficiency enhances drug bioavailability during drug administration and release profile.

IX.1 Discussion

A summary of the PAINS and GAINS of the SuperLip technique, compared to the other processes reported in the literature, is provided in **Table XI.2**.

Table XI.2 *Summary of the PAINS and GAINS of other liposomes production methods Vs. SuperLip*

Other methods PAINS	**SuperLip method GAINS**
Micrometric dimensions	Nanometric dimensions
High solvent residue	Low solvent residue
Low encapsulation efficiencies	Encapsulation efficiencies
Post-processing steps	1-shot production
Batch layout	Continuous and replicable

Supercritical assisted Liposome formation successfully demonstrated to overcome many limitations linked to traditional production methods of liposomes. Exploiting the high diffusion coefficient of supercritical carbon dioxide, liposomes of nanometric and sub-micrometric mean dimensions were obtained, with a better control of particle size distributions than previously proposed processes.

Control of liposomes diameter was one of the key challenge in the vesicles production, especially at nanometric level. This thesis revealed that in the case of SuperLip, the parameter that mainly controls liposome diameter is GLR-EL.

Another relevant result of this study is the reduction of the solvent residue changing GLR-EL, i.e. changing the ethanol mole fraction in the EL.

For this reason, a very low amount of ethanol is dissolved in liposome water suspension, using this technique. This guarantees high biocompatibility of the vesicles in biomedical applications.

Nanometric dimensions of liposomes were achieved “one shot”, without the need of post-processing steps such as extrusion or sonication, that are often reported in the literature to be time consuming and expensive.

The encapsulation efficiency of the chosen compounds were high up to 99 %, an exceptional result if compare with the 20-30 % of conventional techniques.

Moreover, the continuous layout of the process guaranteed homogeneous and repeatable results; whereas, in the batch layouts of several conventional techniques, this was not guaranteed. The continuity of SuperLip process also gave the possibility to design a scale up of the system to the industrial level.

IX.2 Future perspectives

In the **future**, there are many applications that could be studied with liposomes produced with SuperLip:

- Sequestration of oxygen into liposomes for oxygen therapies
- Atomic Force Microscopic characterizations for liposome mechanical properties
- Rheological measurement of liposomes viscosity in gel bulks
- Citotoxicity and internalization experiments to study *in vitro* cell response.
- Production of surface-modified liposomes with improved target-delivery functions

Bibliography

ABDEL-ZAHER, A. O., ABDEL-HADY, R. H., MAHMOUD, M. M. & FARRAG, M. M. Y. 2008. The potential protective role of alpha-lipoic acid against acetaminophen-induced hepatic and renal damage. *Toxicology,* 243**,** 261-270.

ADLERCREUTZ, H. & MAZUR, W. 1997. Phyto-oestrogens and Western diseases. *Annals of Medicine,* 29**,** 95-120.

AKASHI, K., MIYATA, H., ITOH, H. & KINOSITA, K., JR. 1996. Preparation of giant liposomes in physiological conditions and their characterization under an optical microscope. *Biophys J,* 71**,** 3242-50.

AKBARZADEH, A., REZAEI-SADABADY, R., DAVARAN, S., JOO, S. W., ZARGHAMI, N., HANIFEHPOUR, Y., SAMIEI, M., KOUHI, M. & NEJATI-KOSHKI, K. 2013. Liposome: classification, preparation, and applications. *Nanoscale Res Lett,* 8**,** 102.

AKHAVAN, S., ASSADPOUR, E., KATOUZIAN, I. & JAFARI, S. M. 2018. Lipid nano scale cargos for the protection and delivery of food bioactive ingredients and nutraceuticals. . *Trends in Food Science & Technology,* 74**,** 132-146.

ALIAKBARIAN, B., CASAZZA, A. A. & PEREGO, P. 2011. Valorization of olive oil solid waste using high pressure-high temperature reactor. *Food Chemistry,* 128**,** 704-710.

ALIAKBARIAN, B., PALMIERI, D., CASAZZA, A. A., PALOMBO, D. & PEREGO, P. 2012. Antioxidant activity and biological evaluation of olive pomace extract. *Natural Product Research,* 26**,** 2280-2290.

ALVAREZ-RIVERA, F., FERNANDEZ-VILLANUEVA, D., CONCHEIRO, A. & ALVAREZ-LORENZO, C. 2016. alpha-Lipoic Acid in Soluplus (R) Polymeric Nanomicelles for Ocular Treatment of Diabetes-Associated Corneal Diseases. *Journal of Pharmaceutical Sciences,* 105**,** 2855-2863.

ANWEKAR, H., PATEL, S. & SINGHAI, A. K. 2011. Liposome as drug carriers. *International Journal of Pharmacy & Life Sciences,* 2**,** 945-951.

ATEFE, R., FATHI, M. & JAFARI, S. M. 2018. Nanoencapsulation of hydrophobic and low-soluble food bioactive compounds within different nanocarriers. *Food Hydrocolloids*.

BAE, Y. U., HUH, J. W., KIM, B. K., PARK, H. Y., SEU, Y. B. & DOH, K. O. 2016. Enhancement of liposome mediated gene transfer by adding cholesterol and cholesterol modulating drugs. *Biochimica Et Biophysica Acta-Biomembranes,* 1858**,** 3017-3023.

BALL, R. L., BAJAJ, P. & WHITEHEAD, K. A. 2017. Achieving long-term stability of lipid nanoparticles: examining the effect of pH, temperature, and lyophilization. *Int J Nanomedicine,* 12**,** 305-315.

BANDARA, H. M. H. N., HERPIN, M. J., KOLACNY, D., HARB, A., ROMANOVICZ, D. & SMYTH, H. D. C. 2016. Incorporation of Farnesol Significantly Increases the Efficacy of Liposomal Ciprofloxacin against Pseudomonas aeruginosa Biofilms in Vitro. *Molecular Pharmaceutics,* 13**,** 2760-2770.

BANGHAM, A. D. 1992. Liposomes: realizing their promise. *Hosp Pract (Off Ed),* 27**,** 51-6, 61-2.

BANGHAM, A. D. 1993. Liposomes: the Babraham connection. *Chem Phys Lipids,* 64**,** 275-85.

BANGHAM, A. D. 2005. Liposomes and the physico-chemical basis of unconsciousness. *FASEB J,* 19**,** 1766-8.

BANGHAM, A. D., STANDISH, M. M. & WATKINS, J. C. 1965. Diffusion of univalent ions across the lamellae of swollen phospholipids. *J Mol Biol,* 13**,** 238-52.

BARANI, H. & MONTAZER, M. 2008a. A review on applications of liposomes in textile processing. *J Liposome Res,* 18**,** 249-62.

BARANI, H. & MONTAZER, M. 2008b. A review on applications of liposomes in textile processing. *Journal of Liposome Research,* 18**,** 249-262.

BARENHOLZ, Y., BOMBELLI, C., BONICELLI, M. G., DI PROFIO, P., GIANSANTI, L., MANCINI, G. & PASCALE, F. 2011. Influence of lipid composition on the thermotropic behavior and size distribution of mixed cationic liposomes. *J Colloid Interface Sci,* 356**,** 46-53.

BARTH, D., CHOUCHI, D., DELLA PORTA, G., REVERCHON, E. & PERRUT, M. 1994. Desorption of lemon peel oil by supercritical carbon dioxide: deterpenation and psoralens elimination. *The Journal of Supercritical Fluids,* 7**,** 177-183.

BASKARAN, Y., PERIYASAMY, V. & VENKATRAMAN, A. C. 2010. Investigation of antioxidant, anti-inflammatory and DNA-protective properties of eugenol in thioacetamide-induced liver injury in rats. *Toxicology,* 268**,** 204-212.

BECKMAN, C. H. 2000. Phenolic-storing cells: keys to programmed cell death and periderm formation in wilt disease resistance and in general defence responses in plants? *Physiological and Molecular Plant Pathology,* 57**,** 101-110.

BENECH, R. O., KHEADR, E. E., LARIDI, R., LACROIX, C. & FLISS, I. 2002. Inhibition of Listeria innocua in cheddar cheese by addition of nisin Z in liposomes or by in situ production in mixed culture. *Appl Environ Microbiol,* 68**,** 3683-90.

BERGER, N., SACHSE, A., BENDER, J., SCHUBERT, R. & BRANDL, M. 2001. Filter extrusion of liposomes using different devices: comparison of liposome size, encapsulation efficiency, and process characteristics. *International Journal of Pharmaceutics,* 223**,** 55-68.

BERTRAND, N., BOUVET, C., MOREAU, P. & LEROUX, J. C. 2010. Transmembrane pH-gradient liposomes to treat cardiovascular drug intoxication. *ACS Nano,* 4**,** 7552-8.

BIESALSKI, H. K. 2002. Free radical theory of aging. *Current Opinion in Clinical Nutrition and Metabolic Care,* 5**,** 5-10.

BLANQUET, S., GARRAIT, G., BEYSSAC, E., PERRIER, C., DENIS, S., HEBRARD, G. & ALRIC, M. 2005. Effects of cryoprotectants on the viability and activity of freeze dried recombinant yeasts as novel oral drug delivery systems assessed by an artificial digestive system. *European Journal of Pharmaceutics and Biopharmaceutics,* 61**,** 32-39.

BLUME, G. & CEVC, G. 1990. Liposomes for the sustained drug release in vivo. *Biochimica et Biophysica Acta,* 1029**,** 91-7.

BOCHOT, A., COUVREUR, P. & FATTAL, E. 2000. Intravitreal administration of antisense oligonucleotides: Potential of liposomal delivery. *Progress in Retinal and Eye Research,* 19**,** 131-147.

BOZZUTO, G., & MOLINARI, A. (2015). 2015. Liposomes as nanomedical devices. International journal of nanomedicine, 10, 975. *International Journal of Nanomedicine,* 10**,** 975-999.

BRANDWILLIAMS, W., CUVELIER, M. E. & BERSET, C. 1995. Use of a Free-Radical Method to Evaluate Antioxidant Activity. *Food Science and Technology-Lebensmittel-Wissenschaft & Technologie,* 28**,** 25-30.

BRUNNER, G. 2013. Gas extraction: an introduction to fundamentals of supercritical fluids and the application to separation processes. *Springer Science & Business Media,* 4.

CAMPARDELLI, R., BALDINO, L. & REVERCHON, E. 2015. Supercritical fluids applications in nanomedicine. *Journal of Supercritical Fluids,* 101**,** 193-214.

CAMPARDELLI, R., ESPIRITO SANTO, I., ALBUQUERQUE, E. C., DE MELO, S. V., DELLA PORTA, G. & REVERCHON, E. 2016a. Efficient encapsulation of proteins in submicro liposomes using a supercritical fluid assisted continuous process. *Journal of Supercritical Fluids,* 107**,** 163-169.

CAMPARDELLI, R., ESPIRITO SANTO, I., ALBUQUERQUE, E. C., VIEIRA DE MELO, S., DELLA PORTA, G. & REVERCHON, E. 2016b. Efficient encapsulation of proteins in submicro liposomes using a supercritical fluid assisted continuous process. *The Journal of Supercritical Fluids,* 107**,** 163-169.

CAMPARDELLI, R., TRUCILLO, P. & REVERCHON, E. 2016c. A Supercritical Fluid-Based Process for the Production of Fluorescein-Loaded Liposomes. *Industrial & Engineering Chemistry Research,* 55**,** 5359-5365.

CAMPARDELLI, R., TRUCILLO, P. & REVERCHON, E. 2018. Supercritical assisted process for the efficient production of liposomes containing antibiotics for ocular delivery. *Journal of Co2 Utilization,* 25**,** 235-241.

CASCIOLA, M., BONHENRY, D., LIBERTI, M., APOLLONIO, F. & TAREK, M. 2014. A molecular dynamic study of cholesterol rich lipid membranes: comparison of electroporation protocols. *Bioelectrochemistry,* 100**,** 11-7.

CATHCART, K., PATEL, A., DIES, H., RHEINSTADTER, M. C. & FRADIN, C. 2015. Effect of Cholesterol on the Structure of a Five-Component Mitochondria-Like Phospholipid Membrane. *Membranes (Basel),* 5**,** 664-84.

CEVALLOS-CASALS, B. A. & CISNEROS-ZEVALLOS, L. 2010. Impact of germination on phenolic content and antioxidant activity of 13 edible seed species. *Food Chemistry,* 119**,** 1485-1490.

CHAN, J., EL MAGHRABY, G. M. M., CRAIG, J. P. & ALANY, R. G. 2007. Phase transition water-in-oil microemulsions as ocular drug delivery systems: In vitro and in vivo evaluation. *International Journal of Pharmaceutics,* 328**,** 65-71.

CHEN, H. D., PAN, H., LI, P. P., WANG, H., WANG, X., PAN, W. S. & YUAN, Y. 2016. The potential use of novel chitosan-coated deformable liposomes in an ocular drug delivery system. *Colloids and Surfaces B-Biointerfaces,* 143**,** 455-462.

CHEN, X., LIU, J., DING, J. & DING, K. Y. 2015. Characteristics of Aldehyde Reactive Dyes for Leather Dyeing and Retanning Process. *Journal of the American Leather Chemists Association,* 110**,** 338-345.

CHOI, M. J., SOOTTITANTAWAT, A., NUCHUCHUA, O., MIN, S. G. & RUKTANONCHAI, U. 2009. Physical and light oxidative properties of eugenol encapsulated by molecular inclusion and emulsion-diffusion method. *Food Research International,* 42**,** 148-156.

CHU, P. T. & WEN, H. W. 2013. Sensitive detection and quantification of gliadin contamination in gluten-free food with immunomagnetic beads based liposomal fluorescence immunoassay. *Anal Chim Acta,* 787**,** 246-53.

CODERCH, L., FONOLLOSA, J., DE PERA, M., ESTELRICH, J., DE LA MAZA, A. & PARRA, J. L. 2000. Influence of cholesterol on liposome fluidity by EPR: Relationship with percutaneous absorption. *Journal of Controlled Release,* 68**,** 85-95.

CODERCH, L., LOPEZ, O., DELAMAZA, A., MANICH, A. M., PARRA, J. L. & CEGARRA, J. 1997. Internal lipid wool structure modification due to a nonionic auxiliary used in dyeing at low temperatures. *Textile Research Journal,* 67**,** 131-136.

CODERCH, L., OLIVA, M., PONS, M., DE LA MAZA, A., MANICH, A. M. & PARRA, J. L. 1996. Percutaneous penetration of liposomes using the tape stripping technique. *International Journal of Pharmaceutics,* 139**,** 197-203.

COLAS, J. C., SHI, W., RAO, V. S., OMRI, A., MOZAFARI, M. R. & SINGH, H. 2007. Microscopical investigations of nisin-loaded nanoliposomes prepared by Mozafari method and their bacterial targeting. *Micron,* 38**,** 841-7.

COLLINS, J. J. & PHILLIPS, M. C. 1982. The stability and structure of cholesterol-rich codispersions of cholesterol and phosphatidylcholine. *J Lipid Res,* 23**,** 291-8.

CROMMELIN, D. J., VAN RENSEN, A. J., WAUBEN, M. H. & STORM, G. 1999. Liposomes in autoimmune diseases: selected applications in immunotherapy and inflammation detection. *J Control Release,* 62**,** 245-51.

DAGLIA, M. 2012. Polyphenols as antimicrobial agents. *Current Opinion in Biotechnology,* 23**,** 174-181.

DE LEONARDIS, A., ANGELICO, R., MACCIOLA, V. & CEGLIE, A. 2013. Effects of polyphenol enzymatic-oxidation on the oxidative stability of virgin olive oil. *Food Research International,* 54**,** 2001-2007.

DE MARCO, I., IANNONE, R., MIRANDA, S. & RIEMMA, S. 2017. An environmental study on starch aerogel for drug delivery applications: effect of plant scale-up. *The International Journal of Life Cycle Assessment***,** 1-12.

DE PAZ, E., MARTÍN, Á. & COCERO, M. J. 2012. Formulation of β-carotene with soybean lecithin by PGSS (Particles from Gas Saturated Solutions)-drying. *The Journal of Supercritical Fluids,* 72**,** 125-133.

DEAMER, D. W. 2010. From "banghasomes" to liposomes: a memoir of Alec Bangham, 1921-2010. *FASEB J,* 24**,** 1308-10.

DELADINO, L., ANBINDER, P. S., NAVARRO, A. S. & MARTINO, M. N. 2007. Co-crystallization of yerba mate extract (Ilex paraguariensis) and mineral salts within a sucrose matrix. *Journal of Food Engineering,* 80**,** 573-580.

DELAMAZA, A., MARSAL, A., COT, J., MANICH, A. & PARRA, J. L. 1992. Liposomes in Leather Dyeing - Stability of Dye-Liposome Systems and Applications. *Journal of the American Leather Chemists Association,* 87**,** 459-465.

DESAI, K. G. H. & PARK, H. J. 2005. Recent developments in microencapsulation of food ingredients. *Drying Technology,* 23**,** 1361-1394.

DEVI, K. P., NISHA, S. A., SAKTHIVEL, R. & PANDIAN, S. K. 2010. Eugenol (an essential oil of clove) acts as an antibacterial agent against Salmonella typhi by disrupting the cellular membrane. *Journal of Ethnopharmacology,* 130**,** 107-115.

DICKINSON, E. & WHYMAN, R. H. 1996. Colloidal properties of model oil-in-water food emulsion stabilized separately by as1-casein and j-casein. *Food Emulsions and Foams,* 40-229.

DISALVO, E. A. & BOUCHET, A. M. 2014. Electrophoretic mobility and zeta potential of liposomes due to arginine and polyarginine adsorption. *Colloids and Surfaces A: Physicochemical and Engineering Aspects,* 440**,** 170-174.

DONG, Y. X., DONG, P., HUANG, D., MEI, L. L., XIA, Y. W., WANG, Z. H., PAN, X., LI, G. & WU, C. B. 2015. Fabrication and characterization of silk fibroin-coated liposomes for ocular drug delivery. *European Journal of Pharmaceutics and Biopharmaceutics,* 91**,** 82-90.

DOPPALAPUDI, S., JAIN, A., CHOPRA, D. K. & KHAN, W. 2017. Psoralen loaded liposomal nanocarriers for improved skin penetration and efficacy of topical PUVA in psoriasis. *Eur J Pharm Sci,* 96**,** 515-529.

DRAGAN, S., ANDRICA, F., SERBAN, M. C. & TIMAR, R. 2015. Polyphenols-Rich Natural Products for Treatment of Diabetes. *Current Medicinal Chemistry,* 22**,** 14-22.

DURLING, N. E., CATCHPOLE, O. J., TALLON, S. J. & GREY, J. B. 2007a. Measurement and modelling of the ternary phase equilibria for high pressure carbon dioxide-ethanol-water mixtures. *Fluid Phase Equilibria,* 252**,** 103-113.

DURLING, N. E., CATCHPOLE, O. J., TALLON, S. J. & GREY, J. B. 2007b. Measurement and modelling of the ternary phase equilibria for high pressure carbon dioxide–ethanol–water mixtures. *Fluid Phase Equilibria,* 252**,** 103-113.

EICHHORN, U., HELBIG, B., KLOCKING, R., SCHWEIZER, H. & SPROSSIG, M. 1985. Comparison of the Antiviral Activity of Enzymatically and Non-Enzymatically Produced Phenol Substance Polymerides (Pkp) by Means of Cr-51 Release Test in Coxsackie-Virus A9-Infected Fl-Cells. *Pharmazie,* 40**,** 282-282.

EL-ZAWAHRY, M. M., EL-MALLAH, M. H. & EL-SHAMI, S. 2009. An innovative study on dyeing silk fabrics by modified phospholipid liposomes. *Coloration Technology,* 125**,** 164-171.

EL-ZAWAHRY, M. M., EL-SHAMI, S. & EL-MALLAH, M. H. 2007. Optimizing a wool dyeing process with reactive dye by liposome microencapsulation. *Dyes and Pigments,* 74**,** 684-691.

ELOY, J. O., CLARO DE SOUZA, M., PETRILLI, R., BARCELLOS, J. P., LEE, R. J. & MARCHETTI, J. M. 2014. Liposomes as carriers of hydrophilic small molecule drugs: strategies to enhance encapsulation and delivery. *Colloids and Surfaces B: Biointerfaces,* 123**,** 345-63.

ESPIRITO SANTO, I., CAMPARDELLI, R., ALBUQUERQUE, E. C., VIEIRA DE MELO, S., DELLA PORTA, G. & REVERCHON, E. 2014a. Liposomes preparation using a supercritical fluid assisted continuous process. *Chemical Engineering Journal,* 249**,** 153-159.

ESPIRITO SANTO, I., CAMPARDELLI, R., ALBUQUERQUE, E. C., VIEIRA DE MELO, S. A. B., REVERCHON, E. & DELLA PORTA, G. 2015a. Liposomes Size Engineering by Combination of Ethanol Injection and Supercritical Processing. *Journal of Pharmaceutical Sciences,* 104**,** 3842-3850.

ESPIRITO SANTO, I., CAMPARDELLI, R., CABRAL ALBUQUERQUE, E., VIEIRA DE MELO, S., DELLA PORTA, G. & REVERCHON, E. 2014b. Liposomes preparation using a supercritical fluid assisted continuous process. *Chemical Engineering Journal,* 249**,** 153-159.

ESPIRITO SANTO, I., CAMPARDELLI, R., CABRAL ALBUQUERQUE, E., VIEIRA DE MELO, S. A. B., REVERCHON, E. & DELLA PORTA, G. 2015b. Liposomes Size Engineering by Combination of Ethanol Injection and Supercritical Processing. *Journal of Pharmaceutical Sciences,* 104**,** 3842-3850.

FAETH, G. M. 1990. Structure and atomization properties of dense turbolent sprays. *23rd Symposium on Combustion/The Combustion Institute***,** 1345-1352.

FALCAO, L. & ARAUJO, M. E. M. 2018. Vegetable Tannins Used in the Manufacture of Historic Leathers. *Molecules,* 23.

FANG, Z. X. & BHANDARI, B. 2010. Encapsulation of polyphenols - a review. *Trends in Food Science & Technology,* 21**,** 510-523.

FILION, M. C. & PHILLIPS, N. C. 1997. Toxicity and immunomodulatory activity of liposomal vectors formulated with cationic lipids toward immune effector cells. *Biochimica et Biophysica Acta,* 1329**,** 345-56.

FILIPE, V., HAWE, A. & JISKOOT, W. 2010. Critical evaluation of Nanoparticle Tracking Analysis (NTA) by NanoSight for the measurement of nanoparticles and protein aggregates. *Pharm Res,* 27**,** 796-810.

FLOURY, J., DESRUMAUX, A. & LARDIERES, J. 2000. Effect of high-pressure homogenization on droplet size distributions and rheological properties of model oil-in-water emulsions. *Innovative Food Science & Emerging Technologies,* 1**,** 127-134.

FRANZE, S., MARENGO, A., STELLA, B., MINGHETTI, P., ARPICCO, S. & CILURZO, F. 2018. Hyaluronan-decorated liposomes as drug delivery systems for cutaneous administration. *Int J Pharm,* 535**,** 333-339.

FREDERIKSEN, L., ANTON, K., VAN HOOGEVEST, P., KELLER, H. R. & LEUENBERGER, H. 1997. Preparation of liposomes encapsulating water-soluble compounds using supercritical carbon dioxide. *J Pharm Sci,* 86**,** 921-8.

FURNERI, P. M., FRESTA, M., PUGLISI, G. & TEMPERA, G. 2000. Ofloxacin-loaded liposomes: In vitro activity and drug accumulation in bacteria. *Antimicrobial Agents and Chemotherapy,* 44**,** 2458-2464.

GARCON, N. M., SIX, H. R., FRAZER, J., HAZLEWOOD, C., GILBERT, B. E. & KNIGHT, V. 1989. Liposomes of Enviroxime and Phosphatidylcholine - Definition of the Drug - Phospholipid Interactions. *Antiviral Research,* 11**,** 89-98.

GARG, A. & SINGH, S. 2011. Enhancement in antifungal activity of eugenol in immunosuppressed rats through lipid nanocarriers. *Colloids and Surfaces B-Biointerfaces,* 87**,** 280-288.

GELLERSTEDT, G., PETTERSON, E. L. 1975. Light-induced Oxidation of The Behaviour of Structural Units Containing a Ring-conjugated Double Bond. *Acta Chem. Scand. B,* 29**,** 1005-1010.

GIBIS, M., ZEEB, B. & WEISS, J. 2014. Formation, characterization, and stability of encapsulated hibiscus extract in multilayered liposomes. *Food Hydrocolloids,* 38**,** 28-39.

GOUIN, S. 2004. Microencapsulation: industrial appraisal of existing technologies and trends. *Trends in Food Science & Technology,* 15**,** 330-347.

GREGORIADIS, G. 2016. *Liposome Technology: Liposome Preparation and Related Techniques*, CRC Press.

GUAN, Y. G., WU, J. & ZHONG, Q. X. 2016. Eugenol improves physical and chemical stabilities of nanoemulsions loaded with beta-carotene. *Food Chemistry,* 194**,** 787-796.

GULIY, O. I., MARKINA, L. N., IGNATOV, O. V., SHCHEGOLEV, S. Y., ZAITSEVA, I. S., BUNIN, V. D. & IGNATOV, V. V. 2005. The effect of ampicillin on the electrophysical properties of Escherichia coli cells. *Microbiology,* 74**,** 111-115.

GULSEN, D. & CHAUHAN, A. 2004. Ophthalmic drug delivery through contact lenses. *Investigative Ophthalmology & Visual Science,* 45**,** 2342-2347.

HAGIWARA, K., GOTO, T., ARAKI, M., MIYAZAKI, H. & HAGIWARA, H. 2011. Olive polyphenol hydroxytyrosol prevents bone loss. *European Journal of Pharmacology,* 662**,** 78-84.

HARMAN, D. 2006. Free Radical Theory of Aging: An Update Increasing the Functional Life Span. *Understanding and Modulating Aging,* 1067**,** 10-21.

HOSNY, K. M. 2009. Preparation and evaluation of thermosensitive liposomal hydrogel for enhanced transcorneal permeation of ofloxacin. *AAPS PharmSciTech,* 10**,** 1336-42.

HWANG, S. H., MAITANI, Y., QI, X. R., TAKAYAMA, K. & NAGAI, T. 1999. Remote loading of diclofenac, insulin and fluorescein isothiocyanate labeled insulin into liposomes by pH and acetate gradient methods. *Int J Pharm,* 179**,** 85-95.

HWANG, T. L., LEE, W. R., HUA, S. C. & FANG, J. Y. 2007. Cisplatin encapsulated in phosphatidylethanolamine liposomes enhances the in vitro cytotoxicity and in vivo intratumor drug accumulation against melanomas. *Journal of Dermatological Science,* 46**,** 11-20.

IMMORDINO, M. L., DOSIO, F. & CATTEL, L. 2006. Stealth liposomes: review of the basic science, rationale, and clinical applications, existing and potential. *Int J Nanomedicine,* 1**,** 297-315.

IMURA, T., GOTOH, T., OTAKE, K., YODA, S., TAKEBAYASHI, Y., YOKOYAMA, S., TAKEBAYASHI, H., SAKAI, H., YUASA, M. & ABE, M. 2003a. Control of physicochemical properties of liposomes using a supercritical reverse phase evaporation method. *Langmuir,* 19**,** 2021-2025.

IMURA, T., OTAKE, K., HASHIMOTO, S., GOTOH, T., YUASA, M., YOKOYAMA, S., SAKAI, H., RATHMAN, J. F. & ABE, M. 2003b. Preparation and physicochemical properties of various soybean lecithin liposomes using supercritical reverse phase evaporation method. *Colloids and Surfaces B: Biointerfaces,* 27**,** 133-140.

JAAFAR-MAALEJ, C., DIAB, R., ANDRIEU, V., ELAISSARI, A. & FESSI, H. 2010. Ethanol injection method for hydrophilic and lipophilic drug-loaded liposome preparation. *J Liposome Res,* 20**,** 228-43.

JAHN, A., VREELAND, W. N., DEVOE, D. L., LOCASCIO, L. E. & GAITAN, M. 2007. Microfluidic directed formation of liposomes of controlled size. *Langmuir,* 23**,** 6289-93.

JAIN, N. K., MISHRA, V. & MEHRA, N. K. 2013. Targeted drug delivery to macrophages. *Expert Opin Drug Deliv,* 10**,** 353-67.

JIANG, Y., WU, N., FU, Y. J., WANG, W., LUO, M., ZHAO, C. J., ZU, Y. G. & LIU, X. L. 2011. Chemical composition and antimicrobial activity of the essential oil of Rosemary. *Environmental Toxicology and Pharmacology,* 32**,** 63-68.

JONE, A. 2013. Liposomes: A Short Review. *Journal of Pharmaceutical Sciences and Research,* 5**,** 181-183.

KALOMIRAKI, M., THERMOS, K. & CHANIOTAKIS, N. A. 2016. Dendrimers as tunable vectors of drug delivery systems and biomedical and ocular applications. *International Journal of Nanomedicine,* 11**,** 1-12.

KARANTH, H. & MURTHY, R. S. 2007. pH-sensitive liposomes--principle and application in cancer therapy. *J Pharm Pharmacol,* 59**,** 469-83.

KARBSTEIN, H., AND HELMAR SCHUBERT. " 1995. Developments in the continuous mechanical production of oil-in-water macro-emulsions. *Chemical Engineering and Processing: Process Intensification* 34**,** 205-211.

KATOH, S., SOHMA, Y., MORI, Y., FUJITA, R., SADA, E., KISHIMURA, M. & FUKUDA, H. 1993. Homogeneous immunoassay of polyclonal antibodies by use of antigen-coupled liposomes. *Biotechnology and Bioengineering,* 41**,** 862-867.

KELLER, B. C. 2001. Liposomes in nutrition. *Trends in Food Science & Technology,* 12**,** 25-31.

KHANDAN, O., FAMILI, A., KAHOOK, M. Y. & RAO, M. P. 2012. Titanium-Based, Fenestrated, In-Plane Microneedles for Passive Ocular Drug Delivery. *2012 Annual International Conference of the Ieee Engineering in Medicine and Biology Society (Embc)***,** 6572-6575.

KHANDAN, O., KAHOOK, M. Y. & RAO, M. P. 2016. Fenestrated microneedles for ocular drug delivery. *Sensors and Actuators B-Chemical,* 223**,** 15-23.

KHEIR, J. N., SCHARP, L. A., BORDEN, M. A., SWANSON, E. J., LOXLEY, A., REESE, J. H., BLACK, K. J., VELAZQUEZ, L. A., THOMSON, L. M., WALSH, B. K., MULLEN, K. E., GRAHAM, D. A., LAWLOR, M. W., BRUGNARA, C., BELL, D. C. & MCGOWAN, F. X., JR. 2012. Oxygen gas-filled microparticles provide intravenous oxygen delivery. *Sci Transl Med,* 4**,** 140ra88.

KIM, D. S., JUNG, Y. J. & KIM, Y. M. 2001. Synthesis and properties of dextran-linked ampicillin. *Drug Development and Industrial Pharmacy,* 27**,** 97-101.

KORE, U. B. & SHUKLA, S. R. 2017. Ionic-liquid-assisted mixed alkali system for reactive dye fixation in a batch process - optimisation through response surface methodology. *Coloration Technology,* 133**,** 325-333.

KYU, P. I. 2006. Development of eco-friendly polymeric softening agents for reduction of COD effluent loads in leather dyeing process. *7th Asian International Conference of Leather Science and Technology Sect 1 and 2***,** 1-7.

LAJUNEN, T., HISAZUMI, K., KANAZAWA, T., OKADA, H., SETA, Y., YLIPERTTULA, M., URTTI, A. & TAKASHIMA, Y. 2014. Topical drug delivery to retinal pigment epithelium with

microfluidizer produced small liposomes. *European Journal of Pharmaceutical Sciences,* 62**,** 23-32.
LANKALAPALLI, S., TENNETI, V. S. V. K. & NIMMALI, S. K. 2015. Design and Development of Vancomycin Liposomes. *Indian Journal of Pharmaceutical Education and Research,* 49**,** 208-215.
LAOUINI, A., JAAFAR-MAALEJ, C., LIMAYEM-BLOUZA, I., SFAR, S., CHARCOSSET, C. & FESSI, H. Preparation, characterization and applications of liposomes: state of the art. *Journal of colloid Science and Biotechnology,* 1**,** 147-168.
LAOUINI, A., JAAFAR-MAALEJ, C., SFAR, S., CHARCOSSET, C. & FESSI, H. 2011. Liposome preparation using a hollow fiber membrane contactor-Application to spironolactone encapsulation. *International Journal of Pharmaceutics,* 415**,** 53-61.
LARSSON, M., HILL, A. & DUFFY, J. 2012. Suspension stability; why particle size, zeta potential and rheology are important. *Ann. Trans. Nordic Rheol. Soc,* 20**,** 209-214.
LASIC, D. D. 1998. Novel applications of liposomes. *Trends Biotechnol,* 16**,** 307-21.
LAURENTI, R., REDWOOD, M., PUIG, R. & FROSTELL, B. 2017. Measuring the Environmental Footprint of Leather Processing Technologies. *Journal of Industrial Ecology,* 21**,** 1180-1187.
LE BOURLAIS, C., ACAR, L., ZIA, H., SADO, P. A., NEEDHAM, T., & LEVERGE, R. 1998. Ophthalmic drug delivery systems—recent advances. *Progress in retinal and eye research,* 17**,** 33-58.
LEE, S. C., SHIN, E. C. & KIM, W. J. 2014. Dyeing Properties of Natural Leather Using Red Natural Dyes. *Journal of the Society of Leather Technologists and Chemists,* 98**,** 252-258.
LEI, X. P., LEWIS, D. M. & WANG, Y. N. 1992. The Production of Level Fast Dyeings on Wool with Nucleophilic Dyes and a Cross-Linking Agent. *Journal of the Society of Dyers and Colourists,* 108**,** 383-387.
LESOIN, L., BOUTIN, O., CRAMPON, C. & BADENS, E. 2011a. CO2/water/surfactant ternary systems and liposome formation using supercritical CO2: A review. *Colloids and Surfaces A: Physicochemical and Engineering Aspects,* 377**,** 1-14.
LESOIN, L., CRAMPON, C., BOUTIN, O. & BADENS, E. 2011b. Development of a continuous dense gas process for the production of liposomes. *The Journal of Supercritical Fluids* 60**,** 51-62.
LESOIN, L., CRAMPON, C., BOUTIN, O. & BADENS, E. 2011c. Preparation of liposomes using the supercritical anti-solvent (SAS) process and comparison with a conventional method. *The Journal of Supercritical Fluids,* 57**,** 162-174.
LEUNG, S. S., MORALES, S., BRITTON, W., KUTTER, E. & CHAN, H. K. 2018. Microfluidic-assisted bacteriophage encapsulation into liposomes. *International journal of pharmaceutics,* 545**,** 176-182.

LI, C. & DENG, Y. 2004. A novel method for the preparation of liposomes: freeze drying of monophase solutions. *J Pharm Sci,* 93**,** 1403-14.

LI, J., WANG, X., ZHANG, T., WANG, C., HUANG, Z., LUO, X. & DENG, Y. 2015. A review on phospholipids and their main applications in drug delivery systems. *Asian Journal of Pharmaceutical Sciences,* 10**,** 81-98.

LI, P., TANG, Y. P. & JIN, F. J. 2011a. Soft-Sensing Method of Color Measurement in Batch Dyeing Process of Knitted Cotton with Reactive Dyes. *2011 Chinese Control and Decision Conference, Vols 1-6***,** 1796-+.

LI, X., CHEN, D., LE, C., ZHU, C., GAN, Y., HOVGAARD, L. & YANG, M. 2011b. Novel mucus-penetrating liposomes as a potential oral drug delivery system: preparation, in vitro characterization, and enhanced cellular uptake. *Int J Nanomedicine,* 6**,** 3151-62.

LIAN, T. & HO, R. J. 2001. Trends and developments in liposome drug delivery systems. *J Pharm Sci,* 90**,** 667-80.

LIANG, H., BRIGNOLE-BAUDOUIN, F., RABINOVICH-GUILATT, L., MAO, Z., RIANCHO, L., FAURE, M. O., WARNET, J. M., LAMBERT, G. & BAUDOUIN, C. 2008. Reduction of quaternary ammonium-induced ocular surface toxicity by emulsions: an in vivo study in rabbits. *Molecular Vision,* 14**,** 204-216.

LIGLER, F. S., BREDEHORST, R., TALEBIAN, A., SHRIVER, L. C., HAMMER, C. F., SHERIDAN, J. P., VOGEL, C. W. & GABER, B. P. 1987. A homogeneous immunoassay for the mycotoxin T-2 utilizing liposomes, monoclonal antibodies, and complement. *Anal Biochem,* 163**,** 369-75.

LIKHITWITAYAWUID, K. 2008. Stilbenes with tyrosinase inhibitory activity. *Current Science,* 94**,** 44-52.

LIU, D. & HUANG, L. 1989. Role of cholesterol in the stability of pH-sensitive, large unilamellar liposomes prepared by the detergent-dialysis method. *Biochim Biophys Acta,* 981**,** 254-60.

LIU, D., MORI, A. & HUANG, L. 1992. Role of liposome size and RES blockade in controlling biodistribution and tumor uptake of GM1-containing liposomes. *Biochim Biophys Acta,* 1104**,** 95-101.

LIU, H., LEONAS, K. K. & ZHAO, Y. P. 2010. Antimicrobial Properties and Release Profile of Ampicillin from Electrospun Poly(epsilon-caprolactone) Nanofiber Yarns. *Journal of Engineered Fibers and Fabrics,* 5**,** 10-19.

LIU, W., YE, A., LIU, W., LIU, C., & SINGH, H. 2013. Stability during in vitro digestion of lactoferrin-loaded liposomes prepared from milk fat globule membrane-derived phospholipids. *Journal of Diary Science,* 96**,** 2061-2070.

LOHANI, A., VERMA, A., JOSHI, H., YADAV, N. & KARKI, N. 2014. Nanotechnology-based cosmeceuticals. *ISRN Dermatol,* 2014**,** 843687.

LOPES, L. B., SCARPA, M. V., SILVA, G. V., RODRIGUES, D. C., SANTILLI, C. V. & OLIVEIRA, A. G. 2004. Studies on the encapsulation of diclofenac in small unilamellar liposomes of soya phosphatidylcholine. *Colloids Surf B Biointerfaces,* 39**,** 151-8.

LOZADA-CASTRO, J. J. & SANTOS-DELGADO, M. J. 2016. Determination of free cholesterol oxide products in food samples by gas chromatography and accelerated solvent extraction: influence of electron-beam irradiation on cholesterol oxide formation. *Journal of the Science of Food and Agriculture,* 96**,** 4215-23.

LUISI, P. L., WALDE, P. & OBERHOLZER, T. 1998. Lipid vesicles as possible intermediates in the origin of life. *Current Opinion in Colloid & Interface Science,* 4**,** 33-39.

LUO, X. J., QIN, Q. P., LI, Y. L. & YANG, Y. 2013. Spectroscopic Studies on the Binding Properties of Ofloxacin and Human Telomeric G-quadruplex DNA. *Advances in Chemical, Material and Metallurgical Engineering, Pts 1-5,* 634-638**,** 1062-1065.

M. J. COCERO, A. MARTÍN, F. MATTEA & S. VARONA 2009. Encapsulation and co-precipitation processes with supercritical fluids: Fundamentals and applications. *Journal of Supercritical Fluids,* 47**,** 546-555.

MAHERANI, B., ARAB-TEHRANY, E., MOZAFARI, M. R., GAIANI, C. & LINDER, M. 2011. Liposomes: A Review of Manufacturing Techniques and Targeting Strategies. *Current Nanoscience,* 7**,** 436-452.

MAHRHAUSER, D. S., REZNICEK, G., KOTISCH, H., BRANDSTETTER, M., NAGELREITER, C., KWIZDA, K. & VALENTA, C. 2015. Semi-solid fluorinated-DPPC liposomes: Morphological, rheological and thermic properties as well as examination of the influence of a model drug on their skin permeation. *Int J Pharm,* 486**,** 350-5.

MAITANI, Y. 2010. Lipoplex formation using liposomes prepared by ethanol injection. *Methods Mol Biol,* 605**,** 393-403.

MALAM, Y., LOIZIDOU, M. & SEIFALIAN, A. M. 2009. Liposomes and nanoparticles: nanosized vehicles for drug delivery in cancer. *Trends Pharmacol Sci,* 30**,** 592-9.

MANACH, C., SCALBERT, A., MORAND, C., REMESY, C. & JIMENEZ, L. 2004. Polyphenols: food sources and bioavailability. *American Journal of Clinical Nutrition,* 79**,** 727-747.

MANDAL, S., NATARAJAN, S., SURESH, S., CHANDRASEKAR, R., JOTHI, G., MURALIDHARAN, C. & MANDAL, A. B. 2015. Layered clay aqueous dispersion as a novel dye leveling agent in

leather processing: Synthesis, characterization and application studies. *Applied Clay Science,* 115**,** 17-23.

MANNA, L., CAROTENUTO, C., NIGRO, R., LANCIA, A. & DI NATALE, F. 2017. Primary atomization of electrified water sprays. *The Canadian Journal of Chemical Engineering,* 95**,** 1781-1788.

MANNERMAA, E., VELLONEN, K. S. & URTTI, A. 2006. Drug transport in corneal epithelium and blood-retina barrier: Emerging role of transporters in ocular pharmacokinetics. *Advanced Drug Delivery Reviews,* 58**,** 1136-1163.

MANTOVANI, A., ALLAVENA, P., SICA, A. & BALKWILL, F. 2008. Cancer-related inflammation. *Nature,* 454**,** 436-444.

MARIE, P., PERRIER-CORNET, J. M. & GERVAIS., P. 2002. Influence of major parameters in emulsification mechanisms using a high-pressure jet. *Journal of Food Engineering* 53**,** 43-51.

MARSAL, A., MANICH, A. M., DE CASTELLAR, M. D., COT, J. & MARTINEZ, D. 2002. Use of liposomes as auxiliary products in hide dyeing process. *Journal of the American Leather Chemists Association,* 97**,** 23-33.

MARSAL, A., MANICH, A. M., DE CASTELLAR, M. D., COT, J. & MARTINEZ, D. 2003. Use of liposomes as auxiliary products in the hide dyeing process. Influence on the organoleptic and mechanical properties of dyed leather. *Journal of the American Leather Chemists Association,* 98**,** 132-138.

MARTI, M., DE LA MAZA, A., PARRA, J. L. & CODERCH, L. 2014. Role of Liposomes in Textile Dyeing. *Liposomes, Lipid Bilayers and Model Membranes: From Basic Research to Application***,** 401-414.

MARTI, M., DE LA MAZA, A., PARRA, J. L., CODERCH, L. & SERRA, S. 2001. Dyeing wool at low temperatures: New method using liposomes. *Textile Research Journal,* 71**,** 678-682.

MCCLEMENTS, D. J. 2015. Encapsulation, protection, and release of hydrophilic active components: potential and limitations of colloidal delivery systems. *Adv Colloid Interface Sci,* 219**,** 27-53.

MEISNER, D., & MEZEI, M. 1995. Liposome ocular delivery systems. *Advanced drug delivery reviews,* 16**,** 75-93.

MEURE, L. A., FOSTER, N. R. & DEHGHANI, F. 2008. Conventional and dense gas techniques for the production of liposomes: a review. *AAPS PharmSciTech,* 9**,** 798-809.

MEURE, L. A., KNOTT, R., FOSTER, N. R. & DEHGHANI, F. 2009. The depressurization of an expanded solution into aqueous media for the bulk production of liposomes. *Langmuir,* 25**,** 326-37.

MONTAZER, M., ZOLFAGHARI, A., TOLIAT, T. & MOGHADAM, M. B. 2009. Modification of wool surface by liposomes for dyeing with weld. *Journal of Liposome Research,* 19**,** 173-179.

MOURTZINOS, I., KALOGEROPOULOS, N., PAPADAKIS, S. E., KONSTANTINOU, K. & KARATHANOS, V. T. 2008. Encapsulation of nutraceutical monoterpenes in beta-cyclodextrin and modified starch. *Journal of Food Science,* 73**,** S89-S94.

MOZAFARI, M. R. 2005a. Liposomes: an overview of manufacturing techniques. *Cell Mol Biol Lett,* 10**,** 711-9.

MOZAFARI, M. R. 2005b. Liposomes: An overview of manufacturing techniques. *Cellular & Molecular Biology Letters,* 10**,** 711-719.

MOZAFARI, M. R., REED, C. J., ROSTRON, C., KOCUM, C. & PISKIN, E. 2002. Construction of stable anionic liposome-plasmid particles using the heating method: a preliminary investigation. *Cell Mol Biol Lett,* 7**,** 923-7.

MUNDADA, A. S. & AVARI, J. G. 2009. In Situ Gelling Polymers in Ocular Drug Delivery Systems: A Review. *Critical Reviews in Therapeutic Drug Carrier Systems,* 26**,** 85-118.

NAGAHIRO, I., MORA, B. N., BOASQUEVISQUE, C. H., SCHEULE, R. K. & PATTERSON, G. A. 2000. Toxicity of cationic liposome-DNA complex in lung isografts. *Transplantation,* 69**,** 1802-5.

NAVARATNAM, S. & CLARIDGE, J. 2000. Primary photophysical properties of ofloxacin. *Photochemistry and Photobiology,* 72**,** 283-290.

NEDOVIC, V., KALUSEVIC, A., MANOJLOVIC, V., LEVIC, S. & BUGARSKI, B. 2011. An overview of encapsulation technologies for food applications. *11th International Congress on Engineering and Food (Icef11),* 1**,** 1806-1815.

NEETHIRAJAN, S. & JAYAS, D. S. 2011. Nanotechnology for the Food and Bioprocessing Industries. *Food and Bioprocess Technology,* 4**,** 39-47.

NIESMAN, M. R. 1992. The Use of Liposomes as Drug Carriers in Ophthalmology. *Critical Reviews in Therapeutic Drug Carrier Systems,* 9**,** 1-38.

NIESMAN, M. R., KHOOBEHI, B. & PEYMAN, G. A. 1992. Encapsulation of sodium fluorescein for dye release studies. *Invest Ophthalmol Vis Sci,* 33**,** 2113-9.

NII, T. & ISHII, F. 2005a. Encapsulation efficiency of water-soluble and insoluble drugs in liposomes prepared by the microencapsulation vesicle method. *International Journal of Pharmaceutics,* 298**,** 198-205.

NII, T. & ISHII, F. 2005b. Encapsulation efficiency of water-soluble and insoluble drugs in liposomes prepared by the microencapsulation vesicle method. *Int J Pharm,* 298**,** 198-205.

NOGUEIRA, E., GOMES, A. C., PRETO, A. & CAVACO-PAULO, A. 2015. Design of liposomal formulations for cell targeting. *Colloids and Surfaces B: Biointerfaces,* 136**,** 514-526.

OCHOWIAK, M. 2012. The effervescent atomization of oil-in-water emulsions. *Chemical Engineering and Processing: Process Intensification,* 52**,** 92-101.

ONYEJI, C. O., NIGHTINGALE, C. H., NICOLAU, D. P. & QUINTILIANI, R. 1994. Efficacies of liposome-encapsulated clarithromycin and ofloxacin against Mycobacterium avium-M. intracellulare complex in human macrophages. *Antimicrob Agents Chemother,* 38**,** 523-7.

OTAKE, K., IMURA, T., SAKAI, H. & ABE, M. 2001. Development of a new preparation method of liposomes using supercritical carbon dioxide. *Langmuir,* 17**,** 3898-3901.

OTAKE, K., SHIMOMURA, T., GOTO, T., IMURA, T., FURUYA, T., YODA, S., TAKEBAYASHI, Y., SAKAI, H. & ABE, M. 2006. Preparation of liposomes using an improved supercritical reverse phase evaporation method. *Langmuir,* 22**,** 2543-50.

OUSSOREN, C. & STORM, G. 2001. Liposomes to target the lymphatics by subcutaneous administration. *Adv Drug Deliv Rev,* 50**,** 143-56.

OUSSOREN, C., ZUIDEMA, J., CROMMELIN, D. J. & STORM, G. 1997. Lymphatic uptake and biodistribution of liposomes after subcutaneous injection. II. Influence of liposomal size, lipid compostion and lipid dose. *Biochim Biophys Acta,* 1328**,** 261-72.

PACKER, L., WITT, E. H. & TRITSCHLER, H. J. 1995. Alpha-Lipoic Acid as a Biological Antioxidant. *Free Radical Biology and Medicine,* 19**,** 227-250.

PAGE, C., FENNEN, J. & GAGLIARDINO, D. 2009. Leather Dyes - Properties and Analysis. *Xxx Congress of the International Union of Leather Technologists & Chemists Societies, Proceedings***,** 167-174.

PAINI, M., ALIAKBARIAN, B., CASAZZA, A. A., LAGAZZO, A., BOTTER, R. & PEREGO, P. 2015a. Microencapsulation of phenolic compounds from olive pomace using spray drying: A study of operative parameters. *Lwt-Food Science and Technology,* 62**,** 177-186.

PAINI, M., ALIAKBARIAN, B., CASAZZA, A. A., PEREGO, P., RUGGIERO, C. & PASTORINO, L. 2015b. Chitosan/dextran multilayer microcapsules for polyphenol co-delivery. *Materials Science & Engineering C-Materials for Biological Applications,* 46**,** 374-380.

PALEOS, C. M., TSIOURVAS, D. & SIDERATOU, Z. 2016. Triphenylphosphonium Decorated Liposomes and Dendritic Polymers: Prospective Second Generation Drug Delivery Systems for Targeting Mitochondria. *Mol Pharm,* 13**,** 2233-41.

PALMIERI, D., ALIAKBARIAN, B., CASAZZA, A. A., FERRARI, N., SPINELLA, G., PANE, B., CAFUERI, G., PEREGO, P. & PALOMBO, D. 2012. Effects of polyphenol extract from olive

pomace on anoxia-induced endothelial dysfunction. *Microvascular Research,* 83**,** 281-289.

PANDEY, K. B. & RIZVI, S. I. 2009. Plant polyphenols as dietary antioxidants in human health and disease. *Oxidative Medicine and Cellular Longevity,* 2**,** 270-278.

PAPADIA, K., MARKOUTSA, E. & ANTIMISIARIS, S. G. 2014. A simplified method to attach antibodies on liposomes by biotin-streptavidin affinity for rapid and economical screening of targeted liposomes. *J Biomed Nanotechnol,* 10**,** 871-6.

PAPUC, C., CRISTE, R., DURDUN, N., UNTEA, A. & NICORESCU, V. 2010. The Effect of Some Mineral and Phytogenic Additives Rich in Polyphenols on Lipid Peroxidation Process. *Revista De Chimie,* 61**,** 920-924.

PARDUE, R. L. & WHITE, C. A. 1997. Pharmacokinetic evaluation of liposomal encapsulated ampicillin in male and female rats. *Biopharmaceutics & Drug Disposition,* 18**,** 279-292.

PARK, S. J., CHOI, S. G., DAVAA, E. & PARK, J. S. 2011. Encapsulation enhancement and stabilization of insulin in cationic liposomes. *Int J Pharm,* 415**,** 267-72.

PATEL, N., NAKRANI, H., RAVAL, M. & SHETH, N. 2016. Development of loteprednol etabonate-loaded cationic nanoemulsified in-situ ophthalmic gel for sustained delivery and enhanced ocular bioavailability. *Drug Delivery,* 23**,** 3712-3723.

PATIL, Y. P. & JADHAV, S. 2014. Novel methods for liposome preparation. *Chem Phys Lipids,* 177**,** 8-18.

PAUSE, B. 2007. Application of phase change and shape memory materials in medical textiles. *Smart Textiles for Medicine and Healthcare: Materials, Systems and Applications***,** 74-87.

PEER, D. & MARGALIT, R. 2004. Loading mitomycin C inside long circulating hyaluronan targeted nano-liposomes increases its antitumor activity in three mice tumor models. *Int J Cancer,* 108**,** 780-9.

PERKINS, W. R., MINCHEY, S. R., AHL, P. L. & JANOFF, A. S. 1993. The determination of liposome captured volume. *Chem Phys Lipids,* 64**,** 197-217.

PERRIER-CORNET, J. M., P. M. & GERVAIS., P. 2005. Comparison of emulsification efficiency of protein-stabilized oil-in-water emulsions using jet, high pressure and colloid mill homogenization. *Journal of Food Engineering,* 66**,** 211-217.

PHAM, T. T., JAAFAR-MAALEJ, C., CHARCOSSET, C. & FESSI, H. 2012. Liposome and niosome preparation using a membrane contactor for scale-up. *Colloids Surf B Biointerfaces,* 94**,** 15-21.

PLATZER, B. & MAURER, G. 1989. A Generalized Equation of State for Pure Polar and Nonpolar Fluids. *Fluid Phase Equilibria,* 51**,** 223-236.

POPOWCHAK, S., HARRIS, A., REECK, M., PERLER, A. & MARTIN, B. 1996. Ocular hypotension after exercise: Role of colloid osmotic pressure. *Investigative Ophthalmology & Visual Science,* 37**,** 3745-3745.

POSTE, G. & FIDLER, I. J. 1980. The pathogenesis of cancer metastasis. *Nature,* 283**,** 139-46.

PRAKASH, A. J., ARAVINDHAN, R., FATHIMA, N. N. & RAO, J. R. 2016. Dyeing of Chamois Leather using Water Soluble Sulphur Dyes. *Journal of the American Leather Chemists Association,* 111**,** 383-388.

PRIYA, G. K., ABU JAVID, M. M., GEORGE, A., AARTHY, M., ANBARASAN, S. D., KAMINI, N. R., GOWTHAMAN, M. K., ARAVINDHAN, R., GANESH, S., CHANDRASEKAR, R. & AYYADURAI, N. 2016. Next generation greener leather dyeing process through recombinant green fluorescent protein. *Journal of Cleaner Production,* 126**,** 698-706.

PUREV, N., BURGERT, L., PRICHYSTAL, P., HRDINA, R., KUHN, J., CERNY, M. & OYUNTULKHUUR, J. 2013. Dyeing of leather with microencapsulated acid dye. *Coloration Technology,* 129**,** 412-417.

RAFIDINARIVO, H. & DELMAS, M. 1996. A new process of leather dyeing in solvent medium. *Journal of the Society of Leather Technologists and Chemists,* 80**,** 6-10.

RAMALDES, G. A., DEVERRE, J.-R., GROGNET, J.-M., PUISIEUX, F. & FATTAL, E. 1996. Use of an enzyme immunoassay for the evaluation of entrapment efficiency and in vitro stability in intestinal fluids of liposomal bovine serum albumin. *International Journal of Pharmaceutics,* 143**,** 1-11.

RAVIKUMAR, M., MODERY, C. L., WONG, T. L. & GUPTA, A. S. 2012. Peptide-decorated liposomes promote arrest and aggregation of activated platelets under flow on vascular injury relevant protein surfaces in vitro. *Biomacromolecules,* 13**,** 1495-502.

REITZ, R. D. 1978. Atomization and other breakup regimes of a liquid jet.

REVERCHON, E., AMBRUOSI, A. & SENATORE, F. 1994. Isolation of peppermint oil using supercritical CO2 extraction. *Flavour and Fragrance Journal,* 9**,** 19-23.

ROGERS, J. A. & ANDERSON, K. E. 1998. The potential of liposomes in oral drug delivery. *Crit Rev Ther Drug Carrier Syst,* 15**,** 421-80.

ROSA, R., PINI, M., NERI, P., CORSI, M., BIANCHINI, R., BONANNI, M. & FERRARI, A. M. 2017. Environmental sustainability assessment of a new degreasing formulation for the tanning cycle within leather manufacturing. *Green Chemistry,* 19**,** 4571-4582.

ROY, U., SENGUPTA, S., BANERJEE, P., DAS, P., BHOWAL, A. & DATTA, S. 2018. Assessment on the decolourization of textile dye (Reactive Yellow) using Pseudomonas sp immobilized on fly ash: Response surface methodology Chock for optimization and toxicity evaluation. *Journal of Environmental Management,* 223**,** 185-195.

SAHOO, S. K. & LABHASETWAR, V. 2003. Nanotech approaches to drug delivery and imaging. *Drug Discov Today,* 8**,** 1112-20.

SALGADO, M., SANTOS, F., RODRÍGUEZ-ROJO, S., REIS, R. L., DUARTE, A. R. C. & COCERO, M. J. 2017. Development of barley and yeast β-glucan aerogels for drug delivery by supercritical fluids. *Journal of CO2 Utilization,* 22**,** 262-269.

SANCHO, M. & MACH, N. 2015. Effects of Wine Polyphenols on Cancer Prevention. *Nutricion Hospitalaria,* 31**,** 535-551.

SANKARAM, M. B. & THOMPSON, T. E. 1990. Interaction of cholesterol with various glycerophospholipids and sphingomyelin. *Biochemistry,* 29**,** 10670-10675.

SANTO, I. E., CAMPARDELLI, R., ALBUQUERQUE, E. C., DE MELO, S. V., DELLA PORTA, G. & REVERCHON, E. 2014. Liposomes preparation using a supercritical fluid assisted continuous process. *Chemical Engineering Journal,* 249**,** 153-159.

SANTO, I. E., CAMPARDELLI, R., ALBUQUERQUE, E. C., VIEIRA DE MELO, S. A., REVERCHON, E. & DELLA PORTA, G. 2015. Liposomes Size Engineering by Combination of Ethanol Injection and Supercritical Processing. *J Pharm Sci,* 104**,** 3842-50.

SARISOZEN, C., SALZANO, G. & TORCHILIN, V. P. 2015. Recent advances in siRNA delivery. *Biomol Concepts,* 6**,** 321-41.

SASAKI, H., KARASAWA, K., HIRONAKA, K., TAHARA, K., TOZUKA, Y. & TAKEUCHI, H. 2013. Retinal drug delivery using eyedrop preparations of poly-L-lysine-modified liposomes. *European Journal of Pharmaceutics and Biopharmaceutics,* 83**,** 364-369.

SATHISH, M., MADHAN, B., SREERAM, K. J., RAO, J. R. & NAIR, B. U. 2016. Alternative carrier medium for sustainable leather manufacturing - a review and perspective. *Journal of Cleaner Production,* 112**,** 49-58.

SAUVAGE, F. X., BACH, B., MOUTOUNET, M. & VERNHET, A. 2010. Proteins in white wines: Thermo-sensitivity and differential adsorbtion by bentonite. *Food Chemistry,* 118**,** 26-34.

SCALBERT, A. & MAZUR, A. 2002. Dietary polyphenols and the prevention of cardiovascular diseases - State of the art. *Cardiovascular Dieseases 2002***,** 351-357.

SCARMEAS, N., STERN, Y., TANG, M. X., MAYEUX, R. & LUCHSINGER, J. A. 2006. Mediterranean diet and risk for Alzheimer's disease. *Annals of Neurology,* 59**,** 912-921.

SCHUMACHER, I. & MARGALIT, R. 1997. Liposome-encapsulated ampicillin: physicochemical and antibacterial properties. *J Pharm Sci,* 86**,** 635-41.

SEBAALY, C., GREIGE-GERGES, H., AGUSTI, G., FESSI, H. & CHARCOSSET, C. 2016a. Large-scale preparation of clove essential oil and eugenol-loaded liposomes using a membrane contactor and a pilot plant. *Journal of Liposome Research,* 26**,** 126-138.

SEBAALY, C., GREIGE-GERGES, H., STAINMESSE, S., FESSI, H. & CHARCOSSET, C. 2016b. Effect of composition, hydrogenation of phospholipids and lyophilization on the characteristics of eugenol-loaded liposomes prepared by ethanol injection method. *Food Bioscience,* 15**,** 1-10.

SHAHEEN, S. M., SHAKIL AHMED, F. R., HOSSEN, M. N., AHMED, M., AMRAN, M. S. & UL-ISLAM, M. A. 2006. Liposome as a carrier for advanced drug delivery. *Pak J Biol Sci,* 9**,** 1181-1191.

SHAKER, S., GARDOUH, A. R. & GHORAB, M. M. 2017. Factors affecting liposomes particle size prepared by ethanol injection method. *Res Pharm Sci,* 12**,** 346-352.

SHARMA, D., E., A. A. A. & R., T. L. 2018. An updated review on: liposomes as drug delivery systems. *PharmaTutor,* 6**,** 50-62.

SHEVELEVA, I. A., BELOKUROVA, O. A., SHCHEGLOVA, T. L. & MEL'NIKOV, B. N. 2003. Polyfunctional properties of liposomes in preparation of textile materials. *Fibre Chemistry,* 35**,** 48-52.

SIVAKUMAR, V., SWAMINATHAN, G., RAO, P. G. & RAMASAMI, T. 2009. Ultrasound-aided leather dyeing: a preliminary investigation on process parameters influencing ultrasonic technology for large-scale production. *International Journal of Advanced Manufacturing Technology,* 45**,** 41-54.

SOLAYMAN, M., ALI, Y., ALAM, F., ISLAM, M. A., ALAM, N., KHALIL, M. I. & GAN, S. H. 2016. Polyphenols: Potential Future Arsenals in the Treatment of Diabetes. *Current Pharmaceutical Design,* 22**,** 549-565.

SPATARO, G., MALECAZE, F., TURRIN, C. O., SOLER, V., DUHAYON, C., ELENA, P. P., MAJORAL, J. P. & CAMINADE, A. M. 2010. Designing dendrimers for ocular drug delivery. *European Journal of Medicinal Chemistry,* 45**,** 326-334.

STONE, W. L. & SMITH, M. 2004. Therapeutic uses of antioxidant liposomes. *Molecular Biotechnology,* 27**,** 217-230.

SUBCZYNSKI, W. K., WISNIEWSKA, A., YIN, J.-J., HYDE, J. S. & KUSUMI, A. 1994. Hydrophobic Barriers of Lipid Bilayer Membranes Formed by Reduction of Water Penetration by Alkyl Chain Unsaturation and Cholesterol. *Biochemistry,* 33**,** 7670-7681.

SUETSUGU, S., KURISU, S. & TAKENAWA, T. 2014a. Dynamic shaping of cellular membranes by phospholipids and membrane-deforming proteins. *Physiol Rev,* 94**,** 1219-48.

SUETSUGU, S., KURISU, S. & TAKENAWA, T. 2014b. Dynamic shaping of cellular membranes by phospholipids and membrane-deforming proteins. *Physiological Reviews,* 94**,** 1219-48.

SZOKA, F., JR. & PAPAHADJOPOULOS, D. 1978. Procedure for preparation of liposomes with large internal aqueous space and high capture by reverse-phase evaporation. *Proc Natl Acad Sci U S A,* 75**,** 4194-8.

TAAMALLI, A., ARRAEZ-ROMAN, D., ZARROUK, M., VALVERDE, J., SEGURA-CARRETERO, A. & FERNANDEZ-GUTIERREZ, A. 2012. The Occurrence and Bioactivity of Polyphenols in Tunisian Olive Products and by-Products: A Review. *Journal of Food Science,* 77**,** R83-R92.

TADASAS, K., & KAYAHARA, H. 1983. Initial steps of eugenol degradation pathway of a microorganism. *Agricultural and Biological Chemistry,* 47**,** 2639-2640.

TARANTINO, G., BRILLI, E., ZAMBITO, Y., GIORDANO, G. & EQUITANI, F. 2015. Sucrosomial Iron®: a new highly Bioavaible oral iron supplement. *Blood,* 126**,** 4561-4566.

TERAHARA, N. 2015. Flavonoids in Foods: A Review. *Natural Product Communications,* 10**,** 521-528.

TILA, D., GHASEMI, S., YAZDANI-ARAZI, S. N. & GHANBARZADEH, S. 2015. Functional liposomes in the cancer-targeted drug delivery. *J Biomater Appl,* 30**,** 3-16.

TIWARI, G., TIWARI, R., SRIWASTAWA, B., BHATI, L., PANDEY, S., PANDEY, P. & BANNERJEE, S. K. 2012. Drug delivery systems: An updated review. *Int J Pharm Investig,* 2**,** 2-11.

TORCHILIN, V. P. 2005. Recent advances with liposomes as pharmaceutical carriers. *Nat Rev Drug Discov,* 4**,** 145-60.

TRUCILLO, P., CAMPARDELLI, R., ALIAKBARIAN, B., PEREGO, P. & REVERCHON, E. 2018a. Supercritical assisted process for the encapsulation of olive pomace extract into liposomes. *Journal of Supercritical Fluids,* 135**,** 152-159.

TRUCILLO, P., CAMPARDELLI, R. & REVERCHON, E. 2017. Supercritical CO2 assisted liposomes formation: Optimization of the lipidic layer for an efficient hydrophilic drug loading. *Journal of Co2 Utilization,* 18**,** 181-188.

TRUCILLO, P., CAMPARDELLI, R. & REVERCHON, E. 2018b. Encapsulation of Hydrophilic and Lipophilic Compounds in Nanosomes Produced with a Supercritical Based Process. *Advances in Bionanomaterials, Bionam 2016***,** 23-35.

TRUCILLO, P., CAMPARDELLI, R. & REVERCHON, E. 2018c. Production of liposomes loaded with antioxidants using a supercritical CO2 assisted process. *Powder Technology,* 323**,** 155-162.

TUREK, C. & STINTZING, F. C. 2013. Stability of Essential Oils: A Review. *Comprehensive Reviews in Food Science and Food Safety,* 12**,** 40-53.

UHL, P., PANTZE, S., STORCK, P., PARMENTIER, J., WITZIGMANN, D., HOFHAUS, G., HUWYLER, J., MIER, W. & FRICKER, G. 2017. Oral delivery of vancomycin by tetraether lipid liposomes. *European Journal of Pharmaceutical Sciences,* 108**,** 111-118.

ULRICH, A. S. 2002. Biophysical aspects of using liposomes as delivery vehicles *Bioscience Reports,* 22**,** 129-149.

VAISHYA, R. D., KHURANA, V., PATEL, S. & MITRA, A. K. 2014. Controlled ocular drug delivery with nanomicelles. *Wiley Interdisciplinary Reviews-Nanomedicine and Nanobiotechnology,* 6**,** 422-437.

VALADI, H., EKSTROM, K., BOSSIOS, A., SJOSTRAND, M., LEE, J. J. & LOTVALL, J. O. 2007. Exosome-mediated transfer of mRNAs and microRNAs is a novel mechanism of genetic exchange between cells. *Nat Cell Biol,* 9**,** 654-9.

VAN ELK, M., LORENZATO, C., OZBAKIR, B., OERLEMANS, C., STORM, G., NIJSEN, F., DECKERS, R., VERMONDEN, T. & HENNINK, W. E. Alginate microgels loaded with temperature sensitive liposomes for magnetic resonance imageable drug release and microgel visualization. *European Polymer Journal.*

VANDAMME, T. F. 2002. Microemulsions as ocular drug delivery systems: recent developments and future challenges. *Progress in Retinal and Eye Research,* 21**,** 15-34.

VENBA, R., JAWAHAR, M., JOTHI, G., DAKSHINAMOORTHY, D., DEEPIKA, A., BABU, N. K. C. & RAMESH, K. N. 2015. Studies on Solubilized Sulfur Dyes for Coloring Leather. *Journal of the American Leather Chemists Association,* 110**,** 177-185.

VINAYAGAM, R., JAYACHANDRAN, M. & XU, B. J. 2016. Antidiabetic Effects of Simple Phenolic Acids: A Comprehensive Review. *Phytotherapy Research,* 30**,** 184-199.

VISSERS, M. N., ZOCK, P. L. & KATAN, M. B. 2004. Bioavailability and antioxidant effects of olive oil phenols in humans: a review. *European Journal of Clinical Nutrition,* 58**,** 955-965.

VOINEA, M. & SIMIONESCU, M. 2002. Designing of 'intelligent' liposomes for efficient delivery of drugs. *J Cell Mol Med,* 6**,** 465-74.

VOLF, I., IGNAT, I., NEAMTU, M. & POPA, V. I. 2014. Thermal stability, antioxidant activity, and photo-oxidation of natural polyphenols. *Chemical Papers,* 68**,** 121-129.

WANG, H., ZHAO, P., LIANG, X., GONG, X., SONG, T., NIU, R. & CHANG, J. 2010. Folate-PEG coated cationic modified chitosan – Cholesterol liposomes for tumor-targeted drug delivery. *Biomaterials,* 31**,** 4129-4138.

WATWE, R. M. & BELLARE, J. R. 1995. Manufacture of Liposomes - a Review. *Current Science,* 68**,** 715-724.

WEERAKODY, R., FAGAN, P. & KOSARAJU, S. L. 2008. Chitosan microspheres for encapsulation of alpha-lipoic acid. *International Journal of Pharmaceutics,* 357**,** 213-218.

WEN-CHYANTSAI & S.H.RIZVI, S. 2016. Liposomal microencapsulation using the conventional methods and novel supercritical fluid processes. *Trends in Food Science & Technology,* 55**,** 61-71.

WILLIAMSON, G. & MANACH, C. 2005. Bioavailability and bioefficacy of polyphenols in humans. II. Review of 93 intervention studies. *American Journal of Clinical Nutrition,* 81**,** 243s-255s.

WINK, M. 1997. Compartmentation of secondary metabolites and xenobiotics in plant vacuoles. *Advances in Botanical Research Incorporating Advances in Plant Pathology, Vol 25,* 25**,** 141-169.

WOODLE, M. C. & LASIC, D. D. 1992. Sterically stabilized liposomes. *Biochim Biophys Acta,* 1113**,** 171-99.

WORANUCH, S. & YOKSAN, R. 2013. Eugenol-loaded chitosan nanoparticles: I. Thermal stability improvement of eugenol through encapsulation. *Carbohydrate Polymers,* 96**,** 578-585.

WU, G., MIKHAILOVSKY, A., KHANT, H. A., FU, C., CHIU, W. & ZASADZINSKI, J. A. 2008. Remotely triggered liposome release by near-infrared light absorption via hollow gold nanoshells. *J Am Chem Soc,* 130**,** 8175-7.

YAMAGUCHI, M., UEDA, K., ISOWAKI, A., OHTORI, A., TAKEUCHI, H., OHGURO, N. & TOJO, K. 2009. Mucoadhesive Properties of Chitosan-Coated Ophthalmic Lipid Emulsion Containing Indomethacin in Tear Fluid. *Biological & Pharmaceutical Bulletin,* 32**,** 1266-1271.

YANG, S., LIU, C., LIU, W., YU, H., ZHENG, H., ZHOU, W. & HU, Y. 2013. Preparation and characterization of nanoliposomes entrapping medium-chain fatty acids and vitamin C by lyophilization. *Int J Mol Sci,* 14**,** 19763-73.

YOSHIMOTO, M., TAMURA, R. & NATSUME, T. 2013. Liposome clusters with shear stress-induced membrane permeability. *Chem Phys Lipids,* 174**,** 8-16.

ZHANG, J., GUAN, P. P., WANG, T. Y., CHANG, D., JIANG, T. Y. & WANG, S. L. 2009. Freeze-dried liposomes as potential carriers for ocular administration of cytochrome c against selenite cataract formation. *Journal of Pharmacy and Pharmacology,* 61**,** 1171-1178.

ZHANG, L., ZHANG, H. Y., HUANG, F. C., HUANG, Q., LIU, C. & LI, J. R. 2016. Study on the clinical value of alprostadil combined with alpha-lipoic acid in treatment of type 2 diabetes mellitus patients with erectile dysfunction. *European Review for Medical and Pharmacological Sciences,* 20**,** 3930-3933.

ZHANG, R., KULKARNI, K. A. & KULKARNI, A. P. 2000. Oxidation of eugenol by purified human term placental peroxidase. *Placenta,* 21**,** 234-240.

ZHAO, L., ZHOU, Y., GAO, Y., MA, S., ZHANG, C., LI, J., WANG, D., LI, X., LI, C., LIU, Y. & LI, X. 2015. Bovine serum albumin nanoparticles for delivery of tacrolimus to reduce its kidney uptake and functional nephrotoxicity. *Int J Pharm,* 483**,** 180-7.

ZHONG, J. & DAI, L. C. 2011. Liposomal preparation by supercritical fluids technology. *African Journal of Biotechnology,* 10**,** 16406-16413.

ZHOU, F. & LI, B. 2015. Exonuclease III-Assisted Target Recycling Amplification Coupled with Liposome-Assisted Amplification: One-Step and Dual-Amplification Strategy for Highly Sensitive Fluorescence Detection of DNA. *Anal Chem,* 87**,** 7156-62.

Abbreviation list

DDS: Drug Delivery Systems,
SUV: Single Unilamellar Vesicles,
MUV: Medium Unilamellar Vesicles,
LUV: Large Unilamellar Vesicles,
GUV: Giant Unilamellar Vesicles,
OLV: OligoLamellar Vesicles,
MLV: MultiLamellar Vesicles,
MVV: MultiVesicular Vesicles,
EE: Encapsulation Efficiency,
PDI: Polidispersity Index,
SD: Standard Deviation,
MD: Mean Diameter,
PSD: Particle Size Distribution,
SCF: SupercCritical Fluids,
SC-CO_2: Supercritical Carbon Dioxide,
GLR-EL: Gas to Liquid Ratio of the Expanded Liquid,
FBSA: Albumin fluorescein isothiocyanate
PC: Phosphatidylcholine,
PE: Phosphatidylethanolamine,
Chol: Cholesterol,
EUG: Eugenol
SuperLip: Supercritical assisted Liposome formation,
FV: Formation Vessel,
H: Homogenizer,
Sep: Separator,
FE-SEM: Field-Emission Scanning Electron Microscope,
TEM: Transmission Electron Microscope,
SAS: Supercritical Anti-Solvent,
RESS: Rapid Expansion of a Supercritical Solution,
HPLC: High Performance Liquid Chromatography,
Eug: Eugenol,
A: Ampicillin,
OF: Ofloxacin,
PGSS: Particles from gas saturated solution,
GI: GastroIntestinal tract,
PEG: PolyEthylene Glycol
SCRPE: SuperCritical fluid Reverse Phase Evaporation
NTA: Nanoparticle Tracking Analysis
MW: Molecular Weight
TE: Trapment Efficiency
RVE: Reverse phase Evaporation Vesicles

TLH: Thin Layer Hydration
LOM: Lipid Oxygen containing Microparticles
BSA: Bovine Serum Albumin
PIC: polyinosinic-polycytidylic acid,
NIR: Near Infrared,
HNG: Hollow Gold Nanospheres,
TSL: Temperature Sensitive Liposomes,
SR: Solvent Residue
F: Farnesol
V: Vancomycin
TRL: Technology Readiness Level
CF: Cash Flow
ROS: Return on Interest
IRR: Internal Rate of Return
EBTDA: Earnings Before Interest, Tax, Depreciation and Amortization